

Bioanalysis and clinical pharmacology of tyrosine kinase inhibitors

ISBN/EAN: 978-90-393-5906-8

© 2013 Nienke Lankheet, Utrecht

Cover design: Nienke Lankheet & Laura Lammers

Printed and layout by: Gildeprint Drukkerijen – www.gildeprint.nl

Printed on FSC certified paper

Bioanalysis and clinical pharmacology of tyrosine kinase inhibitors

Bioanalyse en klinische farmacologie
van tyrosine kinase remmers

(met een samenvatting in het Nederlands)

Proefschrift

ter verkrijging van de graad van doctor aan de Universiteit Utrecht
op gezag van de rector magnificus, prof.dr. G.J. van der Zwaan,
ingevolge het besluit van het college voor promoties
in het openbaar te verdedigen
op woensdag 13 februari 2013 des middags te 2.30 uur

door

Annie Gerda Lankheet

geboren op 27 april 1984
te Haaksbergen

Promotoren:

Prof.dr. J.H. Beijnen

Prof.dr. J.H.M. Schellens

Co-promotor:

Dr. A.D.R. Huitema

The research described in this thesis was performed at the Department of Pharmacy & Pharmacology of the Slotervaart Hospital / the Netherlands Cancer Institute, Amsterdam, The Netherlands and the Department of Medical Oncology of the Netherlands Cancer Institute, Amsterdam, The Netherlands.

Publication of this thesis was financially supported by:

The Netherlands Laboratory for Anticancer Drug Formulation (NLADF), Amsterdam, The Netherlands

Pfizer B.V., Capelle a/d IJssel, The Netherlands

Roche Nederland B.V., Woerden, The Netherlands

PharmChem Inc., Fort Worth, Texas, USA

Utrecht Institute of Pharmaceutical Sciences (UIPS), Utrecht, The Netherlands



'Angst is mar veur eben, spiet is veur altied'

~ Daniel Lohues, 2008

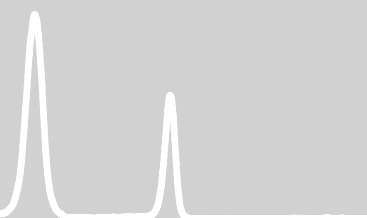
Contents

<i>Preface</i>	11
Chapter 1 Bioanalysis	
1.1 Method development and validation for the quantification of dasatinib, erlotinib, gefitinib, imatinib, lapatinib, nilotinib, sorafenib and sunitinib in human plasma by liquid chromatography coupled with tandem mass spectrometry <i>Biomedical Chromatography. September 17, 2012. Published ahead of print</i>	19
1.2 Quantification of sunitinib and Ndesethyl sunitinib in human EDTA plasma by liquid chromatography coupled with electrospray ionization tandem mass spectrometry: validation and application in routine therapeutic drug monitoring <i>Therapeutic Drug Monitoring, in press</i>	43
1.3 Development and clinical validation of a method for the quantification of sunitinib and N-desethyl sunitinib in dried blood spots <i>Experimental chapter</i>	61
1.4 Determination of sunitinib and its active metabolite N-desethyl sunitinib in sweat of a patient <i>Journal of Analytical Toxicology 2011;35(8):558-65.</i>	83
1.5 Quantitative determination of erlotinib and O-desmethyl erlotinib in human EDTA plasma and lung tumor tissue <i>Bioanalysis 2012; 4(21):2563-77.</i>	101
1.6 A validated assay for the quantitative analysis of vatalanib in human EDTA plasma by liquid chromatography coupled with electrospray ionization tandem mass spectrometry <i>Journal of Chromatography B 2009; 877: 3625–3630.</i>	125

Chapter 2	<i>Clinical Pharmacology</i>	
2.1	Plasma concentrations of tyrosine kinase inhibitors imatinib, erlotinib and sunitinib in routine clinical outpatient cancer care <i>Submitted for publication</i>	141
2.2	Pharmacokinetically-guided sunitinib dosing: A feasibility study in patients with advanced solid tumors <i>Manuscript in preparation</i>	159
2.3	The effect of seasonal variation and secretion of sunitinib in sweat on the development of hand-foot syndrome <i>Submitted for publication</i>	177
2.4	Correlation between plasma erlotinib concentrations and treatment outcome during alternating erlotinib-chemotherapy dosing schedules and erlotinib monotherapy in non-small cell lung cancer <i>Submitted for publication</i>	193
2.5	Intratumoral and serum concentrations of erlotinib in non-small cell lung cancer patients treated with neo-adjuvant erlotinib therapy <i>Submitted for publication</i>	211
	<i>Conclusions and perspectives</i>	223
	<i>Summary</i>	233
	<i>Nederlandse samenvatting</i>	237
	<i>Dankwoord</i>	243
	<i>Curriculum Vitae</i>	249
	<i>List of publications</i>	251



Preface



R1
R2
R3
R4
R5
R6
R7
R8
R9
R10
R11
R12
R13
R14
R15
R16
R17
R18
R19
R20
R21
R22
R23
R24
R25
R26
R27
R28
R29
R30
R31
R32
R33
R34
R35
R36
R37
R38
R39

Preface

Cancer is the second leading cause of death worldwide, after cardiovascular diseases, and accounted for 7.6 million deaths (13% of all deaths) in 2008 [1]. As a result of decades of cancer research, and consequently the availability of multiple effective chemotherapeutic agents and hormone treatments, the mortality of several cancer types began to decrease by the early 1990s. Chemotherapeutic therapies are, however, accompanied by severe toxicities, since their unspecific interaction with intracellular structures do not discriminate between fast growing cancer cells and healthy cells. Though, in 1996 cancer treatment underwent a pivotal change by the proof of principle that a drug (imatinib) was able to target a specific molecular abnormality in chronic myeloid leukemia (CML) cells. Targeting molecular abnormalities that are unique to cancer cells, provided a therapy that would be less toxic to healthy cells in which these abnormalities are absent. Moreover, when the first clinical data of imatinib showed efficacy in patients with CML, the belief that targeted therapy could convert certain types of cancer into manageable chronic diseases was strongly encouraged [2].

Imatinib is a drug belonging to the class of tyrosine kinase inhibitors (TKIs). TKIs are targeted agents which are rationally designed to compete with adenosine-5'- triphosphate (ATP) for the ATP binding pocket within the intracellular domain of several oncogenic tyrosine kinase receptors. Thereby, TKIs block the intracellular signalling pathways of these receptors ultimately leading to inhibition of processes that are important for tumor growth, including angiogenesis, cell proliferation and migration [3]. To date, eleven TKIs have been approved for use in several types of cancer in Europe. In addition, a dozen experimental TKIs are being investigated in pre-clinical and early phase clinical studies. As shown in table 1, most TKIs have been approved after application for orphan drug designation or by conditional approval. In both circumstances, an accelerated marketing authorisation is accomplished. During this accelerated process, it is solely assessed whether the benefits for public health outweigh the risks inherent in the fact that the applicant still has to provide comprehensive data on safety and efficacy. Thus, post-marketing there is still need to obtain additional information on safety, efficacy and optimal use of TKIs [4].

R1
R2
R3
R4
R5
R6
R7
R8
R9
R10
R11
R12
R13
R14
R15
R16
R17
R18
R19
R20
R21
R22
R23
R24
R25
R26
R27
R28
R29
R30
R31
R32
R33
R34
R35
R36
R37
R38
R39

R1
R2
R3
R4
R5
R6
R7
R8
R9
R10
R11
R12
R13
R14
R15
R16
R17
R18
R19
R20
R21
R22
R23
R24
R25
R26
R27
R28
R29
R30
R31
R32
R33
R34
R35
R36
R37
R38
R39

Table 1. Overview of tyrosine kinase inhibitors with marketing authorisation [4].

TKI	Year of authorisation	Type of approval	Indication for use
Imatinib	2001	Orphan drug	Chronic myeloid leukemia (BCR-ABL positive) Dermatofibrosarcoma protuberans Gastrointestinal stromal tumor Hypereosinophilic syndrome Myelodysplastic or myeloproliferative diseases Acute lymphoblastic leukemia
Erlotinib	2005	Complete	Non-small cell lung cancer Pancreatic carcinoma
Sunitinib	2006	Complete	Renal cell carcinoma Gastrointestinal stromal tumor Neuroendocrine tumor
Sorafenib	2006	Orphan drug	Renal cell carcinoma Hepatocellular carcinoma
Dasatinib	2006	Orphan drug	Chronic myeloid leukemia (BCR-ABL positive) Acute lymphoblastic leukemia
Nilotinib	2007	Orphan drug	Chronic myeloid leukemia (BCR-ABL positive)
Lapatinib	2008	Conditional	Mamma carcinoma (HER2 positive)
Gefitinib	2009	Complete	Non-small cell lung cancer
Pazopanib	2010	Conditional	Renal cell carcinoma
Vandetanib	2012	Conditional	Medullary thyroid carcinoma
Axitinib	2012	Complete	Renal cell carcinoma

TKIs are orally, daily administered drugs that are currently prescribed at fixed doses. However, considerable pharmacokinetic inter-individual variability has been observed for all TKIs in daily practice. Variability in drug exposure is probably due to patient non-compliance (for example due to drug-related toxicity), drug interactions with co-medication and variability in oral drug availability and metabolic clearance. Moreover, correlation of pharmacokinetic parameters for drug exposure (trough level, area under the time-concentration curve (AUC)) with treatment efficacy and toxicity has been established for most of the TKIs. Hence, the large inter-individual variability in systemic exposure in combination with the positive exposure-efficacy relationship and low therapeutic index of TKIs, form a rationale for therapeutic drug monitoring (TDM) of these drugs. TDM might contribute to for instance a more optimal and tailor-made TKI treatment by improving therapeutic efficacy, decreasing risk for toxicity, detecting pharmacokinetic drug-drug interactions and monitoring adherence. However, before TDM of TKIs can be introduced as part of the standard of care, validated standardized bio-analytical assays have to be developed for TKIs and their active metabolites. In addition, efficacy and toxicity in relation to plasma exposure as well as therapeutic levels have to be defined for each TKI. Eventually, the efficacy and safety of TDM should be evaluated in prospective clinical trials [5].

Therefore, the aim of this thesis project was to develop bio-analytical assays to quantify TKIs in different biological matrices, and to apply these assays to clinical studies in order to increase the knowledge of TKI exposure in correlation with treatment outcome and toxicity.

Hence, six bio-analytical methods were developed to quantify the exposure of TKIs and their active metabolites in different biological matrices using high pressure liquid chromatography coupled with tandem mass spectrometry (HPLC-MS/MS): **Chapter 1.1**, **Chapter 1.2**, **Chapter 1.5**, and **Chapter 1.6** present bio-analytical methods using the conventional plasma matrix; **Chapter 1.3** discusses the development of a method using patient-friendly dried blood spots sampling; quantification of sunitinib and erlotinib in less conventional matrices sweat and lung tumor tissue is described in **Chapter 1.4** and **Chapter 1.5**, respectively.

Clinical studies to further explore the clinical pharmacology of TKIs are discussed in **Chapter 2**. In **Chapter 2.1** we present an observational study evaluating the plasma concentrations of imatinib, erlotinib and sunitinib in routine clinical practice in relation to the predefined therapeutic trough plasma levels of these TKIs. We also investigated plasma trough concentrations of sunitinib in an interventional study in which sunitinib was dosed individually based on measured plasma concentrations. The feasibility and safety of this pharmacokinetic guided sunitinib dosing regimen are discussed in **Chapter 2.2**. Patients treated with sunitinib suffer frequently from skin toxicity which severely impairs daily living [6]. The pathogenesis of this toxicity is unknown yet [6]. **Chapter 2.3** describes an exploratory study in which sunitinib secretion in sweat as cause of skin toxicity is investigated. Little is known about antagonistic pharmacodynamic interactions between erlotinib and chemotherapeutic agents which make sequential administrations of these agents necessary [7]. In **Chapter 2.4**, we present a study investigating the correlation between erlotinib plasma levels during administration of chemotherapeutic agents and treatment outcome. In **Chapter 2.5**, we studied erlotinib levels within lung tumor tissue after neo-adjuvant therapy to assess erlotinib tumor penetration.

Finally, in the general discussion the results of all studies are discussed and put into perspective.

R1
R2
R3
R4
R5
R6
R7
R8
R9
R10
R11
R12
R13
R14
R15
R16
R17
R18
R19
R20
R21
R22
R23
R24
R25
R26
R27
R28
R29
R30
R31
R32
R33
R34
R35
R36
R37
R38
R39

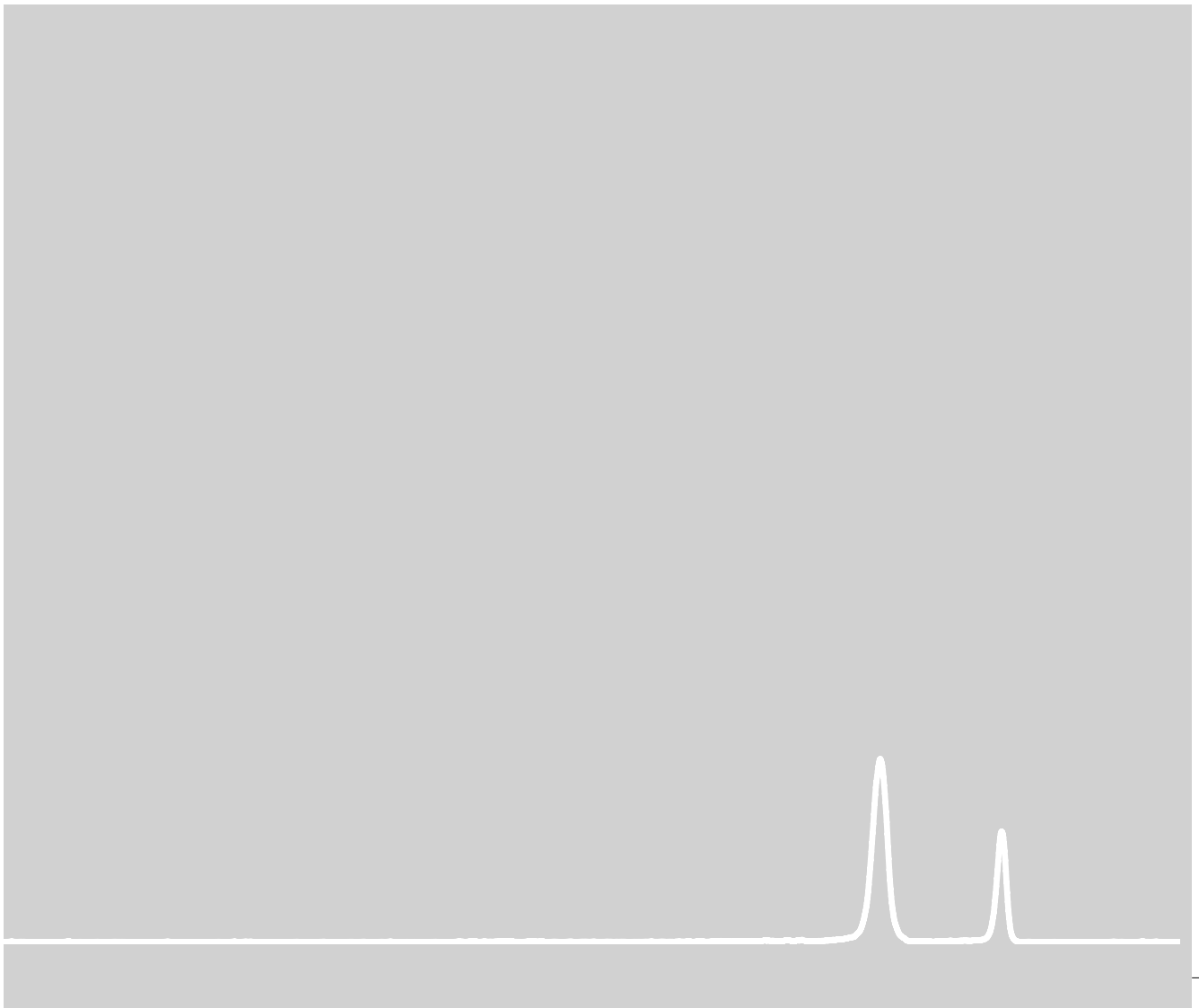
R1
R2
R3
R4
R5
R6
R7
R8
R9
R10
R11
R12
R13
R14
R15
R16
R17
R18
R19
R20
R21
R22
R23
R24
R25
R26
R27
R28
R29
R30
R31
R32
R33
R34
R35
R36
R37
R38
R39

References

1. World Health Organization (WHO). WHO health topic - Cancer - Data and statistics. Available at: <http://www.who.int/cancer/en/index.html>. Date accessed: October 15, 2012 . 2012.
2. DeVita VT, Rosenberg SA. Two hundred years of cancer research. *N Engl J Med* 2012; 366: 2207-14.
3. Krause DS, Van Etten RA. Tyrosine kinases as targets for cancer therapy. *N Engl J Med* 2005; 353: 172-87.
4. European Medicines Agency (EMA). European Public Assessment Reports. Available at: <http://www.ema.europa.eu/ema/>. Date accessed: October 15, 2012 . 2012.
5. Gao B, Yeap S, Clements A et al. Evidence for Therapeutic Drug Monitoring of Targeted Anticancer Therapies. *J Clin Oncol* 2012; Published ahead of print.
6. Lacouture ME, Wu S, Robert C et al. Evolving strategies for the management of hand-foot skin reaction associated with the multitargeted kinase inhibitors sorafenib and sunitinib. *The Oncologist* 2008; 13: 1001-11.
7. Li T, Ling YH, Goldman ID et al. Schedule-dependent cytotoxic synergism of pemetrexed and erlotinib in human non-small cell lung cancer cells. *Clin Cancer Res* 2007; 13: 3413-22.

Chapter 1

Bioanalysis of Tyrosine Kinase Inhibitors





Chapter 1.1

Method development and validation for the quantification of dasatinib, erlotinib, gefitinib, imatinib, lapatinib, nilotinib, sorafenib and sunitinib in human plasma by liquid chromatography coupled with tandem mass spectrometry

Nienke A.G. Lankheet
Michel J.X. Hillebrand
Hilde Rosing
Jan H.M. Schellens
Jos H. Beijnen
Alwin D.R. Huitema

Biomedical Chromatography. September 17, 2012. Epublished ahead of print



R1
R2
R3
R4
R5
R6
R7
R8
R9
R10
R11
R12
R13
R14
R15
R16
R17
R18
R19
R20
R21
R22
R23
R24
R25
R26
R27
R28
R29
R30
R31
R32
R33
R34
R35
R36
R37
R38
R39

Abstract

To support pharmacokinetic (PK)-guided dosing in individual patients, a fast and accurate method for simultaneous determination of anticancer tyrosine kinase inhibitors (TKIs) dasatinib, erlotinib, gefitinib, imatinib, lapatinib, nilotinib, sorafenib and sunitinib in human plasma was developed using high-performance liquid chromatography and detection with tandem mass spectrometry (HPLC-MS/MS). Stable isotopically labelled compounds of the eight different TKIs were used as internal standards. Plasma proteins were precipitated and an aliquot of supernatant was directly injected onto a reversed phase chromatography system consisting of a Gemini C18 column (50 x 2.0 mm ID, 5.0 µm particle size) and then compounds were eluted with a gradient. The outlet of the column was connected to a triple quadrupole mass spectrometer with electrospray interface. Ions were detected in the positive multiple reaction monitoring mode. This method was validated over a linear range from 20.0 to 10,000 ng/mL for erlotinib, gefitinib, imatinib, lapatinib, nilotinib and sorafenib and a linear range from 5.00 to 2,500 ng/mL for dasatinib and sunitinib. Results from the validation study demonstrated good intra- and inter-assay accuracy (<13.1%) and precision (10.0%) for all analytes. This method is now successfully applied for routine therapeutic drug monitoring (TDM) purposes in patients treated with the investigated TKIs.

Introduction

The introduction of selective tyrosine kinase inhibitors (TKIs) for treatment of various malignancies has significant impact on the management of these diseases. TKIs are directed against tyrosine kinases, which play an essential role in the transduction of growth signals in cells [1]. Currently, nine TKIs are approved for various indications in Europe, namely dasatinib, erlotinib, gefitinib, imatinib, lapatinib, nilotinib, pazopanib, sorafenib and sunitinib.

Despite proven efficacy, cases of treatment failure, drug toxicity and suboptimal response have been reported in TKI therapy [2]. The failure of TKIs most likely arises from a combination of tumour and host related factors that contribute to pharmacokinetic variability and/or induction of resistance to these agents [2-4].

Relations between treatment outcome (adverse effects and/or treatment failure) and plasma concentrations have been described for several TKIs [2,4-6]. Additionally, high pharmacokinetic variability (both interpatient and inpatient) in plasma levels was found. This suggests that plasma levels may be more predictive than absolute dose in predicting treatment response and adverse effects [4,7-9]. Therefore, therapeutic drug monitoring (TDM) is proposed to prevent failure of TKIs by reducing drug toxicity, reducing drug resistance and achieving a good level of adherence with a higher likelihood of treatment response on a patient-by-patient basis. This may be even more important in special circumstances, as for example organ dysfunction, the use of co-medication leading to potential drug-drug interactions, suspected non-compliance and occurrence of side effects. Moreover, rational quantification of TKI plasma levels can provide a better understanding of treatment failure or suboptimal response in patients receiving TKIs [6].

Several bioanalytical assays for quantification TKIs in plasma have been published thus far. Majority of these assays have been developed to determine single TKIs in human plasma [10-17]. Besides, eight simultaneous assays for multiple TKIs have been published; including six assays for the determination of at most six TKIs simultaneously [18-23]; one assay for the simultaneous determination of eight TKIs similar to the compounds in the present method [24]; and one assay for the simultaneous determination of nine TKI's, namely axitinib, dasatinib, erlotinib, gefitinib, imatinib, lapatinib, nilotinib, sunitinib and sorafenib [7]. The assay of Couchman et al. is developed using online, automated sample preparation, which is less labour intensive than conventional sample pre-treatments. However, appropriateness of this method for routine TDM purposes is limited, since majority of hospitals are not equipped with the required TurboFlow HPLC system. In the method of Bouchet et al. solid phase extraction (SPE) was used as sample pre-treatment procedure with 300 µL sample volumes [7]. We apply protein precipitation (PP) which is fast and a simple one-step procedure with minor costs and requiring only 50 µL of plasma for the simultaneous determination of dasatinib, erlotinib, gefitinib, imatinib, lapatinib, nilotinib, sorafenib and sunitinib. This method is now routinely used in our laboratory for therapeutic drug monitoring of patients treated with these TKIs.

R1
R2
R3
R4
R5
R6
R7
R8
R9
R10
R11
R12
R13
R14
R15
R16
R17
R18
R19
R20
R21
R22
R23
R24
R25
R26
R27
R28
R29
R30
R31
R32
R33
R34
R35
R36
R37
R38
R39

R1
R2
R3
R4
R5
R6
R7
R8
R9
R10
R11
R12
R13
R14
R15
R16
R17
R18
R19
R20
R21
R22
R23
R24
R25
R26
R27
R28
R29
R30
R31
R32
R33
R34
R35
R36
R37
R38
R39

Materials and methods

Chemicals and materials

Reference standards and internal standards were provided by the following manufacturers: Dasatinib monohydrate ($C_{22}H_{26}ClN_7O_2S \cdot H_2O$), erlotinib hydrochloride ($C_{22}H_{23}N_3O_4 \cdot HCl$), gefitinib ($C_{22}H_{24}N_4ClFO_3$), imatinib mesylate ($C_{29}H_{31}N_7O \cdot CH_4SO_3$), lapatinib ditosylate ($C_{29}H_{26}ClFN_4O_4S \cdot (C_7H_8O_3S)_2$), nilotinib ($C_{22}H_{26}ClN_7O_2S$), sorafenib tosylate ($C_{21}H_{16}N_4ClF_3O_3 \cdot C_7H_8O_3S$), sunitinib maleate ($C_{22}H_{27}FN_4O_2 \cdot C_4H_6O_5$) by Sequoia Research Products (Oxford, United Kingdom), dasatinib- 2H_8 ($C_{22}H_{18}ClN_7O_2SD_8$), erlotinib- $^{13}C_6$ ($C_{16}^{13}C_6H_{23}N_3O_4$), nilotinib- 2H_3 ($C_{22}H_{23}ClN_7O_2SD_3$), sunitinib- $^2H_{10}$ ($C_{22}H_{17}FN_4O_2D_{10}$) stable isotopes by Toronto Research Chemicals (North York, ON, Canada) and gefitinib- 2H_8 ($C_{22}H_{16}N_4ClFO_3D_8$), imatinib- $^{13}C_2^2H_3$ ($C_{28}^{13}CH_{28}N_7OD_3$), lapatinib- $^{13}C_2^2H_7$ ($C_{28}^{13}CH_{19}ClFN_4O_4SD_7$), sorafenib- $^{13}C_2^2H_3$ ($C_{20}^{13}CH_{13}N_4ClF_3O_3D_3$) stable isotopes by Alsa Chim (Illkirch, France). The chemical structures of the TKIs are depicted in Figure 1. HPLC-grade acetonitrile and methanol were purchased from Biosolve (Valkenswaard, The Netherlands). HPLC grade Lichrosolve water and ammonia 25% were obtained from Merck (Darmstadt, Germany). Blank human plasma with EDTA as anticoagulant was obtained from Slotervaart Hospital (Amsterdam, The Netherlands).

Chromatography and Mass spectrometry

Chromatographic separation was carried out using an HPLC system (LC-20AD Prominence binary solvent delivery system) with a column oven, DGU-20A3 online degasser and a SIL-HTc autosampler set to 4°C (all: Shimadzu, Kyoto, Japan). A reversed phase system with a Gemini C18 column (50 x 2.0 mm ID, 5.0 µm particle size; Phenomenex, Torrance, CA, USA) protected with a Securityguard Gemini precolumn (4 x 2.0 mm ID, 5.0 µm particle size; Phenomenex) was thermostatted at 40 °C. The injection volume was 10 µL. Compounds were eluted applying a linear gradient at a flow rate of 250 µL/min. The mobile phase consisted of a mixture of 10 mM ammonium hydroxide in water at pH 10.5 (A) and 1 mM ammonium hydroxide in methanol (B). Before each new injection the column was reconditioned for 3 minutes with 55% B (v/v) resulting in a total run time of 10 min. The chromatographic separation conditions are given in Table 1. The divert valve was directed to waste during the first 1.0 min and last 3.0 min to prevent the contamination of the mass spectrometer.

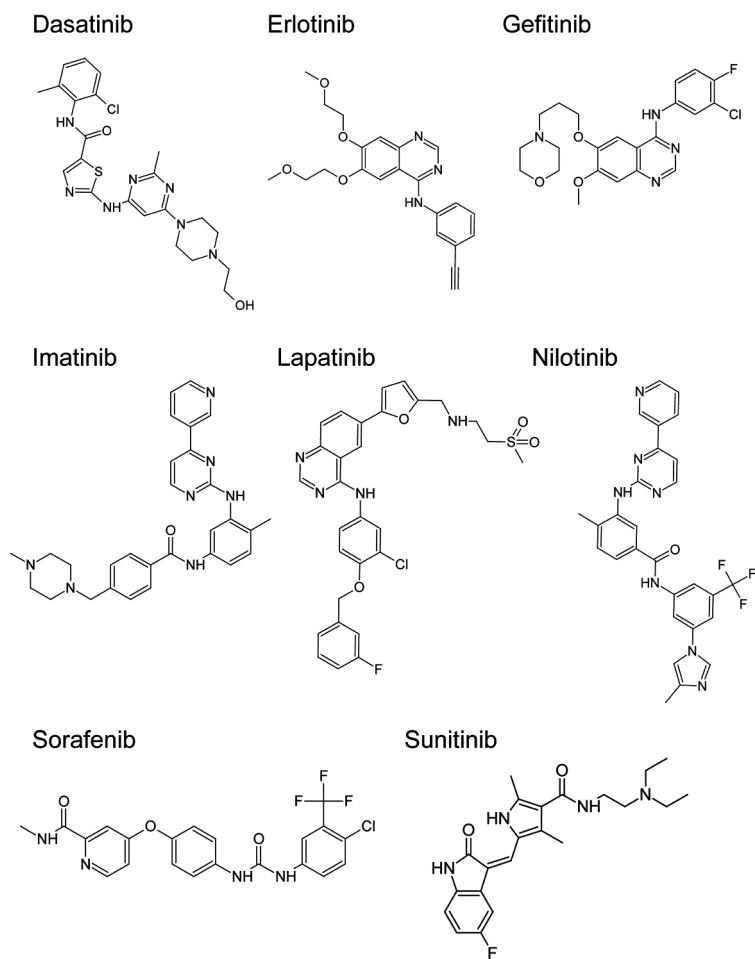


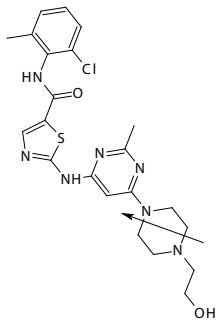
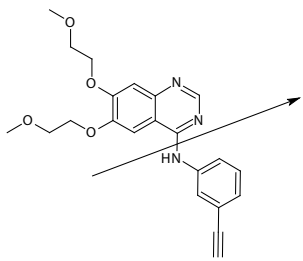
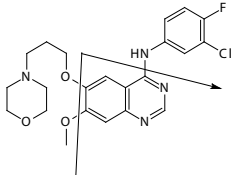
Figure 1. Chemical structures of eight tyrosine kinase inhibitors

Table 1. Gradient composition during the HPLC-run

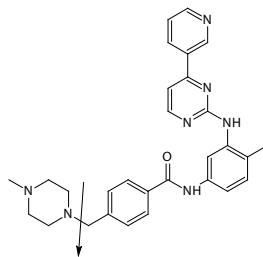
Time (min)	Flow (mL/min)	Ammonium hydroxide in water 10 mM (% v/v)	Ammonium hydroxide in MeOH 1 mM (% v/v)
0.0	0.25	45	55
0.5	0.25	45	55
3.0	0.25	20	80
6.0	0.25	20	80
6.1	0.25	5	95
8.0	0.25	5	95
8.1	0.25	45	55
10.0	0.25	45	55

Determination of the analytes and the internal standards was performed on a TSQ Quantum Ultra triple quadrupole mass spectrometer equipped with an electrospray ionisation source (ESI) operating in the positive ion mode (Thermo Fisher Scientific, Waltham, MA, USA). For quantification, multiple reaction monitoring (MRM) chromatograms were acquired with LCquan™ software version 2.5 (Thermo Fisher Scientific). Positive ions were created at atmospheric pressure and the quadrupoles were operating in unit resolution (0.7 Da). Proposed fragmentation pathways for the analytes are shown in Table 2 and the ESI-MS/MS operating parameters are listed in Table 3.

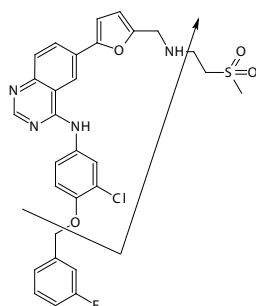
Table 2. Selected transitions and proposed fragmentation pathways of all analytes

Compound	Mass transition (<i>m/z</i>)	Proposed fragmentation pathway
Dasatinib	488 → 401	
Erlotinib	394 → 278	
Gefitinib	447 → 128	

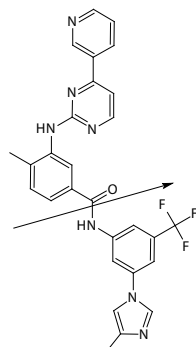
Imatinib 494 → 394



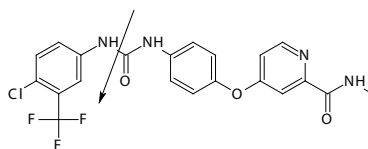
Lapatinib 581 → 365



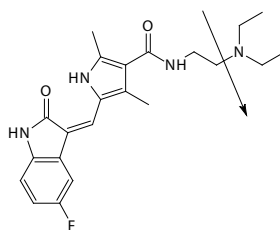
Nilotinib 530 → 289



Sorafenib 465 → 252



Sunitinib 399 → 326



R1
R2
R3
R4
R5
R6
R7
R8
R9
R10
R11
R12
R13
R14
R15
R16
R17
R18
R19
R20
R21
R22
R23
R24
R25
R26
R27
R28
R29
R30
R31
R32
R33
R34
R35
R36
R37
R38
R39

Table 3. Mass spectrometer settings

Parameter	Setting
Run duration	10 min
Ionspray voltage	3,0 kV
Sheath gas (N ₂)	35 psi
Auxiliary gas (N ₂)	15 psi
Ion sweep gas (N ₂)	2 psi
Tube lens offset	12 V
Capillary temperature	350 °C
Collision pressure (argon)	1,5 mTorr
Chrom filter peak width	10 s

Table 3b. Compound specific mass spectrometer settings

Compound	Precursor ion (m/z)	Production (m/z)	Dwell time (ms)	Collision energy (eV)	Tube lens (V)	Mean RT (min)
Dasatinib	488.2	401.1	30	29	102	3.3
Dasatinib- ² H ₈	496.2	406.2	30	29	129	
Erlotinib	394.2	278.0	30	32	102	3.5
Erlotinib- ¹³ C ₆	400.2	342.2	30	24	103	
Gefitinib	447.3	128.1	30	27	80	4.1
Gefitinib- ² H ₈	455.3	136.2	30	27	83	
Imatinib	494.3	394.2	30	26	109	3.4
Imatinib- ¹³ C, ² H ₃	498.3	394.2	30	26	118	
Lapatinib	581.1	365.1	30	37	118	4.6
Lapatinib- ¹³ C, ² H ₇	589.1	365.1	30	42	108	
Nilotinib	530.2	289.1	30	28	112	4.3
Nilotinib- ² H ₃	533.2	289.0	30	29	121	
Sorafenib	465.1	252.1	30	33	118	4.4
Sorafenib- ¹³ C, ² H ₃	469.1	256.1	30	33	114	
Sunitinib	399.2	326.1	30	21	97	3.7 and 4.5
Sunitinib- ² H ₁₀	409.3	326.1	30	21	91	(Z/E-enantiomers)

Preparation of calibration standards and quality control samples

For all TKIs sets of stock solutions were prepared from two independent weightings; one for the calibration standards and one for the quality control (QC) samples. Stock solutions containing 2.0 mg/mL of the free base were prepared in DMSO in a volumetric flask. For sunitinib the stock solution concentration was 1.0 mg/mL. Stock solutions of the stable isotope labeled internal standards were prepared in methanol at a concentration of approximately 1.0 mg/mL for dasatinib-²H₈, nilotinib-²H₃, gefitinib-²H₈, imatinib-¹³C,²H₃ and sorafenib-¹³C,²H₃. Stock solutions of stable isotope labeled erlotinib-¹³C₆, sunitinib-²H₁₀ and lapatinib-¹³C,²H₇ were prepared in methanol at a concentration of approximately 0.5 mg/mL.

A 1,000 ng/mL working solution of the internal standards was prepared by dilution of 100 µL of stock solutions of the internal standards for dasatinib, nilotinib, gefitinib, imatinib and sorafenib and 200 µL of the stock solution of the internal standards erlotinib, lapatinib and sunitinib in a total volume of 100 mL methanol.

For preparation of the calibration standards, working solutions were prepared by dilution of 500 µL of the stock solutions for imatinib, sorafenib, nilotinib, lapatinib, erlotinib and gefitinib, 250 µL of the dasatinib stock solution and 125 µL of the sunitinib stock solution in a total volume of 5.0 mL methanol. Of each working solutions, in the range from 400 to 200,000 ng/ml for erlotinib, gefitinib, imatinib, lapatinib, nilotinib and sorafenib and in the range from 100 to 50,000 ng/ml for dasatinib and sunitinib, a volume of 50 µL was added to 950 µL of control human EDTA plasma to obtain calibration standards in the range from 20.0 to 10,000 and from 5.0 to 2,500 ng/mL, respectively.

Four working solutions in the range from 400 to 160,000 ng/mL and from 100 to 40,000 ng/ml were prepared by dilution of independently prepared analyte stock solutions in methanol. To obtain QC samples containing 20.0, 40.0, 800, 8,000 ng/mL for erlotinib, gefitinib, imatinib, lapatinib, nilotinib and sorafenib and 5.00, 10.0, 200, 2,000 ng/mL for dasatinib and sunitinib in plasma, 50 µL of each working solution was added to 950 µL of control human EDTA plasma. The stock and working solutions in methanol were stored at -20 oC until use. During the validation process calibration standards and quality control samples were prepared freshly before each run.

To establish the accuracy and precision of the method in samples with concentrations above the upper limit of quantification (ULOQ), a sample containing 20,000 ng/mL of erlotinib, gefitinib, imatinib, lapatinib, nilotinib and sorafenib and 5,000 ng/mL of dasatinib and sunitinib were spiked. Samples were then diluted ten times in control human EDTA plasma before processing.

Sample preparation

Protein precipitation was used as sample pre-treatment. To 50 µL of plasma, 20 µL of internal standard working solution (1000 ng/mL) and 150 µL of acetonitril (-20 °C) were added. After vortex mixing for 15 s, samples were centrifuged at 15,000 x g for 15 min. A volume of 50 µL of the clear supernatant was diluted with 50 µL of eluent A (10 mM ammonium hydroxide in water) before injection of 10 µL onto the column.

Validation procedures

A full validation of the assay was performed according to the FDA guidelines for validation of bio-analytical assays including linearity, inaccuracy, precision, specificity, selectivity, cross-analyte/ internal standard interference, recovery, ion suppression, carry-over and stability [25,26].

R1
R2
R3
R4
R5
R6
R7
R8
R9
R10
R11
R12
R13
R14
R15
R16
R17
R18
R19
R20
R21
R22
R23
R24
R25
R26
R27
R28
R29
R30
R31
R32
R33
R34
R35
R36
R37
R38
R39

Results and discussion

Chromatography

A chromatographic system had to be developed with conditions suitable for quantification of eight analytes with a wide range in polarity. Mobile phases with different pH values were tested. A mobile phase with 10 mM ammonium hydroxide in water (pH 10.3) (eluent A) and 1 mM ammonium hydroxide in methanol (eluent B) showed the best overall MS response for all compounds. Column stability under alkaline conditions was established by successive analyses of more than 500 analytical samples in a pharmacokinetic study. Additionally, the number of plates of the column in the first analytical runs did not differ from the number of plates after more than three months of extensive column usage.

A stepwise gradient showed apparent tailing of peaks ($A_s \approx 2.5$). Improved peak shapes ($A_s \approx 1.1$) were accomplished using a linear gradient from 55% to 80% in 2.5 minutes. The analytical run time of the present method is 10 minutes. All compounds were eluted within 5 minutes after injection. However, a total run time of less than 10 min was not possible, since a 1.9 min phase with 95% eluent B had to be introduced into the method to diminish a memory effect from the column and a re-equilibration phase of 2 min with 55% B (v/v) had to be implemented after the gradient to ensure that the analytical column was stabilized at the starting conditions before the next injection, as shown in Table 1.

Typical chromatograms of samples at lower limit of quantification (LLOQ) are depicted in Figure 2. At LLOQ level a signal to noise ratio (S/N-ratio) of >10 was obtained for all analytes. In the chromatograms of sunitinib and sunitinib- $^2\text{H}_{10}$ two peaks with the same molecular mass/mass transition were present. This is due to the presence of E/Z configurations in solution, as reported before [21,27,28]. The retention times of sunitinib were 3.7 and 4.5 min for the E- and Z-isomers, respectively. The isomerization reaction of the Z-isomer into the E-isomer is induced by exposure to light and is reversible. The reverse isomerisation reaction already took place when samples were placed in the dark autosampler during an analytical run, leading to different proportions of E- and Z-isomers in samples over time. Since both isomers showed equal MS responses, the sum of the single reaction monitoring (SRM) responses of both separated isomers of the analytes and internal standard were used to process the data [21,27,28]. Consequently, protection from light during shipment, handling and processing of samples was not necessary.

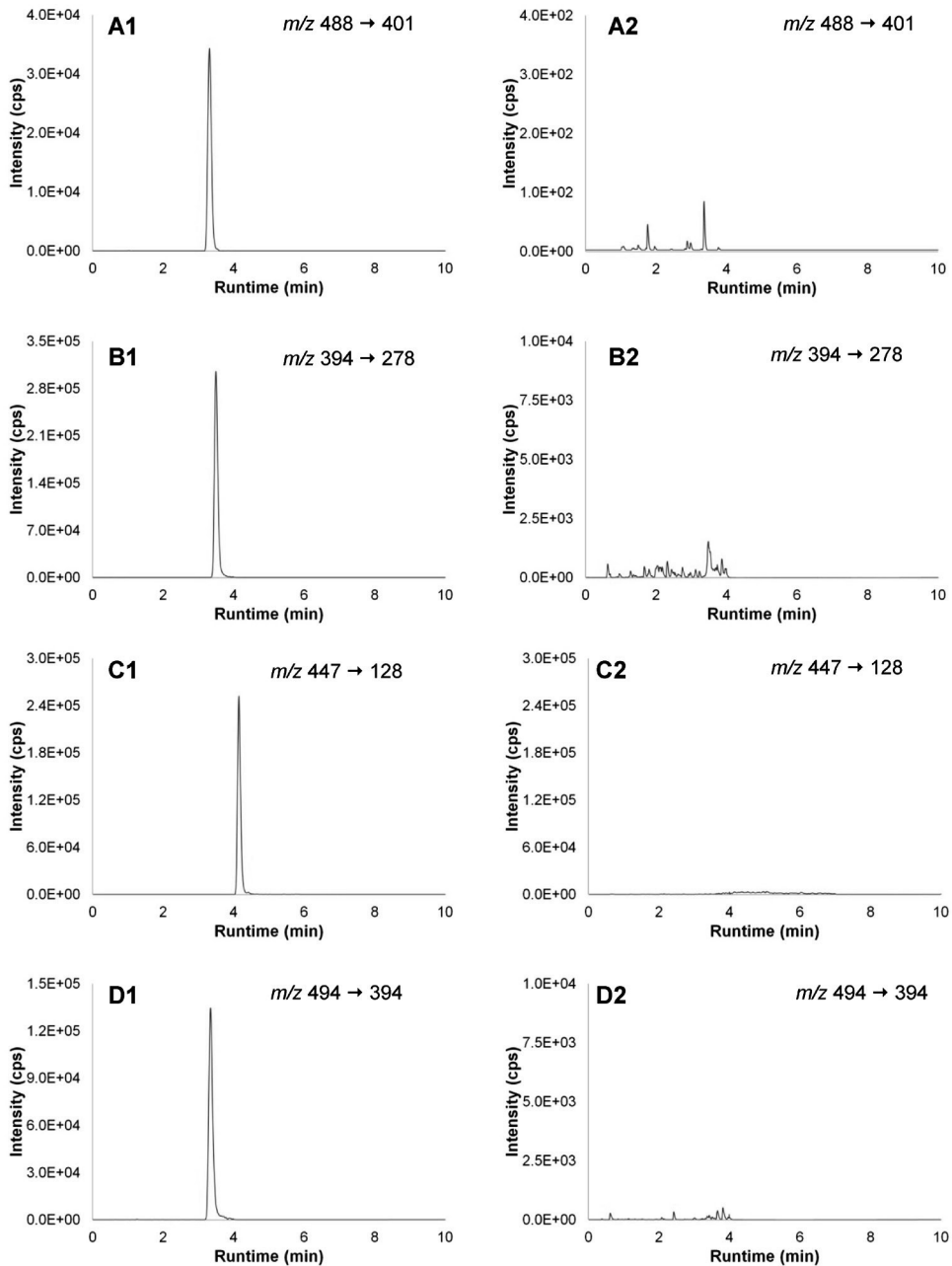


Figure 2. Chromatograms of LLOQ (-1) and blank (-2) samples of TKIs in plasma: dasatinib (A), erlotinib (B), gefitinib (C), imatinib (D), lapatinib (E), nilotinib (F), sorafenib (G) and sunitinib (H).

R1
R2
R3
R4
R5
R6
R7
R8
R9
R10
R11
R12
R13
R14
R15
R16
R17
R18
R19
R20
R21
R22
R23
R24
R25
R26
R27
R28
R29
R30
R31
R32
R33
R34
R35
R36
R37
R38
R39

R1
R2
R3
R4
R5
R6
R7
R8
R9
R10
R11
R12
R13
R14
R15
R16
R17
R18
R19
R20
R21
R22
R23
R24
R25
R26
R27
R28
R29
R30
R31
R32
R33
R34
R35
R36
R37
R38
R39

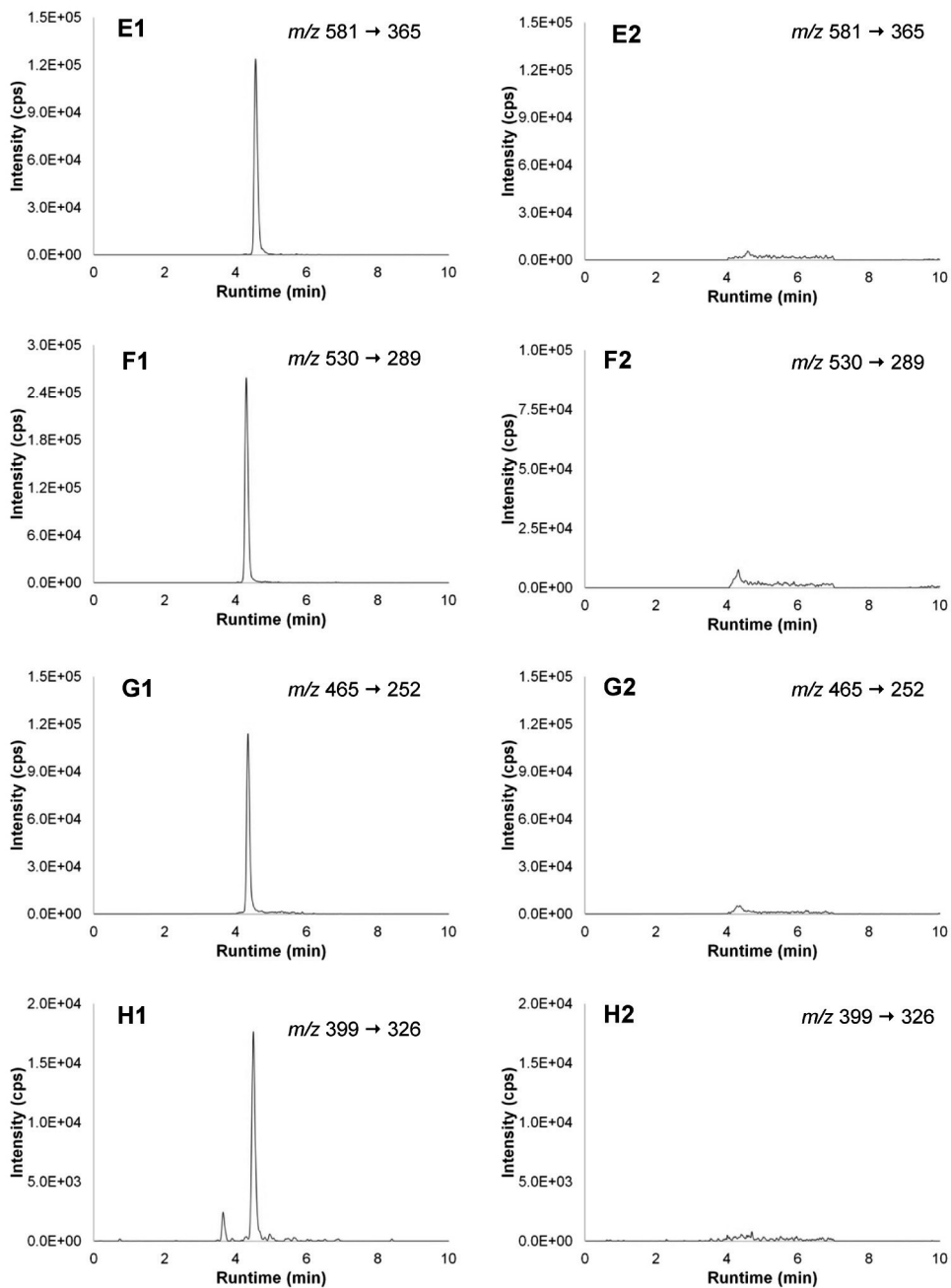


Figure 2. Continued. Chromatograms of LLOQ (-1) and blank (-2) samples of TKIs in plasma: dasatinib (A), erlotinib (B), gefitinib (C), imatinib (D), lapatinib (E), nilotinib (F), sorafenib (G) and sunitinib (H).

Mass spectrometry

During optimization of the mass spectrometric parameters, the Q1 spectra of all compounds showed the singly charged molecular ion as most intense ion. MS/MS experiments were carried out to determine the most abundant product ions for MRM. When a sample with erlotinib-¹³C₆ (m/z 400 to 284) at ULOQ level was processed, a peak was detected in the mass transition window of the most abundant product ion of sunitinib (m/z 399 to 283). Since the retention times of both compounds were overlapping (3.5 and 3.7 minutes), this cross analyte interference issue had to be solved. Increment of the unit mass resolution of the quadruples from 0.7 Da to 0.2 Da could not prevent the cross interference between sunitinib and erlotinib-¹³C₆. Therefore, more specific transitions with less abundant product ions were chosen and optimized for both erlotinib-¹³C₆ (m/z 400 to 342) and sunitinib (m/z 399 to 326). Using these alternative mass transitions, cross analyte interference between those compounds was negligible. Moreover, even using this less abundant product ion, the MS response of sunitinib was sufficient to achieve a S/N ratio > 10 at the LLOQ level. The proposed fragmentation pathways for the chosen transitions of the analytes are shown in Figure 2. Analytes and internal standards could be detected with the electrospray source operating in the positive mode.

Validation experiments

Linearity. Eight non-zero plasma calibration standards were prepared and analysed in duplicate in three separate analytical runs. The linear regression of the ratio of the areas of the analyte and the internal standard peaks versus the concentration were weighted with a weighing factor of 1/x² (where x=concentration). The linearity was evaluated by means of back-calculated concentrations of the calibration standards. The assay was linear over the validated concentration range from 20.0 to 10,000 ng/mL of erlotinib, gefitinib, imatinib, lapatinib, nilotinib and sorafenib in human plasma. For dasatinib and sunitinib the linear validated concentration range was from 5.00 to 2,500 ng/mL. Correlation coefficients (r²) were at least 0.993. The deviation from the nominal concentrations should be within ±20% for the LLOQ and within ±15% for the other concentrations with coefficient of variation (CV) values less than 20% and 15% for both the LLOQ and the other concentrations, respectively. At all concentration levels inaccuracies were within -10.0 and 7.5% with CV values less than 6.40% for all analytes.

Inaccuracy and precision. The intra- and inter-assay performance data are presented in Table 4. Inaccuracy and precision of the assay were established by analysing QC samples with analyte concentrations at the lower limit of quantification (LLOQ) and in the low, mid and high concentration ranges of the calibration curves. Five replicates of each QC sample were measured in three separate analytical runs. The coefficient of variation (CV%) was used to report the intra- and inter-assay precision. The intra- and inter-assay inaccuracies should be within ±20% for the LLOQ and ±15% for all other concentrations. The precisions CV% should be less than 20% for the LLOQ and less than 15% for all other concentrations [26]. The intra-assay inaccuracies (% bias) for

R1
R2
R3
R4
R5
R6
R7
R8
R9
R10
R11
R12
R13
R14
R15
R16
R17
R18
R19
R20
R21
R22
R23
R24
R25
R26
R27
R28
R29
R30
R31
R32
R33
R34
R35
R36
R37
R38
R39

R1
R2
R3
R4
R5
R6
R7
R8
R9
R10
R11
R12
R13
R14
R15
R16
R17
R18
R19
R20
R21
R22
R23
R24
R25
R26
R27
R28
R29
R30
R31
R32
R33
R34
R35
R36
R37
R38
R39

all analytes in human EDTA plasma were within $\pm 13.1\%$ for all concentration levels. The intra-assay precisions (CV%) for the analytes were less than 10.0% for all concentration levels and all compounds. In conclusion, the validated range for erlotinib, gefitinib, imatinib, lapatinib, nilotinib and sorafenib based on 50 mL human EDTA plasma was from 20.0-10,000 ng/mL and for dasatinib and sunitinib the validated range based on 50 mL human EDTA plasma was from 5.00-2,500 ng/mL. Samples with analyte concentrations above the ULOQ (5,000 ng/mL and 20,000 ng/mL) were diluted 10 times with control drug-free human EDTA plasma. These samples were processed in 5-fold and measured in one analytical run to assess the accuracy and precision. The intra-assay inaccuracy for diluted samples was within 7.90% and the intra-assay precision was less than 4.20% for all analytes. When concentrations above the ULOQ level are expected, samples can be diluted 10 times with control drug-free human EDTA plasma. Inaccuracies and precisions fulfilled the requirements [25].

Specificity and selectivity. To investigate whether endogenous compounds from plasma could interfere with the detection of the analyte or the internal standard, six different batches of control drug-free human EDTA plasma were prepared as double blanks (containing neither analyte nor internal standard) and LLOQ samples.

Samples were processed and analysed according to the described procedures. Areas of peaks co-eluting with the analytes should not exceed 20% of the area at the LLOQ level. In MRM chromatograms of six batches of control drug-free EDTA plasma no co-eluting peaks >20% of analyte peak areas at the LLOQ level were found and also no co-eluting peaks >5% of the internal standards were detected. The deviation of the nominal concentration for the LLOQ samples should be within $\pm 20\%$ for at least 67% of the samples. All analytes fulfilled these criteria. For lapatinib and sunitinib, in only one out of six spiked LLOQ plasma samples (17%) the deviation of the nominal concentration exceeded 20%, namely 22.9% for lapatinib and 25.0% for sunitinib. Therefore analyte/internal standard selectivity and specificity of the assay were considered acceptable.

Table 4. Assay performance data

Nominal concentration (ng/mL)	Inaccuracy (%) (n=15)	Mean intra-assay precision (%) (n=15)	Inter-assay precision (%) (n=15)
Dasatinib			
5.10	-1.30	9.1	11.3
10.2	2.5	3.1	4.7
204	4.9	2.6	3.3
2037	10.7	3.7	5.0
Erlotinib			
18.9	2.7	1.5	3.9
37.7	1.1	2.1	3.7
754	1.1	2.2	2.8
7544	-0.9	3.0	3.8
Gefitinib			
20.5	1.5	5.4	6.2
41.0	-0.1	3.0	3.8
820	1.7	2.9	3.5
8204	-5.0	2.9	3.5
Imatinib			
19.8	3.9	5.2	5.5
39.5	1.4	3.0	3.6
790	1.3	2.6	2.8
7904	-3.5	3.8	4.4
Lapatinib			
20.1	3.4	6.0	6.5
40.1	-0.8	3.3	3.4
802	3.8	2.1	3.5
8020	-4.9	3.2	3.9
Nilotinib			
19.9	0.0	4.3	4.8
39.9	0.6	2.5	4.1
794	2.7	2.5	2.9
7944	-4.3	2.6	3.1
Sorafenib			
21.6	4.1	6.3	8.0
43.2	0.7	2.7	2.7
864	0.5	2.9	3.1
8636	-1.7	4.1	4.3
Sunitinib			
5.20	-1.3	5.4	11.7
10.3	0.8	2.6	6.0
207	-0.2	2.8	3.4
2066	-5.9	2.6	3.2

R1
R2
R3
R4
R5
R6
R7
R8
R9
R10
R11
R12
R13
R14
R15
R16
R17
R18
R19
R20
R21
R22
R23
R24
R25
R26
R27
R28
R29
R30
R31
R32
R33
R34
R35
R36
R37
R38
R39

R1
R2
R3
R4
R5
R6
R7
R8
R9
R10
R11
R12
R13
R14
R15
R16
R17
R18
R19
R20
R21
R22
R23
R24
R25
R26
R27
R28
R29
R30
R31
R32
R33
R34
R35
R36
R37
R38
R39

Cross analyte interference. To investigate possible cross interference between analytes and internal standards, a cross interference check was performed. Drug-free human EDTA plasma was spiked with all analytes separately at ULOQ level and these samples were processed without internal standard. Also drug-free plasma samples with separate internal standards were processed. The response of any interfering peak with the same retention time as the analytes should be less than 20% of the response of a LLOQ sample. The response of any interfering peak with the same retention time as the internal standards should be less than 5% of the internal standard response. One of the cross-analyte/internal standard interference samples did not fulfil these requirements. Namely, in a sample processed with imatinib- $^{13}\text{C}_2,^2\text{H}_3$ the response of the interfering peak with the same retention time as imatinib was approximately 38% of the response of a LLOQ sample. This cross interference originated from a 4.0% (CV 1.9%) impurity of the imatinib- $^{13}\text{C}_2,^2\text{H}_3$ reference standard. Duplicate blank samples (containing only internal standard) processed and analysed in five different analytical runs showed a constant interference of 3.7% (CV 3.3%) of the imatinib- $^{13}\text{C}_2,^2\text{H}_3$ internal standard in the window of imatinib. Therefore, the contribution of the interfering peaks is equal for all samples that are processed within an analytical batch. This is reflected in the y-axis intercept of the calibration curve for imatinib (mean: 0.28) compared to the other compounds (mean < 0.003). The results for cross interference were found to be acceptable and no relating problems were expected during quantification of the imatinib. However, the interference can be reduced more elegantly by decreasing the concentration of imatinib- $^{13}\text{C}_2,^2\text{H}_3$ in the internal standard working solution to approximately 200 ng/mL.

Matrix effect. The relative matrix factor is defined as a ratio of the analyte peak response ratio in the presence of matrix ions to the analyte peak response ratio in the absence of matrix ions. The relative matrix factor was examined in triplicate at two concentrations (low and high concentrations) by comparing the area ratio of processed blanks spiked with analyte with those unprocessed samples in precipitation reagent. The mean relative matrix factors detected for all analytes are shown in Table 5. The relative matrix factor was 1.10 with CV values of less than or equal to 5.5%.

Extraction recovery. The protein precipitation (PP) extraction recovery of the analytes was determined in triplicate at two concentrations by comparing the analytical response of processed samples with those of processed blanks spiked with analyte (representing 100% recovery). The mean PP recoveries were between 50 and 75% for all analytes and are shown in Table 5. Although, this extraction recovery was relatively low, the sensitivity of PP with ACN as sample pre-treatment was adequate, since the desired LLOQ for all analytes were achieved with a S/N >10. Moreover, the robustness of this sample pre-treatment method was sufficient with CV values less than 15.2% over the entire concentration range. Protein precipitation seemed to be a fast and simple one-step sample pre-treatment procedure for the analysis of TKIs in plasma.

Carry-over. Carry-over was tested by injecting two processed blank matrix samples sequentially after injecting an ULOQ sample. The response in the first blank matrix at the retention times of analytes and internal standards should be less than 20% of the response of a LLOQ sample. In our method, observed carry over seemed to arise from contamination of the autosampler needle and the divert valve due to adsorption of the analyte after multiple injections. Contamination in the divert valve was reduced by performing multiple valve switches (>15) during the equilibration of the column before each analytical run. Contamination of the autosampler needle was diminished by using an acidic flush solvent (1% formic acid in ACN) instead of 100% methanol and increasing the rinse dip time from 5s to 30s. Using this method the carry over test fulfilled the criteria for dasatinib (0.4%), erlotinib (2.1%), gefitinib (7.8%), imatinib (7.9%), nilotinib (17.9%) and sorafenib (1.9%). For lapatinib and sunitinib still an apparent carry over of respectively 42.1% and 20.6% was observed in a processed blank sample injected directly after an ULOQ sample. However, in the second blank sample in a row injected after an ULOQ sample the carry over was only 13.1% and 9.9% for lapatinib and sunitinib, respectively. Therefore, sunitinib and lapatinib samples should be distributed equally across the entire batch of samples, preventing carry-over effects of these two analytes.

Stability. The stability of all TKIs in spiked human EDTA plasma after three freeze/thaw cycles from nominally -20 °C to ambient temperatures was investigated in triplicate at two concentrations. Additionally, the stability of all analytes in human EDTA plasma kept at -20°C for 1.5 months and at ambient temperature for 48 hours was investigated at three concentrations. The analytes were considered to be stable in the matrix or final extract if 85–115% of the initial concentrations was recovered. All analytes were stable in human plasma for at least three freeze (-20 °C) / thaw cycles. Short term stability of the analytes in plasma at ambient temperatures is established up to at least 48 h and long term stability in plasma at -20°C up to at least 1 month. Experiments to establish long term stability in plasma at -20°C for a longer period of time are still ongoing.

The processed sample stability of the TKIs at 2-8 °C was established at three concentrations (low, mid and high level) after 8 days. Re-injection reproducibility was established and therefore an analytical run can be re-injected after at least 48 h of storage in the autosampler at 4 °C.

For dasatinib, lapatinib, nilotinib, sorafenib and sunitinib the stability of stock solutions at -20°C was determined in triplicate. Analytes were considered to be stable in stock solutions if 90-110% of the initial concentration was found. Long term stock solution stability at -20°C was established for stock solutions of sunitinib (22 months), sorafenib (30 months), dasatinib (32 months), lapatinib (32 months) and nilotinib (32 months). For erlotinib, imatinib and gefitinib long term stability of stock solutions at -20°C is still ongoing.

R1
R2
R3
R4
R5
R6
R7
R8
R9
R10
R11
R12
R13
R14
R15
R16
R17
R18
R19
R20
R21
R22
R23
R24
R25
R26
R27
R28
R29
R30
R31
R32
R33
R34
R35
R36
R37
R38
R39

Table 5. Matrix effect and extraction data

Nominal concentration (ng/mL)	Matrix factor (n=3)	CV%	Protein precipitation recovery (%) (n=3)	CV%
Dasatinib				
10.2	1.09	1.2	54.7	13.6
2037	1.08	5.5	54.4	4.3
Erlotinib				
37.7	1.06	0.4	66.1	4.6
7544	1.09	1.1	67.4	10.9
Gefitinib				
41.0	1.09	2.4	68.3	6.1
8204	1.08	1.2	72.3	6.3
Imatinib				
39.5	1.07	3.4	67.3	9.2
7904	1.10	2.7	74.2	5.8
Lapatinib				
40.1	1.13	2.0	62.8	9.3
8020	1.11	1.4	71.5	9.1
Nilotinib				
39.9	1.08	2.7	62.9	2.9
7944	1.09	0.4	75.0	8.8
Sorafenib				
43.2	1.11	1.7	60.9	3.4
8636	1.12	2.7	67.1	15.2
Sunitinib				
10.3	1.09	4.9	68.4	9.5
2066	1.13	1.1	71.5	4.0

Application for routine therapeutic drug monitoring

As can be deduced from the validation results, the developed assay fulfilled the requirements of the FDA guidelines for validation of bio-analytical assays [25]. Additionally, this method is definitely suitable for clinical application with regard to: e.g. the variety of compounds it covers, sensitivity, range, selectivity and reproducibility.

Originally, we aimed to develop an assay including all currently approved TKIs. However, since pazopanib treatment gives substantially higher plasma levels (trough levels > 20,000 ng/mL) compared to the other compounds [29], the MS source and detector became saturated. Linearity of pazopanib calibration curves was only observed in a range with a maximum of 10,000 ng/mL. Even the use of suboptimal conditions in the MS, as for example less abundant product ions, low collision energy, high resolution and low ionspray voltage, could not prevent saturated and non-linear MS responses for pazopanib. For this reason, our method was restricted to eight currently

approved and most widely used TKIs, namely dasatinib, erlotinib, gefitinib, imatinib, lapatinib, nilotinib, sorafenib and sunitinib.

Pharmacokinetic and pharmacodynamic correlations of imatinib [6], erlotinib [30], lapatinib [31] and sunitinib [32] in patients have already been studied and for these compounds target trough plasma levels have been mentioned in literature. Target trough levels for imatinib, erlotinib, lapatinib and sunitinib are around 1,000 ng/mL, 1,200 ng/mL, 300 ng/mL and 50 ng/mL, respectively. Therefore, a range from 20.0 to 10,000 ng/mL was chosen for the quantification of imatinib, erlotinib and lapatinib, and a lower range from 5.00 to 2,500 ng/mL was chosen for sunitinib to cover the clinically relevant concentration ranges. Namely, results below the range of 20.0 and 5.00 ng/mL, respectively, were not supposed to provide any relevant information for clinical decision-making. Based on phase I and II trials, the lower concentration range was chosen for dasatinib [12]. Additionally, also based on clinical studies, the higher concentration range was chosen for gefitinib [33], nilotinib [34] and sorafenib [35]. To obtain the required sensitivity level of the described method, only a small volume of plasma (50 μ L) was necessary for the sample pre-treatment. Therefore, this method is applicable in clinical pharmacokinetic studies, but it may also be useful for preclinical experiments and studies in which small sample volumes may be expected.

Combination therapy of TKIs has not been implemented in common practice yet. However, combination therapy of different TKIs has already been mentioned as strategy to overcome development of resistance against these drugs by inducing a more rapid and effective response [36]. In case of combination regimens it is even more useful to have a method in which various TKIs can be quantified in one single analytical run. Despite overlapping retention times of the peaks of the different TKIs, our method showed compound selectivity and specificity. Therefore, simultaneous quantification of the compounds in one method is applicable.

As mentioned before, column stability and assay reproducibility under alkaline conditions was established during extensive use of the developed chromatographic method. Additionally, incurred sample reproducibility of a set of study samples has been established using two different batches of stock solutions to prepare calibration and validation samples. Re-analysis of 30% of a set study samples with the new batch calibration and validation samples was performed half a year after the original measurement. For all samples deviations from the mean results were at most 8.48% indicating a good method reproducibility.

In our hospital the present bio-analytical method has been used regularly to support PK-guided dosing in individual patients as part of the standard follow-up and to substantiate clinical observations for example in case of extreme toxicity, treatment failure, altered drug absorption and drug-drug interactions. In these cases, a request from the physician is being sent to our laboratory together with the patient plasma sample. These requests are in particular concerning determination of imatinib, sunitinib and erlotinib plasma levels, since effective target plasma levels for these drugs already have been determined [6,30,32]. Implementation of the fast and simultaneous method for rational quantification of TKIs in our hospital is supporting therapy optimization on a patient-by-

R1
R2
R3
R4
R5
R6
R7
R8
R9
R10
R11
R12
R13
R14
R15
R16
R17
R18
R19
R20
R21
R22
R23
R24
R25
R26
R27
R28
R29
R30
R31
R32
R33
R34
R35
R36
R37
R38
R39

R1 patient basis and is providing better understanding of treatment failure and suboptimal response
R2 in patients receiving TKIs.

R3 Besides, the method is being used successfully to support various clinical pharmacokinetics
R4 studies to provide data to increase the knowledge on pharmacokinetic-pharmacodynamic (PK-PD)
R5 relationships of various TKIs which had been inconclusive or unavailable thus far. Study protocols
R6 concerning these studies all have been approved by the Institutional Ethics Committee of our
R7 hospital.

R8 **Conclusion**

R9 We have developed and validated a fast LC-MS/MS method for the simultaneous, quantitative
R10 analysis of eight TKIs (i.e. dasatinib, erlotinib, gefitinib, imatinib, lapatinib, nilotinib, sorafenib and
R11 sunitinib) in human K-EDTA plasma. Human plasma spiked with these TKIs was pre-treated by
R12 protein precipitation with acetonitrile and addition of stable isotope labeled internal standards
R13 of all different TKIs. Chromatography was performed under alkaline conditions. A linear dynamic
R14 range from 20.0 to 10,000 ng/ml has been validated for erlotinib, gefitinib, imatinib, lapatinib,
R15 nilotinib and sorafenib and from 5.00 to 2,500 ng/mL for dasatinib and sunitinib with high accuracy
R16 and precision. The method is robust, easy to perform and has shown to be applicable in routine
R17 therapeutic drug monitoring of TKIs. Moreover, the simultaneous determination of eight different
R18 TKIs in a single analytical run serves a high throughput of a heterogeneous batch of therapeutic
R19 drug monitoring (TDM) samples of patients on TKI therapy.
R20
R21
R22
R23
R24
R25
R26
R27
R28
R29
R30
R31
R32
R33
R34
R35
R36
R37
R38
R39

References

1. Krause DS, Van Etten RA. Tyrosine kinases as targets for cancer therapy. *N Engl J Med* 2005; 353: 172-87.
2. Apperley JF. Part I: mechanisms of resistance to imatinib in chronic myeloid leukaemia. *Lancet Oncol* 2007; 8: 1018-29.
3. Ross DM, Hughes TP. Current and emerging tests for the laboratory monitoring of chronic myeloid leukaemia and related disorders. *Pathology* 2008; 40: 231-46.
4. Widmer N, Decosterd LA, Leyvraz S et al. Relationship of imatinib-free plasma levels and target genotype with efficacy and tolerability. *Br J Cancer* 2008; 98: 1633-40.
5. Larson RA, Druker BJ, Guilhot F et al. Imatinib pharmacokinetics and its correlation with response and safety in chronic-phase chronic myeloid leukemia: a subanalysis of the IRIS study. *Blood* 2008; 111: 4022-8.
6. Picard S, Titier K, Etienne G et al. Trough imatinib plasma levels are associated with both cytogenetic and molecular responses to standard-dose imatinib in chronic myeloid leukemia. *Blood* 2007; 109: 3496-9.
7. Bouchet S, Chauzit E, Ducint D et al. Simultaneous determination of nine tyrosine kinase inhibitors by 96-well solid-phase extraction and ultra performance LC/MS-MS. *Clin Chim Acta* 2011; 412: 1060-7.
8. Delbaldo C, Chatelut E, Re M et al. Pharmacokinetic-pharmacodynamic relationships of imatinib and its main metabolite in patients with advanced gastrointestinal stromal tumors. *Clin Cancer Res* 2006; 12: 6073-8.
9. Teng JF, Mabasa VH, Ensom MH. The role of therapeutic drug monitoring of imatinib in patients with chronic myeloid leukemia and metastatic or unresectable gastrointestinal stromal tumors. *Ther Drug Monit* 2012; 34: 85-97.
10. Bai F, Freeman BB, III, Fraga CH et al. Determination of lapatinib (GW572016) in human plasma by liquid chromatography electrospray tandem mass spectrometry (LC-ESI-MS/MS). *J Chromatogr B Analyt Technol Biomed Life Sci* 2006; 831: 169-75.
11. Bakhtiar R, Lohne J, Ramos L et al. High-throughput quantification of the anti-leukemia drug STI571 (Gleevec) and its main metabolite (CGP 74588) in human plasma using liquid chromatography-tandem mass spectrometry. *J Chromatogr B Analyt Technol Biomed Life Sci* 2002; 768: 325-40.
12. Dai G, Pfister M, Blackwood-Chirchir A et al. Importance of characterizing determinants of variability in exposure: application to dasatinib in subjects with chronic myeloid leukemia. *J Clin Pharmacol* 2008; 48: 1254-69.
13. de Bruijn P, Sleijfer S, Lam MH et al. Bioanalytical method for the quantification of sunitinib and its n-desethyl metabolite SU12662 in human plasma by ultra performance liquid chromatography/tandem triple-quadrupole mass spectrometry. *J Pharm Biomed Anal* 2010; 51: 934-41.
14. Masters AR, Sweeney CJ, Jones DR. The quantification of erlotinib (OSI-774) and OSI-420 in human plasma by liquid chromatography-tandem mass spectrometry. *J Chromatogr B Analyt Technol Biomed Life Sci* 2007; 848: 379-83.
15. Parise RA, Egorin MJ, Christner SM et al. A high-performance liquid chromatography-mass spectrometry assay for quantitation of the tyrosine kinase inhibitor nilotinib in human plasma and serum. *J Chromatogr B Analyt Technol Biomed Life Sci* 2009; 877: 1894-900.
16. Zhao M, Hartke C, Jimeno A et al. Specific method for determination of gefitinib in human plasma, mouse plasma and tissues using high performance liquid chromatography coupled to tandem mass spectrometry. *J Chromatogr B Analyt Technol Biomed Life Sci* 2005; 819: 73-80.
17. Zhao M, Rudek MA, He P et al. A rapid and sensitive method for determination of sorafenib in human plasma using a liquid chromatography/tandem mass spectrometry assay. *J Chromatogr B Analyt Technol Biomed Life Sci* 2007; 846: 1-7.

R1
R2
R3
R4
R5
R6
R7
R8
R9
R10
R11
R12
R13
R14
R15
R16
R17
R18
R19
R20
R21
R22
R23
R24
R25
R26
R27
R28
R29
R30
R31
R32
R33
R34
R35
R36
R37
R38
R39

R1
R2
R3
R4
R5
R6
R7
R8
R9
R10
R11
R12
R13
R14
R15
R16
R17
R18
R19
R20
R21
R22
R23
R24
R25
R26
R27
R28
R29
R30
R31
R32
R33
R34
R35
R36
R37
R38
R39

18. Chahbouni A, den Burger JC, Vos RM et al. Simultaneous quantification of erlotinib, gefitinib, and imatinib in human plasma by liquid chromatography tandem mass spectrometry. *Ther Drug Monit* 2009; 31: 683-7.
19. De Francia S, D'Avolio A, De Martino F et al. New HPLC-MS method for the simultaneous quantification of the antileukemia drugs imatinib, dasatinib, and nilotinib in human plasma. *J Chromatogr B Analyt Technol Biomed Life Sci* 2009; 877: 1721-6.
20. Gotze L, Hegele A, Metzelder SK et al. Development and clinical application of a LC-MS/MS method for simultaneous determination of various tyrosine kinase inhibitors in human plasma. *Clin Chim Acta* 2012; 413: 143-9.
21. Haouala A, Zanolari B, Rochat B et al. Therapeutic Drug Monitoring of the new targeted anticancer agents imatinib, nilotinib, dasatinib, sunitinib, sorafenib and lapatinib by LC tandem mass spectrometry. *J Chromatogr B Analyt Technol Biomed Life Sci* 2009; 877: 1982-96.
22. Honeywell R, Yarzadah K, Giovannetti E et al. Simple and selective method for the determination of various tyrosine kinase inhibitors used in the clinical setting by liquid chromatography tandem mass spectrometry. *J Chromatogr B Analyt Technol Biomed Life Sci* 2010; 878: 1059-68.
23. Hsieh Y, Galviz G, Zhou Q et al. Hydrophilic interaction liquid chromatography/tandem mass spectrometry for the simultaneous determination of dasatinib, imatinib and nilotinib in mouse plasma. *Rapid Commun Mass Spectrom* 2009; 23: 1364-70.
24. Couchman L, Birch M, Ireland R et al. An automated method for the measurement of a range of tyrosine kinase inhibitors in human plasma or serum using turbulent flow liquid chromatography-tandem mass spectrometry. *Anal Bioanal Chem* 2012; 403: 1685-95.
25. U.S. Food and Drug Administration: Centre for Drug Evaluation and Research. Guidance for Industry: Bioanalytical Method Validation. Available at: <http://www.fda.gov/downloads/Drugs/GuidanceComplianceRegulatoryInformation/Guidances/UCM070107.pdf> Date accessed March 12, 2012. 2001.
26. Viswanathan CT, Bansal S, Booth B et al. Quantitative bioanalytical methods validation and implementation: best practices for chromatographic and ligand binding assays. *Pharm Res* 2007; 24: 1962-73.
27. Lankheet NA, Blank CU, Mallo H et al. Determination of sunitinib and its active metabolite N-desethylsunitinib in sweat of a patient. *J Anal Toxicol* 2011; 35: 558-65.
28. Sparidans RW, Iusuf D, Schinkel AH et al. Liquid chromatography-tandem mass spectrometric assay for the light sensitive tyrosine kinase inhibitor axitinib in human plasma. *J Chromatogr B Analyt Technol Biomed Life Sci* 2009; 877: 4090-6.
29. Yau T, Chen PJ, Chan P et al. Phase I dose-finding study of pazopanib in hepatocellular carcinoma: evaluation of early efficacy, pharmacokinetics, and pharmacodynamics. *Clin Cancer Res* 2011; 17: 6914-23.
30. Hidalgo M, Siu LL, Nemunaitis J et al. Phase I and pharmacologic study of OSI-774, an epidermal growth factor receptor tyrosine kinase inhibitor, in patients with advanced solid malignancies. *J Clin Oncol* 2001; 19: 3267-79.
31. Burris HA, III, Hurwitz HI, Dees EC et al. Phase I safety, pharmacokinetics, and clinical activity study of lapatinib (GW572016), a reversible dual inhibitor of epidermal growth factor receptor tyrosine kinases, in heavily pretreated patients with metastatic carcinomas. *J Clin Oncol* 2005; 23: 5305-13.
32. Houk BE, Bello CL, Poland B et al. Relationship between exposure to sunitinib and efficacy and tolerability endpoints in patients with cancer: results of a pharmacokinetic/pharmacodynamic meta-analysis. *Cancer Chemother Pharmacol* 2010; 66: 357-71.
33. Gross ME, Leichman L, Lowe ES et al. Safety and pharmacokinetics of high-dose gefitinib in patients with solid tumors: results of a phase I study. *Cancer Chemother Pharmacol* 2012; 69: 273-80.
34. Larson RA, Yin OQ, Hochhaus A et al. Population pharmacokinetic and exposure-response analysis of nilotinib in patients with newly diagnosed Ph+ chronic myeloid leukemia in chronic phase. *Eur J Clin Pharmacol* 2012; 68: 723-33.

35. Strumberg D, Clark JW, Awada A et al. Safety, pharmacokinetics, and preliminary antitumor activity of sorafenib: a review of four phase I trials in patients with advanced refractory solid tumors. *Oncologist* 2007; 12: 426-37.
36. Druker BJ. Circumventing resistance to kinase-inhibitor therapy. *N Engl J Med* 2006; 354: 2594-6.

R1
R2
R3
R4
R5
R6
R7
R8
R9
R10
R11
R12
R13
R14
R15
R16
R17
R18
R19
R20
R21
R22
R23
R24
R25
R26
R27
R28
R29
R30
R31
R32
R33
R34
R35
R36
R37
R38
R39



Chapter 1.2

Quantification of sunitinib and N-desethyl sunitinib in human EDTA plasma by liquid chromatography coupled with electrospray ionization tandem mass spectrometry: validation and application in routine therapeutic drug monitoring

Nienke A.G. Lankheet
Neeltje Steeghs
Hilde Rosing
Jan H.M. Schellens
Jos H. Beijnen
Alwin D.R. Huitema

Therapeutic Drug Monitoring, in press



R1
R2
R3
R4
R5
R6
R7
R8
R9
R10
R11
R12
R13
R14
R15
R16
R17
R18
R19
R20
R21
R22
R23
R24
R25
R26
R27
R28
R29
R30
R31
R32
R33
R34
R35
R36
R37
R38
R39

Abstract

Background. Given the low therapeutic index, the large inter-individual variability in systemic exposure and the positive exposure-efficacy relationship of sunitinib, there is a rationale for therapeutic drug monitoring (TDM) of sunitinib. To support TDM, a method for determination of sunitinib and its active metabolite (N-desethyl sunitinib) has been developed and validated.

Methods. For determination of sunitinib and N-desethyl sunitinib in human EDTA plasma samples high-performance liquid chromatography and detection with tandem mass-spectrometry (HPLC-MS/MS) was used. Validation experiments according to FDA guidelines were performed. In addition, the results of 25 analytical runs with 58 patient samples using 8 calibrators and 3 levels of quality control samples per analysis were compared with the results of analyses using only 3 calibrators and 1 quality control sample in order to accelerate sample turnaround time. The method comparison experiment was performed according to international guidelines.

Results. The HPLC-MS/MS method was validated over a linear range from 2.5 to 500 ng/mL using 50 μ L plasma volumes, with good intra- and inter-assay accuracy and precision. In addition, the mean of the absolute differences between the compared methods was only -0.66 ng/mL (mean of relative differences -0.85%), which is not a clinically relevant difference.

Conclusion. This method has been applied successfully for routine TDM purposes for patients treated with sunitinib. Moreover, reliable results with a rapid turnaround time were obtained when performing a short analytical run containing only three calibrators and one quality control sample.

Introduction

Sunitinib (Sutent®) is an orally available inhibitor of VEGFR, PDGFR, c-KIT, and FLT-3 kinase activity. Sunitinib has proven efficacy as a single agent in several solid tumor types and is approved for use in advanced renal cell cancer (RCC), and imatinib-resistant or -intolerant gastrointestinal stromal tumors (GISTs) [1,2].

Recent findings demonstrated a positive dose-efficacy relationship for sunitinib treatment, indicating that it should be the aim to dose patients as high as possible [3]. Target total plasma concentrations of sunitinib plus active metabolite (N-desethyl sunitinib) are in the range 50 to 100 ng/mL, as deduced from pharmacokinetic/pharmacodynamic preclinical data [4-8]. Total trough concentrations below 50 ng/mL have been associated with decreased therapeutic efficacy whilst concentrations above 100 ng/mL have been associated with an increased risk for toxicity [6]. Given the low therapeutic index, the large inter-individual variability in systemic exposure, and the positive exposure-efficacy relationship of sunitinib, there is a rationale for therapeutic drug monitoring of this drug [3,6,9].

High-performance liquid chromatography coupled to tandem mass-spectrometry (HPLC-MS/MS) is becoming the gold standard analytical method for therapeutic drug monitoring, since it results in better sensitivity and selectivity than e.g. conventional antibody-based immunoassays [10]. Several validated bioanalytical assays for the determination of sunitinib have been reported [11-20]. Of these, five assays have also incorporated the determination of the active metabolite (N-desethyl sunitinib) [11,13,14,17,19]. Barratté et al. and Lankheet et al. described the quantification of both compounds in the alternative biomatrices tissue and sweat, respectively, instead of plasma [11,17]. Etienne-Grimaldi et al. used ultraviolet (UV) detection [12,14]. Only two bioanalytical assays for the determination of sunitinib and metabolite in plasma using HPLC-MS/MS have been published to date [13,19]. Both assays require a minimum plasma sample volume of 100 µL during sample pretreatment. Besides, the assay of De Bruijn et al. uses labor-intensive liquid-liquid extraction as the sample pretreatment method [13]. In addition, both assays have insufficient calibration ranges [13,19]. Trough plasma concentrations during sunitinib therapy are typically in a range from approximately 10 to 200 ng/mL for sunitinib and from 5 to 100 ng/mL for N-desethyl sunitinib [6]. However, the ranges that were validated in the publications of Rodamer et al. and De Bruijn et al. were from 0.06 to 100 ng/mL and 0.200 to 50.0 ng/mL, respectively. Thus, they do not cover the expected range of clinical trough concentrations [13,19]. Therefore, we report the development and validation of a method for determination of sunitinib and its active metabolite (N-desethyl sunitinib) using 50 µL of human plasma and HPLC-MS/MS with a linear range from 2.5 to 500 ng/mL for both compounds. In addition, we report the application and robustness of this method using only three calibrators and one QC sample per analytical run, leading to a more rapid turnaround time for therapeutic drug monitoring of patients treated with sunitinib.

R1
R2
R3
R4
R5
R6
R7
R8
R9
R10
R11
R12
R13
R14
R15
R16
R17
R18
R19
R20
R21
R22
R23
R24
R25
R26
R27
R28
R29
R30
R31
R32
R33
R34
R35
R36
R37
R38
R39

Materials and methods

Chemicals and materials

Reference standards and internal standards were provided by the following manufacturers: Sunitinib maleate ($C_{22}H_{27}FN_4O_2 \cdot C_4H_6O_5$) by Sequoia Research Products (Oxford, United Kingdom), N-desethyl sunitinib ($C_{20}H_{23}FN_4O_2$) by Toronto Research Chemicals (North York, ON, Canada), sunitinib- $^2H_{10}$ ($C_{22}H_{23}FN_4O_2D_{10}$) and N-desethyl sunitinib- 2H_5 ($C_{20}H_{23}FN_4O_2D_5$) stable isotope by Alsa Chim (Illkirch, France). The chemical structures of sunitinib, N-desethyl sunitinib, sunitinib- $^2H_{10}$ and N-desethyl SNN- 2H_5 are depicted in Figure 1. HPLC-grade acetonitrile and methanol were purchased from Biosolve (Valkenswaard, The Netherlands). Distilled water was obtained from B.Braun (Melsungen, Germany). Formic acid 98-100% was purchased from Merck (Darmstadt, Germany). Drug-free human plasma with EDTA as anticoagulant was obtained from the Slotervaart Hospital (Amsterdam, The Netherlands).

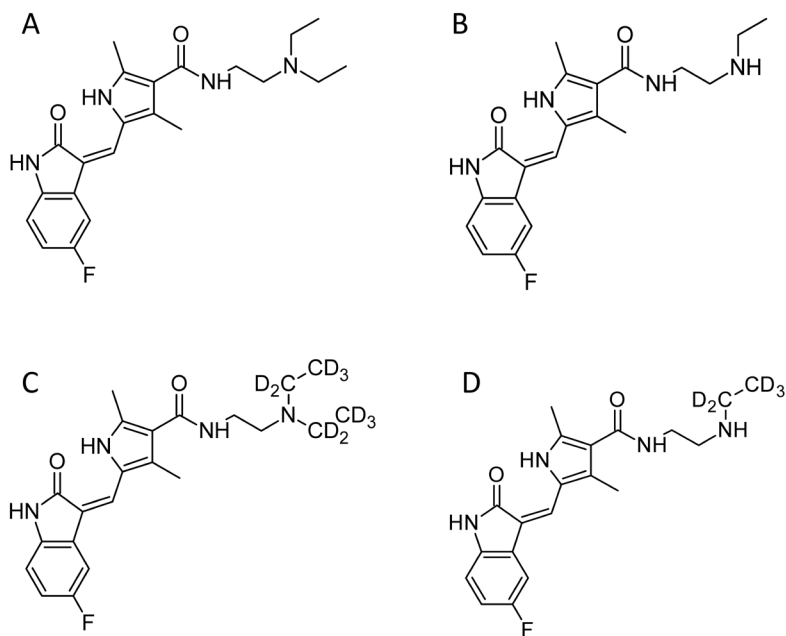


Figure 1. Chemical structures of sunitinib (A), N-desethyl sunitinib (B), sunitinib- $^2H_{10}$ (C) and N-desethyl sunitinib- 2H_5 (D).

Chromatography and Mass-spectrometry

Chromatographic separation was carried out using an HPLC system (LC-20AD Prominence binary solvent delivery system) with a column oven, DGU-20A3 online degasser and a SIL-HTc controller (all: Shimadzu, Kyoto, Japan) and a cooled autosampler (4 °C). A reversed phase system was used with a Synergi Fusion-RP 80 column, 150 x 2.0 mm ID, 4.0 µm particle size (Phenomenex, Torrance, CA, USA) protected by a Securityguard Synergi Fusion precolumn, 4 x 2.0 mm ID, 4.0 mm particle size (Phenomenex, Torrance, CA, USA) maintained at 40 °C. The injection volume was 10 µL. Gradient elution was used at a flow rate of 250 µL/min. The mobile phase consisted of a mixture of 0.1% formic acid in water (A) and 0.1% formic acid in methanol (B) starting at 25% of eluent B for 0.9 minute followed by a quick linear increase to 55% of eluent B within 0.1 minute. This mobile phase composition was maintained for 4.2 minutes. Sequentially, before each injection the column was reconditioned for 4.8 minutes with 25% B (v/v) resulting in a total run time of 10 min. The divert valve was directed to waste during the first 1.0 min and last 2.5 min to prevent the introduction of endogenous compounds into the mass-spectrometer.

Table 1. Mass spectrometer settings

Parameter	Setting
Run duration	10 min
Ionspray voltage	4,5 kV
Sheath gas (N ₂)	35 psi
Auxiliary gas (N ₂)	15 psi
Ion sweep gas (N ₂)	2 psi
Tube lens offset	12 V
Capillary temperature	350 °C
Collision pressure (argon)	1,5 mTorr
Chrom filter peak width	10 s

	Sunitinib	N-desethyl sunitinib	Sunitinib-D10	N-desethyl sunitinib-D5
Q1 mass	399 amu	371 amu	409 amu	376 amu
Q3 mass	283 amu	283 amu	283 amu	283 amu
Dwell time	30 ms	30 ms	30 ms	30 ms
Collision energy	30 V	23 V	32 V	24 V
Tube lens voltage	97 V	81 V	91 V	81 V

Determination of sunitinib, N-desethyl sunitinib and the internal standards (ISTD) was performed on a TSQ Quantum Ultra triple quadrupole mass-spectrometer equipped with an electrospray ionisation source (ESI) operating in the positive ion mode (Thermo Fisher Scientific, Waltham, MA, USA). For quantification, multiple reaction monitoring (MRM) chromatograms were acquired with LCQuan™ software version 2.5 (Thermo Fisher Scientific). Positive ions were created at atmospheric pressure and the quadrupoles were operating in unit resolution (0.7 Da). Mass transitions from m/z 399 to 283 for sunitinib, m/z 371 to 283 for N-desethyl sunitinib, m/z 409 to 283 for sunitinib-

$^2\text{H}_{10}$ and m/z 376 to 283 for N-desethylsunitinib- $^2\text{H}_5$ were optimised (see Figure 2). The ESI-MS/MS operating parameters used in this study are listed in Table 1.

Preparation of calibrators and quality control samples

A set of stock solutions of sunitinib and N-desethyl sunitinib were prepared from two independent weightings; one for the calibrators and one for the quality control (QC) samples. Approximately 2.8 mg of sunitinib maleate was weighted accurately and dissolved in 2 mL of DMSO in a volumetric flask to give a 1.0 mg/mL stock solution of the free-base. Approximately 0.75 mg of N-desethyl sunitinib was weighted accurately and dissolved in 750 μL of DMSO in a volumetric flask to give a 1.0 mg/mL stock solution. Stock solutions of the ISTD sunitinib- $^2\text{H}_{10}$ and N-desethyl sunitinib- $^2\text{H}_5$ were made in methanol at a concentration of approximately 1.0 mg/mL. A 100 ng/mL working solution of the ISTD was prepared by dilution of the stock solution in methanol. For the preparation of the calibrators, working solutions in the range from 50.0 to 10,000 ng/ml were used. These working solutions were prepared by dilution of sunitinib and N-desethyl sunitinib stock solutions in methanol. A volume of 50 μL of each working solution was added to 950 μL of drug-free human EDTA plasma to obtain calibrators in the range 2.5 to 500 ng/ml.

Four working solutions in the range from 50.0 to 8,000 ng/ml were prepared by dilution of independently prepared sunitinib and N-desethyl sunitinib stock solutions in methanol. To obtain QC samples of 2.5, 5.0, 40.0, 400 ng/mL in plasma, 50 μL of each working solution was added to 950 μL of drug-free human EDTA plasma. The stock and working solutions in methanol and precipitation reagent were stored at -20°C until use.

To establish the accuracy and precision of the method when samples above the upper limit of quantification (ULOQ) were quantified, a sample containing 5,000 ng/mL sunitinib and N-desethyl sunitinib was spiked. Before processing, this sample was then diluted ten times in drug-free human EDTA plasma.

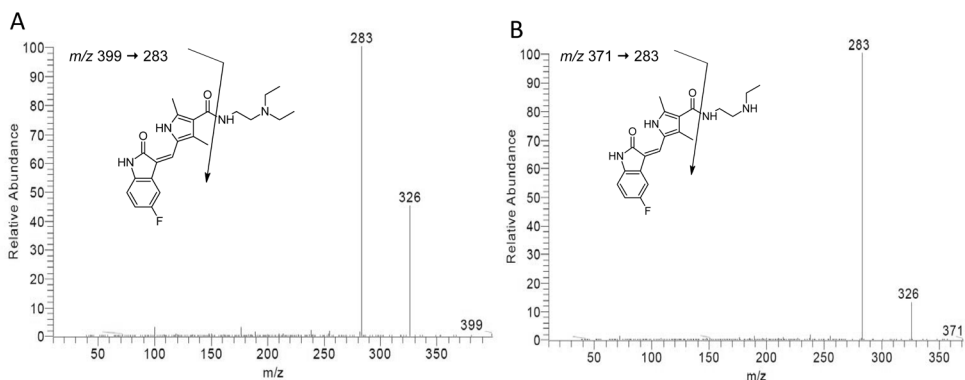


Figure 2. MS/MS product ion scan of sunitinib (A; precursor ion m/z 399) and N-desethyl sunitinib (B; precursor ion m/z 371).

Sample preparation

Protein precipitation with acetonitrile (at -20 °C) was used as sample pre-treatment. This protein precipitation reagent was stored at -20 °C and was kept refrigerated until directly before use, since the low temperature of the reagent contributed to more efficient protein precipitation. To 50 µL of plasma, 20 µL of ISTD working solution (100 ng/mL) and 150 µL of protein precipitation reagent were added. After vortex mixing for 15 s, samples were centrifuged at 15,000 x g for 15 min. A volume of 50 µL of the clear supernatant was diluted with 50 µL of eluent A (0.1% formic acid in water) before injection onto the column.

Validation procedures

A full validation of the assay was performed according to the FDA guidelines for validation of bioanalytical assays including linearity, inaccuracy, precision, specificity, selectivity, cross-analyte/internal standard interference, recovery, ion suppression, carry-over and stability [21-23].

Clinical suitability for routine therapeutic drug monitoring

The validated sunitinib and N-desethyl sunitinib assay was used to perform therapeutic drug monitoring of patients on a continuous once daily dosing regimen in a Phase I trial conducted in multiple centers in the Netherlands [24]. This study was approved by the local institutional review boards and informed consent was given according to the Declaration of Helsinki. In all participating centers EDTA samples were collected and, thereafter, sent directly to the laboratory by ordinary mail at ambient temperature. After receipt of the samples, within 36 h after blood draw, plasma was harvested and stored at -20°C until analysis.

In accordance with international guidelines [21-23], the analytical run for quantification of sunitinib and N-desethyl sunitinib in patient samples consisted of a blank sample (processed matrix sample without analyte and without ISTD) and a zero sample (processed matrix with ISTD), calibrators at a minimum of 6 concentration levels in duplicate, at least 3 levels of QC samples (low, medium and high) in duplicate and patient samples. Thus, at least 26 injections were required for a complete analytical run using the validated assay including one patient sample. However, to assure reduced turnaround time of the trough concentration determination and optimal use of the laboratory's HPLC-MS/MS system, applicability of a shorter run with fewer calibrators and QC samples was investigated. Therefore, a method-comparison experiment was performed according to international guidelines for method comparison [25]. Twenty five analytical runs including 58 patient samples were analysed using both the standard format and a version using a format with fewer calibrators and QC samples. The latter consisted of a blank sample, a zero sample, three calibrators (5.0, 50.0 and 250 ng/mL), one QC sample at medium level (40.0 ng/mL) and patient samples. For the standard analytical run the deviation from the nominal concentrations should be within ±20% for the LLOQ and within ±15% for the other concentrations for at least 75% of the calibrators and for at least 67% of the QC samples. In addition, at each QC level and at the

R1
R2
R3
R4
R5
R6
R7
R8
R9
R10
R11
R12
R13
R14
R15
R16
R17
R18
R19
R20
R21
R22
R23
R24
R25
R26
R27
R28
R29
R30
R31
R32
R33
R34
R35
R36
R37
R38
R39

R1
R2
R3
R4
R5
R6
R7
R8
R9
R10
R11
R12
R13
R14
R15
R16
R17
R18
R19
R20
R21
R22
R23
R24
R25
R26
R27
R28
R29
R30
R31
R32
R33
R34
R35
R36
R37
R38
R39

highest and lowest calibration level at least one out of two samples has to fulfill the criteria for maximum deviation from nominal concentrations [23]. Acceptance criteria for the short analytical run were more stringent, namely all calibrators and the mid level QC sample should be within $\pm 15\%$ of nominal values. Total trough concentrations resulting from the standard method and the abbreviated method were compared, using the standard method as a reference method, and the difference between the two methods was determined. The methods were considered to be equivalent if 85-115% of the initial concentrations measured with the standard method were found using the abbreviated method.

Results and discussion

Chromatography and Mass-spectrometry

A gradient starting on 25% eluent B was followed by a stepwise increase to a gradient with 55% eluent B at a flow rate of 0.25 mL per min. Typical chromatograms for samples at the lower limit of quantification (LLOQ) are depicted in Figures 3 and 4. At the LLOQ (2.5 ng/mL) a signal to noise ratio (S/N-ratio) of >10 was obtained. This LLOQ was determined based on the clinically relevant range of sunitinib and its metabolite, namely concentrations below 2.5 ng/mL are not supposed to be clinically relevant and so need not be quantified accurately. In the chromatograms of sunitinib, N-desethyl sunitinib and sunitinib- $^2\text{H}_{10}$, N-desethyl sunitinib- $^2\text{H}_5$ two peaks with the same molecular mass/mass transition were present. This is due to the presence of E/Z configurations in solution, as has been reported before (see figure 5) [13,15,17,26,27]. The retention times of sunitinib were 4.6 and 5.2 min. for the E- and Z-isomers, respectively. For the E- and Z-isomers of N-desethyl sunitinib the retention times were 4.5 and 4.9 min., respectively. In the pharmaceutical formulation of sunitinib mainly the Z-isomer is present. The isomerization reaction of the Z-isomer into the E-isomer is induced by exposure to light and occurs ex-vivo in plasma samples and other solutions. The isomerisation reaction is reversible and in our experiments the reverse reaction from E-isomer to Z-isomer already took place when samples were placed in a dark autosampler during an analytical run, leading to different proportions of E- and Z-isomers in samples over time. Since both isomers showed equal MS responses, the sum of the SRM responses of both separated isomers of the analytes and ISTD were used to process the data [13,15,17]. Consequently, protection from light during shipment, handling and processing of samples was not necessary.

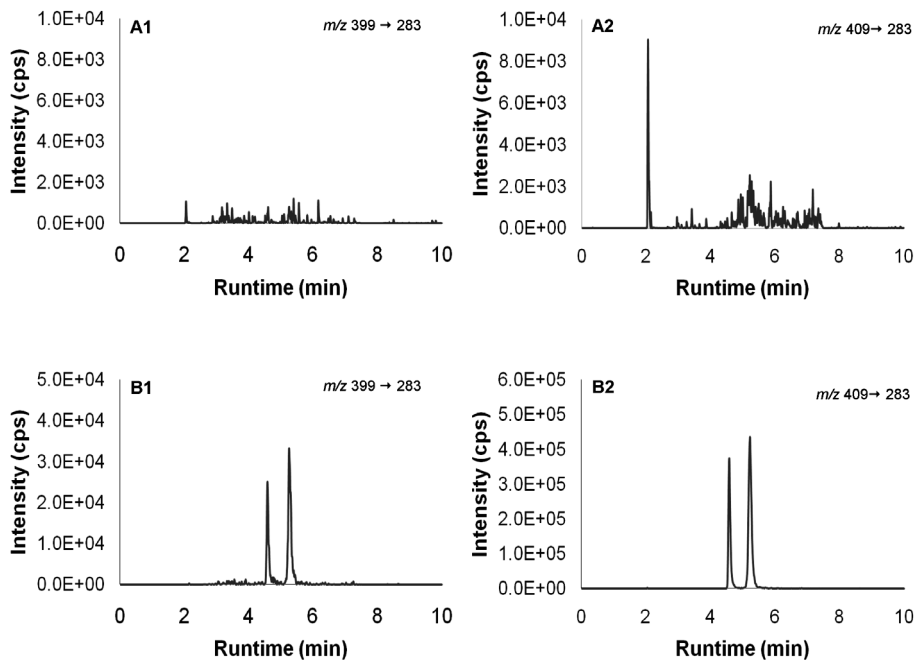


Figure 3. Representative LC-MS/MS chromatograms of a blank human plasma sample (A1, sunitinib; A2, internal standard sunitinib- $^2\text{H}_{10}$) and of a spiked human plasma sample at the LLOQ of 2.5 ng/mL (B1, sunitinib; B2, internal standard sunitinib- $^2\text{H}_{10}$). E/Z isomers of sunitinib eluted at around 4.6 and 5.2 minutes, respectively.

During optimization of the mass-spectrometric parameters, the Q1 spectrum of sunitinib and N-desethyl sunitinib showed the singly charged molecular ion as most intense ion at m/z 399 and 371, respectively. For the ISTD sunitinib- $^2\text{H}_{10}$ and N-desethyl sunitinib- $^2\text{H}_5$ the most intense peak in the Q1 spectrum also corresponded to the singly charged molecular ion at m/z 409 and 376, respectively.

R1
R2
R3
R4
R5
R6
R7
R8
R9
R10
R11
R12
R13
R14
R15
R16
R17
R18
R19
R20
R21
R22
R23
R24
R25
R26
R27
R28
R29
R30
R31
R32
R33
R34
R35
R36
R37
R38
R39

R1
R2
R3
R4
R5
R6
R7
R8
R9
R10
R11
R12
R13
R14
R15
R16
R17
R18
R19
R20
R21
R22
R23
R24
R25
R26
R27
R28
R29
R30
R31
R32
R33
R34
R35
R36
R37
R38
R39

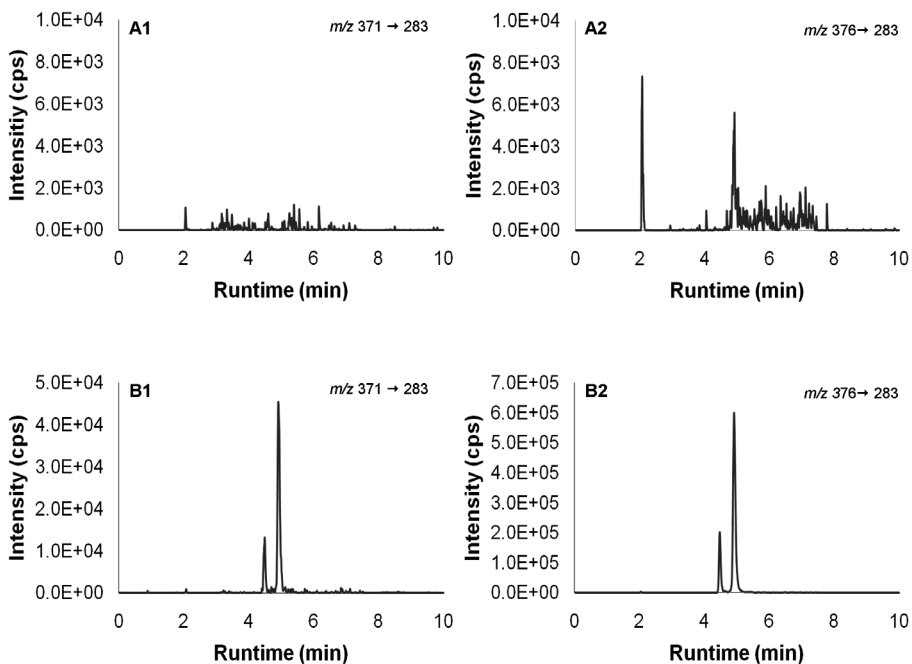


Figure 4. Representative LC-MS/MS chromatograms of a blank human plasma sample (A1, N-desethyl sunitinib; A2, internal standard N-desethyl sunitinib- 2H_3) and of a spiked human plasma sample at the LLOQ of 2.5 ng/mL (B1, N-desethyl sunitinib; B2, internal standard N-desethyl sunitinib- 2H_3). E/Z isomers of sunitinib eluted at around 4.5 and 4.9 minutes, respectively.

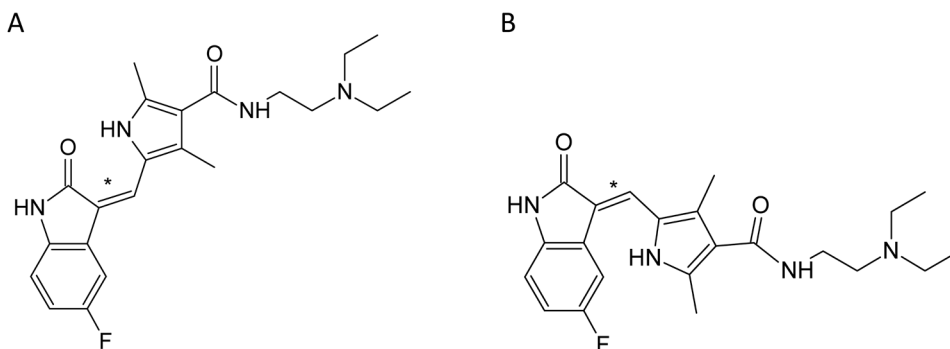


Figure 5. Both isomer forms of sunitinib: A) Sunitinib Z-isomer; B) Sunitinib E-isomer.

Validation experiments

Linearity. Eight non-zero plasma calibrators were prepared and analysed in duplicate in three separate analytical runs. The linear regression of the ratio of the areas of the analyte and the ISTD peaks versus the concentration were weighted with a weighting factors of $1/x^2$ (where x =concentration). The linearity was evaluated by means of back-calculated concentrations of the calibrators. The assay was linear over the validated concentration range from 2.5 to 500 ng/mL of sunitinib and N-desethyl sunitinib in human plasma. Correlation coefficients (r^2) were at least 0.989. The deviation from the nominal concentrations should be within $\pm 20\%$ for the LLOQ and within $\pm 15\%$ for the other concentrations. Coefficients of variation (CV) values were less than 20% and 15% for the LLOQ and other concentrations, respectively [22]. At all calibration levels inaccuracies were within -8.26 and 11.4% with CV values less than 8.21% for sunitinib in plasma. For N-desethyl sunitinib the inaccuracies were within -7.25 and 10.2% with CV values less than 10.3%.

Inaccuracy and precision. The intra- and inter-assay performance data are presented in Table 2. Inaccuracy and precision of the assay were established by analysing QC samples with analyte concentrations at the lower limit of quantification (LLOQ) and in the low, mid and high concentration ranges of the calibration curves. Five determinations of each QC sample were measured in three separate analytical runs. The coefficient of variation (CV%) was used to report the intra- and inter-assay precision. The intra- and inter-assay inaccuracies should be within $\pm 20\%$ for the LLOQ and $\pm 15\%$ for all other concentrations. The precisions, CV%, should be less than 20% for the LLOQ and less than 15% for all other concentration [22]. The intra-assay inaccuracies (% bias) for sunitinib and N-desethyl sunitinib in human EDTA plasma were within $\pm 13.8\%$ for all concentrations. The intra-assay precisions (CV%) for the analytes were less than 9.78% for all concentrations. Thus, the validated range for sunitinib and N-desethyl sunitinib based on 50 mL human EDTA plasma was from 2.5-500 ng/mL. Samples with analyte concentrations above the ULOQ (5,000 ng/mL) were diluted 10 fold with drug-free human EDTA plasma. These samples were processed in 5 replicates and measured in one analytical run to assess the accuracy and precision. The intra-assay inaccuracy for diluted samples was 5.14 and 4.73% and the intra-assay precision was 0.86 and 3.55% for sunitinib and N-desethyl sunitinib, respectively. When concentrations above 500 ng/mL are expected, samples can be diluted 10 fold with drug-free human EDTA plasma. Inaccuracies and precisions fulfilled the requirements [21,22].

Selectivity. To investigate whether endogenous compounds from plasma interfered with the detection of the analytes or the ISTDs, six different batches of drug-free human EDTA plasma were prepared as double blanks (containing neither analyte nor ISTD) and LLOQ samples. Samples were processed and analysed according to the described procedures. Areas of peaks co-eluting with the analytes should not exceed 20% of the area at the LLOQ [22]. In MRM chromatograms of six batches of drug-free EDTA plasma no co-eluting peaks $>20\%$ of the sunitinib and N-desethyl sunitinib peak area at the LLOQ level were found and also no co-eluting peaks $>5\%$ of the ISTDs were detected [22]. The deviation of the nominal concentration for the LLOQ samples should be

R1
R2
R3
R4
R5
R6
R7
R8
R9
R10
R11
R12
R13
R14
R15
R16
R17
R18
R19
R20
R21
R22
R23
R24
R25
R26
R27
R28
R29
R30
R31
R32
R33
R34
R35
R36
R37
R38
R39

within $\pm 20\%$ [21,22] and were between -1.83 and 7.63% for sunitinib and -7.04 and 19.2% for and N-desethyl sunitinib.

Cross analyte interference. To investigate possible cross interference between sunitinib, N-desethyl sunitinib and ISTDs, a cross interference check was performed. Drug-free human EDTA plasma was spiked at ULOQ level and was processed without ISTD. Also drug-free plasma with only ISTD sunitinib- $^2\text{H}_{10}$ and N-desethyl sunitinib- $^2\text{H}_5$ was processed. The response of any interfering peak with the same retention time as sunitinib or N-desethyl sunitinib should be less than 20% of the response of a LLOQ sample. The response of any interfering peak with the same retention time as the ISTD should be less than 5% of the response of the ISTD [21]. Cross-analyte/ISTD interferences of the assay fulfilled these requirements.

Table 2. Assay performance data for sunitinib and N-desethyl sunitinib in plasma.

Analyte	Nominal conc. (ng/mL)	Inter-day imprecision (%CV)	Intra-day imprecision (%CV)	Overall inaccuracy (% bias)
<i>Sunitinib</i>	2.47	7.67	9.78	5.99
	4.94	6.38	9.25	6.16
	39.5	5.92	6.31	8.04
	395	7.72	8.75	-1.37
<i>N-desethyl sunitinib</i>	2.50	6.79	9.04	4.91
	5.00	6.37	6.95	7.44
	40.0	5.15	4.02	9.12
	400	8.93	9.77	-1.60

Conc., concentration; Dev, Deviation; CV, coefficient of variation.

All QC samples have been tested in 3 batches of 5 replicates on three different days.

Overall inaccuracy (% bias) = calculated value/nominal value * 100%.

Recovery and matrix effect. The protein precipitation (PP) recovery of sunitinib and its metabolite was determined in triplicate at two concentrations (5.0 and 400 ng/mL) by comparing the analytical response of processed samples with those of processed blanks spiked with analyte (representing 100% recovery). The mean PP recovery was 100% (CV% 8.1) and 101% (CV% 5.0) for sunitinib and N-desethyl sunitinib, respectively. The ISTD normalized matrix factor is defined as the ratio of the analyte peak response in the presence of matrix ions to the analyte peak response in the absence of matrix ions [28]. The ISTD normalized matrix factor was examined in triplicate at two concentrations (5.0 and 400 ng/mL) by comparing the area ratios of processed blanks spiked with sunitinib and N-desethyl sunitinib and unprocessed samples (acetonitrile spiked with sunitinib and N-desethyl sunitinib). The mean ISTD normalized matrix factor detected for sunitinib and N-desethyl sunitinib in plasma was 1.14 (CV% 2.7) and 1.13 (CV% 2.8), respectively. Ionization enhancement was observed for both analytes when analyzed in the presence of matrix ions. Nevertheless, the reproducibility of the assay was adequate, since signal enhancement was constant at different concentration levels with a CV% less than 3%.

Carry over. Carry-over was tested by injecting two processed blank matrix samples sequentially after injecting an ULOQ sample. The response in the first blank matrix at the retention times of sunitinib, N-desethyl sunitinib and ISTD should be less than 20% of the response of a LLOQ sample [21]. Carry-over of 6.31% and 7.05% of the LLOQ for sunitinib and N-desethyl sunitinib, was observed in a processed blank sample injected after an ULOQ sample.

Stability. Stability data are summarized in Table 3. The stability of sunitinib and N-desethyl sunitinib in spiked human EDTA plasma after three freeze/thaw cycles from nominally -20 °C to ambient temperatures and after 72 hours at ambient temperature was investigated in triplicate at two concentrations. In addition, the long-term stability of sunitinib and N-desethyl sunitinib in spiked human EDTA plasma kept at -20°C for 1.5 months was investigated in triplicate. The analytes were considered to be stable in the matrix or final extract if 85–115% of the nominal concentrations was recovered [22]. Sunitinib and N-desethyl sunitinib were stable in human plasma for at least three freeze (-20 °C) / thaw cycles. Short-term stability of the analyte at ambient temperatures was established up to at least 72 h and long-term stability in plasma at -20°C up to at least 1.5 months.

The processed sample stability of sunitinib and N-desethyl sunitinib at 2-8 °C was investigated at three concentrations (5.0, 40.0 and 400 ng/mL) after 7 days. Both analytes were stable in the final extract for at least 7 days at nominally 2-8 °C. The re-injection reproducibility was determined after 3 days of storage in the autosampler (4 °C). Re-injection reproducibility was established and an analytical run can be re-injected after at least 3 days of storage in the autosampler at 4 °C. Stability of stock solutions of sunitinib, N-desethyl sunitinib stored at ambient temperature for 6 h and at -20°C for 22 months was established in triplicate.

Table 3. Stability data for sunitinib and N-desethyl sunitinib

Conditions	Sunitinib*	N-desethyl sunitinib*	No. of replicates	No. of conc. levels
Freeze/thaw stability in plasma				
3 cycles	93.6 ± 5.4	94.6 ± 2.7	6	2
Short-term stability in plasma				
Ambient, 72 h	97.7 ± 2.9	96.5 ± 5.3	12	2
Long-term stability in plasma				
-20°C, 1.5 months	90.4 ± 7.1	91.1 ± 6.1	9	3
Final extract stability				
2-8°C, 7 days	113.3 ± 6.0	95.9 ± 14.5	9	3
Re-injection reproducibility				
4°C, 3 days	107.9 ± 9.5	95.3 ± 5.4	9	3
Stock solution stability				
Ambient, 6h	102.9 ± 4.7	106.0 ± 11.7	2	1
-20°C, 22 months	101.6 ± 2.4	93.9 ± 2.0	2	1

* [Mean Remaining from Baseline (%) ± CV (%)]

R1
R2
R3
R4
R5
R6
R7
R8
R9
R10
R11
R12
R13
R14
R15
R16
R17
R18
R19
R20
R21
R22
R23
R24
R25
R26
R27
R28
R29
R30
R31
R32
R33
R34
R35
R36
R37
R38
R39

Clinical suitability for routine therapeutic drug monitoring

During a period of eight months 25 analytical runs including 58 patient samples for TDM were performed according to the validated assay procedures. The method proved to be very robust, since none of these runs had to be rejected. Sequentially, data of those runs were analysed using both the standard run format and the format with fewer calibrators and QC samples. Comparing the results of the two methods, the plotted regression line was almost equal to the line of identity, indicating a marginal difference between the methods (correlation coefficient of 0.998) (see Figure 6). In addition, a regression test was performed and showed no statistically significant constant error with an y-axis intercept of 0.63 (95% confidence interval (CI) = -0.666 - 1.93). The slope of the regression line was 0.979 (95% CI = 0.961 - 0.997), which indicated a statistically significant proportional error. However, this proportional error was very small and was not thought to be clinically relevant. The mean of the absolute differences between the methods was only -0.66 ng/mL (mean of relative differences -0.85%). In addition, the deviations of the total trough concentrations in the patient samples were between -10.2 and 5.87% (see Figure 7), which fulfils the criterion of a maximum bias of $\pm 15\%$.

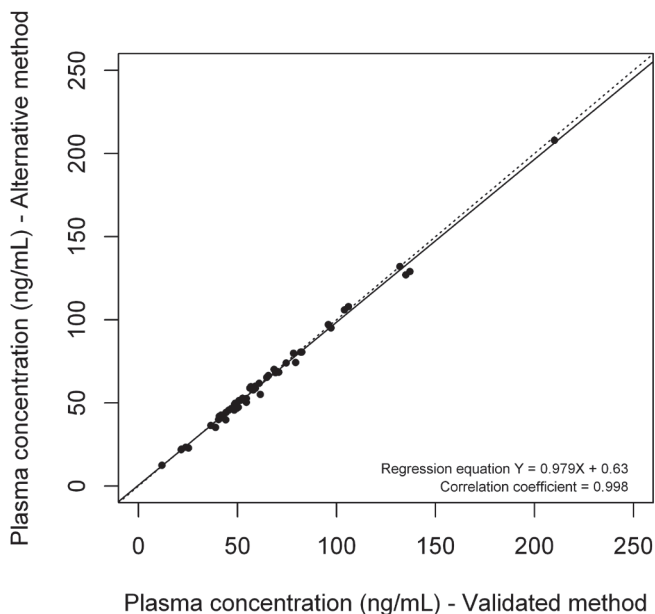


Figure 6. Scatter plot of method comparison: results of the alternative method plotted against the validated method. Solid line: linear regression line; Dotted line: line of identity.

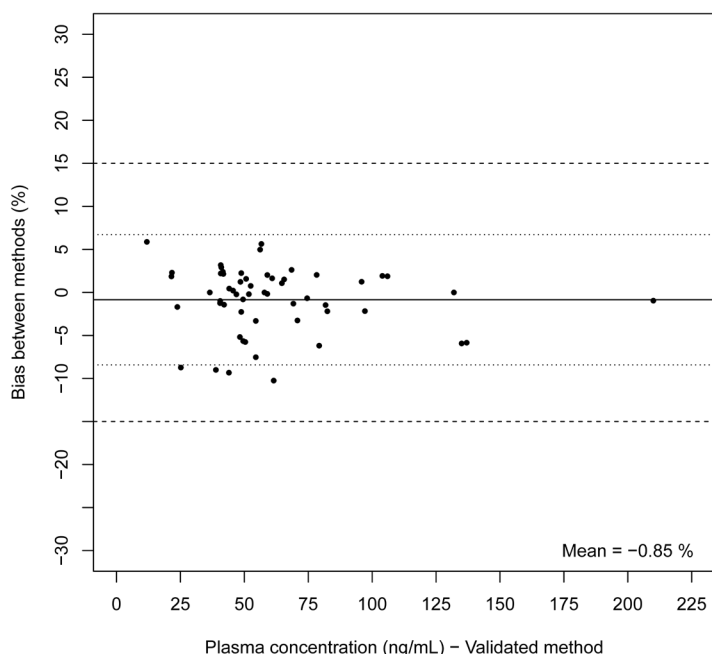


Figure 7. Bias plot of method comparison: the relative bias of the measured concentration between the two methods (%) plotted against the sunitinib total plasma concentrations. Dotted line: 95% confidence interval of bias; Dashed line: maximal permitted bias.

In our study, the cut-off value for dose escalation is a total trough concentration of less than 50 ng/mL. Total trough concentrations below this are supposed to be subtherapeutic and should therefore lead to a dose increase if the patient does not show any severe toxicities. In only one out of 58 patient samples the advice for dose modification was different based on the abbreviated method. In this case the first, conventional analysis resulted in a total trough concentration of 50.4 ng/mL and the second analysis in 46.9 ng/mL, which is a deviation of -5.75%. This deviation is less than the inter-assay precision or repeatability (CV%) of the validated assay which is $\pm 9.78\%$. For this reason, the alternative method with fewer injections has proved to be interchangeable with the conventional analytical run composition. Thus, for cases of TDM that require a fast turnaround time, the time-saving analytical run composition can give reliable results within a much shorter time frame.

Conclusion

We have developed and validated a fast LC-MS/MS method for the quantitative analysis of sunitinib and N-desethyl sunitinib in human plasma. Human EDTA plasma with sunitinib and N-desethyl sunitinib were pre-treated by protein precipitation with acetonitrile and the addition

R1
R2
R3
R4
R5
R6
R7
R8
R9
R10
R11
R12
R13
R14
R15
R16
R17
R18
R19
R20
R21
R22
R23
R24
R25
R26
R27
R28
R29
R30
R31
R32
R33
R34
R35
R36
R37
R38
R39

R1
R2
R3
R4
R5
R6
R7
R8
R9
R10
R11
R12
R13
R14
R15
R16
R17
R18
R19
R20
R21
R22
R23
R24
R25
R26
R27
R28
R29
R30
R31
R32
R33
R34
R35
R36
R37
R38
R39

of ISTD sunitinib-²H₁₀ and N-desethyl sunitinib-²H₅. Chromatography was performed under acidic conditions. A linear dynamic range from 2.5 to 500 ng/ml has been validated with high accuracy and precision. The method is robust, easy to perform and has been shown to be applicable for routine TDM of sunitinib. Moreover, application of this method using only three calibrators and one QC sample per analytical run has been proved to give reliable results with a more rapid turnaround time.

References

1. Demetri GD, van Oosterom AT, Garrett CR et al. Efficacy and safety of sunitinib in patients with advanced gastrointestinal stromal tumour after failure of imatinib: a randomised controlled trial. *Lancet* 2006; 368: 1329-38.
2. Motzer RJ, Michaelson MD, Redman BG et al. Activity of SU11248, a multitargeted inhibitor of vascular endothelial growth factor receptor and platelet-derived growth factor receptor, in patients with metastatic renal cell carcinoma. *J Clin Oncol* 2006; 24: 16-24.
3. Houk BE, Bello CL, Poland B et al. Relationship between exposure to sunitinib and efficacy and tolerability endpoints in patients with cancer: results of a pharmacokinetic/pharmacodynamic meta-analysis. *Cancer Chemother Pharmacol* 2010; 66: 357-71.
4. Abrams TJ, Murray LJ, Pesenti E et al. Preclinical evaluation of the tyrosine kinase inhibitor SU11248 as a single agent and in combination with "standard of care" therapeutic agents for the treatment of breast cancer. *Mol Cancer Ther* 2003; 2: 1011-21.
5. Abrams TJ, Lee LB, Murray LJ et al. SU11248 inhibits KIT and platelet-derived growth factor receptor beta in preclinical models of human small cell lung cancer. *Mol Cancer Ther* 2003; 2: 471-8.
6. Faivre S, Delbaldo C, Vera K et al. Safety, pharmacokinetic, and antitumor activity of SU11248, a novel oral multitarget tyrosine kinase inhibitor, in patients with cancer. *J Clin Oncol* 2006; 24: 25-35.
7. Mendel DB, Laird AD, Xin X et al. In vivo antitumor activity of SU11248, a novel tyrosine kinase inhibitor targeting vascular endothelial growth factor and platelet-derived growth factor receptors: determination of a pharmacokinetic/pharmacodynamic relationship. *Clin Cancer Res* 2003; 9: 327-37.
8. Murray LJ, Abrams TJ, Long KR et al. SU11248 inhibits tumor growth and CSF-1R-dependent osteolysis in an experimental breast cancer bone metastasis model. *Clin Exp Metastasis* 2003; 20: 757-66.
9. de Jonge ME, Huitema AD, Schellens JH et al. Individualised cancer chemotherapy: strategies and performance of prospective studies on therapeutic drug monitoring with dose adaptation: a review. *Clin Pharmacokinet* 2005; 44: 147-73.
10. Ivanova M, Artusi C, Polo G et al. High-throughput LC-MS/MS method for monitoring sunitinib and everolimus in the routine clinical laboratory. *Clin Chem Lab Med* 2011; 49: 1151-8.
11. Baratte S, Sarati S, Frigerio E et al. Quantitation of SU11248, an oral multi-target tyrosine kinase inhibitor, and its metabolite in monkey tissues by liquid chromatograph with tandem mass spectrometry following semi-automated liquid-liquid extraction. *J Chromatogr A* 2004; 1024: 87-94.
12. Blanchet B, Saboureau C, Benichou AS et al. Development and validation of an HPLC-UV-visible method for sunitinib quantification in human plasma. *Clin Chim Acta* 2009; 404: 134-9.
13. de Bruijn P, Sleijfer S, Lam MH et al. Bioanalytical method for the quantification of sunitinib and its n-desethyl metabolite SU12662 in human plasma by ultra performance liquid chromatography/tandem triple-quadrupole mass spectrometry. *J Pharm Biomed Anal* 2010; 51: 934-41.
14. Etienne-Grimaldi MC, Renee N, Izzedine H et al. A routine feasible HPLC analysis for the anti-angiogenic tyrosine kinase inhibitor, sunitinib, and its main metabolite, SU12662, in plasma. *J Chromatogr B Analyt Technol Biomed Life Sci* 2009; 877: 3757-61.
15. Haouala A, Zanolari B, Rochat B et al. Therapeutic Drug Monitoring of the new targeted anticancer agents imatinib, nilotinib, dasatinib, sunitinib, sorafenib and lapatinib by LC tandem mass spectrometry. *J Chromatogr B Analyt Technol Biomed Life Sci* 2009; 877: 1982-96.
16. Honeywell R, Yazdani K, Giovannetti E et al. Simple and selective method for the determination of various tyrosine kinase inhibitors used in the clinical setting by liquid chromatography tandem mass spectrometry. *J Chromatogr B Analyt Technol Biomed Life Sci* 2010; 878: 1059-68.

R1
R2
R3
R4
R5
R6
R7
R8
R9
R10
R11
R12
R13
R14
R15
R16
R17
R18
R19
R20
R21
R22
R23
R24
R25
R26
R27
R28
R29
R30
R31
R32
R33
R34
R35
R36
R37
R38
R39

R1
R2
R3
R4
R5
R6
R7
R8
R9
R10
R11
R12
R13
R14
R15
R16
R17
R18
R19
R20
R21
R22
R23
R24
R25
R26
R27
R28
R29
R30
R31
R32
R33
R34
R35
R36
R37
R38
R39

17. Lankheet NA, Blank CU, Mallo H et al. Determination of sunitinib and its active metabolite N-desethylsunitinib in sweat of a patient. *J Anal Toxicol* 2011; 35: 558-65.
18. Minkin P, Zhao M, Chen Z et al. Quantification of sunitinib in human plasma by high-performance liquid chromatography-tandem mass spectrometry. *J Chromatogr B Analyt Technol Biomed Life Sci* 2008; 874: 84-8.
19. Rodamer M, Elsingerhorst PW, Kinzig M et al. Development and validation of a liquid chromatography/tandem mass spectrometry procedure for the quantification of sunitinib (SU11248) and its active metabolite, N-desethyl sunitinib (SU12662), in human plasma: application to an explorative study. *J Chromatogr B Analyt Technol Biomed Life Sci* 2011; 879: 695-706.
20. Zhou Q, Gallo JM. Quantification of sunitinib in mouse plasma, brain tumor and normal brain using liquid chromatography-electrospray ionization-tandem mass spectrometry and pharmacokinetic application. *J Pharm Biomed Anal* 2010; 51: 958-64.
21. European Medicines Agency (EMA). Guideline on bioanalytical method validation. Available at: http://www.ema.europa.eu/docs/en_GB/document_library/Scientific_guideline/2011/08/WC500109686.pdf. Date accessed November 16, 2011. 2010.
22. U.S. Food and Drug Administration: Centre for Drug Evaluation and Research. Guidance for Industry: Bioanalytical Method Validation. <http://www.fda.gov/downloads/Drugs/GuidanceComplianceRegulatoryInformation/Guidances/UCM070107.pdf>. Date accessed March 21, 2011. 2011.
23. Viswanathan CT, Bansal S, Booth B et al. Quantitative bioanalytical methods validation and implementation: best practices for chromatographic and ligand binding assays. *Pharm Res* 2007; 24: 1962-73.
24. Steeghs N. Use of Individual Pharmacokinetically (PK)-Guided Sunitinib Dosing: A Feasibility Study in Patients With Advanced Solid Tumors (NCT01286896). Available at: <http://clinicaltrials.gov/ct2/show/NCT01286896?term=NCT01286896&rank=1>. Date accessed April 15, 2012. 2012.
25. Clinical and Laboratory Standards Institute (CLSI). Method Comparison and Bias Estimation Using Patient Samples; Approved Guideline - Second Edition. NCCLS document EP9-A2. Available at: <http://www.jslab.cn/data/2006/EP09-A2.pdf>. Date accessed March 21, 2012. 2010.
26. Sistla A, Shenoy N. Reversible Z-E isomerism and pharmaceutical implications for SU5416. *Drug Dev Ind Pharm* 2005; 31: 1001-7.
27. Sparidans RW, Iusuf D, Schinkel AH et al. Liquid chromatography-tandem mass spectrometric assay for the light sensitive tyrosine kinase inhibitor axitinib in human plasma. *J Chromatogr B Analyt Technol Biomed Life Sci* 2009; 877: 4090-6.
28. Bansal S, DeStefano A. Key elements of bioanalytical method validation for small molecules. *AAPS J* 2007; 9: E109-E114.

Chapter 1.3

Development and clinical validation of a method
for the quantification of sunitinib and N-desethyl
sunitinib in dried blood spots

Nienke A.G. Lankheet
Alexander B.P. van der Straeten
Hilde Rosing
Jan H.M. Schellens
Jos H. Beijnen
Alwin D.R. Huitema

Experimental chapter



R1
R2
R3
R4
R5
R6
R7
R8
R9
R10
R11
R12
R13
R14
R15
R16
R17
R18
R19
R20
R21
R22
R23
R24
R25
R26
R27
R28
R29
R30
R31
R32
R33
R34
R35
R36
R37
R38
R39

Abstract

Background. Dried blood spot (DBS) sampling is a patient-friendly technique with several advantages over the classical way of performing therapeutic drug monitoring (TDM) using plasma after venapuncture. Therefore, a sunitinib DBS assay was developed. Since target concentrations for TDM of sunitinib are defined in plasma, there is also need to establish the relationship between DBS and plasma concentrations.

Methods. An LC-MS/MS method for quantitative analysis of sunitinib and N-desethyl sunitinib in DBS, using different filter paper cards (pure cellulose based Whatman 903 and impregnated DMPK-B paper cards), has been developed and validated. For clinical validation of DMPK-B paper cards, paired plasma and DBS samples were collected and analyzed. Theoretical plasma concentrations were calculated from DBS concentrations by correcting for haematocrit level and blood-to-plasma ratio. The results of the plasma and DBS method were compared using linear regression and Bland-Altman analysis.

Results. Methods with both filter paper cards have been validated with high accuracy and precision. Only DMPK-B paper cards, impregnated to inhibit conversion of sunitinib, could be used to quantify sunitinib and N-desethyl sunitinib separately. However, DBS specific method validation parameters, e.g. spotted blood volume, haematocrit level and spot homogeneity were found to influence accuracy and precision of the assay using DMPK-B cards. Additionally, when comparing sunitinib and N-desethyl sunitinib concentrations resulting from the standard plasma method and the DBS method using DMPK-B paper cards, the two methods did not show adequate correlation enabling the use of these cards in clinical practice.

Conclusions. DMPK-B cards are not suitable for TDM of sunitinib by patient self-sampling in a non-hospital based setting, since haematocrit, blood volume and spot homogeneity were found to be very critical in DBS quality using these type of cards. Use of these cards should, therefore, be limited to strictly regulated settings where volumetric pipette are used to spot equally distributed, fixed volumes of blood. Further research is warranted for the development of a DBS method for sunitinib and N-desethyl sunitinib.

Introduction

Sunitinib (Sutent®) is an orally available multiple kinase inhibitor. Sunitinib has proven efficacy as single agent in several solid tumor types and is approved for use in advanced renal cell cancer (RCC), imatinib-resistant or -intolerant gastrointestinal stromal tumors (GISTs) and neuroendocrine tumors (NETs) [1-3].

Recent findings demonstrated a strong dose-efficacy relationship for sunitinib treatment [4]. Given a low therapeutic index, large inter-individual variability in systemic exposure, and the positive exposure-efficacy relationship of sunitinib, therapeutic drug monitoring (TDM) may represent a practical tool to improve the outcome of patients receiving sunitinib leading to therapy optimization on a patient-by-patient basis [4-6].

Current clinical practice for TDM is to measure drug concentrations in plasma, obtained by venous blood sampling in the outpatient clinic. Therefore, we previously developed a high-performance liquid chromatography coupled with tandem mass spectrometry (HPLC-MS/MS) method for the quantification of sunitinib and its active metabolite, N-desethyl sunitinib, in human EDTA plasma (see Chapter 1.2). However, this manner of performing TDM has several limitations. For example, measuring real trough levels (exactly 24h after intake of sunitinib) is not always feasible at the outpatient clinic, since most patients on a sunitinib regimen take their medication early in the morning or late in the evening. In the last decade, many publications have been published in which dried blood spots (DBS) are used for TDM of e.g. antiretroviral drugs [7,8], anti-epileptics [9-11], anti-malarials [12,13], antibiotics [14,15], drugs of abuse [16]. DBS sampling for TDM enables sample collection by means of a simple fingerprick. This patient-friendly technique has several advantages over the classic way of performing TDM, e.g.: 1) It allows pharmacokinetic studies in non-hospital based settings, allowing self-sampling of trough levels at home at consecutive occasions; 2) There is no need for use of anticoagulant containing sampling tubes and plasma separation. Therefore, the logistics and storage of DBS samples are much less complicated [17,18].

However, since the target concentrations for TDM of sunitinib are defined in plasma samples, there is need to establish the relationship between DBS and plasma concentrations. Due to binding of the drugs to components in blood that are not present in plasma or due to differences in venous and capillary blood, the concentrations of drugs and metabolites in DBS and plasma are not necessarily equal [18]. Therefore, the DBS to plasma ratio of sunitinib and its metabolite has to be defined in simultaneously drawn DBS and plasma samples of patients on sunitinib therapy. Here, we report development and validation of a method to quantify sunitinib and N-desethyl sunitinib on DBS paper cards. We also report the results of a clinical validation to define the relationship between DBS and plasma concentrations of sunitinib and N-desethyl sunitinib to facilitate clinical implementation of DBS sampling.

R1
R2
R3
R4
R5
R6
R7
R8
R9
R10
R11
R12
R13
R14
R15
R16
R17
R18
R19
R20
R21
R22
R23
R24
R25
R26
R27
R28
R29
R30
R31
R32
R33
R34
R35
R36
R37
R38
R39

R1
R2
R3
R4
R5
R6
R7
R8
R9
R10
R11
R12
R13
R14
R15
R16
R17
R18
R19
R20
R21
R22
R23
R24
R25
R26
R27
R28
R29
R30
R31
R32
R33
R34
R35
R36
R37
R38
R39

Materials and methods

Bio-analytical conditions and materials

For the bio-analytical development and validation the chemicals, materials and chromatographic and mass spectrometric conditions used for the dried blood spot (DBS) methods are equal to conditions of the earlier described method for the analysis of sunitinib and N-desethyl sunitinib in human EDTA plasma (see Chapter 1.2).

For collection of DBS, pure cellulose based filter cards (Whatman 903 Protein Saver cards) and Whatman™ FTA™ DMPK-B DBS filter paper cards were purchased from Whatman Nederland B.V (Den Bosch, The Netherlands). Whatman™ foil bags and desiccant packages for storage of DBS samples were provided by GE Healthcare (Buckinghamshire, UK). BD Microtainer® Contact-activated lancets for capillary blood collection (1.8 mm) were obtained from BD (Plymouth, UK). Freshly drawn drug-free whole blood with EDTA as anticoagulant was obtained from healthy donors in the Slotervaart Hospital (Amsterdam, The Netherlands) using 3.5 mL BD Vacutainer® EDTA sampling tubes provided by BD (Plymouth, UK).

Preparation of calibration standards and QC samples

DBS calibration standards and QC samples were prepared from whole blood working solutions spiked with sunitinib and N-desethyl sunitinib in a range from 10.0 to 500 ng/mL by transferring 30 µL (for DMPK-B paper card) or 40 µL (for pure cellulose paper card) of the whole blood working solutions on the paper cards with a volumetric pipette. Thereafter, the blood spots were left to dry overnight at ambient temperatures. Calibration standards and QC samples were prepared freshly for each run and processed and analysed in duplicate.

Extraction procedure

A 0.25 inch diameter disc was punched out of the dried blood spot, ensuring an area completely filled with blood was obtained. The disc was transferred to a 2 mL amber coloured Eppendorf tube and 100 µL of extraction solution (acetonitrile – methanol (1:1, v/v) containing both stable isotopically labeled internal standards of sunitinib and N-desethyl sunitinib) was added. Sunitinib and N-desethyl sunitinib were extracted from the dried blood spots by sonication for 30 min. The tubes were centrifuged for 2 min. at 23,100 x g. The clear extract was transferred to a 1.5 mL amber colored Eppendorf tube (i.e. partly processed DBS extract) and was evaporated till dryness at 40°C under a gentle flux of nitrogen. Subsequently, the dry extract was reconstituted with 50 µL of reconstitution solution (acetonitrile – methanol – water (1:1:1, v/v/v)). After vortex mixing for 30 s, the clear final extracts were transferred to a glass autosampler vial with insert (i.e. final DBS extract).

Bio-analytical validation procedures

Assay validation was performed according to the FDA guidelines for validation of bio-analytical assays [19,20]. For the quantification methods using different types of cards, linearity, inaccuracy, precision, cross-analyte/internal standard interference, recovery, matrix effect and carry-over were tested. Additionally, DBS specific validation tests, including determination of the effect of spotted blood volume, haematocrit, and spot homogeneity on the validity of both types of paper cards, were performed as recommended by the European Bioanalysis Forum (EBF) [21,22].

Clinical validation procedures

The only method to quantify sunitinib and N-desethyl sunitinib separately was using DMPK-B cards and, therefore, this method was proposed to be the most elegant way to analyse patient samples. For this reason, the DMPK-B cards were used during the clinical validation. For the clinical validation, paired plasma and DBS samples of patients on a continuous once daily sunitinib dosing regimen in a Phase I trial conducted in multiple centres in the Netherlands were collected [23]. This study was approved by the local institutional review boards and informed consent was provided by each participant before inclusion in the study. Patients were recruited between April 2011 and June 2012.

DBS samples were obtained within one hour before or after the collection of EDTA whole blood by venous sampling from each patient during regular study visits to the outpatient clinic. EDTA plasma samples were obtained from the EDTA whole blood samples after centrifugation and were stored at -20°C until analysis. DBS sampling was performed using an automatic lancet after sterile cleaning of the skin. The first drop of blood was discarded and subsequent drops were collected on DMPK-B paper cards. DBS samples were dried overnight at ambient temperature at the outpatient clinic and thereafter shipped to the laboratory in a foil bag with a desiccant package. After receipt, the DBS samples were processed to DBS extract the same day. Analysis of the DBS samples was performed using the currently described method and analysis of the plasma samples was performed using the previously validated method for the quantification of sunitinib and N-desethyl sunitinib in human EDTA plasma (see Chapter 1.2).

When using DBS samples, haematocrit levels have an effect on blood viscosity leading to differences in diffusion properties of blood on the paper card. Therefore, a considerable variation can occur in the blood volume represented by a punched out circle from the DBS [17]. In our patient population a wide range of haematocrit values is expected due to disease state and haematological toxicity of sunitinib therapy. Therefore, significant bias due to haematocrit variation is not inconceivable, when using qualification standards and QC samples of healthy volunteers with normal haematocrit levels. For this reason, haematocrit levels were determined at the day of the DBS (and plasma) sample collection as part of the weekly follow-up study examinations. If necessary, a correction for bias related to haematocrit level would be implemented to make a more reasonable interpretation of pharmacokinetic data derived from DBS samples.

R1
R2
R3
R4
R5
R6
R7
R8
R9
R10
R11
R12
R13
R14
R15
R16
R17
R18
R19
R20
R21
R22
R23
R24
R25
R26
R27
R28
R29
R30
R31
R32
R33
R34
R35
R36
R37
R38
R39

R1 Additionally, an effect of haematocrit level in quantification of DBS samples may result in bias of
R2 measured concentrations of analytes which are partitioned into erythrocytes as well as plasma
R3 [7,24,25]. This makes a direct comparison between results of DBS and plasma samples inaccurate. To
R4 calculate the correlation between plasma and whole blood concentrations, it is important to know
R5 the blood-to-plasma ratio of an analyte [18,25]. Theoretical plasma concentrations ($\text{Plasma}_{[\text{analyte}]}$)
R6 can be calculated from DBS concentrations using the following formula, as previously proposed
R7 by Li et al. [18]:
R8

$$\text{Plasma}_{[\text{analyte}]} = (\text{DBS}_{[\text{analyte}]} / [1 - \text{haematocrit}]) \times (1 - f_{\text{BC}})$$

R10
R11 where f_{BC} is the fraction of an analyte distributed into blood cells. An analyte with a higher f_{BC} has
R12 a higher blood-to-plasma ratio [18]. Despite sunitinib and N-desethyl sunitinib are highly bound
R13 to plasma proteins for 95% and 90%, respectively [26], both compounds are preferably partitioned
R14 into erythrocytes with blood-to-plasma ratios of 1.8 and 3.0, respectively, as derived from studies in
R15 monkeys [27]. Consequently, the fractions sunitinib and N-desethyl sunitinib distributed into blood
R16 cells (f_{BC}) of are 0.643 and 0.75, respectively.
R17

R18 The method-comparison experiment for plasma and DBS samples was performed according to
R19 International Guidelines for Method Comparison and Bias Estimation using Patient Samples from
R20 the CLSI [28]. Sunitinib and N-desethyl sunitinib trough concentrations resulting from the standard
R21 plasma method and the alternative DBS method were compared using linear regression and the
R22 Bland-Altman approach [29]. Subsequently, the difference between two methods was determined
R23 and the methods were considered to be equivalent if 85-115% of the initial concentration measured
R24 with the standard, validated plasma method was found using the DBS method [19,20,28].
R25

R26 Results

R27 *Method development*

R28 *Pure cellulose paper cards*

R29 Conventionally, pure cellulose paper cards (Whatman Protein Saver card 903) have been used for
R30 DBS [7-16]. However, it was established that sunitinib was converted to N-desethyl sunitinib on
R31 these cards during a cross analyte interference check. In general, it is assumed that analytes are
R32 very stable on DBS paper cards that are protected against moisture, since the DBS matrix seems
R33 to stabilize many analytes [17]. However, in our DBS samples spiked with sunitinib, a substantial
R34 amount of N-desethyl sunitinib was formed (>10%). To investigate the cause of the N-desethyl
R35 sunitinib formation, different experiments were performed. From these experiments it was
R36 concluded that the conversion of sunitinib to its metabolite was not due to substances originating
R37 from the paper card or sample pre-treatment. From a subsequent experiment, in which the drying
R38 process of the DBS was monitored, it could be deduced that presence of whole blood and drying
R39

in the air were essential for the conversion of sunitinib into its metabolite. It has been assumed that biotransformation of sunitinib only occurs in vivo and is solely catalyzed by liver microsomal cytochrome P450 enzyme 3A4 [30-32]. However, it was also suggested that hemoproteins in red blood cells, e.g. horse radish peroxidase, myoglobin and oxyhemoglobin, are able to catalyze peroxide-mediated N-demethylation of xenobiotics [30-32]. Probably, hemoproteins are released from lysing red blood cells during the drying process of the DBS, which leads to biotransformation of sunitinib into its N-desethyl metabolite. The chemical structures of sunitinib and N-desethyl sunitinib are shown in Figure 1. As for TDM of sunitinib the target level is based on the sum of sunitinib and N-desethyl sunitinib (total trough level) [6], conversion of sunitinib into N-desethyl sunitinib during drying of the DBS eventually does not lead to a different total trough level. However, such a pragmatic approximation can only be used for accurate determination of the sum concentration and is, apparently, less elegant than a method in which both analytes are quantified separately.

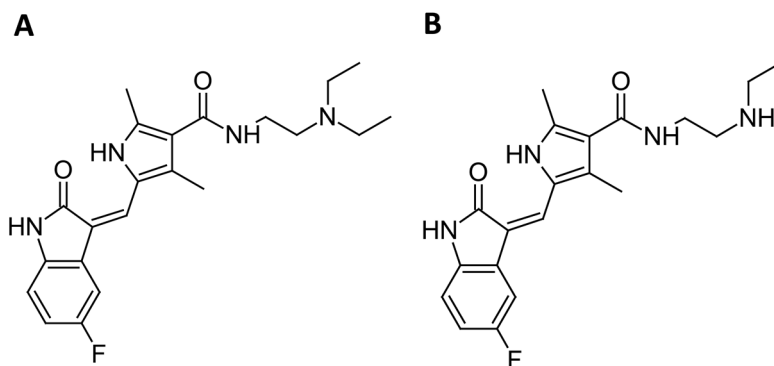


Figure 1. Chemical structures of sunitinib (A), N-desethyl sunitinib (B).

FTA DMPK-B cards

To circumvent the conversion of sunitinib in N-desethyl sunitinib on the cellulose paper cards, it was considered to use recently developed DBS paper cards which are chemically treated with reagents that, upon contact, lyse cells and denature proteins (FTA DMPK-B cards impregnated with thiocyanate salts and FTA DMPK-A cards impregnated with sodium lauryl sulphate (GE Healthcare, Buckinghamshire, UK)). The sunitinib blood spot drying process was monitored on these types of cards at different time points (0, 1, 2, 3 and 20 h) after spiking. The DMPK-A paper card did not completely block the conversion process, however, the DMPK-B paper card with thiocyanate salts completely blocked the conversion of sunitinib into its N-desethyl metabolite, as shown in Figure 2. Therefore, the DMPK-B paper card was used for further bio-analytical and clinical validation of an DBS method for the quantification of sunitinib and N-desethyl sunitinib separately.

R1
R2
R3
R4
R5
R6
R7
R8
R9
R10
R11
R12
R13
R14
R15
R16
R17
R18
R19
R20
R21
R22
R23
R24
R25
R26
R27
R28
R29
R30
R31
R32
R33
R34
R35
R36
R37
R38
R39

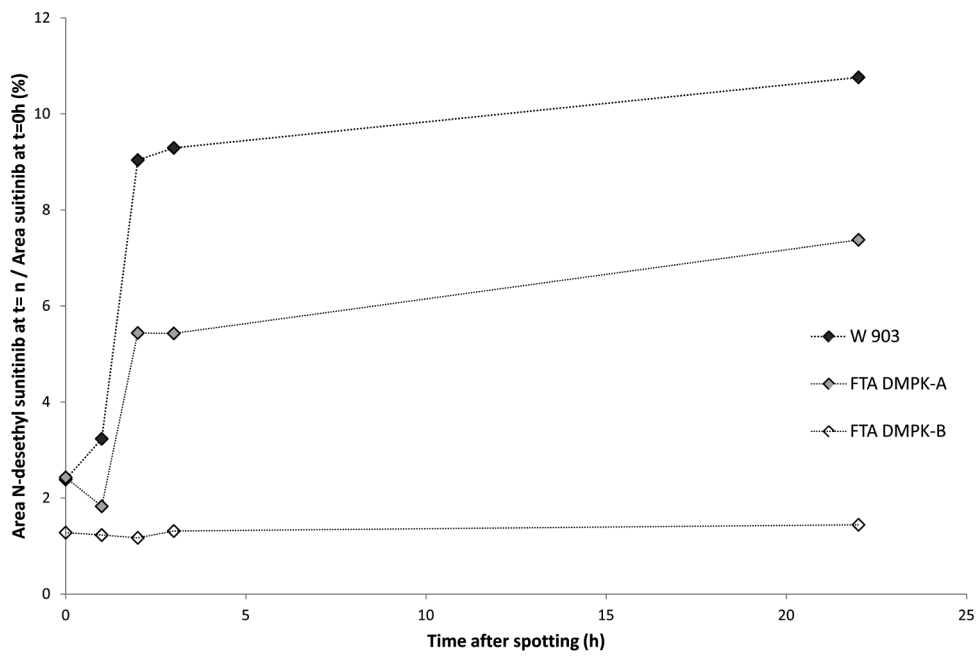


Figure 2. Formation of N-desethyl sunitinib in DBS samples spiked with sunitinib during the drying process on three different card types (conventional Whatman 903 pure cellulose paper card; sodium lauryl sulphate impregnated DMPK-A paper card; thiocyanate salt impregnated DMPK-B paper card). The formation of N-desethyl sunitinib is shown as an area ratio of the N-desethyl sunitinib area at the specific time point and the area of sunitinib at t= 0h.

As a major point of concern for using the DMPK-B cards, however, we found that blood spots on DMPK-B paper appeared considerably less homogenous than on pure cellulose based paper. This lack of spot homogeneity is clearly shown by presence of a 'halo' of lighter colour on the outer edge of the spots, as shown in Figure 3. Additionally, the variation in appearance of the DBS with different haematocrit values already gave an indication that haematocrit levels strongly influence spot size and spot homogeneity. Namely, spot size was inversely correlated to haematocrit level. Moreover, the quality of patient DBS samples on DMPK-B paper cards, regarding homogeneity and volume of blood spotted on the paper card, was highly variable (see Figure 3).

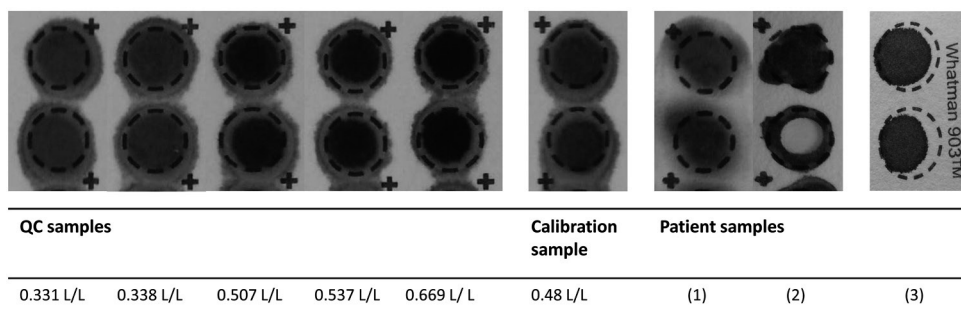


Figure 3. Appearance of DBS: 5 QC samples of a haematocrit range; calibration sample of Ht 0.48 L/L; representative patient samples with excessively large blood volume (1) and bad spot homogeneity (2) on DMPK-B paper cards; and a representative patient sample with good spot homogeneity (3) on Whatman 903 pure cellulose based paper card.

Extraction procedure

In the procedure for extraction of sunitinib and N-desethyl sunitinib from the DBS it is preferable to retain blood components and thiocyanate salts on the paper card. For protein precipitation in plasma samples acetonitrile and methanol are effective. Therefore, different mixtures containing these solvents were tested for their extraction capabilities for sunitinib and N-desethyl sunitinib from DBS. Mixtures including water were tested, because N-desethyl sunitinib is soluble in water. However, all mixtures including water were unsuitable, since blood components were also extracted from the DBS, leading to a very low signal to noise ratio. The highest signal to noise ratio was obtained using a mixture of acetonitrile – methanol (1:1, v/v).

Additionally, the influence of sonication time on the signal to noise ratio of sunitinib and N-desethyl sunitinib was investigated. The highest signal to noise ratio was obtained by sonication for 30 minutes. Therefore, the final extraction method was sonication of the DBS during 30 min with 100 μ L acetonitril – methanol (1:1, v/v) containing both internal standards. Additionally, to circumvent any solvent effect after injection of the samples in the chromatographic system with methanol and water, the dry extracts were reconstituted in acetonitril – methanol – water (1:1:1, v/v/v).

During method development, it was observed that the MS signal of N-desethyl sunitinib decreased substantially when DBS samples on cellulose or DMPK-B paper cards were stored for more than one week at ambient temperature. Since this decrease of signal was firstly assigned as a stability issue, tandem mass spectrometry and orbitrap experiments were performed to investigate whether biodegradation products of N-desethyl sunitinib could be detected in extracts of DBS on DMPK-B paper cards that had been stored for several months at ambient temperature. However, no signs of biodegradation of N-desethyl sunitinib were found. Additionally, we addressed the issue that probably some diffusion of N-desethyl sunitinib through the DBS paper card occurred during storage at ambient temperature. However, it was observed that the relative amounts of N-desethyl

sunitinib in the center, perimeter and outside the DBS did not differ between freshly prepared DBS and DBS stored at ambient temperature for several months. Therefore, it was assumed that the recovery of N-desethyl sunitinib decreased over time when the DBS were stored at ambient temperature. In an experiment in which 8 sequential extractions were performed on DBS samples with different storage durations at ambient temperature (2 weeks and 18 weeks) a difference was found in the total recovery of N-desethyl sunitinib between samples of both time points, whereas the recovery of sunitinib in all samples was equal (see Table 1). The exact mechanism for the increased retention of N-desethyl sunitinib on the DBS paper card is not elucidated, but probably the secondary amine, which is not present in the parent drug, interacts irreversibly with the DBS paper card [33]. To avoid this problem, patient samples were processed partly to DBS extracts directly after shipment (i.e. within 5 days after DBS collection). For patient DBS samples and QC samples, the first part of the extraction procedure, including 30 min of sonication, was used to obtain partly processed DBS extracts of samples. These DBS extracts were stored at -20°C until further analysis. The second part of the extraction process, including evaporation and reconstitution to obtain final extracts, was performed on the day of the LC-MS/MS measurements. Calibration standards and a second set of QC samples were prepared freshly for each analytical run and the whole extraction procedure of these samples was performed at once.

Table 1. Extraction recovery of sunitinib and N-desethyl sunitinib in DBS samples on DMPK-B paper cards after different storage times (2 weeks and 18 weeks) at ambient temperature.

Analyte	Duration of storage at amb. temp. (weeks)	Area ratio	
		Recovery first extraction	Total recovery of 8 sequential extractions
Sunitinib	2	0.015	0.040
	18	0.015	0.040
N-desethyl sunitinib	2	0.027	0.032
	18	0.018	0.026

Validation experiments

General validation experiments

The results of general assay validation experiments for quantification sunitinib and N-desethyl sunitinib on DMPK-B cards and for quantification of the sum of sunitinib and N-desethyl sunitinib on Whatman 903 cards are depicted in Table 2. These results all fulfilled the criteria for bio-analytical assay validation [19,20]. The intra- and inter-assay performance data of both assays are presented in Table 3 and also fulfilled the criteria [19,20].

Table 2. Assay validation parameters for sunitinib and N-desethyl sunitinib on DMPK-B paper cards and the sum of sunitinib and N-desethyl sunitinib on Whatman 903 paper cards.

Validation parameter		DMPK-B		Whatman 903
		<i>Sunitinib</i>	<i>N-desethyl sunitinib</i>	<i>Sum</i>
Linearity	Linear range (ng/mL)	10.0 - 500	10.0 - 500	10.0 - 1,000
	Accuracy (%Bias)	97.5 - 100.6	98.9 - 102.0	96.9 - 104.1
	Precision (CV%)	< 5.67	< 4.51	< 5.75
	Correlation (R ²)	0.995	0.997	0.991
Recovery	Extraction recovery (%)	76.6	74.1	42.2
	<i>Precision (CV%)</i>	11.1	10.3	6.0
Matrix effect	Matrix factor	1.07	0.53	1.19
	<i>Precision (CV%)</i>	1.92	11.7	4.75
Carry over	After ULOQ sample (% of LLOQ)	8.32	7.59	3.50
Selectivity (in 6 batches of whole blood)	Accuracy (%Bias)	84.5 – 91.0	82.5 – 95.6	NA
	Interference (% of LLOQ)	< 6.29	< 5.40	NA

Sum, sum of sunitinib and N-desethyl sunitinib; CV, coefficient of variation; R², correlation coefficient; ULOQ, upper limit of quantification; LLOQ, lower limit of quantification; NA, not available.

Accuracy (%Bias) = calculated value/nominal value * 100%

The cross analyte interference test for the analytes on pure cellulose based cards showed conversion of sunitinib in N-desethyl sunitinib. Using the DMPK-B cards, the interfering peak response in the N-desethyl sunitinib window after injection of calibration samples containing solely sunitinib sample accounted for at most 0.434% of the total SRM response of N-desethyl sunitinib. Therefore, the contribution of the interfering peaks to the total SRM response was negligible and the results for cross interference were found to be acceptable.

The analytes were considered to be stable in the matrix or final extract if 85–115% of the nominal concentrations was recovered [19,20]. Sunitinib and N-desethyl sunitinib were stable in DBS for at most 5 days at ambient temperature at Whatman 903 and at DMPK-B cards and for 4 months at -20°C at DMPK-B cards. Partly processed DMPK-B DBS extracts were stable up to at least 4 months at -20°C and for at least one freeze/thaw cycle. Additionally, both analytes were stable in the final extract at least 33 days at nominally 2-8 °C. Re-injection reproducibility was established and an analytical run can be re-injected after at least 25 days of storage in the autosampler at 4 °C. Stability of stock solutions of sunitinib, N-desethyl sunitinib stored at ambient temperature for 6 hours and at -20°C for 22 months was established in triplicate.

Dried blood spot specific validation experiments

Dried blood spot specific validation experiments include determination of the impact of spotted blood volume, haematocrit, and spot homogeneity on the validity of the dried blood spot method [21,22]. For the DBS specific tests deviations of the nominal concentrations within 85-115% were considered acceptable.

R1
R2
R3
R4
R5
R6
R7
R8
R9
R10
R11
R12
R13
R14
R15
R16
R17
R18
R19
R20
R21
R22
R23
R24
R25
R26
R27
R28
R29
R30
R31
R32
R33
R34
R35
R36
R37
R38
R39

Dried blood spot volume. The influence of the volume of whole blood, used to spot a DBS, on the accuracy and precision of Whatman 903 paper cards was investigated by spotting different volumes (20, 40, 60 μ L) on paper cards in triplicate at two concentration levels and concentrations were subsequently quantified on calibration curves obtained from 40 μ L spots. At all different volumes and concentration levels, inaccuracies were within -4.13 and 5.74% with CV values less than 6.79% for the sum of sunitinib and N-desethyl sunitinib concentrations in DBS. For DMPK-B cards the same experiment was performed with volumes of 20, 30, 40, 50 μ L and subsequent quantification on calibration curves obtained from 30 μ L spots. At all different volumes and concentration levels, inaccuracies were within -8.82 and 13.0% with CV values less than 4.69% for sunitinib in DBS. For N-desethyl sunitinib the inaccuracies were within -7.51 and 16.0% with CV values less than 4.70%. However, for both analytes the concentration measured on DMPK-B paper cards was directly correlated to the volume of blood spotted with the highest analyte concentrations found in DBS with the highest volume spotted. These results show that spot volume did influence the amount of analyte present in the punched-out disc from DMPK-B paper cards. For sunitinib all spotted volumes (20 to 50 μ L) fulfilled the criteria and for N-desethyl a spotted volume of 20 to 40 μ L can be used without need to correct for the blood volume spotted.

Haematocrit effect. The effect of haematocrit and spot homogeneity using pure cellulose based paper cards has been extensively tested thus far [24,25,34]. Acceptable effects of haematocrit were seen by Wilhelm et al. when using a haematocrit range from 0.20 to 0.72 L/L and, moreover, using a range from 0.30 to 0.59 L/L negligible effects of haematocrit were seen [25]. Deniff et al. also observed that assay bias on Whatman 903 paper cards was within 15% for a clinically relevant haematocrit range from 0.28 to 0.67 L/L using different analytes [34]. The impact of variations in haematocrit values on the spot size and assay performance using DMPK-B paper cards was evaluated experimentally in a clinically relevant range of haematocrit levels from 0.33 to 0.67 L/L. EDTA whole blood of a volunteer was used to prepare QC samples with five different haematocrit levels by adding the appropriate volume of plasma to the centrifuged blood, followed by gentle mixing. The haematocrit level was then measured for each blood sample using a Cell Dyn Hematology analyser (Abbot Diagnostics, Lake Forest, IL). After spiking the blood samples with sunitinib and N-desethyl sunitinib, 30 μ L of blood was spotted on DBS paper cards. Subsequently, blood spots were dried overnight at ambient temperatures and analysed. A linear correlation was found between haematocrit levels and the measured concentrations of both sunitinib and N-desethyl sunitinib with correlation coefficients of 0.991 and 0.983, respectively, as shown in Figure 4. The inaccuracies exceeded 15% deviation from nominal concentrations when haematocrit levels deviate approximately more than 0.06 L/L from the haematocrit levels of the calibration samples. Therefore, a correction based on haematocrit level is required when patient DBS samples are quantified.

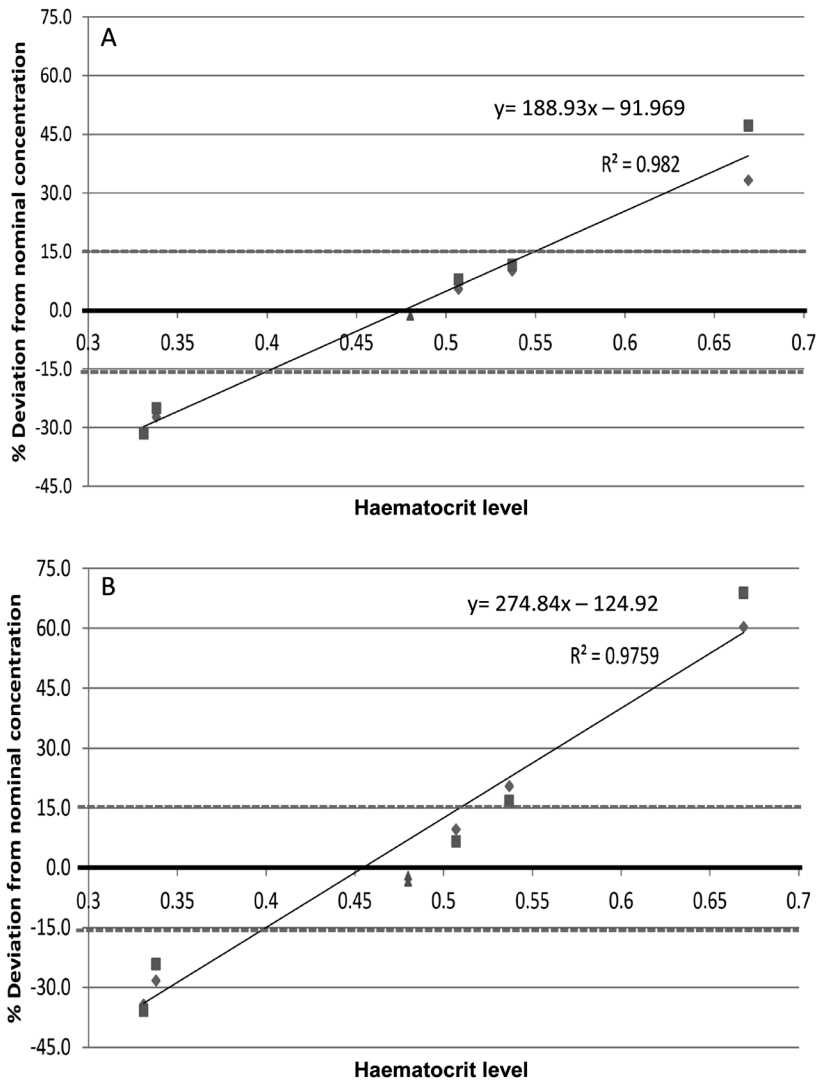


Figure 4. Influence of haematocrit level on the (A) sunitinib and (B) N-desethyl sunitinib concentration found in DBS samples on DMPK-B paper cards (defined as % deviation from the nominal concentration). The lozenges represents samples at QC low level (20.0 ng/mL), the squares represent samples at QC high level (400 ng/mL) and the triangles represent QC samples that were prepared of whole blood with the same haematocrit level as the calibration samples.

R1
R2
R3
R4
R5
R6
R7
R8
R9
R10
R11
R12
R13
R14
R15
R16
R17
R18
R19
R20
R21
R22
R23
R24
R25
R26
R27
R28
R29
R30
R31
R32
R33
R34
R35
R36
R37
R38
R39

R1
R2
R3
R4
R5
R6
R7
R8
R9
R10
R11
R12
R13
R14
R15
R16
R17
R18
R19
R20
R21
R22
R23
R24
R25
R26
R27
R28
R29
R30
R31
R32
R33
R34
R35
R36
R37
R38
R39

Spot homogeneity. The influence of the location in the DBS, at which the discs were punched out, on the accuracy and precision was investigated by punching discs from the center and perimeter of a DBS at two different concentration levels. For this experiment a smaller punch (0.125 inch diameter) was used to allow multiple punches from a single DBS. For discs punched from the centre and perimeters of the DBS on Whatman 903 paper cards the inaccuracies were acceptable, namely between -3.4 and -10.3%. Using DMPK-B paper cards, inaccuracies for discs punched from the center of the DBS were between 0.556 and 7.64% for both analytes. However, for discs punched from the perimeters of the DBS the inaccuracies were substantially higher, namely between -12.3 and -18.5%. To get a representative sample, it is therefore necessary to punch a disc out of the centre of a spot with a big enough punch (0.25 inch diameter).

Clinical suitability for routine therapeutic drug monitoring

For the clinical validation of sunitinib and N-desethyl sunitinib quantification on DMPK-B paper cards, in total 77 paired plasma and DBS samples of 32 patients were collected. The mean haematocrit value of patient samples was 0.39 L/L (SD 0.05 L/L). Since these haematocrit values were substantially lower than haematocrit values of calibration and QC samples (0.48 L/L), the bias introduced by this discrepancy was corrected. Therefore, the following formulas, based on the results of the haematocrit effect test during method validation (Figure 4), were used:

$$\text{Corrected DBS}_{\text{sunitinib}} = \frac{\text{DBS}_{\text{sunitinib}}}{100 + ((188.93 \times \text{Haematocrit}) - 91.969)} \times 100$$

$$\text{Corrected DBS}_{\text{N-desethyl sunitinib}} = \frac{\text{DBS}_{\text{N-desethyl sunitinib}}}{100 + ((274.84 \times \text{Haematocrit}) - 124.92)} \times 100$$

However, after correction for haematocrit effect of the DBS paper card and calculation of theoretical plasma concentrations using haematocrit level and blood-to-plasma distribution ratio, still inadequate precision was found when comparing theoretical plasma concentrations derived from DBS samples with measured plasma concentrations (see Figure 5). For sunitinib the relationship between measured plasma concentrations and theoretical plasma concentrations were adequately distributed around the line of identity. However, for N-desethyl sunitinib a structural difference was found between theoretical and measured plasma concentrations. The deviations between the results of the plasma method and DBS method exceeded a maximum tolerated bias of 15% for both compounds, as shown in the Bland-Altman plots in Figure 6. Therefore, the two methods did not show adequate correlation.

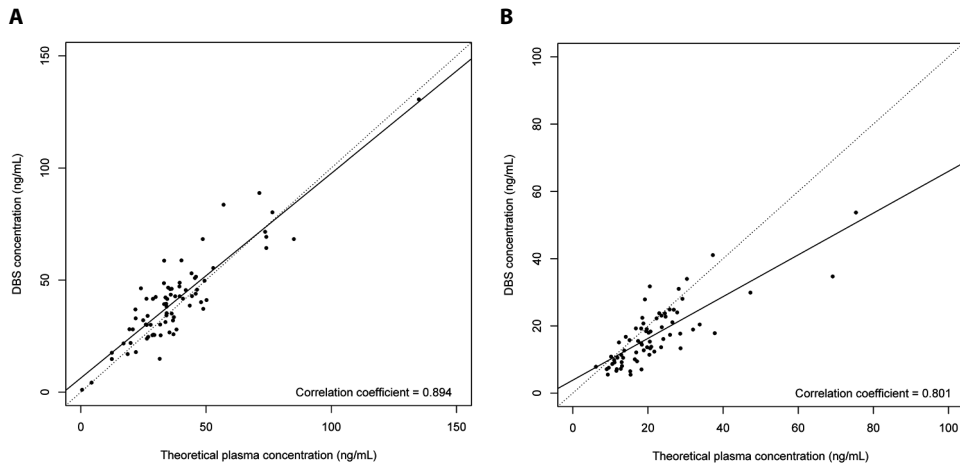


Figure 5. Theoretical plasma concentrations of DMPK-B paper cards plotted against measured plasma concentrations for (A) sunitinib and (B) N-desethyl sunitinib. The broken line is the line of true identity.

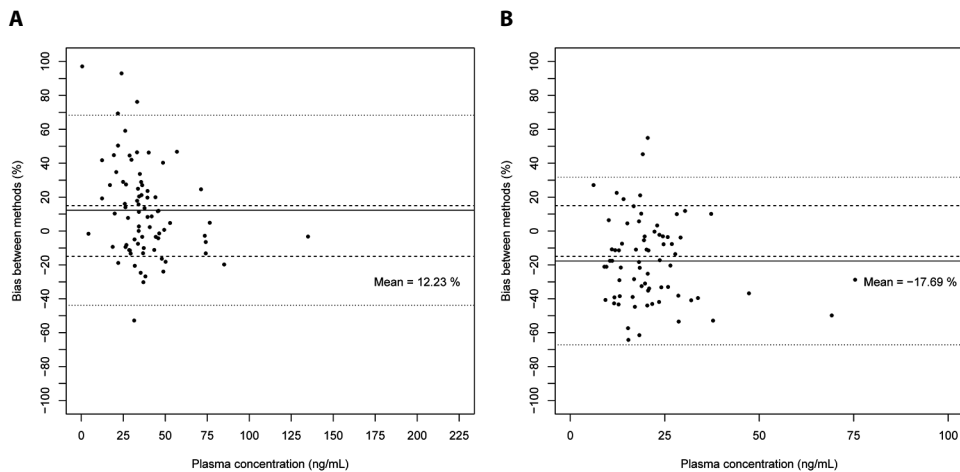


Figure 6. Bland-Altman plots for (A) sunitinib and (B) N-desethyl sunitinib of the clinical validation on DMPK-B paper cards. The continuous line is the mean bias, the dotted lines represent the 95% confidence interval and the broken lines represent the criterium of maximum deviation ($\pm 15\%$).

Discussion

The method validation of DBS on pure cellulose paper cards and DMPK-B paper cards showed good results based on general validation parameters. However, during validation of DBS specific parameters, e.g. spotted blood volume, haematocrit level and spot homogeneity were found to influence the accuracy and precision of the assay using DBS on DMPK-B cards. In addition, inadequate precision was found when comparing theoretical plasma concentrations derived from

R1
R2
R3
R4
R5
R6
R7
R8
R9
R10
R11
R12
R13
R14
R15
R16
R17
R18
R19
R20
R21
R22
R23
R24
R25
R26
R27
R28
R29
R30
R31
R32
R33
R34
R35
R36
R37
R38
R39

R1
R2
R3
R4
R5
R6
R7
R8
R9
R10
R11
R12
R13
R14
R15
R16
R17
R18
R19
R20
R21
R22
R23
R24
R25
R26
R27
R28
R29
R30
R31
R32
R33
R34
R35
R36
R37
R38
R39

DBS samples on DMPK-B cards with measured plasma concentrations. Since adequate accuracy and precision of both the plasma and DBS method were observed during general bio-analytical method validation, the lack of precision during method comparison was expected to be caused by paper characteristics rather than HPLC-MS/MS assay performance. Assay performance was tested on DBS of equal blood volumes (30µL per spot) spotted using a volumetric pipette. Therefore, spots were all the same size, the same haematocrit and equally distributed through the paper card avoiding bias introduced by effect of haematocrit, spot volume or bad spot homogeneity. On the contrary, patient DBS samples were obtained from a finger prick. Consequently, the quality of patient DBS samples, regarding homogeneity and volume of blood spotted on the paper card, was highly variable. Since haematocrit was directly correlated to deviation from the nominal value, a correction for this effect can be made when a patient's haematocrit level is known. Hence, it is still necessary to collect a paired venous whole blood sample by at the outpatient clinic to correct for patient's current haematocrit level. However, correction is not possible for spotted blood volume and spot homogeneity and, therefore, these determinants seem to be pivotal in quantification of sunitinib and N-desethyl sunitinib in DBS samples on DMPK-B paper cards. Moreover, Deniff et al. also observed that the performance of DMPK-B paper cards was inferior to pure cellulose based paper cards (Whatman 903, DMPK-C) and DMPK-A cards based on blood spot appearance and assay bias introduced by haematocrit level even within a normal haematocrit range (0.28-0.67 L/L) [34]. The effect of haematocrit level on DBS results on DMPK-B cards compared to pure cellulose based paper cards was confirmed by O'Mara et al [24]. Probably, it is for this reason that no clinical methods using DMPK-B cards have been reported to date. Thus, not fulfilling DBS paper card specific parameters for method validation is most probably the cause of the high imprecision in the results of the clinical validation.

Another probable source of bias is the sample handling of DBS samples after receipt in the laboratory. DBS samples with sunitinib and N-desethyl sunitinib have to be extracted from the paper card at receipt in the laboratory, because of decrease in extraction recovery of N-desethyl sunitinib when DBS samples are stored at room temperature for more than five days. Consequently, patients samples are processed to partly processed extract at different time points. However, when standardized procedures and the same batch of extraction solvent are used during processing and QC samples are processed with patient samples regularly, introduction of bias during this process can be minimized.

Besides high imprecision, N-desethyl sunitinib also showed a structural difference in the correlation between measured plasma concentrations and theoretical plasma concentrations and, therefore, this correlation did not equal the line of true identity. Probably, this structural difference is caused by a discrepancy between the blood-to-plasma ratio of monkeys, used in the calculation of theoretical plasma concentrations, and the actual blood-to-plasma ratio in human, which has not been reported in literature [26,27].

Multiple reasons to prefer the use of DBS instead of plasma in TDM of sunitinib have been mentioned. Firstly, DBS enables collection of real trough level (exactly 24h after intake) in a non-hospital based setting by self-sampling instead of venous sampling in an outpatient clinic [18]. However, when using DMPK-B paper cards to collect DBS, blood spot volume and spot homogeneity are pivotal for DBS quality. For this reason, the paper characteristics of the impregnated DMPK-B cards is inadequate to use for TDM by self-sampling in non-hospital based settings. Secondly, by using DBS sampling for TDM, there is no need for plasma separation directly after blood collection and DBS can be sent by ordinary mail [18]. Therefore, the logistics and storage of DBS samples would be much less complicated even despite the necessary sample handling at receipt at the laboratory and storage of partly processed extracts. Accordingly, in strictly regulated settings of a clinical trials, use of DMPK-B paper cards can be considered when there is need to either simplify logistics or to reduce sample storage volume and to quantify sunitinib and N-desethyl sunitinib separately. In this case, venous blood samples should be transferred to a DMPK-B card by using a volumetric pipette to avoid bias by variability in blood volume and spot homogeneity.

Conclusion

We have developed a LC-MS/MS method for the quantitative analysis of sunitinib and N-desethyl sunitinib in DBS. Since conversion of sunitinib in its N-desethyl metabolite occurred on conventional pure cellulose based DBS paper cards, these cards could only be used to quantify the sum of sunitinib and N-desethyl concentrations. On DMPK-B paper cards, impregnated with thiocyanate salts to denature catabolic enzymes, the conversion of sunitinib was blocked and, therefore, these paper cards could be used to quantify sunitinib and N-desethyl sunitinib separately. The bio-analytical method using either DBS on pure cellulose paper cards or on DMPK-B paper cards has been validated with high accuracy and precision. However, DBS specific method validation parameters, e.g. spotted blood volume, haematocrit level and spot homogeneity were found to influence the accuracy and precision of the assay using DBS on DMPK-B cards. Additionally, when comparing sunitinib and N-desethyl sunitinib trough concentrations in paired patient samples resulting from the standard plasma method and the DBS method on DMPK-B cards, no correlation between the two methods was found. Probably, the lack of correlation between plasma and DBS concentrations is caused by influence of blood spot volume and homogeneity on results of DBS collected using DMPK-B cards. Therefore, use of DMPK-B cards for quantification of sunitinib and N-desethyl sunitinib should be limited to strictly regulated settings where volumetric pipettes are used to spot equally distributed, fixed volumes of blood. Thus, these cards can not be used for patient self-sampling by means of a finger prick.

R1
R2
R3
R4
R5
R6
R7
R8
R9
R10
R11
R12
R13
R14
R15
R16
R17
R18
R19
R20
R21
R22
R23
R24
R25
R26
R27
R28
R29
R30
R31
R32
R33
R34
R35
R36
R37
R38
R39

R1
R2
R3
R4
R5
R6
R7
R8
R9
R10
R11
R12
R13
R14
R15
R16
R17
R18
R19
R20
R21
R22
R23
R24
R25
R26
R27
R28
R29
R30
R31
R32
R33
R34
R35
R36
R37
R38
R39

Future perspectives

Pure cellulose based cards have been successfully used in various clinical applications [7-9,34-37]. Moreover, the effect of haematocrit on assay bias was within 15% for a clinical relevant haematocrit range using different analytes [24,25,34]. Less effect of haematocrit, blood volume and spot homogeneity would be expected when using these conventional paper cards, given the good correlation of the relationship between DBS and plasma samples found in the previously reported applications and our experience during method validation of the sum of sunitinib and N-desethyl sunitinib using these paper cards. Hence, it is plausible that clinical validation of quantification of the sum of sunitinib and N-desethyl sunitinib on conventional cellulose based paper cards would be successful. Therefore, it should be considered to use pure cellulose based paper cards for TDM of total sunitinib levels by self-sampling by means of a finger prick in a non-hospital based setting. This gives the opportunity to use DBS for TDM based on real trough levels and patient-friendly sampling. However, further investigation of the relationship between DBS and plasma samples for the sum of sunitinib and N-desethyl sunitinib is still warranted for clinical validation of this assay. Knowledge on use of DBS for quantitative analysis of drugs is rapidly expanding and, therefore, innovative solutions are expected to be available soon. Encouraging is the recent development of DBS paper cards on which blood cells and plasma are separated directly after spotting [38]. Use of this type of cards could probably overcome the problems with analyte stability due to oxidative catabolism by red blood cell enzymes, since plasma is separated from these cells before drying of the paper card. Moreover, using this type of card, the effect of haematocrit level on assay accuracy would be negligible. Thus, this new type of paper card might be useful in patient self-sampling for TDM of separately quantified sunitinib and N-desethyl sunitinib levels, when it can be confirmed that blood volume and spot homogeneity do not influence assay accuracy.

References

1. Demetri GD, van Oosterom AT, Garrett CR et al. Efficacy and safety of sunitinib in patients with advanced gastrointestinal stromal tumour after failure of imatinib: a randomised controlled trial. *Lancet* 2006; 368: 1329-38.
2. Motzer RJ, Michaelson MD, Redman BG et al. Activity of SU11248, a multitargeted inhibitor of vascular endothelial growth factor receptor and platelet-derived growth factor receptor, in patients with metastatic renal cell carcinoma. *J Clin Oncol* 2006; 24: 16-24.
3. Raymond E, Dahan L, Raoul JL et al. Sunitinib malate for the treatment of pancreatic neuroendocrine tumors. *N Engl J Med* 2011; 364: 501-13.
4. Houk BE, Bello CL, Poland B et al. Relationship between exposure to sunitinib and efficacy and tolerability endpoints in patients with cancer: results of a pharmacokinetic/pharmacodynamic meta-analysis. *Cancer Chemother Pharmacol* 2010; 66: 357-71.
5. de Jonge ME, Huitema AD, Schellens JH et al. Individualised cancer chemotherapy: strategies and performance of prospective studies on therapeutic drug monitoring with dose adaptation: a review. *Clin Pharmacokinet* 2005; 44: 147-73.
6. Faivre S, Delbaldo C, Vera K et al. Safety, pharmacokinetic, and antitumor activity of SU11248, a novel oral multitarget tyrosine kinase inhibitor, in patients with cancer. *J Clin Oncol* 2006; 24: 25-35.
7. Kromdijk W, Mulder JW, Rosing H et al. Use of dried blood spots for the determination of plasma concentrations of nevirapine and efavirenz. *J Antimicrob Chemother* 2012; 67: 1211-6.
8. Ter Heine R, Mulder JW, van Gorp EC et al. Clinical evaluation of the determination of plasma concentrations of darunavir, etravirine, raltegravir and ritonavir in dried blood spot samples. *Bioanalysis* 2011; 3: 1093-7.
9. La Marca G, Malvagias S, Filippi L et al. Rapid assay of topiramate in dried blood spots by a new liquid chromatography-tandem mass spectrometric method. *J Pharm Biomed Anal* 2008; 48: 1392-6.
10. La Marca G, Malvagias S, Filippi L et al. A new rapid micromethod for the assay of phenobarbital from dried blood spots by LC-tandem mass spectrometry. *Epilepsia* 2009; 50: 2658-62.
11. La Marca G, Malvagias S, Filippi L et al. Rapid assay of rufinamide in dried blood spots by a new liquid chromatography-tandem mass spectrometric method. *J Pharm Biomed Anal* 2011; 54: 192-7.
12. Blessborn D, Romsing S, Annerberg A et al. Development and validation of an automated solid-phase extraction and liquid chromatographic method for determination of lumefantrine in capillary blood on sampling paper. *J Pharm Biomed Anal* 2007; 45: 282-7.
13. Blessborn D, Romsing S, Bergqvist Y et al. Assay for screening for six antimalarial drugs and one metabolite using dried blood spot sampling, sequential extraction and ion-trap detection. *Bioanalysis* 2010; 2: 1839-47.
14. La Marca G, Giocaliere E, Villanelli F et al. Development of an UPLC-MS/MS method for the determination of antibiotic ertapenem on dried blood spots. *J Pharm Biomed Anal* 2012; 61: 108-13.
15. La Marca G, Villanelli F, Malvagias S et al. Rapid and sensitive LC-MS/MS method for the analysis of antibiotic linezolid on dried blood spot. *J Pharm Biomed Anal* 2012; 67-68: 86-91.
16. Sausseureau E, Lacroix C, Gaulier JM et al. On-line liquid chromatography/tandem mass spectrometry simultaneous determination of opiates, cocaine and amphetamines in dried blood spots. *J Chromatogr B Analyt Technol Biomed Life Sci* 2012; 885-886: 1-7.
17. Edelbroek PM, Heijden van der J, Stolk LML. Dried blood spot methods in therapeutic drug monitoring: methods, assays, and pitfalls. *Ther Drug Monit* 2009; 31: 327-36.

R1
R2
R3
R4
R5
R6
R7
R8
R9
R10
R11
R12
R13
R14
R15
R16
R17
R18
R19
R20
R21
R22
R23
R24
R25
R26
R27
R28
R29
R30
R31
R32
R33
R34
R35
R36
R37
R38
R39

R1
R2
R3
R4
R5
R6
R7
R8
R9
R10
R11
R12
R13
R14
R15
R16
R17
R18
R19
R20
R21
R22
R23
R24
R25
R26
R27
R28
R29
R30
R31
R32
R33
R34
R35
R36
R37
R38
R39

18. Li W, Tse FL. Dried blood spot sampling in combination with LC-MS/MS for quantitative analysis of small molecules. *Biomed Chromatogr* 2010; 24: 49-65.
19. U.S. Food and Drug Administration: Centre for Drug Evaluation and Research. Guidance for Industry: Bioanalytical Method Validation. Available at: <http://www.fda.gov/downloads/Drugs/GuidanceComplianceRegulatoryInformation/Guidances/UCM070107.pdf>. Date accessed: July 17, 2012. 2001.
20. Viswanathan CT, Bansal S, Booth B et al. Quantitative bioanalytical methods validation and implementation: best practices for chromatographic and ligand binding assays. *Pharm Res* 2007; 24: 1962-73.
21. Timmerman P, White S, Globig S et al. EBF recommendation on the validation of bioanalytical methods for dried blood spots. *Bioanalysis* 2011; 3: 1567-75.
22. Timmerman P, White S, Globig S et al. EBF and dried blood spots: from recommendations to potential resolution. *Bioanalysis* 2011; 3: 1787-9.
23. Steeghs N. Use of Individual Pharmacokinetically (PK)-Guided Sunitinib Dosing: A Feasibility Study in Patients With Advanced Solid Tumors (NCT01286896). Available at: <http://clinicaltrials.gov/ct2/show/NCT01286896?term=NCT01286896&rank=1>. Date accessed April 15, 2012. 2012.
24. O'Mara M, Hudson-Curtis B, Olson K et al. The effect of hematocrit and punch location on assay bias during quantitative bioanalysis of dried blood spot samples. *Bioanalysis* 2011; 3: 2335-47.
25. Wilhelm AJ, den Burger JC, Vos RM et al. Analysis of cyclosporin A in dried blood spots using liquid chromatography tandem mass spectrometry. *J Chromatogr B Analyt Technol Biomed Life Sci* 2009; 877: 1595-8.
26. European Medicines Agency (EMA). Sutent: EPAR - Scientific Discussion. Available at: http://www.ema.europa.eu/docs/en_GB/document_library/EPAR_-_Scientific_Discussion/human/000687/WC500057733.pdf. Date accessed: July 17, 2012. 2007.
27. Haznedar JO, Patyna S, Bello CL et al. Single- and multiple-dose disposition kinetics of sunitinib malate, a multitargeted receptor tyrosine kinase inhibitor: comparative plasma kinetics in non-clinical species. *Cancer Chemother Pharmacol* 2009; 64: 691-706.
28. Clinical and Laboratory Standards Institute (CLSI). Method comparison and Bias Estimation Using Patient Samples; Approved Guideline - Second Edition. NCCLS document EP9-A2. Available at: <http://www.jslab.cn/data/2006/EP09-A2.pdf>. Date accessed: March 3, 2012. 2010.
29. Bland JM, Altman DG. Statistical methods for assessing agreement between two methods of clinical measurement. *Lancet* 1986; 1: 307-10.
30. Kedderis GL, Hollenberg PF. Characterization of the N-demethylation reactions catalyzed by horseradish peroxidase. *J Biol Chem* 1983; 258: 8129-38.
31. Mieyal JJ, Starke DW. Hydroxylation and dealkylation reactions catalyzed by hemoglobin. *Methods Enzymol* 1994; 231: 573-98.
32. Stecca C, Cumps J, Duverger-Van BM. Enzymic N-demethylation reaction catalysed by red blood cell cytosol. *Biochem Pharmacol* 1992; 43: 207-11.
33. Whatman. DBS Technical Tips: Suggestions for Refining and Troubleshooting Dried Biosample Spot Analysis. Available at: <http://www.whatman.com/DMPK.aspx>. Date accessed: October 15, 2012. 2012.
34. Denniff P, Spooner N. The effect of hematocrit on assay bias when using DBS samples for the quantitative bioanalysis of drugs. *Bioanalysis* 2010; 2: 1385-95.
35. Meesters RJ, van Kampen JJ, Reedijk ML et al. Ultrafast and high-throughput mass spectrometric assay for therapeutic drug monitoring of antiretroviral drugs in pediatric HIV-1 infection applying dried blood spots. *Anal Bioanal Chem* 2010; 398: 319-28.
36. Van Schooneveld T, Swindells S, Nelson SR et al. Clinical evaluation of a dried blood spot assay for atazanavir. *Antimicrob Agents Chemother* 2010; 54: 4124-8.

37. Vu DH, Koster RA, Alffenaar JW et al. Determination of moxifloxacin in dried blood spots using LC-MS/MS and the impact of the hematocrit and blood volume. *J Chromatogr B Analyt Technol Biomed Life Sci* 2011; 879: 1063-70.
38. Whatman. Blood separation; product information. Available at: <http://www.whatman.com/PRODBloodSeparation.aspx>. Date accessed: October 15, 2012. 2012.

R1
R2
R3
R4
R5
R6
R7
R8
R9
R10
R11
R12
R13
R14
R15
R16
R17
R18
R19
R20
R21
R22
R23
R24
R25
R26
R27
R28
R29
R30
R31
R32
R33
R34
R35
R36
R37
R38
R39



Chapter 1.4

Determination of sunitinib and its active metabolite N-desethyl sunitinib in sweat of a patient

Nienke A.G. Lankheet
Christian U. Blank
Henk Mallo
Sandra Adriaansz
Hilde Rosing
Jan H.M. Schellens
Jos H. Beijnen
Alwin D.R. Huitema

Journal of Analytical Toxicology 2011;35(8):558-65.



R1
R2
R3
R4
R5
R6
R7
R8
R9
R10
R11
R12
R13
R14
R15
R16
R17
R18
R19
R20
R21
R22
R23
R24
R25
R26
R27
R28
R29
R30
R31
R32
R33
R34
R35
R36
R37
R38
R39

Abstract

Introduction. Skin reactions are side effects of sunitinib therapy with an adverse impact on quality of life often necessitating dose reductions. For conventional antineoplastic agents, such as doxorubicin, previous studies have indicated a possible relationship between sweat excretion and the development of skin toxicity. However, determination of sunitinib and its active metabolite in sweat has not been reported yet.

Method. A sensitive and accurate method for the determination of sunitinib and its active metabolite N-desethyl sunitinib in human sweat was developed using high-performance liquid chromatography coupled to tandem mass spectrometry detection (LC-MS/MS). Sweat samples of a patient treated with sunitinib were collected using Pharmchek™ Drugs of Abuse patches to determine cumulative amounts of sunitinib and metabolite.

Results. Validation of the LC-MS/MS method was performed over a range from 1.0-200 ng/patch with good intra- and interassay accuracies for sunitinib and N-desethyl sunitinib. Ranges of 76-119 and 7.9-10.5 ng/patch for cumulative secretion of sunitinib and metabolite, respectively, were found in patient samples.

Conclusion. To our knowledge this is the first method for determination of cumulative secretion of sunitinib and N-desethyl sunitinib in human sweat samples. Sunitinib and its metabolite were easily detectable in sweat patches of a patient treated with sunitinib.

Introduction

Sunitinib (Sutent®) is an orally available inhibitor of multiple tyrosine kinases. Sunitinib has proven efficacy as single agent in several solid tumor types and is approved for use in advanced renal cell cancer (RCC), and imatinib-resistant or -intolerant gastrointestinal stromal tumors (GISTs) [1,2]. Recent findings demonstrated a positive dose-efficacy relationship for sunitinib treatment, indicating that it should be the aim to dose patients as high as possible [3]. Target plasma concentrations of sunitinib plus active metabolite (N-desethyl sunitinib) are in the range of 50 to 100 ng/mL, as deduced from pharmacokinetic/pharmacodynamic preclinical data [4-8]. However, within this target range some patients already develop severe toxicities.

The most clinically relevant side effect of sunitinib appears to be the development of Hand-Foot Syndrome (HFS). HFS (all grades) occurred in 19% of patients in a pooled analysis of published clinical trials of sunitinib of whom 5% experienced severe HFS (grade 3 or 4) [9,10]. This skin toxicity severely impacts the quality of life of patients treated with sunitinib and thus impairs activities of daily living. Moreover, it can lead to unavoidable dose modifications or dose interruptions, which can negatively affect treatment efficacy [11,12].

The exact pathogenesis of HFS is unknown, but some hypotheses exist concerning the mechanism by which HFS is caused. The primarily affected sites in HFS, the palmoplantar surfaces, have a high density of eccrine glands which continuously excrete sweat [13,14]. Sweat can contain virtually any substance present in blood [15]. For conventional antineoplastic agents, such as doxorubicin, previous studies have indicated a possible relationship between hyperhidrosis on the palms and plantae and the development of skin toxicity [13]. This indicates that sweat functions as a carrier of drug to the skin surface. After excretion on the skin surface, sweat containing the drug may penetrate into the stratum corneum and cause toxicity [13]. However, secretion of sunitinib and its active metabolite N-desethyl sunitinib by the eccrine glands in sweat has not been studied yet [11,12]. Moreover, sweat is a non-conventional biological matrix in bioanalysis and no methods for determination of sunitinib in sweat have been reported in literature hitherto. We report here the development and validation of a method for determination of sunitinib and its active metabolite (N-desethyl sunitinib) in sweat using high performance liquid chromatography coupled to tandem mass spectrometry (HPLC-MS/MS). Additionally, we report the determination of cumulative excretion of sunitinib and its metabolite in samples of a patient treated with sunitinib.

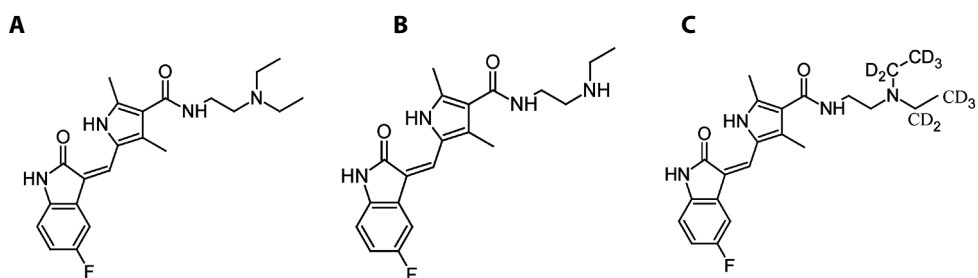
Materials and methods

Chemicals and materials

Reference standards and internal standards were provided by the following manufacturers: Sunitinib maleate ($C_{22}H_{27}FN_4O_2 \cdot C_4H_6O_5$) by Sequoia Research Products (Oxford, United Kingdom), N-desethyl sunitinib ($C_{20}H_{23}FN_4O_2$) by Toronto Research Chemicals (North York, ON, Canada),

R1
R2
R3
R4
R5
R6
R7
R8
R9
R10
R11
R12
R13
R14
R15
R16
R17
R18
R19
R20
R21
R22
R23
R24
R25
R26
R27
R28
R29
R30
R31
R32
R33
R34
R35
R36
R37
R38
R39

R1 sunitinib-²H₁₀ (C₂₂H₂₃FN₄O₂D₁₀) stable isotope by Alsa Chim (Illkirch, France). The chemical
R2 structures of sunitinib, N-desethyl sunitinib and sunitinib-²H₁₀ are depicted in Figure 1. HPLC-grade
R3 acetonitrile and methanol were purchased from Biosolve (Valkenswaard, The Netherlands). Distilled
R4 water was obtained from B. Braun (Melsungen, Germany). Ammonia 25% was purchased from
R5 Merck (Darmstadt, Germany). PharmChek™ Drugs of Abuse patches, used for sweat collection,
R6 were from PharmChem Inc. (Forth Worth, TX, USA).



R16 **Figure 1.** Chemical structures of sunitinib (A), N-desethyl sunitinib (B) and sunitinib-²H₁₀ (C)

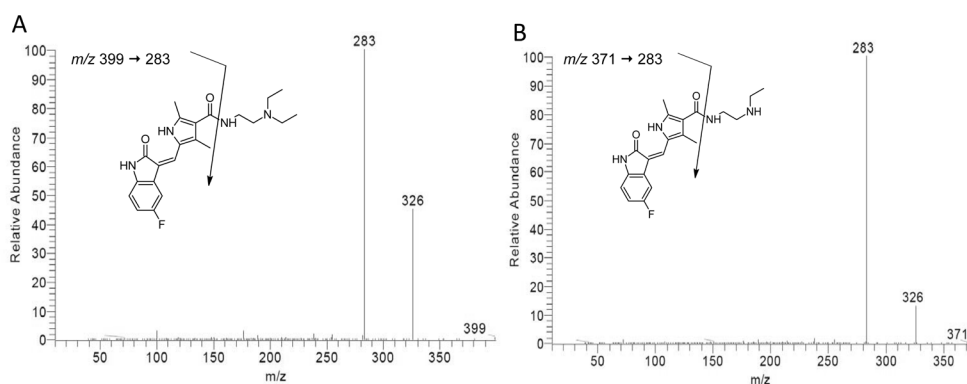
R17
R18 **Instrumentation**

R19 Determination of sunitinib, N-desethyl sunitinib and the internal standard was performed on a
R20 HPLC system (LC-20AD Prominence binary solvent delivery system) with a column oven, DGU-20A3
R21 online degasser and a SIL-HTc controller (all: Shimadzu, Kyoto, Japan) coupled to a TSQ Quantum
R22 Ultra triple quadrupole mass spectrometer equipped with an electrospray ionisation source (ESI)
R23 operating in the positive ion mode (Thermo Fisher Scientific, Waltham, MA, USA). Separation was
R24 carried out on a reversed phase system with a Gemini C₁₈ column (50 x 2.0 mm ID, 5.0 μm particle
R25 size; Phenomenex, Torrance, CA, USA) protected with a Securityguard Gemini precolumn (4 x 2.0
R26 mm ID, 5.0 μm particle size; Phenomenex) and thermostatted at 40 °C. The injection volume was
R27 10 μL. Compounds were eluted on a linear gradient at a flow rate of 250 μL/min. The mobile phase
R28 consisted of a mixture of 10 mM ammonium hydroxide in water at pH 10.5 (A) and 1 mM ammonium
R29 hydroxide in methanol (B). Before each new injection the column was reconditioned for 3 minutes
R30 with 55% B (v/v) resulting in a total run time of 10 min. The chromatographic separation conditions
R31 are given in Table 1. The divert valve was directed to waste during the first 1.5 min and last 2.0 min
R32 to prevent the introduction of endogenous compounds into the mass spectrometer.

Table 1. Gradient composition during the HPLC-run

Time (min)	Flow (mL/min)	Ammonium hydroxide in water 10 mM (% v/v)	Ammonium hydroxide in MeOH 1 mM (% v/v)
0.0	0.25	45	55
0.5	0.25	45	55
3.0	0.25	20	80
6.0	0.25	20	80
6.1	0.25	5	95
8.0	0.25	5	95
8.1	0.25	45	55
10.0	0.25	45	55

For quantification, multiple reaction monitoring (MRM) chromatograms were acquired with LCQuan™ software version 2.5 (Thermo Fisher Scientific). Positive ions were created at atmospheric pressure and the quadrupoles were operating in unit resolution (0.7 Da). Mass transitions from m/z 399 to 283 for sunitinib, m/z 371 to 283 for N-desethyl sunitinib and m/z 409 to 283 for internal standard sunitinib- $^2\text{H}_{10}$ were optimised (see Figure 2). The ESI-MS/MS operating parameters used in this study are listed in Table 2.

**Figure 2.** MS/MS product ion scan of sunitinib (A; precursor ion m/z 399) and N-desethyl sunitinib (B; precursor ion m/z 371).

Preparation of calibration and validation samples

A set of stock solutions of sunitinib and N-desethyl sunitinib were prepared from two independent weightings; one for the calibration standards and one for the validation samples.

For the preparation of the calibration standards, working solutions in the range from 10 to 1,000 ng/ml were used. Four working solutions in the range from 10 to 800 ng/ml were prepared for spiking the validation samples.

For the preparation of all calibration and validation samples sweat patches (Pharmchek™ Drugs of abuse patches, PharmChem Inc.) applied on the upper arm of healthy volunteers for

at least 24 hours were used. Halves of these drug free blank sweat patches were spiked with a volume of working solution to obtain calibration and validation samples with different amounts of sunitinib and N-desethyl sunitinib.

Sample preparation

Sample preparation was performed and validated on sweat patches which were cut into two equal parts to allow re-analysis of study samples when necessary. Half of each patch was cut into smaller parts, which were transferred into a 2 mL Eppendorf tube. To each sample 20 µL internal standard sunitinib-²H₁₀ (100 ng/mL) and 1.5 mL of extraction solvent (methanol) were added. Tubes were closed and shaken for 60 min. Then the extraction solvent was transferred into an Eppendorf tube using a pipette and then evaporated under a gentle flux of nitrogen at 40 °C till dryness. To reconstitute the dry extracts, 100 µL of a mixture of eluent A and eluent B (1:1, v/v) was used. The samples were homogenized by vortex mixing for 30 seconds. To eliminate any present sweat patch fibres, the final extract was centrifuged at 3,000 x g for 1 minute at room temperature. The supernatant was transferred into an autosampler vial and 10 µL were injected onto the HPLC column.

Table 2. Mass spectrometer settings

Parameter	Setting		
Run duration	10 min		
Ionspray voltage	3,0 kV		
Sheath gas (N ₂)	35 psi		
Auxiliary gas (N ₂)	15 psi		
Ion sweep gas (N ₂)	2 psi		
Tube lens offset	12 V		
Capillary temperature	350 °C		
Collision pressure (argon)	1,5 mTorr		
Chrom filter peak width	10 s		
	Sunitinib	N-desethyl sunitinib	Sunitinib-d10
Q1 mass	399 amu	371 amu	409 amu
Q3 mass	283 amu	283 amu	283 amu
Dwell time	30 ms	30 ms	30 ms
Collision energy	30 V	23 V	32 V
Tube lens voltage	97 V	81 V	91 V

Validation experiments

A validation of the assay was performed according to the FDA guidelines for validation of bioanalytical assays including linearity, inaccuracy, precision, specificity, selectivity, cross-analyte/internal standard interference, recovery, ion suppression, carry-over and stability [16,17]. Since blank human sweat is difficult to obtain, procedures for assessment of recovery, ion suppression and stability were performed on just one concentration level of the calibration range.

Calibration curves. Six non-zero calibration samples were prepared by spiking working solutions to sweat patches. The final concentrations were 0.00, 1.00, 5.00, 10.0, 50.0, 100, 200 ng/patch of sunitinib and N-desethyl sunitinib. The lowest calibration sample (1.00 ng/mL) is defined as the lower limit of quantification (LLOQ) and the highest calibration sample (200 ng/mL) is defined as the upper limit of quantification (ULOQ). Calibration samples were analysed in duplicate in three separate analytical runs. The linear regression of the area ratio of the analytes and the internal standard peaks versus the concentration were weighted with weighting factor $1/x^2$. The linearity was evaluated by means of back-calculated concentrations of the calibration standards.

Inaccuracy and precision. Inaccuracy and precision of the assay were established by analysing validation samples with analyte concentrations at the LLOQ and at low, mid and high concentration of the calibration range. The final concentrations were 1.00, 3.00, 20.0 and 160 ng/patch for both analytes. Replicates of each validation sample were measured in three separate analytical runs to evaluate the intra- and inter-assay inaccuracy and precision. Validation samples with analyte concentrations above the ULOQ were processed and diluted 1:10 (v/v) in reconstitution solvent before injection to obtain analyte single reaction monitoring (SRM) responses within the validated range. These samples were processed in 5-fold and measured in a single analytical run with a dilution factor of 1/10 on the internal standard concentration to assess the inaccuracy and precision after dilution. For acceptance, the intra- and inter-assay inaccuracies should be within $\pm 20\%$ for the LLOQ and $\pm 15\%$ for all other concentrations. The precisions CV% should be less than 20% for the LLOQ and less than 15% for all other concentrations.

Specificity and selectivity. To investigate whether endogenous compounds from sweat could interfere with the detection of the analytes or the internal standard, six different batches of control drug-free human sweat patches were prepared as double blanks (containing neither analyte nor internal standard) and LLOQ samples. Areas of peaks co-eluting with the analytes should not exceed 20% of the area at the LLOQ level and 5% of the area at the internal standard level.

Cross analyte interference. To investigate possible cross interference between sunitinib, N-desethyl sunitinib and the internal standard, a cross interference check was performed. Drug-free human sweat was spiked at ULOQ level (with both analytes separately) and was processed without internal standard. Also drug-free human sweat with only internal standard was processed. The response of any interfering peak with the same retention time as sunitinib or N-desethyl sunitinib should be less than 20% of the response of a LLOQ sample.

Matrix effect. Ion suppression was examined by comparing the analytical response of processed blanks spiked with analyte with those of unprocessed samples in reconstitution solvent. Additionally, the matrix factor was calculated by comparing the internal standard corrected analytical response of processed blanks spiked with analyte with those of unprocessed samples in reconstitution solvent.

Recovery. The extraction recovery of the analytes was determined by comparing the analytical response of processed samples with those of processed blanks spiked with analyte.

R1
R2
R3
R4
R5
R6
R7
R8
R9
R10
R11
R12
R13
R14
R15
R16
R17
R18
R19
R20
R21
R22
R23
R24
R25
R26
R27
R28
R29
R30
R31
R32
R33
R34
R35
R36
R37
R38
R39

Carry over. Carry-over was tested by injecting two processed blank matrix samples sequentially after injecting an ULOQ sample. The response in the first blank matrix at the retention times of sunitinib, N-desethyl sunitinib and sunitinib-²H₁₀ should be less than 20% of the response of a LLOQ sample.

Stability. The stability of sunitinib and N-desethyl sunitinib in spiked sweat patches after two freeze/thaw cycles from nominally -20 °C to ambient temperatures and after 7 days at ambient temperatures and skin temperature (32°C) was investigated. Additionally, the long term stability of sunitinib and N-desethyl sunitinib in sweat patches stored at -20°C for 14 months was investigated. The processed sample stability of sunitinib and N-desethyl sunitinib was investigated after 1 day (ambient temperature) and 7 days (2-8 °C). The re-injection reproducibility was determined after 7 days of storage in the autosampler (4 °C). The analytes were considered to be stable in the matrix or final extract if 85–115% of the initial concentrations was recovered.

Patient samples. A 68-year female patient was treated with sunitinib for metastasized renal cell cancer (mRCC). The sunitinib regimen consisted of an on-treatment phase of 4 weeks (days 1-28) followed by an off-treatment phase of 2 weeks (days 29-42). She received a modified dosing scheme with reduced doses (alternating 25 mg on one day and 37.5 mg the other day), but nevertheless she suffered from HFS. To collect sweat samples, sweat patches were applied to the patients upper arm during seven consecutive days of the on-treatment phase (days 22-28) and of the off-treatment phase (days 36-42) (see Figure 3). The patches were stored in accessory plastic bags at -20 °C until analysis.



Figure 3. Time scheme of patch application during the 6 weekly cycle (4 week treatment followed by 2 weeks of no treatment) of sunitinib treatment. Black bars represent the weeks on which the patches were applied.

Results and discussion

Method development

The amount of sunitinib and metabolite in sweat was unknown but expected to be low. However, since it was decided to collect the cumulative amount and not the instantaneous concentration of the drug in sweat for a better reflection of the total skin exposure, assay sensitivity would not be a problem. Sweat samples were collected in a cumulative way by application of the PharmChek™ Drugs of Abuse patches for seven consecutive days. These sweat patches exist of a cellulose absorption pad of 480 by 320 mm covered with an adhesive semi-permeable polyurethane film

layer. Non-volatile substances from sweat will accumulate in the pad. The semi-permeable film layer allows water, oxide and carbondioxide to pass through the patch keeping the skin underneath healthy and preventing from external contamination during the period of application [18].

The sample pre-treatment procedure for sweat patches was derived from previously reported HPLC-MS/MS analyses of the drugs fentanyl and methylphenidate in sweat patches [19,20]. During assay development different sample pre-treatment procedures reported in literature were compared [19,20]: 4.0, 2.0, 1.5 mL methanol and 1.5 mL methanol/water (1:1 v/v) as extraction solvent; evaporation of the extract in one vs. two steps; and using half patches vs. cutting the half patches into smaller parts before extraction. The procedure with the highest SRM responses in combination with a good reproducibility was the method using half patches cut into smaller parts before extraction; extraction with 1.5 mL methanol in 2.0 mL Eppendorf tubes; and evaporation of the extract in one step. Before injection of the reconstituted sweat extract onto the column, an additional centrifugation step was inserted to eliminate any sweat patch fibers present, which could possibly clog the HPLC system after sample injection.

Early in the assay development process it became clear that unused patches spiked with analytes gave higher SRM responses than patches worn by healthy volunteers before spiking with analytes. No stable isotope labelled N-desethyl sunitinib was available to correct for this apparent ion suppression due to matrix effects during the HPLC-MS/MS analysis. For this reason only sweat patches applied on the upper arm of healthy volunteers for at least 24 hours were used for the preparation of calibration and validation samples to take into account any of the matrix effects of sweat and any background signal of the patches. Influence of using batches sweat of different individuals was negligible as established in the selectivity experiments during assay validation.

One half of each patch was used to perform the analysis allowing to perform once a re-analysis on the remaining other half of the patch, when necessary. Sunitinib and N-desethyl sunitinib seemed to be homogeneously distributed through the whole patch, since the analysis of two halves of one patch showed a low variability in result of CV% 4.78 and 6.44 for sunitinib and N-desethyl sunitinib, respectively. So, the use of half a patch was accurate and precise. Moreover, use of half patches did not affect the height of the LLOQ level, because even when using half patches the signal to noise ratio (S/N-ratio) at LLOQ level (1.0 ng/patch) was >100.

Peaks with satisfying peak shapes were obtained when the linear gradient starting on 55% eluent B was followed by an isocratic elution with 80% eluent B at a flow rate of 0.25 mL per min (see Table 1). Typical chromatograms of LLOQ samples are depicted in Figure 4.

R1
R2
R3
R4
R5
R6
R7
R8
R9
R10
R11
R12
R13
R14
R15
R16
R17
R18
R19
R20
R21
R22
R23
R24
R25
R26
R27
R28
R29
R30
R31
R32
R33
R34
R35
R36
R37
R38
R39

R1
R2
R3
R4
R5
R6
R7
R8
R9
R10
R11
R12
R13
R14
R15
R16
R17
R18
R19
R20
R21
R22
R23
R24
R25
R26
R27
R28
R29
R30
R31
R32
R33
R34
R35
R36
R37
R38
R39

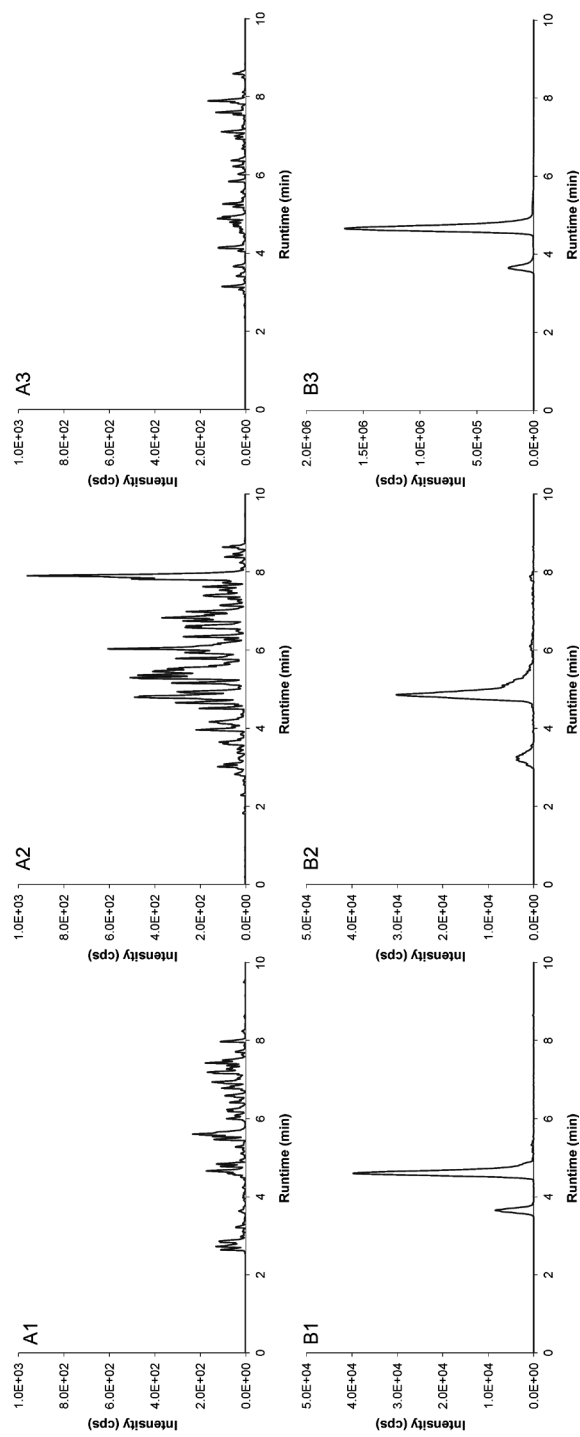


Figure 4. Representative LC-MS/MS chromatograms of a blank human sweat sample (A1, sunitinib; A2, N-desethyl sunitinib; A3, internal standard sunitinib- $^2\text{H}_{10}$) and of a spiked human sweat sample at the LLOQ level of 1.0 ng/patch (B1, sunitinib; B2, N-desethyl sunitinib; B3, internal standard sunitinib- $^2\text{H}_{10}$).

In the chromatograms of sunitinib, N-desethyl sunitinib and sunitinib-²H₁₀ two peaks with the same molecular mass/mass transition were present. This is due to the presence of E/Z configurations in solution, as has been reported before [21-23]. The isomerization reaction of the Z-isomer into the E-isomer is induced by exposure to light and is reversible. The retention times of sunitinib were 3.6 and 4.6 min. for the E- and Z-isomers, respectively. For the E- and Z-isomers of N-desethyl sunitinib the retention times were 3.2 and 4.8 min., respectively. Since both isomers showed equal MS responses, the sum of the SRM responses of both separated isomers of the analytes and internal standard were used to process the data [21].

Validation experiments

Linearity. The assay was linear over the validated concentration range from 1.00 to 200 ng/patch of sunitinib and N-desethyl sunitinib in human sweat. Correlation coefficients (r²) were respectively at least 0.991 and 0.989 for sunitinib and N-desethyl sunitinib.

Inaccuracy and precision. The intra- and inter-assay performance data are presented in Table 3.

Selectivity. In MRM chromatograms of six batches of control drug-free human sweat no interference of endogenous compounds from sweat could be detected with the analyte or the internal standard.

Cross analyte interference. For sunitinib and the internal standard no cross interferences were found. In contrast, when a sample with sunitinib at ULOQ level was processed without internal standard, peaks were detected at the retention time of N-desethyl sunitinib. Additionally, by analyzing academic dilutions of freshly prepared sunitinib stock solution, approximately 1% of the sunitinib area was shown in the mass transition window of N-desethyl sunitinib. This signal was proportional to the signal in processed Cross Analyte Interference samples of sunitinib. Therefore, we conclude that the cross interference originated from the reference standard of sunitinib and did not arise in the samples during processing. The response of the interfering peak in the N-desethyl sunitinib window accounted for at most 7.10% (CV % 4.4) of the total SRM response of N-desethyl sunitinib in the calibration and validation samples. Since the contribution of the interfering peaks was within 15% of deviation from the nominal concentrations, the results for cross interference were found to be acceptable and no relating problems will be expected during quantification of the analytes.

Matrix effect. The matrix effect detected for sunitinib and N-desethyl sunitinib was a suppression of SRM signal of 70.4% and 71.4%, respectively. The observed matrix effect was just partly due to influences of the sweat matrix. Namely, since there was also a discrepancy in SRM signal between final extract of spiked unused patches and spiked unprocessed samples (suppression 30.3% for sunitinib and 18.5% for N-desethyl sunitinib) the suppression seems to be partly due to exogenous compounds originating from the patches. For quantification of sunitinib the stable isotope labelled internal standard (sunitinib-²H₁₀) corrected well for the ion suppression effects (matrix factor 1.04). For quantification of N-desethyl sunitinib the matrix factor was 0.89.

R1
R2
R3
R4
R5
R6
R7
R8
R9
R10
R11
R12
R13
R14
R15
R16
R17
R18
R19
R20
R21
R22
R23
R24
R25
R26
R27
R28
R29
R30
R31
R32
R33
R34
R35
R36
R37
R38
R39

R1
R2
R3
R4
R5
R6
R7
R8
R9
R10
R11
R12
R13
R14
R15
R16
R17
R18
R19
R20
R21
R22
R23
R24
R25
R26
R27
R28
R29
R30
R31
R32
R33
R34
R35
R36
R37
R38
R39

Recovery. For sunitinib the mean extraction recovery was 90.3% and the mean total recovery was 27.6% and for N-desethyl sunitinib the mean extraction recovery was 71.5% and the mean total recovery was 21.6%. Due to the matrix effect the total recovery was very low, but nevertheless this recovery was reproducible (CV% 1.1 for sunitinib and CV% 9.5 for N-desethyl sunitinib).

Carry over. No carry-over was observed since no interfering peaks were detected in processed blank samples injected after an ULOQ sample, due to the use of 100% eluent B after elution of the analytes.

Stability. Sunitinib and N-desethyl sunitinib are stable in sweat patches for at least two freeze (-20 °C) / thaw cycles and in sweat patches at ambient and skin temperatures (20 °C and 32°C, respectively) up to at least 7 days. Additionally, the long term stability of sunitinib and N-desethyl sunitinib in sweat patches stored at -20 °C is at least 14 months. Besides, sunitinib and N-desethyl sunitinib are stable in the final extract at least 24 h at ambient temperature and up to 7 days at nominally 2-8 °C. Re-injection reproducibility was established and an analytical run can be re-injected after at least 7 days of storage in the autosampler at 4 °C.

Table 3. Assay performance data for sunitinib (A) and N-desethyl sunitinib (B).

A) Sunitinib						
Run		Nominal conc. (ng/mL)	Mean calculated conc. (ng/mL)	Inaccuracy (% Dev)	Precision (%CV)	No. of replicates
	1	1.01	1.01	-0.50	0.14	2
	2	1.01	0.97	-3.96	13.1	2
	3	1.01	0.87	-13.9	6.08	3
Inter-assay		1.01	0.94	-7.21	9.41	7
	1	3.04	2.94	4.75	3.57	2
	2	3.04	2.80	-8.06	7.84	2
	3	3.04	2.95	-3.07	6.08	3
Inter-assay		3.04	2.90	-2.26	8.12	7
	1	20.2	22.1	9.51	1.19	2
	2	20.2	22.6	11.9	3.63	2
	3	20.2	21.6	6.86	3.57	3
Inter-assay		20.2	22.0	9.07	3.32	7
	1	162	154	-5.08	2.23	2
	2	162	167	3.12	1.88	2
	3	162	161	-0.82	4.64	3
Inter-assay		162	161	-0.61	4.48	7
B) N-desethyl sunitinib						
Run		Nominal conc. (ng/mL)	Mean calculated conc. (ng/mL)	Inaccuracy (% Dev)	Precision (%CV)	No. of replicates
	1	1.01	1.11	9.55	7.48	2
	2	1.01	1.02	0.50	13.2	2
	3	1.01	0.98	-2.97	3.68	3
Inter-assay		1.01	1.03	1.60	8.63	7
	1	3.04	2.61	-14.3	13.4	2
	2	3.04	2.94	-3.29	12.5	2
	3	3.04	2.98	-1.86	7.16	3
Inter-assay		3.04	2.86	-5.81	10.4	7
	1	20.2	18.0	-10.8	0.48	2
	2	20.2	20.0	-0.89	0.64	2
	3	20.2	19.2	-5.20	8.38	3
Inter-assay		20.2	19.1	-5.57	6.50	7
	1	162	139	-14.2	1.09	2
	2	162	173	6.96	4.33	2
	3	162	157	-3.20	2.98	3
Inter-assay		162	156	-3.43	9.31	7

R1
R2
R3
R4
R5
R6
R7
R8
R9
R10
R11
R12
R13
R14
R15
R16
R17
R18
R19
R20
R21
R22
R23
R24
R25
R26
R27
R28
R29
R30
R31
R32
R33
R34
R35
R36
R37
R38
R39

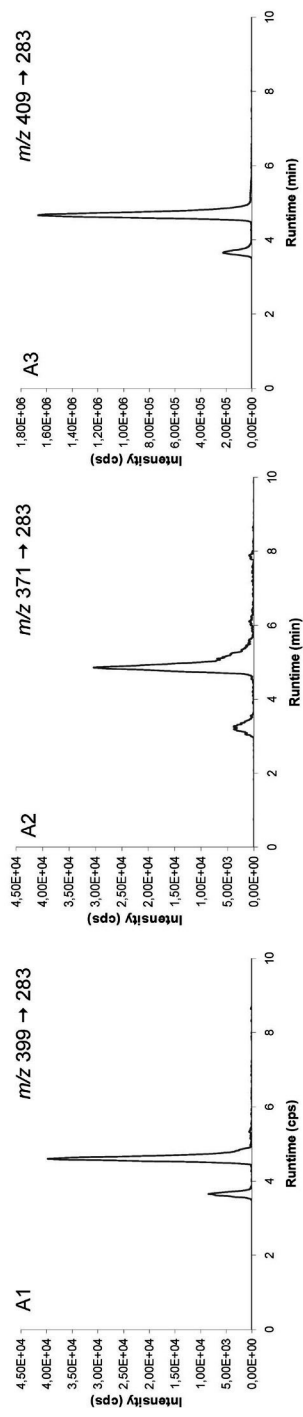


Figure 5. Representative LC-MS/MS chromatograms of a sweat patch applied to the patients upper arm during seven consecutive days of the off-treatment phase (days 36-42) of therapy (A1, sunitinib; A2, N-desethyl sunitinib; A3, internal standard sunitinib- $^2H_{10}$).

Sunitinib in patients' sweat samples

The exposure of drugs to the skin during a certain period of time depends on both the concentration of drugs in sweat and the degree of sweat secretion. Moreover, a patient with a low sunitinib concentration in sweat, but a excessively high sweat excretion would have a higher skin exposure than a patient with a high sunitinib concentration in sweat and practically no sweat excretion. Therefore, the cumulative amount of sunitinib in the patch would probably be of more clinical relevance than the absolute concentration of sunitinib in sweat. Thus, it was decided to collect sweat in a cumulative way by application of the sweat patches for seven consecutive days.

As a proof of concept half a sweat patch of a patient was processed simultaneously with an unused blank patch. This gave satisfying results, since sunitinib and N-desethyl sunitinib were easily detectable in the sweat patch which was applied on the upper arm during seven consecutive days. Typical chromatograms of a patient's sweat patch applied during the off-treatment phase (days 36-42) of therapy are depicted in Figure 5.

In the samples of a patient that were collected during the on-treatment phase and the off-treatment phase of the sunitinib therapy regimen, we found ranges of 76-119 and 7.9-10.5 ng/patch for cumulative secretion of sunitinib and its metabolite, respectively (see Figure 6). These amounts were all within the validated range of 1.0 to 200 ng/patch. Additionally, even in the second week after the administration of sunitinib, the cumulative amounts of sunitinib and N-desethyl sunitinib in the sweat patches were far above the LLOQ.

At LLOQ level (1.0 ng/patch) a signal to noise ratio (S/N-ratio) of >100 was obtained. Since this S/N-ratio is high, quantification of amounts less than 1 ng/patch of sunitinib and metabolite would be possible, but these amounts were not found to be clinically relevant. Our patient samples showed cumulative amounts of sunitinib and N-desethyl sunitinib above the LLOQ even at the end of the off-treatment phase. As expected, the skin exposure to sunitinib and metabolite during the off-treatment phase is lower compared to the on-treatment phase. In plasma N-desethyl sunitinib levels are approximately one third of the sunitinib levels [24]. Besides, due to more hydrophilic properties of the N-desethyl metabolite the secretion onto the skin would be decreased compared to the parent drug [15]. Thereby, the observed difference in sunitinib and N-desethyl sunitinib levels in sweat during treatment can be explained. Strikingly, in the off-treatment phase of our case the cumulative levels of the metabolite were higher compared to the parent drug. This observation can be explained by the difference in elimination half life of both compounds, namely 40-60 h for sunitinib and 80-110 h for N-desethyl sunitinib. As a result, the metabolite remains in plasma for a longer time period and therefore the excretion of this compound in sweat will also be sustained.

R1
R2
R3
R4
R5
R6
R7
R8
R9
R10
R11
R12
R13
R14
R15
R16
R17
R18
R19
R20
R21
R22
R23
R24
R25
R26
R27
R28
R29
R30
R31
R32
R33
R34
R35
R36
R37
R38
R39

R1
R2
R3
R4
R5
R6
R7
R8
R9
R10
R11
R12
R13
R14
R15
R16
R17
R18
R19
R20
R21
R22
R23
R24
R25
R26
R27
R28
R29
R30
R31
R32
R33
R34
R35
R36
R37
R38
R39

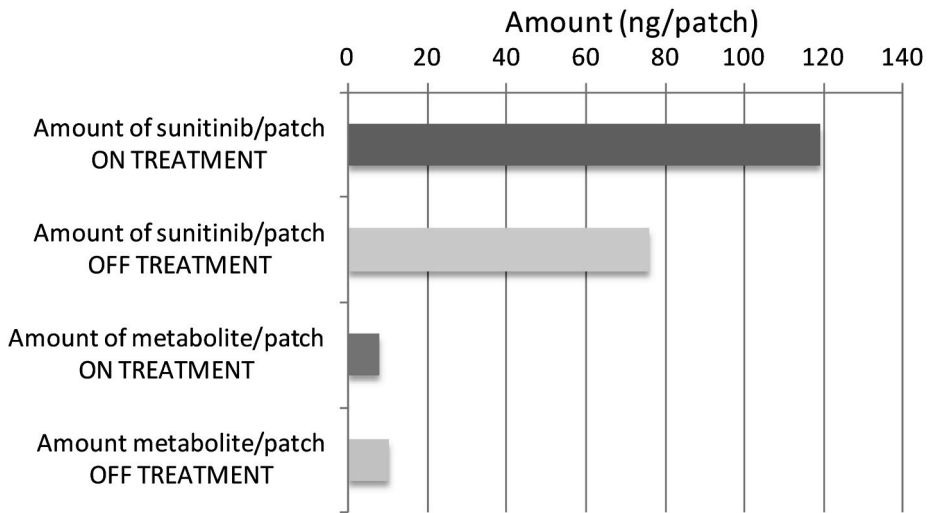


Figure 6. Cumulative amounts of sunitinib and N-desethyl sunitinib in sweat of a patient on sunitinib therapy wearing sweat patches for seven consecutive days during the on-treatment and off-treatment phase.

Conclusion

We have developed and validated a sensitive and easy to perform HPLC-MS/MS method for analysis of sunitinib and N-desethyl sunitinib in human sweat samples. To our knowledge this is the first report of bio-analytical determination of sunitinib secretion in sweat of a patient. Human sweat samples are collected using PharmChek™ Drugs of Abuse Patches. The sweat patches with sunitinib and N-desethyl sunitinib are pre-treated by extraction with methanol and addition of internal standard sunitinib-²H₁₀. A linear dynamic range from 1.0 to 200 ng/patch has been validated. Validation results show that the method is accurate and precise. From our patient samples we concluded that cumulative amounts of sunitinib and N-desethyl sunitinib could be easily detected in human sweat patches applied on the upper arm of a patient during seven consecutive days.

References

1. Demetri GD, van Oosterom AT, Garrett CR et al. Efficacy and safety of sunitinib in patients with advanced gastrointestinal stromal tumour after failure of imatinib: a randomised controlled trial. *Lancet* 2006; 368: 1329-38.
2. Motzer RJ, Michaelson MD, Redman BG et al. Activity of SU11248, a multitargeted inhibitor of vascular endothelial growth factor receptor and platelet-derived growth factor receptor, in patients with metastatic renal cell carcinoma. *J Clin Oncol* 2006; 24: 16-24.
3. Houk BE, Bello CL, Poland B et al. Relationship between exposure to sunitinib and efficacy and tolerability endpoints in patients with cancer: results of a pharmacokinetic/pharmacodynamic meta-analysis. *Cancer Chemother Pharmacol* 2010; 66: 357-71.
4. Abrams TJ, Murray LJ, Pesenti E et al. Preclinical evaluation of the tyrosine kinase inhibitor SU11248 as a single agent and in combination with "standard of care" therapeutic agents for the treatment of breast cancer. *Mol Cancer Ther* 2003; 2: 1011-21.
5. Abrams TJ, Lee LB, Murray LJ et al. SU11248 inhibits KIT and platelet-derived growth factor receptor beta in preclinical models of human small cell lung cancer. *Mol Cancer Ther* 2003; 2: 471-8.
6. Faivre S, Delbaldo C, Vera K et al. Safety, pharmacokinetic, and antitumor activity of SU11248, a novel oral multitarget tyrosine kinase inhibitor, in patients with cancer. *J Clin Oncol* 2006; 24: 25-35.
7. Mendel DB, Laird AD, Xin X et al. In vivo antitumor activity of SU11248, a novel tyrosine kinase inhibitor targeting vascular endothelial growth factor and platelet-derived growth factor receptors: determination of a pharmacokinetic/pharmacodynamic relationship. *Clin Cancer Res* 2003; 9: 327-37.
8. Murray LJ, Abrams TJ, Long KR et al. SU11248 inhibits tumor growth and CSF-1R-dependent osteolysis in an experimental breast cancer bone metastasis model. *Clin Exp Metastasis* 2003; 20: 757-66.
9. Rosenbaum SE, Wu S, Newman MA et al. Dermatological reactions to the multitargeted tyrosine kinase inhibitor sunitinib. *Support Care Cancer* 2008; 16: 557-66.
10. Chu D, Lacouture ME, Weiner E et al. Risk of hand-foot skin reaction with the multitargeted kinase inhibitor sunitinib in patients with renal cell and non-renal cell carcinoma: a meta-analysis. *Clin Genitourin Cancer* 2009; 7: 11-9.
11. Lacouture ME, Wu S, Robert C et al. Evolving strategies for the management of hand-foot skin reaction associated with the multitargeted kinase inhibitors sorafenib and sunitinib. *The Oncologist* 2008; 13: 1001-11.
12. Lacouture ME, Reilly LM, Gerami P et al. Hand foot skin reaction in cancer patients treated with the multikinase inhibitors sorafenib and sunitinib. *Ann Oncol* 2008; 19: 1955-61.
13. Jacobi U, Waibler E, Schulze P et al. Release of doxorubicin in sweat: first step to induce the palmar-plantar erythrodysesthesia syndrome? *Ann Oncol* 2005; 16: 1210-1.
14. Lipworth AD, Robert C, Zhu AX. Hand-foot syndrome (hand-foot skin reaction, palmar-plantar erythrodysesthesia): focus on sorafenib and sunitinib. *Oncology* 2009; 77: 257-71.
15. Rivier L. Techniques for analytical testing of unconventional samples. *Bailliere's Clinical Endocrinology and Metabolism.*, 2000 edition. 2010;147-65.
16. U.S.Food and Drug Administration: Centre for Drug Evaluation and Research. Guidance for Industry: Bioanalytical Method Validation. <http://www.fda.gov/downloads/Drugs/GuidanceComplianceRegulatoryInformation/Guidances/UCM070107.pdf>. 1-5-2001.
17. Viswanathan CT, Bansal S, Booth B et al. Quantitative bioanalytical methods validation and implementation: best practices for chromatographic and ligand binding assays. *Pharm Res* 2007; 24: 1962-73.

R1
R2
R3
R4
R5
R6
R7
R8
R9
R10
R11
R12
R13
R14
R15
R16
R17
R18
R19
R20
R21
R22
R23
R24
R25
R26
R27
R28
R29
R30
R31
R32
R33
R34
R35
R36
R37
R38
R39

18. Hartley M, Crook D. PharmChek Drugs of Abuse Sweat Patch (product information). 2010. Product Information. 1-10-2010.
19. Marchei E, Farre M, Pellegrini M et al. Liquid chromatography-electrospray ionization mass spectrometry determination of methylphenidate and ritalinic acid in conventional and non-conventional biological matrices. *J Pharm Biomed Anal* 2009; 49: 434-9.
20. Schneider S, Ait MB, Schummer C et al. Determination of fentanyl in sweat and hair of a patient using transdermal patches. *J Anal Toxicol* 2008; 32: 260-4.
21. Haouala A, Zanolari B, Rochat B et al. Therapeutic Drug Monitoring of the new targeted anticancer agents imatinib, nilotinib, dasatinib, sunitinib, sorafenib and lapatinib by LC tandem mass spectrometry. *J Chromatogr B Analyt Technol Biomed Life Sci* 2009; 877: 1982-96.
22. Sistla A, Shenoy N. Reversible Z-E isomerism and pharmaceutical implications for SU5416. *Drug Dev Ind Pharm* 2005; 31: 1001-7.
23. Sparidans RW, Iusuf D, Schinkel AH et al. Liquid chromatography-tandem mass spectrometric assay for the light sensitive tyrosine kinase inhibitor axitinib in human plasma. *J Chromatogr B Analyt Technol Biomed Life Sci* 2009; 877: 4090-6.
24. Britten CD, Kabbinavar F, Hecht JR et al. A phase I and pharmacokinetic study of sunitinib administered daily for 2 weeks, followed by a 1-week off period. *Cancer Chemother Pharmacol* 2008; 61: 515-24.

Chapter 1.5

Quantitative determination of erlotinib and O-desmethyl erlotinib in human EDTA plasma and lung tumor tissue

Nienke A.G. Lankheet
Eva. E. Schaake
Hilde Rosing
Jacques A. Burgers
Jan H.M. Schellens
Jos H. Beijnen
Alwin D.R. Huitema

Bioanalysis 2012; 4(21):2563-77.



R1
R2
R3
R4
R5
R6
R7
R8
R9
R10
R11
R12
R13
R14
R15
R16
R17
R18
R19
R20
R21
R22
R23
R24
R25
R26
R27
R28
R29
R30
R31
R32
R33
R34
R35
R36
R37
R38
R39

Abstract

Background. To increase knowledge about lung tumor tissue levels of erlotinib and its primary active metabolite and about erlotinib plasma levels in intercalated dosing schedules, a sensitive and accurate method for determination of erlotinib and O-desmethyl erlotinib (OSI-420) in human plasma and lung tumour tissue has been developed.

Results. A method with high-performance liquid chromatography and detection with tandem mass spectrometry (HPLC-MS/MS) was validated over a linear range from 5 to 2,500 ng/mL in plasma and from 5.0 to 500 ng/mL for lung tumor tissue homogenate (50- 5000 ng/g for lung tumor). Calibration curves in plasma were used to quantify analytes in lung tumor tissue homogenate. Lung tumor tissue of 15 patients has been collected and analyzed with the presented method.

Conclusion. This method has been successfully validated and applied to determine plasma and lung tumor tissue concentrations of erlotinib and O-desmethyl erlotinib in patients with non-small cell lung cancer.

Introduction

Erlotinib is an epidermal growth factor receptor (EGFR) tyrosine kinase inhibitor. Erlotinib is approved for first-line treatment of non-small cell lung cancer (NSCLC) with mutated EFGR, second-line treatment of NSCLC and first-line treatment of advanced pancreatic adenocarcinoma.

Erlotinib drug exposure may be altered by pharmacokinetic drug-drug interactions leading to high inter-patient variability in plasma concentrations [1]. It has been established that the magnitude of the pharmacological effect (tyrosine kinase inhibition) in vitro is concentration dependent. Moreover, in clinical studies trough plasma concentrations of erlotinib and its metabolite O-desmethyl erlotinib (OSI-420) seemed to correlate with treatment outcome [2,3]. At the advised daily dose of erlotinib (150 mg/d) trough plasma concentrations are 1200 (SD 600) ng/mL [2]. To provide an adequate level of tyrosine kinase inhibition minimal trough plasma concentrations of approximately 500 ng/mL are required, based on animal pharmacodynamic studies [2]. Furthermore, an association has been observed between erlotinib plasma exposure and severity of skin toxicity [1]. However, no clear cut-off values for efficacy and toxicity have been established in human, hitherto [1,2]. Therefore, further pharmacokinetic investigations are needed to design individual treatment strategies.

Additionally, pharmacodynamic drug-drug interactions between chemotherapeutics and erlotinib can negatively influence treatment outcome [4]. Since erlotinib interferes with the mechanism of action of chemotherapeutics, intermittent dosing schedules with a wash out period of five days for erlotinib have been introduced for combination therapy regimens [4,5]. In these intermittent schedules it is important that concentrations of erlotinib in plasma are subtherapeutic before the chemotherapeutic drugs are administered and, therefore, this has to be established by determination of erlotinib plasma concentrations. Moreover, since the pharmacodynamic target of erlotinib is located in tumor tissue, knowledge about concentrations of erlotinib in tumor tissue is even more informative [5].

To support the pharmacokinetic analysis in clinical trials, compound specific analytical methods are essential. Five bioanalytical assays for the determination of erlotinib in plasma have been reported so far [2,6-9]. The determination of the active metabolite of erlotinib was only incorporated in three assays [7-9]. None of the assays was validated to analyse erlotinib and O-desmethyl erlotinib in tissue samples. Additionally, these methods require a minimal sample volume of 100-250 μ L during sample pretreatment and have a lower limit of quantification (LLOQ) of 10-12.5 ng/mL [7-9]. For these reasons, the reported methods are not suitable for analysis of our study samples, which include samples with restricted volumes (e.g. tumor tissue homogenates) and with low expected drug concentrations (e.g. tissue homogenates or plasma samples drawn after an erlotinib wash out period). Therefore, we developed and validated a sensitive and specific HPLC-MS/MS method for quantification of erlotinib and O-desmethyl erlotinib in human EDTA plasma and in human lung tumor tissue homogenates with an LLOQ of 5.0 ng/mL in plasma and 50 ng/g in tumor tissue, respectively, using 50 μ L of sample.

R1
R2
R3
R4
R5
R6
R7
R8
R9
R10
R11
R12
R13
R14
R15
R16
R17
R18
R19
R20
R21
R22
R23
R24
R25
R26
R27
R28
R29
R30
R31
R32
R33
R34
R35
R36
R37
R38
R39

Experimental

Chemicals

Reference standards and internal standard (ISTD) were provided by the following manufacturers: erlotinib.HCl ($C_{22}H_{23}N_3O_4 \cdot HCl$) by Sequoia Research Products (Oxford, United Kingdom), O-desmethyl erlotinib ($C_{21}H_{21}N_3O_4$) by Toronto Research Chemicals (North York, Canada), stable isotopically labelled erlotinib- $^{13}C_6$ ($C_{16}^{13}C_6H_{23}N_3O_4 \cdot HCl$) by Alsa Chim (Illkirch, France). The chemical structures of erlotinib, O-desmethyl erlotinib and erlotinib- $^{13}C_6$ are depicted in Figure 1. HPLC-grade acetonitrile and methanol were purchased from Biosolve (Valkenswaard, The Netherlands). HPLC grade Lichrosolve water and formic acid 98-100% were purchased from Merck (Darmstadt, Germany).

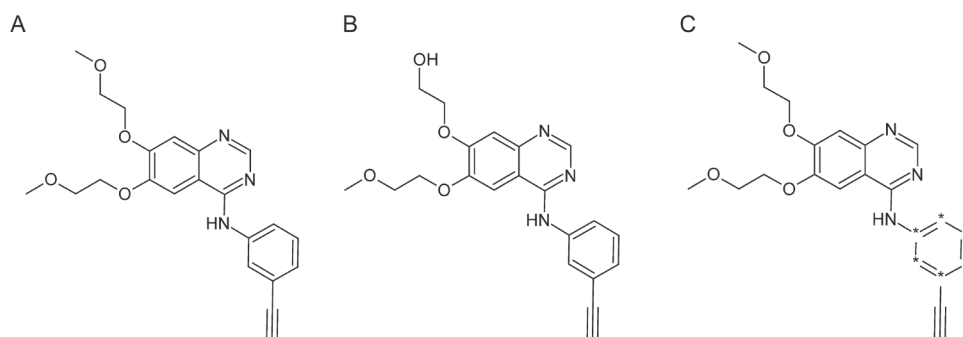


Figure 1. Structural formulas of erlotinib (A), O-desmethyl erlotinib (B) and erlotinib- $^{13}C_6$ (C). (* represents ^{13}C)

Drug-free matrices

Drug-free human plasma with EDTA as anticoagulant was obtained from the Slotervaart Hospital (Amsterdam, The Netherlands) and stored at $-20^{\circ}C$ until use. Drug-free lung tumor tissue was obtained from patients that functioned as a untreated control group to a phase II trial in the Antoni van Leeuwenhoek Hospital (Amsterdam, The Netherlands) [10]. Fresh lung tumor material of resected lung tumors of ten control patients was frozen at $-70^{\circ}C$ directly after surgery. Subsequently, of each lung tumor specimen 50 to 150 mg was weighted accurately. On first sight, the used parts of the tumors were not contaminated with blood. Therefore, no sample clean-up was performed before sample homogenization.

An accurate volume of 500 to 1500 μL of drug-free human EDTA plasma was added to obtain samples containing 100 mg of lung tumor tissue per 1.0 mL of plasma. Lung tumor tissue homogenate was prepared by using a rotor/stator-type mechanical homogenizer until no tissue fibers were visible. Lung tumor tissue homogenate samples were stored at nominally $-20^{\circ}C$ until use.

Chromatographic and mass spectrometric conditions

An HPLC system (LC-20AD Prominence binary solvent delivery system) with a column oven, DGU-20A3 online degasser and a SIL-HTc controller (all: Shimadzu, Kyoto, Japan) and a cooled autosampler (4 °C) were used. Chromatographic separation was carried out at 40 °C on a reversed phase system with a Synergi Fusion-RP 80 column (150 x 2.0 mm ID, 4.0 µm particle size, Phenomenex, Torrance, CA, USA) protected with a Securityguard Synergi Fusion precolumn (4 x 2.0 mm ID, 4.0 mm particle size, Phenomenex). The injection volume was 10 µL. A stepwise gradient was applied at a flow rate of 250 µL/min. The mobile phase consisted of a mixture of 0.1% formic acid in water (A) and 0.1% formic acid in methanol (B). Before each new injection, the column was reconditioned for 4.7 minutes with 25% B (v/v) resulting in a total run time of 10 min. The chromatographic separation conditions are given in Table 1. The divert valve was directed to waste during the first 1.0 min and last 2.5 min to prevent the introduction of endogenous compounds into the mass spectrometer.

Table 1. Gradient composition during the HPLC-run

Time (min)	Flow (mL/min)	0.1% formic acid (v/v) in MeOH	0.1% formic acid (v/v) in water
0.0	0.25	25	75
0.9	0.25	25	75
1.0	0.25	55	45
5.2	0.25	55	45
5.3	0.25	25	75
10.0	0.25	25	75

A TSQ Quantum Ultra triple quadrupole mass spectrometer equipped with an electrospray ionisation source (ESI) operating in the positive ion mode (Thermo Scientific, Waltham, MA, USA) was used. For quantification, multiple reaction monitoring (MRM) chromatograms were acquired with LCQuan™ software version 2.5 (Thermo Scientific). Positive ions were created at atmospheric pressure and the quadrupoles were operating in unit resolution (0.7 Da). Mass transitions from *m/z* 394 to 278 for erlotinib, *m/z* 380 to 278 for O-desmethyl erlotinib and *m/z* 400 to 284 for ISTD erlotinib -¹³C₆ were optimised (see Figure 2). The ESI-MS/MS operating parameters used in this assay are listed in Table 2.

Preparation of calibration standards and validation samples

A set of stock solutions of erlotinib and O-desmethyl erlotinib were prepared from two independent weighings; one for the calibration standards and one for the validation samples. Approximately 2.2 mg of erlotinib.HCl was accurately weighted and dissolved in 1 mL of DMSO in a volumetric flask to give a 1.0 mg/mL stock solution of the free base. Approximately 0.7 mg of O-desmethyl erlotinib.HCl was accurately weighted and dissolved in 1 mL of DMSO in a volumetric flask to give a 0.7 mg/mL stock solution. Stock solutions of the ISTD erlotinib -¹³C₆ were prepared in methanol at a concentration of approximately 500 µg/mL. A 1,000 ng/mL working solution of the ISTD was prepared by dilution of the stock solution in methanol.

R1
R2
R3
R4
R5
R6
R7
R8
R9
R10
R11
R12
R13
R14
R15
R16
R17
R18
R19
R20
R21
R22
R23
R24
R25
R26
R27
R28
R29
R30
R31
R32
R33
R34
R35
R36
R37
R38
R39

For the preparation of the calibration standards, working solutions containing erlotinib and O-desmethyl erlotinib in the range from 100 to 50,000 ng/ml were used. These working solutions were prepared by dilution of erlotinib and O-desmethyl erlotinib stock solutions in methanol. A volume of 50 μ L of each working solution was added to 950 μ L of drug-free human EDTA plasma to obtain calibration standards in the range from 5 to 2,500 ng/mL.

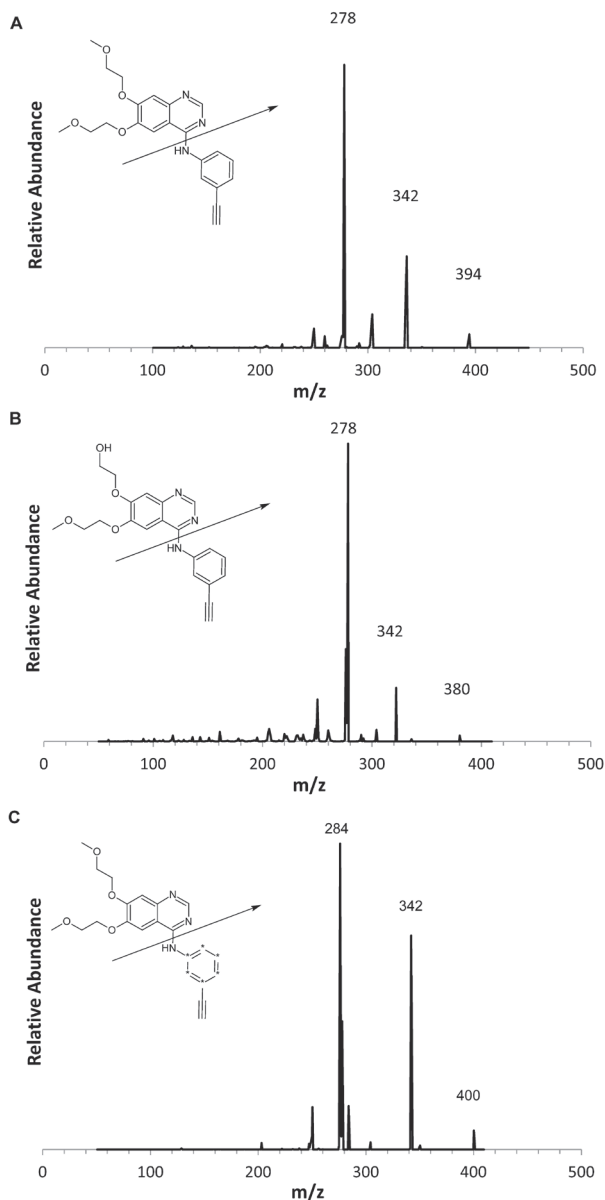


Figure 2. MS/MS product ion scan of erlotinib (A; precursor ion m/z 394), O-desmethyl erlotinib (B; precursor ion m/z 380) and erlotinib-¹³C₆ (C; precursor ion m/z 400; * represents ¹³C)

Five working solutions in the range from 100 to 40,000 ng/ml were prepared by dilution of independently prepared erlotinib and O-desmethyl erlotinib stock solutions in methanol. To obtain validation samples of 5, 10, 400 and 2,000 ng/mL in plasma, 50 µL of each working solution was added to 950 µL of drug-free human EDTA plasma. To obtain validation samples of 5, 10, 80, 400 ng/mL lung tumor tissue homogenate in plasma, 50 µL of each working solution was added to 950 µL of drug-free human tumor tissue homogenate. The stock and working solutions in methanol were stored at nominally -20 °C until use.

During the first two method validation runs validation samples and calibration samples were prepared freshly since the stability of the analytes in the different matrices was not established at that moment. However, the validation samples were prepared independently of the calibration samples by using different stock solutions and working solutions. When short term analyte stability was established, freshly prepared calibration samples and aliquoted validation samples were used for the final validation run.

To establish the accuracy and precision of the method after dilution of samples containing analyte concentrations above the upper limit of quantification (ULOQ), a plasma sample at 5,000 ng/mL erlotinib and O-desmethyl erlotinib was spiked. Before processing, this sample was diluted ten times in drug-free human EDTA plasma.

Table 2. Mass spectrometer settings

Parameter	Setting		
Run duration	10 min		
Ionspray voltage	3.0 kV		
Sheath gas (N2)	35 psi		
Auxiliary gas (N2)	15 psi		
Ion sweep gas (N2)	2 psi		
Tube lens offset	12 V		
Capillary temperature	350 °C		
Collision pressure (argon)	1.5 mTorr		
Chrom filter peak width	10 s		
	Erlotinib	O-desmethyl erlotinib	Erlotinib-¹³C₆
Q1 mass	394 amu	380 amu	400 amu
Q3 mass	278 amu	278 amu	284 amu
Dwell time	30 ms	30 ms	30 ms
Collision energy	32 V	31 V	29 V
Tube lens voltage	102 V	84 V	102 V

Sample pre-treatment

Protein precipitation (PP) was used as sample pre-treatment for plasma and lung tumor tissue homogenate samples. 20 µL of ISTD working solution (1,000 ng/mL) was added to 50 µL of plasma and tissue homogenate sample. Subsequently 150 µL of acetonitrile (-20 °C) was added. After vortex mixing for 15 s, samples were centrifuged at 15,000 x g for 15 min. A volume of 50 µL of the

R1 clear supernatant was diluted with 50 μ L of eluent A (0.1% formic acid in water) before injection of
R2 10 μ L onto the column.

R3 ***Validation procedures***

R4 A full validation of the assay was performed according to the FDA guidelines for validation of
R5 bioanalytical assays including linearity, inaccuracy, precision, specificity, selectivity, cross-analyte/
R6 ISTD interference, recovery, ion suppression, carry-over and stability [11,12].
R7

R8 ***Application of assay in patient blood and tissue samples***

R9 The validated erlotinib and O-desmethyl erlotinib assay was used to measure trough plasma levels
R10 in patients on a sequential dosing regimen in a Phase II trial conducted in multiple centers in
R11 the Netherlands. Patients were treated with erlotinib for 14 days followed by a wash-out period
R12 of 5 days. During the last day of the wash-out period EDTA plasma samples were collected and
R13 then directly sent to the laboratory. Within 48 h after blood draw, plasma was stored at -20°C until
R14 analysis.
R15

R16 Additionally, the validated assay was used to measure erlotinib and O-desmethyl erlotinib
R17 levels in human lung tumor tissue homogenates of patients on a neo-adjuvant continuous
R18 dosing regimen of erlotinib until three days before surgery in a phase II trial in the Antoni van
R19 Leeuwenhoek Hospital (Amsterdam, The Netherlands). Lung tumor tissue homogenates of
R20 patients were obtained using the same procedure as was used for preparation of drug-free lung
R21 tumor tissue homogenates (see Section Drug-free matrices).

R22 Both trials were approved by the local institutional review boards and informed consent was
R23 given according to the Declaration of Helsinki.
R24

R25 **Results and discussion**

R26 ***Method development***

R27 The stable isotopically labeled analogue of erlotinib, erlotinib $^{-13}\text{C}_6$, was used as ISTD to normalize
R28 for variations in the response of erlotinib and O-desmethyl erlotinib. The physical and chemical
R29 similarities between erlotinib $^{-13}\text{C}_6$, erlotinib and O-desmethyl erlotinib, makes this ISTD very
R30 suitable to compensate for variations in the response of the analytes introduced by sample
R31 preparation, injection, and matrix effects. However, during method development erlotinib and the
R32 co-eluting stable isotopically labeled ISTD appeared to suppress each other's responses due to
R33 competition in the electrospray ionisation (ESI) process of the MS source [13,14]. This resulted in
R34 nonlinear calibration curves and high inaccuracies of the validation samples when using an ISTD
R35 solution of 2,000 ng/mL, mainly due to a fluctuation of the ISTD response. Since the extent of
R36 suppression was supposed to be concentration dependent, the concentrations of ISTD solutions
R37 were varied (20, 200, 500, 1,000, 2,000, 20,000 ng/mL). It was expected that an exceptionally
R38 high ISTD concentration would lead to saturation of the electrospray even in presence of low
R39

concentrations of the analyte and would diminish the effect of high analyte concentrations on the ISTD response. However, fluctuation of the ISTD responses was observed at all ISTD concentrations (see Figure 3). In the first part of the calibration range (5,0 – 250 ng/mL) the response of the ISTD signal seemed to be enhanced with increasing analyte concentrations. In contrast, in the second part of the calibration range (250- 2,500 ng/mL) the ISTD signal seemed to be suppressed with increasing analyte concentrations. It was considered that this double-directed effect could be due to cross-interference of analyte into ISTD trace, followed by suppression of ISTD at higher levels. However, this mechanism was not plausible, since cross-analyte interference and selectivity was assessed and the interference of an ULOQ concentration of erlotinib into the ISTD trace was only 0.07% of the LLOQ level of the ISTD. Remarkably, no correlation between ISTD concentration and degree of response fluctuation was observed.

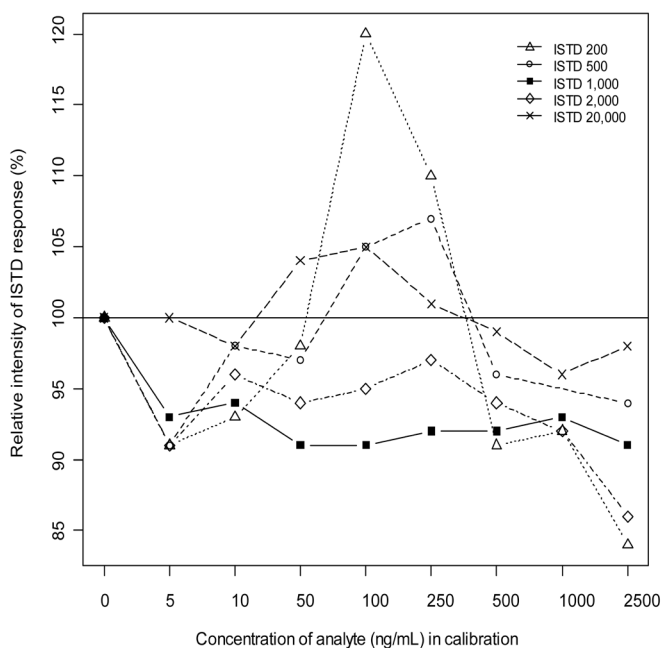


Figure 3. Representative, typical patterns of fluctuating ISTD response using different concentrations of ISTD erlotinib- $^{13}\text{C}_6$ (200, 500, 1,000, 2,000, 20,000 ng/mL) in calibration samples with increasing analyte concentrations (range 5.00 – 2,500 ng/mL) determined using LC-ESI-MS/MS. ISTD response in blank plasma sample processed with ISTD is defined as 100%. This figure shows results that are representative for two experiments performed on different days.

Sequentially, suitability of a HPLC-APCI-MS/MS system in the quantification of erlotinib was investigated, since the ionisation process in atmospheric pressure chemical ionisation (APCI) is known to be less susceptible for ion saturation in the source [13]. The ISTD responses of a set of calibration samples using APCI were not influenced by concentration of analytes. However, the

R1
R2
R3
R4
R5
R6
R7
R8
R9
R10
R11
R12
R13
R14
R15
R16
R17
R18
R19
R20
R21
R22
R23
R24
R25
R26
R27
R28
R29
R30
R31
R32
R33
R34
R35
R36
R37
R38
R39

R1
R2
R3
R4
R5
R6
R7
R8
R9
R10
R11
R12
R13
R14
R15
R16
R17
R18
R19
R20
R21
R22
R23
R24
R25
R26
R27
R28
R29
R30
R31
R32
R33
R34
R35
R36
R37
R38
R39

assay sensitivity was decreased leading to an inevitable and undesirable increase of the lower limit of quantification (LLOQ) to at least 10.0 ng/mL for both analytes. For this reason, it was decided to use the HPLC-ESI-MS/MS system and consequently to tighten the range to 5.0 – 2,500 ng/mL in order to avoid the tremendous effect of the highest calibration level (5,000 ng/mL) on the ISTD response. The ISTD concentration of 20,000 ng/mL showed the smallest deviations from the ISTD response of a plasma sample without analyte, as shown in Figure 3. However, this high ISTD concentration gave signal suppression of erlotinib in the samples, leading to decreased assay sensitivity. The ISTD concentration of 1,000 ng/mL showed the smallest fluctuation in ISTD response over the entire calibration range and was, therefore, used in the validation experiments. This ISTD concentration showed good linearity, accuracy and precision within the validated range, as shown in Figure 4.

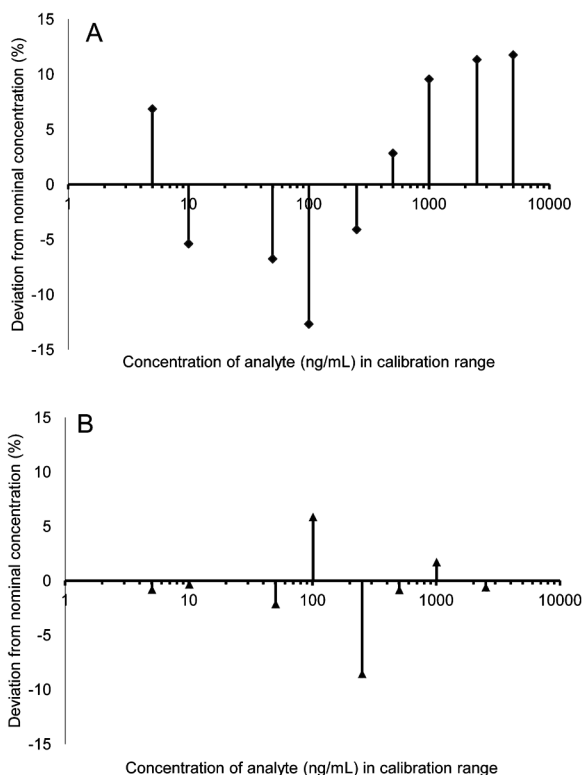


Figure 4. Deviations from nominal erlotinib concentrations based on area ratio responses in samples of a calibration range using different concentrations of ISTD erlotinib-¹³C₆ ((A) 2,000 ng/mL ISTD; (B) 1,000 ng/mL ISTD). This figure shows results that are representative for two experiments performed on different days. Figure 4A, using 2,000 ng/mL ISTD, shows negative deviations from nominal concentrations in the first part of the calibration curve and positive deviations in the second part of the calibration curve, leading to nonlinear calibration curves. Figure 4B, using 1,000 ng/mL ISTD, shows small deviations from nominal concentrations, which are evenly distributed across the calibration range with as a result good linearity of the calibration curve.

Using a stable isotopically labeled ISTD for either a parent drug and for its metabolite risks the problem that the quantification of the metabolite is affected by ISTD ionization suppression in presence of high concentrations of the parent drug. However, it was assumed that this was not an issue in our method, since the effect of erlotinib on the ISTD (in a concentration of 1,000 ng/mL) was not concentration dependent, as shown in Figure 3. Moreover, calibrations curves of the metabolite in presence and absence of erlotinib could both be fitted linear (correlation coefficients 0.9917 and 0.9918, respectively) with inaccuracies <15% (data not shown).

Chromatographic and mass spectrometric conditions

Peaks with satisfying peak shapes were obtained when the stepwise gradient starting on 25% eluent B was followed by a block gradient with 55% eluent B at a flow rate of 0.25 mL per min (see Table 2). Typical chromatograms of LLOQ samples are depicted in Figure 5 and 6. At LLOQ level (5.0 ng/mL) a signal to noise ratio (S/N-ratio) of >10 was obtained. In neither the validation samples nor the patient plasma and tissue samples more than one peak was observed in the mass transition of O-desmethyl erlotinib. Thus, the isomeric forms of O-desmethyl erlotinib (OSI-420 and OSI-413), were not chromatographically separated.

During optimization of the mass spectrometric parameters, the Q1 spectrum of erlotinib and O-desmethyl erlotinib showed the singly charged molecular ion as most intense ion at m/z 394 and 380, respectively. For erlotinib $-^{13}\text{C}_6$ the most intense peak in the Q1 spectrum also corresponded to the singly charged molecular ion at m/z 400. MS/MS experiments were carried out to determine the most abundant product ions for multiple reaction monitoring (MRM). MS/MS product ion scans and the proposed fragmentation pathways for the chosen transitions of erlotinib, O-desmethyl erlotinib and erlotinib $-^{13}\text{C}_6$ are shown in Figure 2. The analytes and the ISTD could be detected with the electrospray source operating in the positive mode.

R1
R2
R3
R4
R5
R6
R7
R8
R9
R10
R11
R12
R13
R14
R15
R16
R17
R18
R19
R20
R21
R22
R23
R24
R25
R26
R27
R28
R29
R30
R31
R32
R33
R34
R35
R36
R37
R38
R39

R1
R2
R3
R4
R5
R6
R7
R8
R9
R10
R11
R12
R13
R14
R15
R16
R17
R18
R19
R20
R21
R22
R23
R24
R25
R26
R27
R28
R29
R30
R31
R32
R33
R34
R35
R36
R37
R38
R39

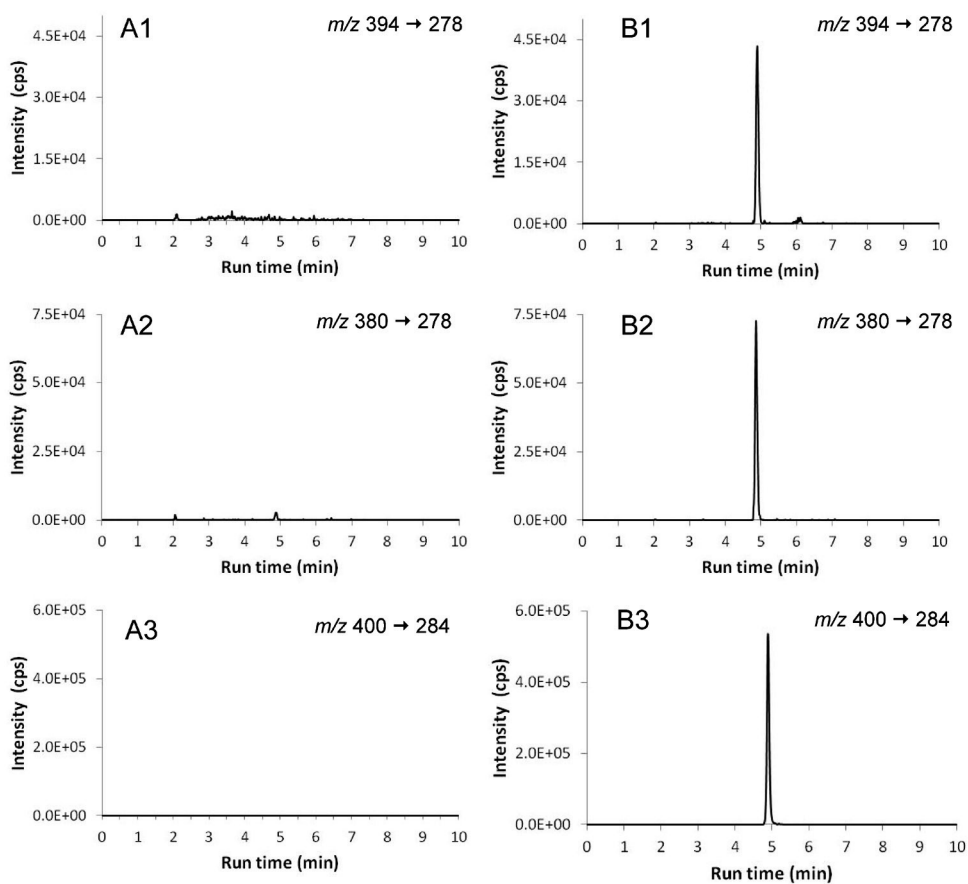


Figure 5. Representative LC-MS/MS chromatograms of a blank human plasma sample (A1, erlotinib; A2, O-desmethyl erlotinib; A3, ISTD erlotinib- $^{13}\text{C}_6$) and of a spiked human plasma sample at the LLOQ level of 5.0 ng/mL (B1, erlotinib; B2, O-desmethyl erlotinib; B3, ISTD erlotinib- $^{13}\text{C}_6$).

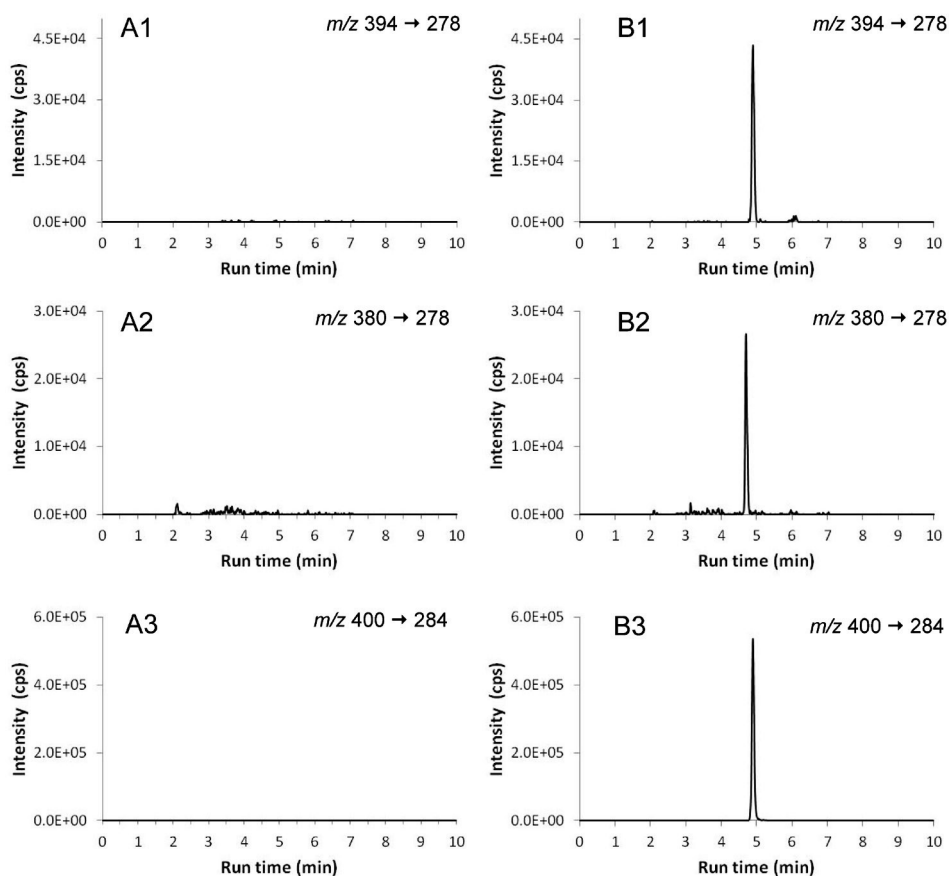


Figure 6. Representative LC-MS/MS chromatograms of a blank human lung tumor tissue homogenate sample (A1, erlotinib; A2, O-desmethyl erlotinib; A3, ISTD erlotinib- $^{13}\text{C}_6$) and of a spiked human lung tumor tissue homogenate sample at the LLOQ level of 5.0 ng/mL (B1, erlotinib; B2, O-desmethyl erlotinib; B3, ISTD erlotinib- $^{13}\text{C}_6$).

Validation experiments

Linearity. Eight non-zero plasma calibration samples were prepared and analysed in duplicate in three separate analytical runs. Calibration curves in plasma were also used to quantify tissue homogenate samples. The linear regression of the ratio of the areas of the analyte and the ISTD peaks versus the concentration were weighted with weighing factor $1/x^2$ (where x =concentration). The linearity was evaluated by means of back-calculated concentrations of the calibration standards. The assay was linear over the validated concentration range from 5.0 to 2,500 ng/mL of erlotinib and O-desmethyl erlotinib in human plasma and from 5.0 to 500 ng/mL for these analytes in lung tumor tissue homogenates. Correlation coefficients (r^2) were at least 0.995. The deviation from the nominal concentrations should be within $\pm 20\%$ for the LLOQ and within $\pm 15\%$ for the

R1
R2
R3
R4
R5
R6
R7
R8
R9
R10
R11
R12
R13
R14
R15
R16
R17
R18
R19
R20
R21
R22
R23
R24
R25
R26
R27
R28
R29
R30
R31
R32
R33
R34
R35
R36
R37
R38
R39

R1 other concentrations with coefficient of variation (CV) values less than 20% and 15% for both the
R2 LLOQ and the other concentrations respectively. At all concentration levels the inaccuracies were
R3 within -6.7 and 7.7% with CV values less than 10.1% for erlotinib and its metabolite in plasma. For
R4 tissue samples the levels the inaccuracies were within -6.0 and 7.4% with CV values less than 7.7%.

R5 **Inaccuracy and precision.** The intra- and inter-assay performance data are presented in Table 3
R6 and 4. Inaccuracy and precision of the assay were established by analysing validation samples
R7 with analyte concentrations at the LLOQ and in the low, mid and high concentration ranges of
R8 the calibration curves. Five determinations of each validation sample were measured in three
R9 separate analytical runs. The coefficient of variation (CV%) was used to report the intra- and inter-
R10 assay precision. The intra- and inter-assay inaccuracies should be within $\pm 20\%$ for the LLOQ and
R11 $\pm 15\%$ for all other concentrations. The precisions CV% should be less than 20% for the LLOQ and
R12 less than 15% for all other concentrations [12]. The intra-assay inaccuracies (% bias) for erlotinib
R13 and O-desmethyl erlotinib in human EDTA plasma were within respectively $\pm 14.0\%$ for all
R14 concentration levels. The intra-assay precisions (CV%) for the analytes were less than 10.0% for all
R15 concentration levels. In conclusion, the validated range for erlotinib and O-desmethyl erlotinib
R16 based on 50 mL human EDTA plasma is from 5.0-2,500 ng/mL. Additionally, the validated range
R17 for erlotinib and O-desmethyl erlotinib based on 50 mL human tissue homogenate is from 5.0-
R18 500 ng/mL. The intra-assay inaccuracies (% bias) for erlotinib and O-desmethyl erlotinib in human
R19 tissue homogenates were within $\pm 12.5\%$ for all concentration levels. The intra-assay precisions
R20 (CV%) for the analytes in this matrix were less than 15.9% for the LLOQ level and less than 13.2% for
R21 the other concentration levels. Samples with analyte concentrations above the ULOQ (2,500 ng/
R22 mL) were diluted 1:10 (v/v) in drug-free human EDTA. These samples were processed in 5-fold and
R23 measured in one analytical run to assess the accuracy and precision. The intra-assay inaccuracy
R24 for diluted samples was -5.0 and -7.4% and the intra-assay precision was 2.1 and 2.5% for erlotinib
R25 and O-desmethyl erlotinib, respectively. When concentrations above 2,500 ng/mL are expected,
R26 samples can be diluted 10 times with drug-free human EDTA plasma. Inaccuracies and precisions
R27 fulfilled the requirements [11].

R28 **Specificity and selectivity.** To investigate whether endogenous compounds from plasma could
R29 interfere with the detection of the analyte or the ISTD, six different batches of drug-free human
R30 EDTA plasma and five different batches of human tissue homogenate were processed as double
R31 blanks (containing neither analyte nor ISTD) and LLOQ samples. Samples were analysed according
R32 to the described procedures. Areas of peaks co-eluting with the analytes should not exceed 20%
R33 of the area at the LLOQ level. In MRM chromatograms of six batches of drug-free EDTA plasma
R34 no interference of endogenous compounds from plasma could be detected with the analyte or
R35 the ISTD. No co-eluting peaks $>20\%$ of the erlotinib and O-desmethyl erlotinib peak area at the
R36 LLOQ level were found and also no co-eluting peaks $>5\%$ of the ISTD were detected. In MRM
R37 chromatograms of five batches of drug-free tissue homogenates no interference of endogenous
R38 compounds from plasma could be detected with the analyte or the ISTD. No co-eluting peaks
R39

>20% of the erlotinib and O-desmethyl erlotinib peak area at the LLOQ level were found and also no co-eluting peaks >5% of ISTD were detected. The deviation of the nominal concentration for the LLOQ samples should be within $\pm 20\%$ and were between -2.1 and 7.6% for erlotinib and -13.0 and 2.6% for O-desmethyl erlotinib in plasma samples. In lung tumor tissue homogenates the deviations of the nominal concentration at the LLOQ level were between -17.0 and 14.2% for erlotinib and -27.2 and 17.4% for O-desmethyl erlotinib. For the metabolite only one out of five LLOQ samples in lung tumor tissue homogenate showed deviation >20%. Therefore, it can be concluded that the method is selective and specific and that endogenous compounds do not interfere with the assay.

R1
R2
R3
R4
R5
R6
R7
R8
R9
R10
R11
R12
R13
R14
R15
R16
R17
R18
R19
R20
R21
R22
R23
R24
R25
R26
R27
R28
R29
R30
R31
R32
R33
R34
R35
R36
R37
R38
R39

Table 3. Assay performance data for erlotinib (A) and O-desmethyl erlotinib (B) in plasma.

A) Erlotinib					
Run	Nominal conc. (ng/mL)	Mean calculated conc. (ng/mL)	Inaccuracy (% Dev)	Precision (%CV)	No. of replicates
1	5.04	5.46	8.40	3.20	5
2	5.04	5.75	14.0	3.69	5
3	5.04	5.39	6.91	3.00	5
Inter-assay	5.04	5.53	9.78	4.22	15
1	10.1	10.1	0.21	4.67	5
2	10.1	10.5	4.11	3.08	5
3	10.1	9.76	-3.36	5.20	5
Inter-assay	10.1	10.1	0.32	5.12	15
1	403	427	6.05	2.73	5
2	403	429	6.47	4.08	5
3	403	433	7.55	2.05	5
Inter-assay	403	430	6.69	2.90	15
1	2015	2152	6.81	2.95	5
2	2015	2154	6.89	5.97	5
3	2015	1995	-0.99	1.37	5
Inter-assay	2015	2100	4.24	5.22	15
B) O-desmethyl erlotinib					
Run	Nominal conc. (ng/mL)	Mean calculated conc. (ng/mL)	Inaccuracy (% Dev)	Precision (%CV)	No. of replicates
1	5.00	5.11	2.11	10.1	5
2	5.00	4.85	-3.07	10.0	5
3	5.00	5.46	9.21	5.93	5
Inter-assay	5.00	5.14	2.75	13.0	15
1	10.0	9.25	-7.46	10.1	5
2	10.0	9.70	-3.05	4.63	5
3	10.0	9.41	-5.90	11.7	5
Inter-assay	10.0	9.45	-5.47	10.5	15
1	400	406	1.70	5.25	5
2	400	411	2.87	6.54	5
3	400	410	2.72	2.82	5
Inter-assay	400	409	2.43	4.76	15
1	2000	2133	6.68	6.35	5
2	2000	2122	6.15	8.73	5
3	2000	1890	-5.48	1.79	5
Inter-assay	2000	2048	2.45	8.30	15

Conc., concentration; Dev, Deviation; CV, coefficient of variation.

Table 4. Assay performance data for erlotinib (A) and O-desmethyl erlotinib (B) in lung tumor tissue homogenates.

A) Erlotinib					
Run	Nominal conc. (ng/mL)	Mean calculated conc. (ng/mL)	Inaccuracy (% Dev)	Precision (%CV)	No. of replicates
1	5.04	5.67	12.5	9.35	2
2	5.04	5.16	2.42	8.19	3
3	5.04	5.08	0.96	13.4	4
Inter-assay	5.04	5.24	4.01	10.7	9
1	10.1	10.1	0.14	0.48	2
2	10.1	10.5	4.04	3.00	3
3	10.1	9.52	-5.77	9.96	4
Inter-assay	10.1	9.98	-1.19	7.62	9
1	80.6	82.3	2.06	1.47	2
2	80.6	84.3	4.64	8.68	3
3	80.6	83.8	4.00	1.46	4
Inter-assay	80.6	83.7	3.78	4.60	9
1	403	451	11.9	3.45	2
2	403	418	3.82	1.07	3
3	403	425	5.48	3.49	4
Inter-assay	403	429	6.36	3.97	9
B) O-desmethyl erlotinib					
Run	Nominal conc. (ng/mL)	Mean calculated conc. (ng/mL)	Inaccuracy (% Dev)	Precision (%CV)	No. of replicates
1	5.00	5.37	7.39	8.76	2
2	5.00	4.75	-5.09	7.82	3
3	5.00	5.35	6.89	15.9	4
Inter-assay	5.00	5.15	3.01	13.3	9
1	10.0	9.36	-6.38	4.84	2
2	10.0	10.6	5.99	10.5	3
3	10.0	9.80	-1.96	13.2	4
Inter-assay	10.0	9.97	-0.29	11.1	9
1	80.0	83.3	4.75	4.67	2
2	80.0	78.6	-1.71	6.32	3
3	80.0	86.8	8.56	4.05	4
Inter-assay	80.0	83.3	4.14	6.26	9
1	400	468	7.28	2.75	2
2	400	422	5.45	6.74	3
3	400	437	9.15	3.78	4
Inter-assay	400	439	9.67	5.82	9

Conc., concentration; Dev, Deviation; CV, coefficient of variation.

R1
R2
R3
R4
R5
R6
R7
R8
R9
R10
R11
R12
R13
R14
R15
R16
R17
R18
R19
R20
R21
R22
R23
R24
R25
R26
R27
R28
R29
R30
R31
R32
R33
R34
R35
R36
R37
R38
R39

Cross analyte interference. To investigate possible cross interference between erlotinib, O-desmethyl erlotinib and ISTD, a cross interference check was performed. Drug-free human EDTA plasma was spiked at ULOQ level and was processed without ISTD. Also drug-free plasma with only ISTD erlotinib- $^{13}\text{C}_6$ was processed. The response of any interfering peak with the same retention time as erlotinib or O-desmethyl erlotinib should be less than 20% of the response of a LLOQ sample. The response of any interfering peak with the same retention time as the ISTD should be less than 5% of the response of the ISTD. No cross-analyte/ISTD standard interference was detected and, therefore, cross-analyte/ISTD interferences of the assay fulfilled the requirements.

Recovery and matrix effect. Recovery and matrix effect were tested in EDTA plasma samples and not in lung tumor tissue homogenates, since these tumor tissue homogenates were scarce and, therefore, difficult to obtain in large quantities. Moreover, since selectivity assessments in different batches of lung tumor tissue homogenate established that endogenous compounds did not interfere with the assay's accuracy, it was assumed that the stable isotopically labeled internal standard corrected for potential matrix effects.

The protein precipitation (PP) recovery of erlotinib and its metabolite was determined at two concentrations (10.0 and 2,000 ng/ml) by comparing the analytical response of processed samples with those of processed blanks spiked with analyte (representing 100% recovery). The mean PP recovery was 71.0% (CV 4.3%) and 73.0% (CV 4.8%) for erlotinib and O-desmethyl erlotinib, respectively.

Ion suppression (matrix factor) was examined by comparing the analytical response of processed blanks spiked with analyte with those unprocessed samples in precipitation reagent. These experiments were performed in triplicate. The mean matrix factor detected for erlotinib and O-desmethyl erlotinib in plasma was 1.14 (CV% 9.5) and 1.14 (CV% 8.0), respectively.

Carry-over. Carry-over was tested by injecting two processed blank matrix samples sequentially after injecting an ULOQ sample. The response in the first blank matrix at the retention times of erlotinib, O-desmethyl erlotinib and erlotinib- $^{13}\text{C}_6$ should be less than 20% of the response of a LLOQ sample. Apparent carry over was observed after injection of spiked plasma samples (28.6% and 26.1% of the LLOQ for erlotinib and O-desmethyl erlotinib, respectively). To solve this carry-over problem a systematic approach, as described before, was used [15,16]. The carry-over seemed to arise from contamination of the autosampler needle and the divert valve due to adsorption of the analyte after multiple injections. Contamination in the divert valve was diminished by performing multiple valve switches (>15) during the equilibration of the column before each analytical run. Contamination of the autosampler needle was diminished by using an acidic flush solvent (1% formic acid in ACN) instead of 100% methanol and increasing the rinse dip time from 5s to 30s. Carry over was reduced to 16.8% and 14.5% of the LLOQ for erlotinib and O-desmethyl erlotinib, respectively, observed in a processed blank sample after injection of an ULOQ sample.

Stability. Stability data are summarized in Table 5. The stability of erlotinib and O-desmethyl erlotinib in spiked human EDTA plasma after three freeze/thaw cycles from nominally -20 °C to

ambient temperatures and after 48 hours at ambient temperature was investigated in triplicate at two concentrations. Additionally, the stability of erlotinib and O-desmethyl erlotinib in spiked human EDTA plasma kept at -20°C for 1.5 months was investigated in triplicate. The analytes were considered to be stable in the matrix or final extract if 85–115% of the initial concentrations was recovered. Erlotinib and O-desmethyl erlotinib are stable in human plasma for at least three freeze (-20 °C) / thaw cycles. Short term stability of the analyte in plasma at ambient temperatures is established up to at least 48 h and at -20°C up to at least 1.5 months.

The processed sample stability of erlotinib and O-desmethyl erlotinib was investigated at three concentrations (10.0, 200 and 2,000 ng/mL) after 7 days (2-8 °C). Both analytes were stable in the final extract at least 7 days at nominally 2-8 °C. Re-injection reproducibility was established and an analytical run can be re-injected after at least 7 days of storage in the autosampler at 4 °C.

Stability of stock solutions of erlotinib, O-desmethyl erlotinib and ISTD stored at ambient temperature for 6 h was established in triplicate. The analyte was considered to be stable in stock solutions if 90-110% of the initial concentration was recovered. Investigation of the long term stability of the analytes in stock solutions and plasma at -20°C is still ongoing.

Application of assay in patient blood and tissue samples

The validated assay was used to support translational research within two Phase II trials of erlotinib in patients with non-small cell lung cancer. Plasma samples and lung tumor tissue samples were collected and thereafter processed and analyzed by the methods described in this report. Subsequently, lung tumor tissue homogenates were quantified on plasma calibration curves.

The bioanalytical assay did not distinguish between the two isomer forms of the primary metabolite of erlotinib, OSI-420 and OSI-413. However, both isomers possess similar pharmacological activity compared to the parent compound [17]. In addition, it was assumed that both isomers possess similar ionization efficiencies. Therefore, quantification of the sum of both isomers is thus justified. In the first trial, the assay was used to measure trough plasma levels after an erlotinib wash-out period of 5 days to ensure that erlotinib levels had reached subtherapeutic levels at that time point. The minimal effective therapeutic level of erlotinib, as deduced from IC₅₀ values after correction for plasma protein binding, is approximately 235 ng/mL [18,19]. Therefore, the assay sensitivity and range (5.0 – 2,500 ng/mL) are sufficient to discriminate between samples underneath and above the therapeutic level of erlotinib.

In the second trial, as a proof of concept, lung tumor tissue homogenates of patients treated with erlotinib until three days before surgery were analysed. Erlotinib levels of approximately 5.0-30 ng/mL (50 - 300 ng/g tissue) and O-desmethyl erlotinib levels of approximately 7.0 ng/mL (70 ng/g tissue) were measured [10]. Therefore, a range of 5.0 – 500 ng/mL in tissue homogenate appeared to be sufficient for analyses of tumor tissue samples of patients treated with erlotinib.

R1
R2
R3
R4
R5
R6
R7
R8
R9
R10
R11
R12
R13
R14
R15
R16
R17
R18
R19
R20
R21
R22
R23
R24
R25
R26
R27
R28
R29
R30
R31
R32
R33
R34
R35
R36
R37
R38
R39

Table 5. Stability data for erlotinib and O-desmethyl erlotinib

Matrix	Conditions	Initial conc. (ng/mL)	Measured conc. (ng/mL)	Dev (%)	CV (%)	No. of replicates
Erlotinib						
Plasma	3 freeze/thaw cycles	10.3	10.4	1.24	13.7	3
Plasma	3 freeze/thaw cycles	1840	1979	7.57	0.90	3
Plasma	Ambient, 48h	100	105	4.32	5.74	3
Plasma	Ambient, 48h	1000	1044	4.33	4.04	3
Plasma	-20°C, 1.5 months	9.76	9.09	-6.78	2.00	2
Plasma	-20°C, 1.5 months	416	410	-1.61	0.04	2
Plasma	-20°C, 1.5 months	1986	1936	-2.53	0.09	2
Final extract (plasma)	2-8°C, 7 days	9.79	10.5	6.89	1.97	2
Final extract (plasma)	2-8°C, 7 days	427	452	5.65	3.13	2
Final extract (plasma)	2-8°C, 7 days	2012	2205	9.59	0.34	2
Final extract (tissue)	2-8°C, 7 days	9.79	10.2	3.88	0.85	2
Final extract (tissue)	2-8°C, 7 days	427	444	3.88	0.57	2
RR	Autosampler 4°C, 7 days	10.1	10.3	1.96	6.65	3
RR	Autosampler 4°C, 7 days	403	427	5.97	0.74	3
RR	Autosampler 4°C, 7 days	2015	2146	6.49	5.71	3
Stock solution (methanol)	Ambient, 6h	1.00 * 10 ⁶	1.08* 10 ⁶	7.80	2.93	3
O-desmethyl erlotinib						
Plasma	3 freeze/thaw cycles	10.0	9.05	-9.05	0.88	3
Plasma	3 freeze/thaw cycles	1804	1882	4.30	0.72	3
Plasma	Ambient, 48h	100	86.7	-13.2	6.16	3
Plasma	Ambient, 48h	1000	1009	11.0	2.30	3
Plasma	-20°C, 1.5 months	9.09	8.61	-5.37	0.72	2
Plasma	-20°C, 1.5 months	390	429	9.93	5.58	2
Plasma	-20°C, 1.5 months	1906	1879	-1.40	1.99	2
Final extract (plasma)	2-8°C, 7 days	9.59	10.0	4.43	0.65	2
Final extract (plasma)	2-8°C, 7 days	410	426	3.88	4.57	2
Final extract (plasma)	2-8°C, 7 days	1930	2054	6.46	0.33	2
Final extract (tissue)	2-8°C, 7 days	9.59	10.2	6.49	10.9	2
Final extract (tissue)	2-8°C, 7 days	410	423	3.24	1.22	2
RR	Autosampler 4°C, 7 days	10.0	9.92	-0.78	5.43	3
RR	Autosampler 4°C, 7 days	400	393	-1.73	3.89	3
RR	Autosampler 4°C, 7 days	2000	2111	5.57	8.43	3
Stock solution (methanol)	Ambient, 6h	1.00 * 10 ⁶	1.08* 10 ⁶	8.09	1.18	3

Conc., concentration; Dev, Deviation; CV, coefficient of variation; RR, re-injection reproducibility; h, hours.

Conclusion

We have developed and validated a fast LC-MS/MS method for the quantitative analysis of erlotinib and O-desmethyl erlotinib in human plasma and lung tumor tissue samples. To our knowledge, this is the first LC-MS/MS method for analysis of erlotinib and O-desmethyl erlotinib in human lung tumor tissue. Human EDTA plasma and human lung tumor tissue homogenate samples with erlotinib and O-desmethyl erlotinib are pre-treated by protein precipitation with acetonitrile after addition of ISTD erlotinib- $^{13}\text{C}_6$. Chromatography is performed under acidic conditions. A linear dynamic range from 5.0 to 2,500 ng/ml has been validated for plasma samples and a range from 5.0 to 500 ng/mL for lung tumor tissue homogenates (50 - 5000 ng/g for lung tumor). Calibration curves in plasma are used to quantify lung tumor tissue homogenate samples. Validation results show that the method is accurate and precise. Proof of concept experiments demonstrated the applicability of the method for quantification of the analytes in clinical samples.

Future perspective

Quantitative analysis of drugs in tissues is important to gain knowledge about drug uptake at the site of action, particularly, for chemotherapeutic drugs that have to be selectively destructive to malignant cells and tissues. In near future, tissue analysis may be increasingly used to support the determination of target levels for optimal therapeutic effects of targeted chemotherapeutic drugs. However, inconsistency between extraction recovery of the drug in calibration samples and patient samples remains one of the major challenges of tissue analysis. To minimize this potential bias, areas for future research should concentrate on new tissue preparation techniques with improved extraction efficiency and reproducibility.

R1
R2
R3
R4
R5
R6
R7
R8
R9
R10
R11
R12
R13
R14
R15
R16
R17
R18
R19
R20
R21
R22
R23
R24
R25
R26
R27
R28
R29
R30
R31
R32
R33
R34
R35
R36
R37
R38
R39

R1
R2
R3
R4
R5
R6
R7
R8
R9
R10
R11
R12
R13
R14
R15
R16
R17
R18
R19
R20
R21
R22
R23
R24
R25
R26
R27
R28
R29
R30
R31
R32
R33
R34
R35
R36
R37
R38
R39

References

1. Thomas F, Rochaix P, White-Koning M et al. Population pharmacokinetics of erlotinib and its pharmacokinetic/pharmacodynamic relationships in head and neck squamous cell carcinoma. *Eur J Cancer* 2009; 45: 2316-23.
2. Hidalgo M, Siu LL, Nemunaitis J et al. Phase I and pharmacologic study of OSI-774, an epidermal growth factor receptor tyrosine kinase inhibitor, in patients with advanced solid malignancies. *J Clin Oncol* 2001; 19: 3267-79.
3. Shepherd FA, Rodrigues PJ, Ciuleanu T et al. Erlotinib in previously treated non-small-cell lung cancer. *N Engl J Med* 2005; 353: 123-32.
4. Li T, Ling YH, Goldman ID et al. Schedule-dependent cytotoxic synergism of pemetrexed and erlotinib in human non-small cell lung cancer cells. *Clin Cancer Res* 2007; 13: 3413-22.
5. Davies AM, Ho C, Lara PN, Jr. et al. Pharmacodynamic separation of epidermal growth factor receptor tyrosine kinase inhibitors and chemotherapy in non-small-cell lung cancer. *Clin Lung Cancer* 2006; 7: 385-8.
6. Lepper ER, Swain SM, Tan AR et al. Liquid-chromatographic determination of erlotinib (OSI-774), an epidermal growth factor receptor tyrosine kinase inhibitor. *J Chromatogr B Analyt Technol Biomed Life Sci* 2003; 796: 181-8.
7. Masters AR, Sweeney CJ, Jones DR. The quantification of erlotinib (OSI-774) and OSI-420 in human plasma by liquid chromatography-tandem mass spectrometry. *J Chromatogr B Analyt Technol Biomed Life Sci* 2007; 848: 379-83.
8. Zhang W, Siu LL, Moore MJ et al. Simultaneous determination of OSI-774 and its major metabolite OSI-420 in human plasma by using HPLC with UV detection. *J Chromatogr B Analyt Technol Biomed Life Sci* 2005; 814: 143-7.
9. Zhao M, He P, Rudek MA et al. Specific method for determination of OSI-774 and its metabolite OSI-420 in human plasma by using liquid chromatography-tandem mass spectrometry. *J Chromatogr B Analyt Technol Biomed Life Sci* 2003; 793: 413-20.
10. Schaake EE, Kappers I, Codrington HE et al. Tumor Response and Toxicity of Neoadjuvant Erlotinib in Patients With Early-Stage Non-Small-Cell Lung Cancer. *J Clin Oncol* 2012; July, 2nd Epub.
11. U.S. Food and Drug Administration: Centre for Drug Evaluation and Research. Guidance for Industry: Bioanalytical Method Validation. <http://www.fda.gov/downloads/Drugs/GuidanceComplianceRegulatoryInformation/Guidances/UCM070107.pdf>. 1-5-2001.
12. Viswanathan CT, Bansal S, Booth B et al. Quantitative bioanalytical methods validation and implementation: best practices for chromatographic and ligand binding assays. *Pharm Res* 2007; 24: 1962-73.
13. Liang HR, Foltz RL, Meng M et al. Ionization enhancement in atmospheric pressure chemical ionization and suppression in electrospray ionization between target drugs and stable-isotope-labeled internal standards in quantitative liquid chromatography/tandem mass spectrometry. *Rapid Commun Mass Spectrom* 2003; 17: 2815-21.
14. Sojo LE, Lum G, Chee P. Internal standard signal suppression by co-eluting analyte in isotope dilution LC-ESI-MS. *Analyst* 2003; 128: 51-4.
15. Dolan JW. Autosampler Carry Over. *LCGC* 2001; 19: 164-8.
16. Dolan J. Attacking Carry Over Problems. *LCGC* 2001; 19: 1050-4.
17. European Medicines Agency (EMA). Erlotinib: EPAR - Scientific Discussion. Available at: http://www.ema.europa.eu/docs/en_GB/document_library/EPAR_-_Scientific_Discussion/human/000618/WC500033991.pdf Date accessed: July 17, 2012. 2-11-2005.

18. Carey KD, Garton AJ, Romero MS et al. Kinetic analysis of epidermal growth factor receptor somatic mutant proteins shows increased sensitivity to the epidermal growth factor receptor tyrosine kinase inhibitor, erlotinib. *Cancer Res* 2006; 66: 8163-71.
19. Sangha R, Davies AM, Lara PN, Jr. et al. Intercalated Erlotinib-Docetaxel Dosing Schedules Designed to Achieve Pharmacodynamic Separation: Results of a Phase I/II Trial. *J Thorac Oncol* 2011; 6: 2112-9.

R1
R2
R3
R4
R5
R6
R7
R8
R9
R10
R11
R12
R13
R14
R15
R16
R17
R18
R19
R20
R21
R22
R23
R24
R25
R26
R27
R28
R29
R30
R31
R32
R33
R34
R35
R36
R37
R38
R39



Chapter 1.6

A validated assay for the quantitative analysis of vatalanib in human EDTA plasma by liquid chromatography coupled with electrospray ionization tandem mass spectrometry

Nienke A.G. Lankheet
Michel J.X. Hillebrand
Marlies. H.G. Langenberg
Hilde Rosing
Alwin D.R. Huitema
Emile E. Voest
Jan H.M. Schellens
Jos H. Beijnen

Journal of Chromatography B 2009; 877: 3625–3630.



R1
R2
R3
R4
R5
R6
R7
R8
R9
R10
R11
R12
R13
R14
R15
R16
R17
R18
R19
R20
R21
R22
R23
R24
R25
R26
R27
R28
R29
R30
R31
R32
R33
R34
R35
R36
R37
R38
R39

Abstract

A sensitive and accurate method for the determination of vatalanib in human EDTA plasma was developed using high-performance liquid chromatography and detection with tandem mass spectrometry. Stable isotopically labeled imatinib was used as internal standard. Plasma proteins were precipitated and an aliquot of the supernatant was directly injected onto a Phenomenex Gemini C18 analytical column (50 x 2.0 mm ID, 5.0 μ m particle size) and then compounds were eluted with a linear gradient. The outlet of the column was connected to a Sciex API 365 triple quadrupole mass spectrometer and ions were detected in positive multiple reaction monitoring mode. The lower limit of quantification was 10 ng/mL (S/N \approx 10, CV \approx 8.4%). This method was validated over a linear range from 10 to 2,500 ng/mL, and results from the validation study demonstrated a good intra- and inter-assay accuracy (inaccuracy \leq 9.57%) and precision (CV \leq 8.81%). This method has been used to determine plasma vatalanib concentrations in patients with advanced solid tumor, enrolled in a Phase I pharmacokinetic trial with the drug.

Introduction

Neovascularization of tumor tissue is essential for tumor growth and metastasis formation. The vascular endothelial growth factor (VEGF) is a multifunctional cytokine involved in neovascularization by increasing vascular permeability and stimulating endothelial cell growth and angiogenesis. VEGF is secreted by tumor cells and macrophages and evokes its effects by binding to cell surface VEGF receptors (VEGFR) on the tumor vascular endothelium[1-3]. The family of VEGFRs consists of three different tyrosine kinase receptors (VEGFR-1, VEGFR-2 and VEGFR-3). Specific inhibition of angiogenesis by blocking tyrosine kinase receptors could prevent growth of tumors and their metastatic potential. Since cell division of endothelial cells in the normal vasculature is rare, inhibition of angiogenic signals by interfering with VEGFR-induced signals selectively targets the vasculature of tumor tissue. Therefore VEGFR targeted therapy is expected to be well tolerated in cancer patients[1,3].

Vatalanib (PTK787/ZK222584) belongs to the class of aminophthalazines and is a potent orally active tyrosine kinase receptor inhibitor blocking all known VEGFRs, with a greater potency against VEGFR-1 and VEGFR-2. In addition, vatalanib also inhibits other tyrosine kinase receptors, such as the platelet-derived growth factor receptor (PDGF), c-kit and c-Fms [3,4]. The intended indication for use of vatalanib is tumors with an overexpression of VEGF or VEGFR. Currently, vatalanib is studied in phase I, II and III trials in several advanced solid tumors, including cancer of the gastrointestinal tract, prostate, breast, ovary, lung, liver and brain [4].

To support the pharmacokinetic analysis in clinical trials, compound specific analytical methods are essential. Analytical methods based on high performance liquid chromatography coupled to tandem mass spectrometry (HPLC-MS/MS) have become irreplaceable in the quantitative analysis of small molecules in biological matrices [5]. However, to date only HPLC-UV methods for determination of vatalanib have been reported in literature [6,7]. Therefore we developed and validated a sensitive and specific HPLC-MS/MS method for quantification of vatalanib in human EDTA plasma.

Experimental

Chemicals and materials

Reference standards and internal standards were provided by the following manufacturers: vatalanib.HCl ($C_{20}H_{15}ClN_4 \cdot HCl$) by Sequoia Research Products (Oxford, United Kingdom), imatinib- $^{13}C, ^2H_3$ ($C_{29}H_{31}N_7O$) stable isotope by Alsa Chim (Illkirch, France). HPLC-grade acetonitrile and methanol were purchased from Biosolve (Valkenswaard, The Netherlands). Distilled water was obtained from B.Braun (Melsungen, Germany). Ammonia 25% was purchased from Merck (Darmstadt, Germany). Blanco plasma with EDTA as anticoagulant was obtained from Slotervaart Hospital (Amsterdam, The Netherlands).

R1
R2
R3
R4
R5
R6
R7
R8
R9
R10
R11
R12
R13
R14
R15
R16
R17
R18
R19
R20
R21
R22
R23
R24
R25
R26
R27
R28
R29
R30
R31
R32
R33
R34
R35
R36
R37
R38
R39

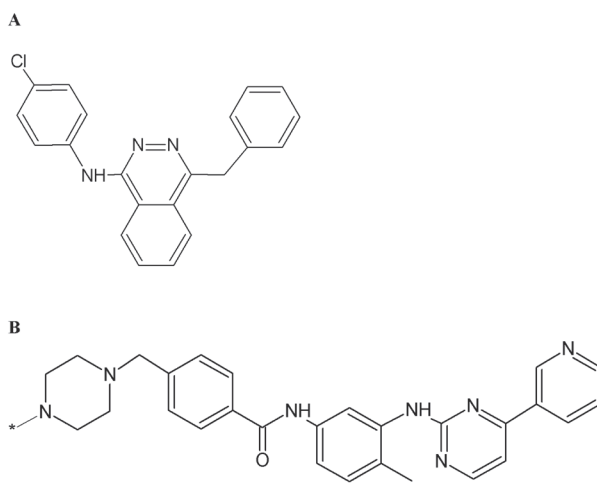


Figure 1. Chemical structures of vatalanib (A) and imatinib- $^{13}\text{C}_2\text{H}_3$ (* Represents the $^{13}\text{C}_2\text{H}_3$ -group, B).

Mass Spectrometric conditions

An API 365 triple quadrupole mass spectrometer (Sciex, ON, Canada) equipped with an electrospray ionization (ESI) source (Sciex) operating in the positive ion mode was used as detector. The ionisation source parameters were: nebulizer gas, 10 arbitrary units (a.u.); curtain gas, 6 a.u.; ionspray voltage, 5000 V; heater gas, 350 °C; turbo gas, 7 L/min. The nebulizer (1.8 L/min) and turbo (7.0 L/min) gases were zero air, while curtain (1.3 mL/min) and collision activated dissociation gas (240×10^{12} molecules/cm²) consisted of nitrogen (grade 5.0). The dwell time was 150 ms with a 5 ms pause between scans. Quadruples operated at unit mass resolution (0.7 Da). Multiple reaction monitoring (MRM) chromatograms were used for quantification. Mass-transitions of from m/z 347 to 311 for vatalanib and m/z 498 to 394 for the internal standard imatinib- $^{13}\text{C}_2\text{H}_3$ were optimised. Data were processed by Analyst software (version 1.4, Sciex).

Chromatographic conditions

Chromatographic separations of vatalanib and the internal standard were carried out using an Agilent 1100 HPLC system (Agilent technologies, Palo Alto, CA, USA) consisting of a binary pump and a cooled autosampler (4 °C). Compounds were eluted on a linear gradient at a flow rate of 250 $\mu\text{L}/\text{min}$. Eluent A consisted of 10 mM ammonium hydroxide in water and eluent B of 1 mM ammonium hydroxide in methanol. At time zero, 55% of eluent B was flushed through the column. After 0.5 min, 80% of eluent B was mixed with 20% of eluent A and this mobile phase composition was maintained for 3 min. Then the gradient composition was changed to a mix of 95% eluent B with 5% of eluent A. This composition was maintained for 1 min and the column was reconditioned for 3.4 min with 55% of eluent B before the next injection. Separation was carried out on a reversed phase system with a Gemini C₁₈ column (50 x 2.0 mm ID, 5.0 μm particle size;

Phenomenex, Torrance, CA, USA) protected with a Securityguard Gemini precolumn (4 x 2,0 mm ID, 5,0 mm particle size; Torrance, CA, USA) and thermostatted at 40 °C. The column outlet was connected to the ESI through a divert valve. The divert valve was directed to waste during the first 2 min to prevent the introduction of endogenous compounds into the mass spectrometer. The total run time was 8 min and sample injections of 10 µL were carried out.

Preparation of calibration standards and validation samples

A set of stock solutions of vatalanib was prepared from two independent weighings; one for the calibration standards and one for the validation samples. Approximately 1.1 mg of vatalanib.HCl was accurately weighted and dissolved in 2 mL of methanol in a volumetric flask to give a 500 µg/mL stock solution of the free base. Stock solutions of the internal standard imatinib-¹³C,²H₃ were made in methanol at a concentration of approximately 1000 µg/mL. A 200 ng/mL working solution of the internal standard was prepared by dilution of the stock solution in methanol. To precipitate the plasma proteins, a mixture of methanol-acetonitrile (1:1, v/v) was used.

For the preparation of the calibration standards, working solutions in the range from 200 to 50,000 ng/ml were used. These working solutions were prepared by dilution of a vatalanib stock solution in methanol. A volume of 50 µL of each working solution was added to 950 µL of control human EDTA plasma to obtain calibration standards in the range from 10 to 2,500 ng/ml.

Four working solutions in the range from 200 to 40,000 ng/ml were prepared by dilution of an independently prepared vatalanib stock solution in methanol. To obtain validation samples of 10, 20, 200 and 2,000 ng/ml, 50 µL of each working solution was added to 950 µL of control human EDTA plasma. The stock and working solutions in methanol and precipitation reagent were stored at nominally -20 °C until use.

To establish the accuracy and precision of the method when samples are quantified above the upper limit of quantification (ULQ), a sample containing 8,000 ng/mL vatalanib was spiked. Before processing, this sample was then diluted ten times in control human EDTA plasma.

Sample pre-treatment

Protein precipitation was used as sample pre-treatment for plasma samples with vatalanib and imatinib-¹³C,²H₃. To 50 µL of plasma sample, 20 µL of internal standard working solution (200 ng/mL) and 150 µL of protein precipitation reagent (-20 °C) were added. After vortex mixing for 15 s, samples were centrifuged at 15,000 x g for 15 min. A volume of 5 µL of the clear supernatant was injected onto the column.

Validation procedures

A full validation of the assay was performed according to the FDA guidelines for validation of bioanalytical assays including linearity, inaccuracy, precision, specificity, selectivity, cross-analyte/internal standard interference, recovery, ion suppression, carry-over and stability [8,9].

R1
R2
R3
R4
R5
R6
R7
R8
R9
R10
R11
R12
R13
R14
R15
R16
R17
R18
R19
R20
R21
R22
R23
R24
R25
R26
R27
R28
R29
R30
R31
R32
R33
R34
R35
R36
R37
R38
R39

R1 Eight non-zero plasma calibration samples were prepared and analysed in duplicate in three
R2 separate analytical runs. The linear regression of the ratio of the areas of the analyte and the internal
R3 standard peaks versus the concentration were weighted. Weighing factors of $1/x$ and $1/x^2$ (where
R4 x =concentration) were tested. In order to establish the best weighting factor, back-calculated
R5 calibration concentrations were determined. The model with the lowest total bias and the most
R6 constant bias across the concentration range was used for further analysis and quantification. The
R7 linearity was evaluated by means of back-calculated concentrations of the calibration standards.
R8 The deviation from the nominal concentrations should be within $\pm 20\%$ for the lower limit of
R9 quantification (LLQ) and within $\pm 15\%$ for the other concentrations with coefficient of variation
R10 (CV) values less than 20% and 15% for both the LLQ and the other concentrations respectively.
R11 Inaccuracy and precision of the assay were established by analysing validation samples with
R12 analyte concentrations at the lower limit of quantification (LLQ) and in the low, mid and high
R13 concentration ranges of the calibration curves. Five determinations of each validation sample were
R14 measured in three separate analytical runs. Samples with vatalanib concentrations above the ULQ
R15 were diluted 1:10 in control human EDTA. These samples were processed in 5-fold and measured in
R16 one analytical run to assess the accuracy and precision. The intra-assay inaccuracy was defined as
R17 the percentage difference between the mean calculated concentration after three analytical runs
R18 and the nominal concentration. The coefficient of variation (CV%) was used to report the intra- and
R19 inter-assay precision. The intra- and inter-assay inaccuracies should be within $\pm 20\%$ for the LLQ and
R20 $\pm 15\%$ for all other concentrations. The precisions CV% should be less than 20% for the LLQ and less
R21 than 15% for all other concentrations [9].

R22 To investigate whether endogenous compounds from plasma could interfere with the
R23 detection of the analyte or the internal standard, six different batches of control drug-free human
R24 EDTA plasma prepared as double blanks (containing neither analyte nor internal standard) and
R25 LLQ samples. Samples were processed and analysed according to the described procedures. Areas
R26 of peaks co-eluting with the analytes should not exceed 20% of the area at the LLQ level. The
R27 deviation of the nominal concentration for the LLQ samples should be within $\pm 20\%$.

R28 To investigate possible cross interference between vatalanib and the internal standard, a
R29 cross interference check was performed. Drug-free human EDTA plasma was spiked at ULQ level
R30 and was processed without internal standard. Also drug-free plasma with only internal standard
R31 imatinib- $^{13}\text{C}_2,^2\text{H}_3$ was processed. The response of any interfering peak with the same retention
R32 time as vatalanib should be less than 20% of the response of a LLQ sample. The response of any
R33 interfering peak with the same retention time as the internal standard imatinib- $^{13}\text{C}_2,^2\text{H}_3$ should be
R34 less than 5% of the response of the internal standard.

R35 The protein precipitation recovery of vatalanib was determined at three concentrations (20,
R36 200 and 2000 ng/ml) by comparing the analytical response of processed samples with those
R37 of processed blanks spiked with analyte (representing 100% recovery). The total recovery was
R38 determined by comparing the analytical response of processed samples with the analytical
R39

response of the unprocessed samples containing only analyte and internal standard in precipitation reagent. Ion suppression (matrix effect) was examined by comparing the analytical response of processed blanks spiked with analyte with those unprocessed samples in precipitation reagent. These experiments were performed in triplicate.

Carry-over was tested by injecting two processed blank matrix samples sequentially after injecting an ULQ sample. The response in the first blank matrix at the retention times of vatalanib and imatinib- $^{13}\text{C},^2\text{H}_3$ should be less than 20% of the response of a LLQ sample.

The stability of vatalanib in spiked human EDTA plasma after three freeze/thaw cycles from nominally $-20\text{ }^\circ\text{C}$ to ambient temperatures was investigated in triplicate at two concentrations (20 ng/mL and 2,000 ng/mL) by comparing validation samples that had been frozen and thawed three times with validation samples that had been prepared freshly. The stability of vatalanib in spiked human EDTA plasma maintained at ambient temperatures for 6 h was evaluated in triplicate at two concentrations and compared to validation samples that were kept at $-20\text{ }^\circ\text{C}$ until processing. The processed sample stability of vatalanib was investigated at two concentrations (20 and 2,000 ng/mL). Hereto, the measured concentrations in a final extract of validation samples after 2 days (ambient temperature) and 7 days ($2\text{--}8\text{ }^\circ\text{C}$) were determined using freshly prepared calibration standards. The re-injection reproducibility was determined after 2 days of storage in the autosampler ($4\text{ }^\circ\text{C}$) and compared with the initial concentrations. The analytes were considered to be stable in the matrix or final extract if 85–115% of the initial concentrations was recovered. Stability of stock solutions of vatalanib and imatinib- $^{13}\text{C},^2\text{H}_3$ stored at ambient temperature for 6 h and at $-20\text{ }^\circ\text{C}$ was assessed in triplicate. The analyte was considered to be stable in stock solutions if 95–105% of the initial concentration was recovered. The internal standard was considered to be stable if 80–120% of the initial concentration was recovered. Determination of long term stability of vatalanib in stock solutions and in plasma at $-70\text{ }^\circ\text{C}$ are currently ongoing.

Results and discussion

Mass spectrometry

During optimization of the mass spectrometric parameters, the Q1 spectrum of vatalanib showed the singly charged molecular ion as most intense ion at m/z 347. For imatinib- $^{13}\text{C},^2\text{H}_3$ the most intense peak in the Q1 spectrum also corresponded to the singly charged molecular ion at m/z 498. The structural formulas of vatalanib and imatinib- $^{13}\text{C},^2\text{H}_3$ are depicted in figure 1. MS/MS experiments were carried out to determine the most abundant product ions for multiple reaction monitoring (MRM). MS/MS product ion scans and the proposed fragmentation pathways for the chosen transitions of vatalanib and imatinib- $^{13}\text{C},^2\text{H}_3$ are shown in figure 2. Vatalanib and the internal standard could be detected with the electrospray source operating in the positive mode. Non-linearity was observed for all calibration curves when 2.5 ng of vatalanib or more was injected onto the column. When injecting a smaller volume of 5 mL supernatant the ULQ was set to 2,500 ng/mL (injection of 2.8 ng onto the column).

R1
R2
R3
R4
R5
R6
R7
R8
R9
R10
R11
R12
R13
R14
R15
R16
R17
R18
R19
R20
R21
R22
R23
R24
R25
R26
R27
R28
R29
R30
R31
R32
R33
R34
R35
R36
R37
R38
R39

R1
R2
R3
R4
R5
R6
R7
R8
R9
R10
R11
R12
R13
R14
R15
R16
R17
R18
R19
R20
R21
R22
R23
R24
R25
R26
R27
R28
R29
R30
R31
R32
R33
R34
R35
R36
R37
R38
R39

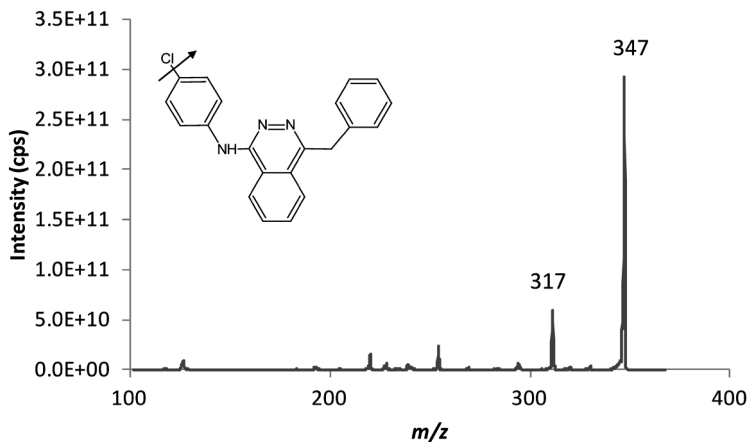


Figure 2A. MS/MS product ion scan of vatalanib (precursor ion m/z 347).

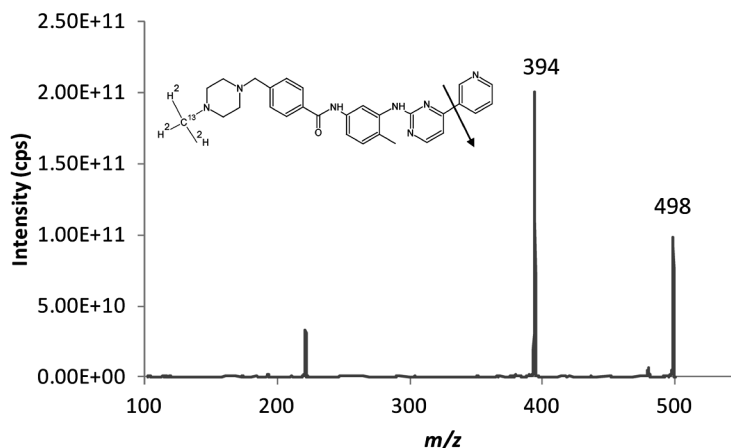


Figure 2B. MS/MS product ion scan of imatinib- $^{13}\text{C}_2\text{H}_3$ (precursor ion m/z 498; * Represents the $^{13}\text{C}_2\text{H}_3$ -group).

Chromatography

Due to the basic properties of vatalanib the best retention was observed using an alkaline mobile phase. In order to retain vatalanib on the column and to establish stable retention times a mobile phase with 10 mM ammonium hydroxide (pH 10.2) was applied. Column stability under alkaline conditions was established by successive analyses of more than 500 analytical samples of a pharmacokinetic study. Additionally, the number of plates of the column in the first analytical runs did not differ from the number of plates after more than three months of extensive column usage.

Since the pH of the aqueous component was ~ 10 , full protonation of the analyte in the mobile phase was not expected. However, the most abundant peaks in the spectrum of vatalanib and imatinib- $^{13}\text{C}_2\text{H}_3$ were the positively charged molecular ions at m/z 347 and 498 respectively.

Protonation of compounds during ESI-MS performed with a basic eluent has been described [10].

Peak shape of compounds eluting on a linear gradient starting at 55% eluent B increasing to 100% B in 2.5 min at a flow rate of 250 μL per min was not symmetrical ($A_s \approx 3$). Improved peak shapes ($A_s \approx 1.1$) were obtained when the linear gradient starting on 55% eluent B was followed by an isocratic elution with 80% eluent B at a flow rate of 250 μL per min. To elute the hydrophobic compound from the column and to decrease the carry over in the HPLC system the amount of modifier was increased by a quick stepwise gradient to 95% of eluent B after elution of vatalanib. Subsequently, the column was reconditioned with 55% B before the next injection (Figure 3). Typical chromatograms are depicted in Figure 4. At LLQ level (10.2 ng/mL) a signal to noise ratio (S/N-ratio) of ± 10 was obtained. Analyte retention times (t_r 3.2 min) were sufficient to separate vatalanib and imatinib- $^{13}\text{C}_2\text{H}_3$ from endogenous interferences.

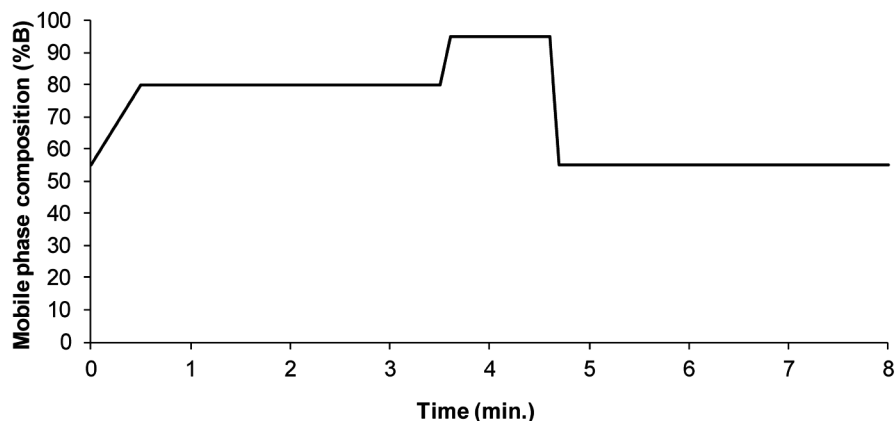


Figure 3. HPLC gradient used in the LC-MS/MS-assay for vatalanib.

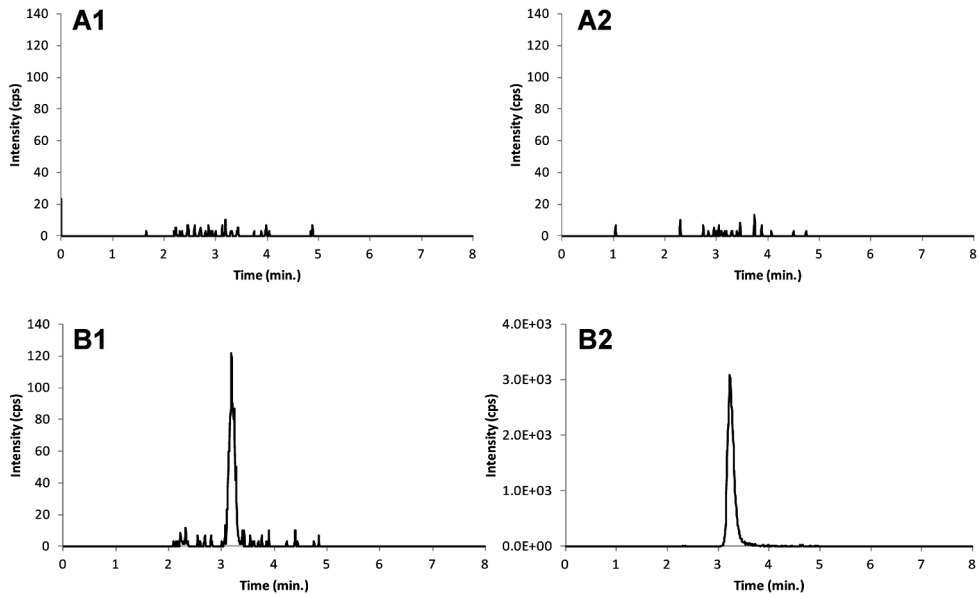
Sample pre-treatment

Protein precipitation (PP) was used as sample pre-treatment, mainly because it is a fast and simple one-step procedure and the costs are very minor. However, PP lacks specificity and selectivity. For vatalanib a 3-fold signal reduction was observed when processed (PP with 100% acetonitrile) and non-processed samples were compared. This could be due to inclusion of the analyte during protein precipitation. To prevent loss of analyte a less strong precipitation fluid consisting of acetonitrile/methanol (1:1, v/v) was tested. This resulted in an increase in peak intensity with 20%. Liquid-liquid extraction with t-butyl methyl ether was tested, but the signal to noise ratio did not improve. Moreover, the sensitivity after protein precipitation was sufficient to quantify vatalanib in plasma within the therapeutic window. Additionally, the robustness of the sample pre-treatment with protein precipitation, determined by degree of variation of area ratio within repetitive measurements, was comparable to the robustness of the method with liquid-liquid

R1
R2
R3
R4
R5
R6
R7
R8
R9
R10
R11
R12
R13
R14
R15
R16
R17
R18
R19
R20
R21
R22
R23
R24
R25
R26
R27
R28
R29
R30
R31
R32
R33
R34
R35
R36
R37
R38
R39

R1 extraction (CV% 4.0 vs 5.0). Therefore, protein precipitation seems to be the most efficient sample
R2 pre-treatment for the analysis of vatalanib.

R3 No deuterated internal standard of vatalanib was available. Therefore, stable isotopes of several
R4 tyrosine kinase inhibitors were tested as potential internal standards in this assay. Imatinib stable
R5 isotope co-eluted with vatalanib and corrected for variations in sample pre-treatment and analysis,
R6 and was therefore chosen as internal standard.



R16 **Figure 4.** Representative LC-MS/MS chromatograms of a blank human EDTA plasma sample (A1, vatalanib; A2,
R17 internal standard imatinib-¹³C₂H₃) and of a spiked human EDTA plasma sample at the LLQ level of 10 ng/mL
R18 (B1, vatalanib; B2, internal standard imatinib-¹³C₂H₃).

R20 **Validation**

R21 The assay was linear over the validated concentration range from 10 to 2,500 ng/mL of vatalanib in
R22 human plasma. The lowest total bias and the most constant bias across the range were obtained
R23 using a weighting factor of 1/x². Correlation coefficients (r²) were at least 0.995. At all concentration
R24 levels the accuracies were within 95.9 and 106.3% with CV values less than 9.14%.

R25 The intra- and inter-assay performance data are presented in Table 1. The intra-assay inaccuracies
R26 (% bias) for vatalanib in human EDTA plasma were within ± 9.57% for all concentration levels. The
R27 intra-assay precisions (CV%) for vatalanib were less than 8.81% for all concentration levels. Samples
R28 above the ULQ (2,500 ng/mL) were diluted 10 times with control drug-free human EDTA plasma.
R29 The intra-assay inaccuracy for diluted samples was 1.22% and the intra-assay precision was 3.23%.
R30 In conclusion, the validated range for vatalanib based on 50 mL human EDTA plasma is from 10.0-
R31 2,500 ng/mL. When concentrations above 2,500 ng/mL are expected, plasma samples can be
R32
R33
R34
R35
R36
R37
R38
R39

diluted 10 times with control drug-free human EDTA plasma. Inaccuracies and precisions fulfilled the requirements [8].

Table 1. Assay performance data for vatalanib.

Run	Nominal conc. (ng/mL)	Mean calculated conc. (ng/mL)	Inaccuracy (% Dev)	Precision (%CV)	No. of replicates
1	10.2	10.8	6.08	5.60	5
2	10.2	11.2	9.57	8.06	5
3	10.2	10.5	3.12	11.4	5
Inter-assay	10.2	10.8	6.25	8.38	15
1	20.5	20.5	-0.20	10.4	5
2	20.5	22.4	9.07	6.27	5
3	20.5	20.4	-0.39	7.69	5
Inter-assay	20.5	21.1	2.83	8.81	15
1	205	192	-6.44	2.94	5
2	205	188	-8.39	2.78	5
3	205	210	2.54	4.38	5
Inter-assay	205	197	-4.10	6.08	15
1	2050	2060	0.49	5.41	5
2	2050	2113	3.05	6.78	5
3	2050	2134	4.10	1.89	5
Inter-assay	2050	2101	2.51	4.79	15

Conc., concentration; Dev, Deviation; CV, coefficient of variation.

In MRM chromatograms of six batches of control drug-free EDTA plasma no interference of endogenous compounds from plasma could be detected with the analyte or the internal standard. No co-eluting peaks >20% of the vatalanib peak area at the LLQ level were found and also no co-eluting peaks >5% of the internal standard imatinib-¹³C,³H₂ were detected. The deviations of the nominal concentration at the LLQ level were between -6.08 and 9.48% for vatalanib and were found to be acceptable.

When a sample of control drug-free human EDTA plasma was only processed with the internal standard imatinib-¹³C,³H₂, no peaks were detected at the retention time of vatalanib. Additionally, when a sample with vatalanib at ULQ level was processed without internal standard, no peaks were detected at the retention time of imatinib-¹³C,³H₂. In conclusion, no cross-analyte/internal standard interference was detected.

The mean matrix effect detected for vatalanib was an enhancement of 4.27% (range 2.91% to 6.59%). For vatalanib the mean PP recovery was 77.8% and the mean total recovery was 82.7%.

During development of the chromatographic system, different gradient systems were tested. Gradient elution with an increase in the amount of modifier by a quick stepwise gradient to 95% of eluent B after elution of vatalanib was chosen and the run time was set to 8 minutes to diminish carry-over due to a memory effect on the HPLC column. During validation of the present system no

carry-over was experienced since no interfering peaks were detected in processed blank samples injected after an ULQ sample.

The stability data for vatalanib are represented in Table 2. Vatalanib is stable in human EDTA plasma for at least three freeze (-20 °C) / thaw cycles and in human EDTA plasma at ambient temperatures up to 6h. Besides, vatalanib is stable in the final extract at nominally 2-8 °C up to 7 days. Re-injection reproducibility was established and an analytical run can be re-injected after at least 48h of storage in the autosampler at 4 °C. Assessment of long term stability of vatalanib in plasma and in stock solutions is still ongoing.

Table 2. Stability data for vatalanib and the internal standard imatinib-¹³C₃H₃.

Matrix	Conditions	Initial conc. (ng/mL)	Measured conc. (ng/mL)	Dev (%)	CV (%)	No. of replicates
Vatalanib						
Plasma	3 freeze (-20°C)/ thaw cycles	19.8	20.3	2.18	4.31	3
Plasma	3 freeze (-20°C)/ thaw cycles	2160	2190	1.39	2.02	3
Plasma	Ambient, 6h	22.1	23.4	5.57	4.05	3
Plasma	Ambient, 6h	2113	2383	12.8	15.8	3
Final extract	2-8°C, 7 days	20.7	20.9	1.29	7.71	3
Final extract	2-8°C, 7 days	2177	2253	3.52	1.25	3
Final extract	Ambient, 48h	20.9	21.5	10.7	3.82	3
Final extract	Ambient, 48h	2120	2235	2.7	4.65	3
RR	Autosampler 4°C, 48h	19.8	20.0	0.67	5.02	3
RR	Autosampler 4°C, 48h	195	204	4.79	2.70	3
RR	Autosampler 4°C, 48h	2057	1997	-2.92	3.93	3
Stock solution (methanol)	Ambient, 6h	0.512 * 10 ⁶	0.497 * 10 ⁶	-2.87	1.35	3
Imatinib-¹³C₃H₃						
Stock solution (methanol)	Ambient, 6h	1.003 * 10 ⁶	0.947 * 10 ⁶	-5.57	2.00	3

Conc., concentration; Dev, Deviation; CV, coefficient of variation; RR, re-injection reproducibility.

Application of assay in patient blood samples

The validated vatalanib assay was used to support a Phase I pharmacokinetic trial of vatalanib in patients with advanced solid tumors [11]. Plasma samples were collected and thereafter processed and analyzed by the methods described in this report. All samples were stored at -70°C until analysis. Because high concentrations were expected at the time points directly after administration of vatalanib, these plasma samples were diluted 10 times with control human EDTA plasma (50 mL

plasma sample with 450 mL control human EDTA plasma) before processing. A representative plasma concentration-time profile for vatalanib after oral administration (dose: 750 mg once-daily) is depicted in figure 5. The mean terminal half-life of vatalanib was calculated to be 5 h. Even 24 h after administration, the vatalanib plasma concentrations are far above the LLQ. These results demonstrate the applicability of the method in clinical pharmacokinetic studies.

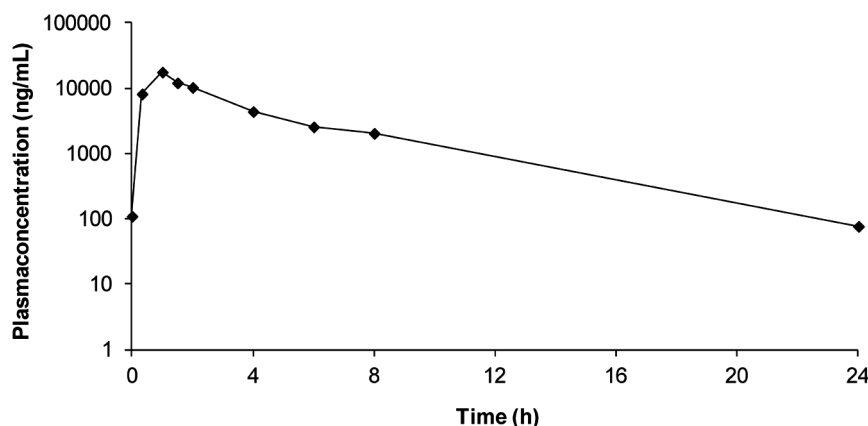


Figure 5. Representative concentration vs. time profile of vatalanib in a patient after one oral dose of vatalanib (750 mg).

Conclusion

We have developed and validated a fast LC-MS/MS method for the quantitative analysis of vatalanib in human plasma samples. Human EDTA plasma samples with vatalanib are pre-treated by protein precipitation with acetonitrile/methanol (1:1, v/v) and addition of internal standard imatinib- $^{13}\text{C}_3,^3\text{H}_2$. Chromatography is performed under alkaline conditions. A linear dynamic range from 10.0 to 2,500 ng/ml was validated. Validation results show that the method is accurate and precise. The method is easy to perform and it has shown to be applicable in clinical pharmacological research. Additionally, since the required sample volume is relatively small (50 mL) and the method has a high sensitivity ($S/N \approx 10$ at 10.2 ng/ml) it may also be useful for studies of vatalanib in which small sample volumes or low concentrations may be expected, such as other biological matrices.

R1
R2
R3
R4
R5
R6
R7
R8
R9
R10
R11
R12
R13
R14
R15
R16
R17
R18
R19
R20
R21
R22
R23
R24
R25
R26
R27
R28
R29
R30
R31
R32
R33
R34
R35
R36
R37
R38
R39

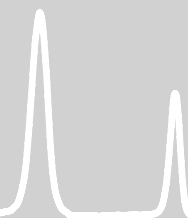
R1
R2
R3
R4
R5
R6
R7
R8
R9
R10
R11
R12
R13
R14
R15
R16
R17
R18
R19
R20
R21
R22
R23
R24
R25
R26
R27
R28
R29
R30
R31
R32
R33
R34
R35
R36
R37
R38
R39

References

1. Moreira IS, Fernandes PA, Ramos MJ. Vascular endothelial growth factor (VEGF) inhibition--a critical review. *Anticancer Agents Med Chem* 2007; 7: 223-45.
2. Senger DR, Van de WL, Brown LF et al. Vascular permeability factor (VPF, VEGF) in tumor biology. *Cancer Metastasis Rev* 1993; 12: 303-24.
3. Wood JM, Bold G, Buchdunger E et al. PTK787/ZK 222584, a novel and potent inhibitor of vascular endothelial growth factor receptor tyrosine kinases, impairs vascular endothelial growth factor-induced responses and tumor growth after oral administration. *Cancer Res* 2000; 60: 2178-89.
4. Jost LM, Gschwind HP, Jalava T et al. Metabolism and disposition of vatalanib (PTK787/ZK-222584) in cancer patients. *Drug Metab Dispos* 2006; 34: 1817-28.
5. Stokvis E, Rosing H, Beijnen JH. Liquid chromatography-mass spectrometry for the quantitative bioanalysis of anticancer drugs. *Mass Spectrom Rev* 2005; 24: 887-917.
6. Morgan B, Thomas AL, Dreves J et al. Dynamic contrast-enhanced magnetic resonance imaging as a biomarker for the pharmacological response of PTK787/ZK 222584, an inhibitor of the vascular endothelial growth factor receptor tyrosine kinases, in patients with advanced colorectal cancer and liver metastases: results from two phase I studies. *J Clin Oncol* 2003; 21: 3955-64.
7. Mross K, Dreves J, Muller M et al. Phase I clinical and pharmacokinetic study of PTK/ZK, a multiple VEGF receptor inhibitor, in patients with liver metastases from solid tumours. *Eur J Cancer* 2005; 41: 1291-9.
8. U.S.Food and Drug Administration: Centre for Drug Evaluation an Research. Guidance for Industry: Bioanalytical Method Validation. Available at: <http://www.fda.gov/downloads/Drugs/GuidanceComplianceRegulatoryInformation/Guidances/UCM070107.pdf>. Date accessed October 14, 2008. 1-5-2001.
9. Viswanathan CT, Bansal S, Booth B et al. Quantitative bioanalytical methods validation and implementation: best practices for chromatographic and ligand binding assays. *Pharm Res* 2007; 24: 1962-73.
10. Stokvis E, Rosing H, Lopez-Lazaro L et al. Quantitative analysis of the novel depsipeptide anticancer drug Kahalalide F in human plasma by high-performance liquid chromatography under basic conditions coupled to electrospray ionization tandem mass spectrometry. *J Mass Spectrom* 2002; 37: 992-1000.
11. Langenberg MH, Witteveen PO, Lankheet AG. Phase I study of combination treatment with PTK 787/ZK 222584 (PTK/ZK) and cetuximab for patients with advanced solid tumors: Safety, pharmacokinetics, pharmacodynamics, and toxicity analysis (abstract). *J Clin Oncol* 2009; 27: (suppl; abstr 2575).

Chapter 2

Clinical Pharmacology of Tyrosine Kinase Inhibitors





Chapter 2.1

Plasma concentrations of tyrosine kinase inhibitors
imatinib, erlotinib and sunitinib in routine clinical
outpatient cancer care

Nienke A.G. Lankheet
Lotte M. Knapen
Jan H.M. Schellens
Jos H. Beijnen
Neeltje Steeghs
Alwin D.R. Huitema

Submitted for publication



R1
R2
R3
R4
R5
R6
R7
R8
R9
R10
R11
R12
R13
R14
R15
R16
R17
R18
R19
R20
R21
R22
R23
R24
R25
R26
R27
R28
R29
R30
R31
R32
R33
R34
R35
R36
R37
R38
R39

Abstract

Background. The objectives of this study were to evaluate plasma concentrations of the tyrosine kinase inhibitors (TKIs) imatinib, erlotinib and sunitinib within several dosing schemes in a cohort of cancer patients in routine clinical practice and to find possible factors related to subtherapeutic plasma concentrations.

Methods. An observational study was performed in an unselected cohort of patients using TKIs for cancer treatment. Randomly timed plasma samples were drawn together with regular laboratory investigations during routine outpatient clinic visits. Plasma concentrations of the TKIs were determined using a validated HPLC-MS/MS method. Trough concentrations were calculated using the interval between last dose intake and blood sampling and the mean elimination half-life of the TKIs and were compared with target trough concentrations. Outpatient medical records were reviewed to collect data on patient- and medication- related factors that could have contributed to variations in TKI plasma concentrations.

Results. Only 26.8%, 88.9% and 51.4% of the calculated trough plasma concentrations of imatinib, erlotinib and sunitinib samples, respectively, reached the predefined therapeutic target (imatinib: 1100 ng/mL, erlotinib: 500 ng/mL, sunitinib: 50 ng/mL). Inter-patient variability was high with coefficients of variation (CV%) of 39.1%, 40.1% and 29.2% for imatinib, erlotinib and sunitinib, respectively. High variation in plasma concentrations could only partly be explained by patient- or medication related factors.

Conclusion. Almost half of the plasma concentrations in the outpatient population appeared to be subtherapeutic with a risk of treatment failure or development of drug resistance. It is not possible to predict which patients are at risk of subtherapeutic plasma concentrations based on patient- or medication related factors. Thus, therapeutic drug monitoring (TDM) is paramount and should be fully implemented in routine cancer care to identify patients that are in need of individual adjusted dosages.

Introduction

Tyrosine kinase inhibitors (TKIs) are targeted agents, which have been introduced in anticancer treatment within the last two decades and became an integral part of this treatment rapidly. Application of these agents in patients with malignant diseases has shown to successfully induce clinical responses in various malignancies [1].

For several TKIs, relationships between plasma concentrations and treatment efficacy and toxicity have been described [2-8]. Pharmacokinetic variability (both interpatient and inpatient) may, therefore, have important clinical consequences. For imatinib, erlotinib and sunitinib, minimal plasma concentration thresholds have been established below which a substantial increase in treatment failure and drug resistance was observed [5,7,9-15].

The ease of oral administration of TKIs enables patients to get their drug regimen in an outpatient setting, which is more patient friendly. However, oral administration also entails the possibility of considerable variation in drug exposure due to patient non-compliance (for example due to drug-related toxicity), drug interactions with co-medication and variability in oral drug availability [16]. Although pharmacokinetic parameters such as metabolic clearance and bioavailability, can vary substantially between individuals and especially during illness [17], TKIs are currently prescribed at a fixed dose. The large inter-individual variability in systemic exposure in combination with the positive exposure-efficacy relationship and low therapeutic index of TKIs, form a rationale for therapeutic drug monitoring (TDM) of these drugs [11,18-21].

We have investigated the occurrence of subtherapeutic TKI plasma concentrations in an outpatient population. In addition, we have studied patient-related (e.g. gender, age, weight) and medication-related (e.g. dose and drug interactions with concomitantly administered drugs) factors that may contribute to the occurrence of subtherapeutic TKI concentrations. The data may unveil some valuable arguments about the role of TDM in an unselected cohort of patients in routine daily clinical practice. Furthermore, the outcome may support further optimization and individualization of TKI therapy.

Methods

Patients

Patients were included if a TKI was part of their anticancer therapy in a period from June 2009 to May 2012. Patients were willing and able to undergo blood sampling. No exclusion criteria were defined, since the cohort of patients should reflect an unselected, 'real life' cohort of patients. For a patient to be evaluable, at least one drug plasma concentration during steady state should be available during the defined period. The study protocol was approved by local independent ethics committees. All patients received information regarding the purpose and conduct of this study and provided written informed consent.

R1
R2
R3
R4
R5
R6
R7
R8
R9
R10
R11
R12
R13
R14
R15
R16
R17
R18
R19
R20
R21
R22
R23
R24
R25
R26
R27
R28
R29
R30
R31
R32
R33
R34
R35
R36
R37
R38
R39

R1 All plasma samples were single randomly timed samples obtained by standardized procedures.
 R2 The samples were drawn together with regular laboratory investigations during routine outpatient
 R3 clinic visits. Time after drug administration (interval between last dose intake and plasma sampling)
 R4 and dosing scheme were documented. Patients of whom dosing scheme or time interval after last
 R5 intake were not available, were excluded from the final analysis.
 R6

R7 **Bioanalysis**

R8 EDTA whole blood samples were centrifuged within 36 hours after collection and, subsequently,
 R9 EDTA plasma was stored at -70°C until analysis. Plasma concentrations of imatinib, erlotinib, sunitinib
 R10 and its active metabolite N-desethyl sunitinib were determined by validated high-performance
 R11 liquid chromatography coupled with tandem mass spectrometry detection (HPLC-MS/MS)
 R12 methods [22]. Lower limits of quantification (LLOQ) were 20 ng/mL for imatinib and erlotinib. For
 R13 sunitinib and its metabolite the LLOQs were 5 ng/mL.
 R14

R15 **Trough plasma concentrations**

R16 For each TKI, trough target plasma concentrations that need to be reached for effective therapy
 R17 were defined based on published data and are shown in Table 1. For each patient sample, trough
 R18 plasma concentrations were compared with the target trough concentrations. Blood samples
 R19 were drawn during follow up visits at the outpatient clinic along with routine laboratory tests. Most
 R20 patients took their medication early in the morning or late in the evening. Therefore, the plasma
 R21 samples were randomly drawn during the dosing interval within this study and trough plasma
 R22 concentrations were not always available. Therefore, trough plasma concentrations were estimated
 R23 using the interval between last dose intake and blood sampling and the mean elimination half life
 R24 of the drugs, as previously proposed by Wang *et al.* [23]. The formulas used for this purpose, were:
 R25

$$R26 \quad 1) \quad Conc_{24h} = Conc_{measured} \cdot 0.5^{\left(\frac{24-interval}{t_{1/2}}\right)}$$

$$R27 \quad 2) \quad Conc_{12h} = Conc_{measured} \cdot 0.5^{\left(\frac{12-interval}{t_{1/2}}\right)}$$

- R29 • $Conc_{24h}$, $Conc_{12h}$ = calculated plasma trough levels for drugs with once daily or twice daily
 R30 administration, respectively.
- R31 • $Conc_{measured}$ = measured drug plasma concentration in ng/mL
- R32 • Interval = interval between last dose intake and blood sampling in hours
- R33 • $t_{1/2}$ = mean terminal half life of the drug in hours
 R34

R35 Formula 1 was used for drugs with once daily administration and formula 2 was used for drugs with
 R36 twice daily administration. Mean elimination half-lives used in the calculation were 18 h, 36 h, 50 h
 R37 and 95 h for imatinib, erlotinib, sunitinib and N-desethyl sunitinib, respectively [11,20,21]. Calculated
 R38 trough concentrations below or above the target trough level were defined as subtherapeutic or
 R39 therapeutic, respectively.

Since more than one sample per patient would be collected, a linear mixed effects model was used to assess inter- and intra-patient variability in trough concentrations.

To calculate dose-corrected plasma concentrations, the most frequently prescribed mean daily doses within our cohort, namely 400 mg for imatinib, 150 mg for erlotinib and 50 mg for sunitinib were used as standard mean daily doses.

Table 1. Target trough plasma concentrations of TKIs

Drug	Target trough level (ng/mL)	Subgroup	References
Imatinib	1000	CML	[7,15]
Imatinib	1110	GIST	[10]
Erlotinib	500	*	[5]
Sunitinib	50-100	* #	[9,11-14]

CML, chronic myeloid leukemia; GIST, gastrointestinal stromal tumor.

* based on preclinical PK-PD data

sum of sunitinib and N-desethyl sunitinib level

Patient data collection

To study patient- and medication- related factors that could have contributed to variations in TKI plasma concentrations, outpatient medical records were reviewed. Data were collected on daily dose, age, gender, weight, liver function tests (ASAT, ALAT), cigarette smoking behavior, tumor type and concomitantly administered drugs.

Toxicity and plasma concentrations

Data on occurrence of adverse events, that were clinically relevant and possibly or probably related to TKI use, were extracted from medical records. It was assessed which TKI plasma concentrations were related to occurrence of toxicity. Subsequently, the prevalence of adverse events in patients with subtherapeutic and therapeutic plasma concentrations was investigated.

Factors influencing plasma concentrations

To assess the correlation between all patient- and medication- related factors (except daily dose) and TKI plasma concentrations, dose-corrected plasma concentrations were used as dose-exposure relationships were found to be linear [12,24,25]. The correlation between patient-related factors age, gender, bodyweight or liver function and TKI plasma concentrations was assessed. Additionally, four medication related factors were investigated. Firstly, the correlation between mean daily TKI dose and TKI plasma concentrations was determined. Secondly, the influence of concomitant medication, which induces or inhibits cytochrome P450 enzyme 3A4 (CYP3A4), was assessed, since TKIs are mainly metabolized via CYP3A4 [11,20,21]. Thirdly, bioavailability of erlotinib and imatinib are known to depend on gastric pH <5.0 and drug efflux transporters (P-glycoprotein (Pgp) and breast cancer resistance protein (BCRP)), respectively. Therefore, the impact of the use

R1
R2
R3
R4
R5
R6
R7
R8
R9
R10
R11
R12
R13
R14
R15
R16
R17
R18
R19
R20
R21
R22
R23
R24
R25
R26
R27
R28
R29
R30
R31
R32
R33
R34
R35
R36
R37
R38
R39

of H₂-antagonists (H2As) and proton pump inhibitors (PPIs), which increase gastric pH and inhibit Pgp and BCRP [26-29], on TKI plasma concentrations was investigated. At last, the effect of cigarette smoking on erlotinib concentrations was investigated, since smoking is known to decrease erlotinib exposure by induction of CYP1A [25]. For all patient- and medication- related factors, correlations with plasma concentrations were tested using linear mixed effect modeling. The likelihood ratio test was used to assess the significance of different parameters (patient- and medication- related factors) in the regression models. A p-value of < 0.05 was considered statistically significant [30]. Additionally, for each plasma concentration that was classified as within approximately the lowest 10th percentile of concentrations, it was investigated whether one of the above mentioned factors could be identified as the cause of the very low plasma concentrations. Although no upper limit of the therapeutic window of plasma trough levels has been defined for TKIs, also extremely high TKI plasma concentrations were investigated in a similar manner. Therefore, involvement of possible patient- and medication- related factors was investigated for the approximately 2.5-5% highest plasma concentrations of each TKI.

Results

Patients and Plasma concentrations

In total, 108 evaluable patients were included in the study with a mean age of 61 years (range 33-83 years). More than half of the patients were female (58%). A total of 246 plasma concentrations was available, yielding a median of 2 plasma concentrations per patient (range 1-7). Characteristics of all patients enrolled are depicted in Table 2 stratified by TKI therapy.

Mean trough plasma concentrations for imatinib, erlotinib and the sum of sunitinib and N-desethyl sunitinib were 926 ng/ml (range 87.0 - 3607), 1010 ng/ml (range 74.9 - 5542) and 51.6 ng/ml (range 14.7 – 93.7), respectively. In the total study population, therapeutic trough plasma concentrations were reached in 55.3% of patient samples. For the particular patient groups using imatinib, erlotinib or sunitinib treatment, therapeutic trough concentrations were reached in 26.8%, 88.9% and 51.4% of patient samples, respectively. The distribution of trough concentrations divided in subtherapeutic and therapeutic plasma concentrations are depicted in Table 3.

Table 2. Characteristics of patients on imatinib, erlotinib and sunitinib therapy

Characteristic	Imatinib		Erlotinib		Sunitinib	
Number of patients	36		41		31	
Number of samples	112		99		35	
Samples per patient (number of pt (%))						
1	9	(25.0)	10	(24.4)	27	(87.1)
2	5	(13.9)	16	(39.0)	4	(12.9)
3	9	(25.0)	6	(14.6)		
4	5	(13.9)	7	(17.1)		
5	4	(11.1)	1	(2.4)		
6	2	(5.6)	1	(2.4)		
7	2	(5.6)				
Gender (number of pt (%))						
male	14	(38.9)	15	(36.6)	16	(51.6)
female	22	(61.1)	26	(63.4)	15	(48.4)
Age (yr) (mean (SD))	60 (11.1)		60 (7.9)		63 (9.9)	
Bodyweight (kg) (mean (SD))	78 (18.7)		75 (15.3)		83 (17.8)	
Tumor type (number of pt (%))						
	GIST	35 (97.2)	NSCLC	41 (100)	mRCC	29 (93.5)
	CLL	1 (2.8)			GIST	2 (6.5)
Dosing scheme (number of pt (%))						
	200 mg QD	2 (5.6)	25 mg QD	1 (2.4)	25 mg QD*	2 (6.5)
	300 mg QD	1 (2.8)	50 mg QD	2 (4.9)	37.5 mg QD*	12 (38.7)
	400 mg QD	31 (86.0)	75 mg QD	2 (4.9)	50 mg QD*	15 (48.4)
	300 mg BID	1 (2.8)	100 mg QD	3 (7.3)	62.5 mg QD*	2 (6.5)
	400 mg BID	1 (2.8)	150 mg QD	32 (78.1)		
			100 mg eod	1 (2.4)		

* patients were treated with sunitinib for 4 weeks followed by 2 weeks off-treatment. Plasma samples were analysed during steady state of the on-treatment phase. BID, twice daily; CLL, chronic lymphocytic leukemia; eod, every other day; GIST, gastrointestinal stromal tumor; mRCC, metastasized renal cell carcinoma; NSCLC, non-small cell lung cancer; pt, patients; QD, once daily; SD, standard deviation.

Table 3. Distribution of (calculated) trough concentrations divided in subtherapeutic and therapeutic concentrations.

TKI	Total			Subtherapeutic		Therapeutic		
	Number	Mean	(CV%)	Number (%)	Mean (CV%)	Number (%)	Mean (CV%)	
Imatinib	112	926	(51.7)	82 (73.2)	712 (32.0)	30 (26.8)	1508 (33.4)	
Erlotinib	99	1011	(68.6)	11 (11.1)	288 (57.9)	88 (88.9)	1101 (61.9)	
Sunitinib	35	51.6	(38.7)	17 (48.6)	35.5 (26.5)	18 (51.4)	68.6 (18.2)	
Total	246			110 (44.7)		136 (55.3)		

CV%, coefficient of variation; Mean, mean plasma concentration in ng/mL; TKI, tyrosine kinase inhibitor.

Large variability in reached trough concentrations was observed for all drugs, as shown in Figure 1. Inter-patient variability in plasma concentrations with variation coefficients (CV%) of 39.1%, 40.1% and 29.2% were found for imatinib, erlotinib and sunitinib, respectively. From 26 patients on imatinib therapy more than one plasma sample was available and intra-patient variability of plasma concentrations in this group was 32.9% (CV%). For erlotinib the intra-patient variability, based on 30 patients with multiple plasma samples, was 35.5% (CV%). Only four patients with multiple plasma samples were included in the sunitinib group and intra-patient variability of total plasma concentrations in those patients was 34.5% (CV%).

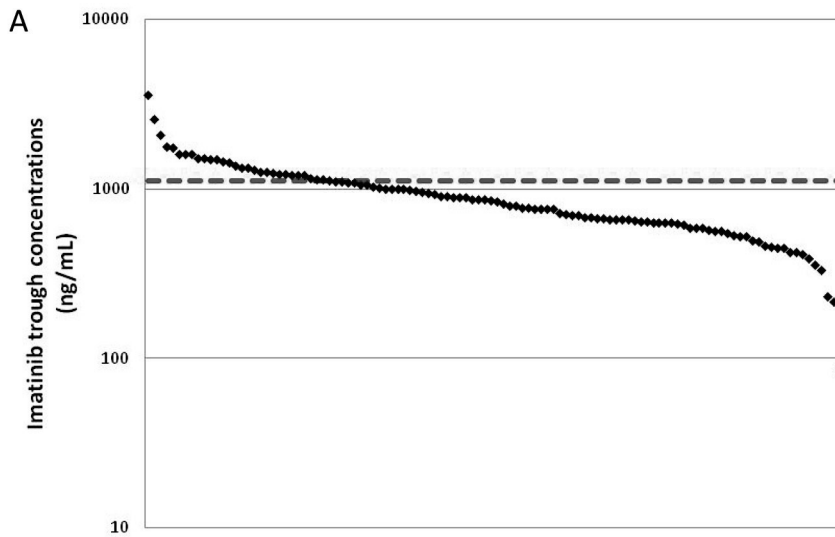


Figure 1. Calculated trough plasma concentrations for all plasma samples of imatinib (A), erlotinib (B), and sunitinib (C) patients. The dashed line represents the therapeutic target level below which trough plasma concentrations were classified as subtherapeutic.

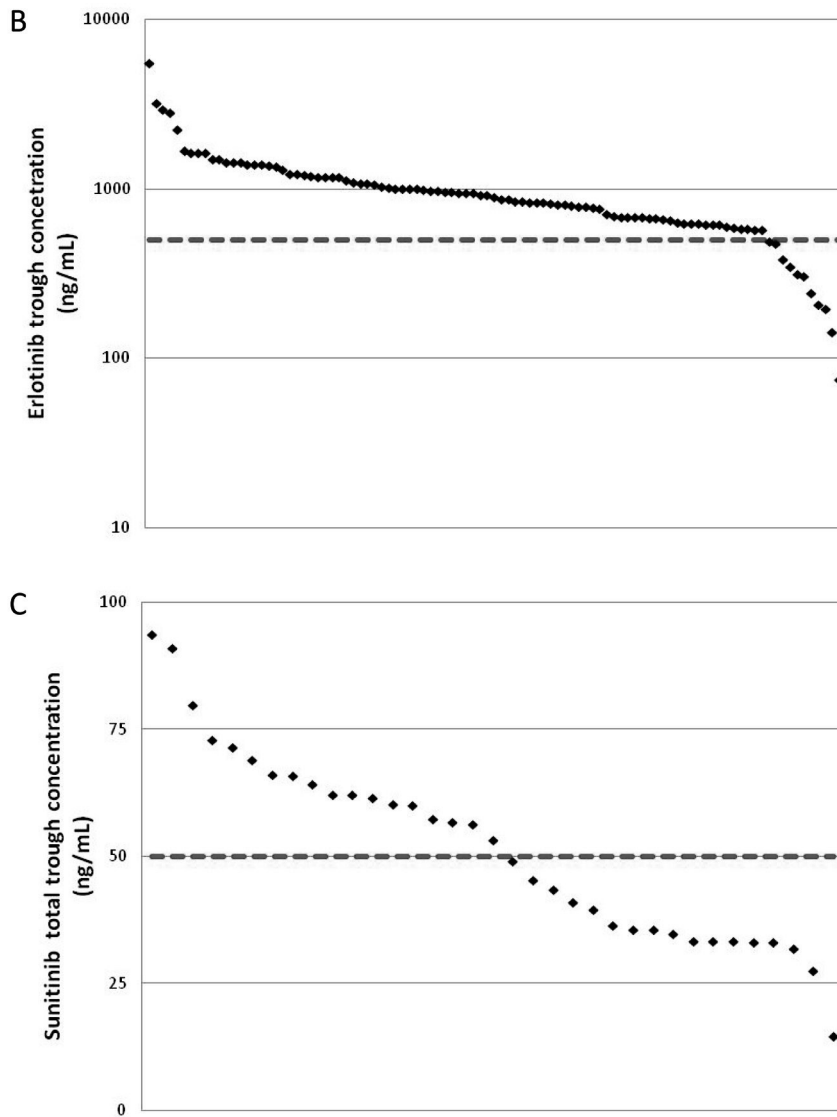


Figure 1. Continued. Calculated trough plasma concentrations for all plasma samples of imatinib (A), erlotinib (B), and sunitinib (C) patients. The dashed line represents the therapeutic target level below which trough plasma concentrations were classified as subtherapeutic.

R1
R2
R3
R4
R5
R6
R7
R8
R9
R10
R11
R12
R13
R14
R15
R16
R17
R18
R19
R20
R21
R22
R23
R24
R25
R26
R27
R28
R29
R30
R31
R32
R33
R34
R35
R36
R37
R38
R39

Trough levels in relation to toxicities

During the study period, 66 patients (61.1%) suffered from toxicities: 19 patients (52.8%) on imatinib therapy, 25 patients (61.0%) on erlotinib therapy, and 22 patients (71.0%) on sunitinib therapy. The incidence of reported adverse events is shown in Table 4. Consequently, four patients groups could be defined, namely (1) patients with subtherapeutic drug concentrations and without toxicities; (2) patients with subtherapeutic drug concentrations and with toxicities; (3) patients with therapeutic drug levels and without toxicities; and (4) patients with therapeutic drug levels and with toxicities. The distribution of patient plasma samples within these four groups is depicted in Figure 2. No difference was observed between mean trough plasma concentrations of patients with or without toxicities, as shown in Figure 3. Toxicities also occurred at subtherapeutic concentrations. For sunitinib and erlotinib the prevalence of toxicities at therapeutic plasma concentrations was higher than at subtherapeutic levels.

Table 4. Incidence of toxicity

Characteristic	Imatinib	Erlotinib	Sunitinib
Patients with toxicity (number (%))	19 (52.8)	25 (61.0)	22 (71.0)
Samples related to toxicity (number (%))	61 (54.4)	64 (64.6)	23 (65.7)
Toxicity (number of pt (% of study pt))			
fatigue	6 (16.7)	skin rash 22 (53.7)	fatigue 9 (29.0)
periorbital edema	6 (16.7)	diarrhea 6 (14.6)	hand foot syndrome 7 (22.6)
nausea	4 (11.1)	blepharitis 4 (9.8)	mucositis 7 (22.6)
skin rash	3 (8.3)	paronychia 4 (9.8)	dysgeusia 4 (12.9)
diarrhea	2 (5.6)	vomiting 2 (4.9)	stomatitis 3 (9.7)
dyspnea	2 (5.6)	fatigue 2 (4.9)	hypertension 2 (6.5)
peripheral edema	2 (5.6)	anorexia 2 (4.9)	anorexia 2 (6.5)
dysgeusia	1 (2.8)	weight loss 1 (2.4)	dyspepsia 2 (6.5)
hypertension	1 (2.8)	dysgeusia 1 (2.4)	vomiting 1 (3.2)
alopecia	1 (2.8)	nausea 1 (2.4)	skin rash 1 (3.2)
anorexia	1 (2.8)		muscle cramps 1 (3.2)
anemia	1 (2.8)		hypo-thyroidism 1 (3.2)

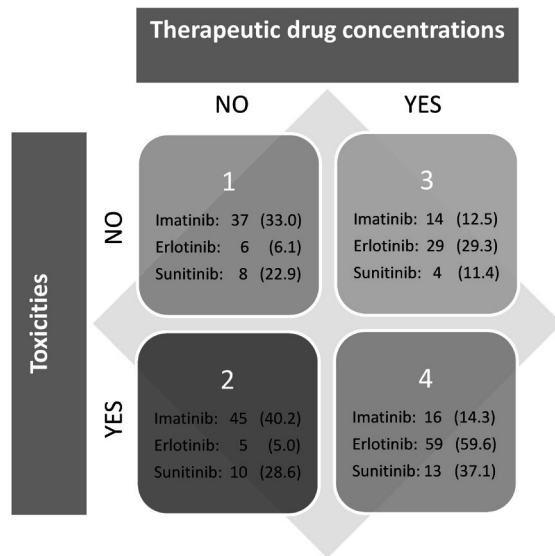


Figure 2. Four subgroups of patients samples can be defined based on whether or not reaching therapeutic drug concentrations and whether or not related to occurrence of toxicities. Distribution of patient samples within these four groups is depicted with number and percentage (within parentheses) of samples for each tyrosine kinase inhibitor.

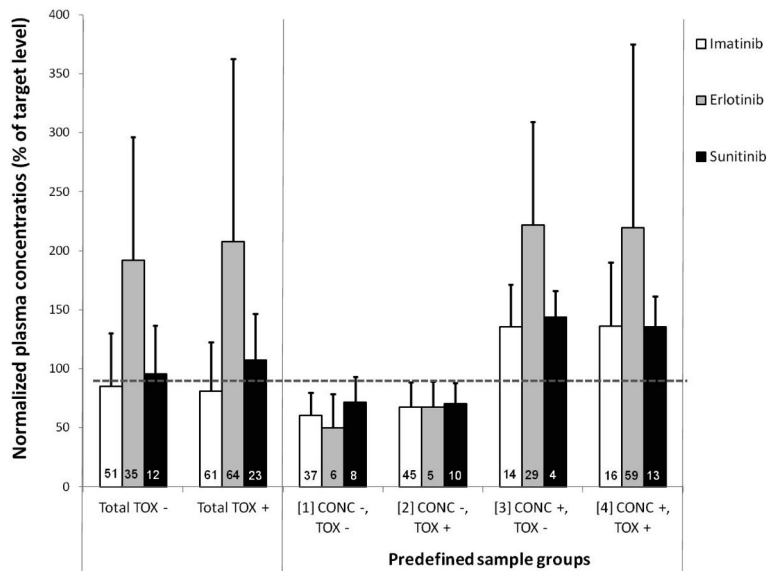


Figure 3. A) Mean TKI plasma concentrations of sample group without occurrence of toxicity (TOX -) and sample group with occurrence of toxicity (TOX +); B) Mean plasma concentrations of four predefined sample groups, namely samples of [1] patients with subtherapeutic drug concentrations (CONC -) and without toxicities (TOX -); [2] patients with subtherapeutic drug concentrations (CONC -) and with toxicities (TOX +); [3] patients with therapeutic drug levels (CONC +) and without toxicities (TOX -); and [4] patients with therapeutic drug levels (CONC +) and with toxicities (TOX +). Error bars represent the relative standard deviation. Numbers in bars represent the sample number of the specific subgroup of samples.

Factors influencing plasma concentrations

Our cohort consisted of patients with a large range of body weights. Despite obesity, all patients with extremely high body weights were treated with standard doses of TKIs. However, no significant effect of body weight on TKI plasma concentrations was observed. No large differences were found in plasma concentrations between different age groups. Additionally, no significant effects of gender on plasma concentrations were observed for erlotinib and sunitinib. For imatinib, plasma concentrations were nearly significantly increased in females (+39%, $p > 0.05$). Slight increases of plasma concentrations were observed for imatinib (+24%, $p > 0.05$) and erlotinib (+23%, $p > 0.05$) with decreasing liver function. For erlotinib concentrations a dose-exposure correlation was shown, but due to large inter-patient variability no linear relationship was found. For imatinib and sunitinib no relationship between dose and plasma concentrations was observed in our patient cohort. The effect of PPIs on erlotinib and imatinib plasma concentrations was not significant (-27.8% ($p > 0.05$) and +8.0% ($p > 0.05$), respectively). A significant increase of sunitinib concentrations (+53%, $p < 0.05$) was observed with concomitant use of PPIs. Eleven plasma samples of two patients, using imatinib concomitantly with CYP3A4-inducers (carbamazepine or phenytoin), showed significantly decreased imatinib plasma concentrations (-58.4%, $p < 0.05$). In one of the patients a dose increase from 400 mg once daily to subsequently 300 mg and 400 mg twice daily was implemented. However, even when comparing measured plasma concentrations instead of dose-corrected plasma concentrations, the imatinib concentrations were significantly decreased (-51.1%, $p < 0.05$). Thus, a doubling of the daily imatinib dose was not sufficient to overcome the effect of CYP3A4 induction by carbamazepine. Five erlotinib concentrations of cigarette smokers were measured and the CYP1A enzyme inducing effect of smoking was correlated to an insignificant decrease of erlotinib concentrations (-37.0%, $p > 0.05$).

Only 11 (11.1%) of the erlotinib samples were below the target level of 500 ng/mL. Among these samples were 2 samples of heavy cigarette smokers; 3 samples of patients with low erlotinib doses (25 mg QD or 150 mg every other day); 5 samples of patients using medication that increases the gastric pH; and 1 sample for which no explanation could be found for subtherapeutic concentrations. Four sunitinib samples (11.4%) were below a total sum concentration of 30 ng/mL. The extremely low concentration in one of the samples could possibly be explained by a high bodyweight of 125 kg. Potential causes for the other low sunitinib concentrations were not identified. Fifteen imatinib samples (13.4%) obtained from 8 different patients were below 500 ng/mL. Seven of those extremely low plasma concentrations were attributed to the drug-drug interactions with CYP3A4 inducing agents, as mentioned above. For the other eight samples no patient- or medication related factor could be identified to explain the subtherapeutic concentrations.

Trough concentrations of imatinib >2000 ng/mL were found in 3 patient samples (2.7%). For two of these samples no explanation was found for the extremely high concentrations. The third sample was of a patient treated with 300 mg imatinib twice daily. Sunitinib plasma concentrations

of >90 ng/mL were measured in two samples (5.7%). One of the patients had a decreased liver function. For erlotinib the highest observed plasma concentrations could possibly all be explained by hepatic dysfunction. Of the 5 patients samples that were >2000 ng/mL (5.1%), all patients suffered from any severity of liver function loss. Remarkably, four patients obtained extremely high erlotinib trough concentrations even in combination with PPIs as co-medication.

Discussion

The objective of this study was to explore the distribution of trough plasma concentrations of imatinib, erlotinib and sunitinib in an unselected cohort of patients. Only 55.3% of the trough plasma concentrations reached the predefined therapeutic target level. In our cohort, the large inter-patient variability of plasma concentrations could only be explained partly by patient- or medication related factors. This implicates that routine TDM may be very valuable for treatment optimization and individualization of these drugs.

As far as we know, this is the first investigation of trough plasma concentrations of various TKIs in an unselected population. Imatinib trough concentrations have been determined previously in different cohorts of patients who were enrolled in clinical trials with strict in- and exclusion criteria (e.g. patients with poor compliance to treatment or using concomitant medication were excluded) [7,10,15]. For imatinib, additionally, some observational studies without exclusion criteria have been performed in which the influence of patient-related factors on plasma trough levels were investigated [8,31,32].

We chose to use an unselected cohort of patients to approach the outpatient cancer patient care as best as possible. In such 'real-life' cohort, variability in drug exposure may be much larger than in clinical trials and consequently response to treatment (efficacy and/or toxicity) may show wider variability. With this observational study design it is, however, difficult to detect factors that significantly affect plasma concentrations. Another drawback of the observational study design is that only clinically relevant toxicity was recorded and, thus, toxicity was not systematically graded according to the common toxicity criteria (CTCAE). However, since the main goal of the study was to explore the range of trough plasma concentrations that were reached in a 'real-life' patient population, it was accepted that only exploratory investigations would be achievable on possible determinants of variation in plasma concentrations and adverse events.

High percentages of samples were subtherapeutic for imatinib and sunitinib, namely 73.2%, and 48.6%, respectively. Since multiple samples per patient were analysed, these percentages do not directly reflect the number of patients that are on a subtherapeutic regimen. Nevertheless, our results are comparable with the percentage of patients reaching subtherapeutic concentrations of imatinib and sunitinib in previously reported studies [7,15,32,33]. The relatively high number of subtherapeutic imatinib concentrations can probably be explained by decreasing imatinib exposure after long-term treatment, as reported by Eechoute *et al.*, since most of patients included

R1
R2
R3
R4
R5
R6
R7
R8
R9
R10
R11
R12
R13
R14
R15
R16
R17
R18
R19
R20
R21
R22
R23
R24
R25
R26
R27
R28
R29
R30
R31
R32
R33
R34
R35
R36
R37
R38
R39

R1
R2
R3
R4
R5
R6
R7
R8
R9
R10
R11
R12
R13
R14
R15
R16
R17
R18
R19
R20
R21
R22
R23
R24
R25
R26
R27
R28
R29
R30
R31
R32
R33
R34
R35
R36
R37
R38
R39

in our study had already been treated with imatinib for several years [23,34]. Although our patient cohort existed of unselected patients, inter-patient variability in trough plasma concentrations (CV%) observed for imatinib (39.1%), erlotinib (40.1%) and sunitinib (29.2%) was comparable to previously reported data [5-7,15,32].

In line with registration studies, patient-related factors age, body weight and gender did not substantially affect trough plasma concentrations due to large inter-patient variabilities [11,20,21]. The nearly significant influence of female gender on imatinib concentrations was corroborated by a previous study [10]. The relationship between decreased liver function and increased plasma concentrations has not been confirmed in other studies thus far [11,20,21]. Analogous to these findings, we only observed a tendency towards higher plasma concentrations of imatinib, erlotinib and sunitinib with decreasing liver function. Concomitant use of CYP3A4-inducing antiepileptic drugs lead to significantly lower plasma concentrations of imatinib. It has previously been reported that imatinib trough concentrations were reduced 2.9-fold when concurrently used with enzyme inducing antiepileptics [35]. This can explain why a twofold imatinib dose increase was not sufficient to reach target trough levels, as observed in a patient using carbamazepine. As expected, decreased erlotinib absorption (-28.7%) with concomitant use of PPIs or H2As was nearly statistically significant within our patient cohort. The increased plasma concentrations of sunitinib in combination with PPIs could not be explained by decreased absorption [36] and it is unknown whether inhibition of Pgp, BCRP or other efflux transporters contributes to increased bioavailability of sunitinib in human [37,38].

No prospective clinical trials have been performed to investigate the safety and efficacy of TDM for imatinib, erlotinib and sunitinib therapy. Thus the ultimate proof that reaching target trough concentrations increases treatment outcome remains to be awaited. However, when assuming that target trough concentrations are needed for adequate treatment responses, four patient groups with different changes for successful therapy can be defined, as was mentioned before in Figure 3. Hence, patient group 3 (therapeutic drug concentrations and no toxicity) are most likely to reach optimal treatment responses. Patients in group 1 (subtherapeutic levels and no toxicity), may benefit from TDM guided dose increases. Patients in group 2 (subtherapeutic levels and toxicity) also need dose adjustments to reach target trough levels, however, TDM would in this case probably not be helpful since toxicities would make dose increases impossible. Patients in group 4 (therapeutic drug concentrations and toxicities) risk treatment discontinuation due these toxicities. Therefore, TDM may support treatment success in these patients by decreasing TKI doses and aiming for TKI concentrations just above the target level. Thus, patients in group 1 and 4 could probably benefit from implementation of routine TDM, which included 47.3%, 65.7% and 60.0% of the patient samples for imatinib, erlotinib and sunitinib in our cohort, respectively.

To identify drugs for which TDM can be an added value in treatment optimization, different criteria are defined [19]. The anticancer drugs imatinib, erlotinib and sunitinib fulfill the five most important criteria. These drugs have a narrow therapeutic index (1) with a steep exposure-response

relationship (2) [4-7,39]. Additionally, a substantial inter-patient variability (3) and relatively small intra-patient variability (4) were observed. Moreover, no easily accessible clinical or laboratory parameter is available that can be used for determining the dosage (5), since no patient- or medication related factors could completely explain the high inter-patient variability in trough concentrations.

In conclusion, around half of the plasma concentrations in the outpatient population appeared to be subtherapeutic. These patients, consequently, could risk treatment failure or development of drug resistance. A large percentage of subtherapeutic and extremely high concentrations could not be explained by patient- or medication related factors. Accordingly, it is not possible to predict which patients need optimization of plasma concentrations through TKI dose adjustment. Thus, TDM could play a crucial role in routine cancer care to identify patients that are in need of individual adjusted dosages.

R1
R2
R3
R4
R5
R6
R7
R8
R9
R10
R11
R12
R13
R14
R15
R16
R17
R18
R19
R20
R21
R22
R23
R24
R25
R26
R27
R28
R29
R30
R31
R32
R33
R34
R35
R36
R37
R38
R39

R1
R2
R3
R4
R5
R6
R7
R8
R9
R10
R11
R12
R13
R14
R15
R16
R17
R18
R19
R20
R21
R22
R23
R24
R25
R26
R27
R28
R29
R30
R31
R32
R33
R34
R35
R36
R37
R38
R39

References

1. Krause DS, Van Etten RA. Tyrosine kinases as targets for cancer therapy. *N Engl J Med* 2005; 353: 172-87.
2. Burris HA, III, Hurwitz HI, Dees EC et al. Phase I safety, pharmacokinetics, and clinical activity study of lapatinib (GW572016), a reversible dual inhibitor of epidermal growth factor receptor tyrosine kinases, in heavily pretreated patients with metastatic carcinomas. *J Clin Oncol* 2005; 23: 5305-13.
3. Calvo E, Rowinsky EK. Effect of epidermal growth factor receptor mutations on the response to epidermal growth factor receptor tyrosine kinase inhibitors: target-based populations for target-based drugs. *Clin Lung Cancer* 2004; 6 Suppl 1: S35-S42.
4. Delbaldo C, Chatelut E, Re M et al. Pharmacokinetic-pharmacodynamic relationships of imatinib and its main metabolite in patients with advanced gastrointestinal stromal tumors. *Clin Cancer Res* 2006; 12: 6073-8.
5. Hidalgo M, Siu LL, Nemunaitis J et al. Phase I and pharmacologic study of OSI-774, an epidermal growth factor receptor tyrosine kinase inhibitor, in patients with advanced solid malignancies. *J Clin Oncol* 2001; 19: 3267-79.
6. Houk BE, Bello CL, Poland B et al. Relationship between exposure to sunitinib and efficacy and tolerability endpoints in patients with cancer: results of a pharmacokinetic/pharmacodynamic meta-analysis. *Cancer Chemother Pharmacol* 2010; 66: 357-71.
7. Larson RA, Druker BJ, Guilhot F et al. Imatinib pharmacokinetics and its correlation with response and safety in chronic-phase chronic myeloid leukemia: a subanalysis of the IRIS study. *Blood* 2008; 111: 4022-8.
8. Widmer N, Decosterd LA, Leyvraz S et al. Relationship of imatinib-free plasma levels and target genotype with efficacy and tolerability. *Br J Cancer* 2008; 98: 1633-40.
9. Abrams TJ, Murray LJ, Pesenti E et al. Preclinical evaluation of the tyrosine kinase inhibitor SU11248 as a single agent and in combination with "standard of care" therapeutic agents for the treatment of breast cancer. *Mol Cancer Ther* 2003; 2: 1011-21.
10. Demetri GD, van Oosterom AT, Garrett CR et al. Efficacy and safety of sunitinib in patients with advanced gastrointestinal stromal tumour after failure of imatinib: a randomised controlled trial. *Lancet* 2006; 368: 1329-38.
11. European Medicines Agency (EMA). Sutent: EPAR - Scientific Discussion. Available at: http://www.ema.europa.eu/docs/en_GB/document_library/EPAR_-_Scientific_Discussion/human/000687/WC500057733.pdf Date accessed: July 17, 2012. 10-1-2007.
12. Faivre S, Delbaldo C, Vera K et al. Safety, pharmacokinetic, and antitumor activity of SU11248, a novel oral multitarget tyrosine kinase inhibitor, in patients with cancer. *J Clin Oncol* 2006; 24: 25-35.
13. Mendel DB, Laird AD, Xin X et al. In vivo antitumor activity of SU11248, a novel tyrosine kinase inhibitor targeting vascular endothelial growth factor and platelet-derived growth factor receptors: determination of a pharmacokinetic/pharmacodynamic relationship. *Clin Cancer Res* 2003; 9: 327-37.
14. Murray LJ, Abrams TJ, Long KR et al. SU11248 inhibits tumor growth and CSF-1R-dependent osteolysis in an experimental breast cancer bone metastasis model. *Clin Exp Metastasis* 2003; 20: 757-66.
15. Picard S, Titier K, Etienne G et al. Trough imatinib plasma levels are associated with both cytogenetic and molecular responses to standard-dose imatinib in chronic myeloid leukemia. *Blood* 2007; 109: 3496-9.
16. Klumpen HJ, Samer CF, Mathijssen RH et al. Moving towards dose individualization of tyrosine kinase inhibitors. *Cancer Treat Rev* 2011; 37: 251-60.

17. Slaviero KA, Clarke SJ, Rivory LP. Inflammatory response: an unrecognised source of variability in the pharmacokinetics and pharmacodynamics of cancer chemotherapy. *Lancet Oncol* 2003; 4: 224-32.
18. Gao B, Yeap S, Clements A et al. Evidence for Therapeutic Drug Monitoring of Targeted Anticancer Therapies. *J Clin Oncol* 2012.
19. de Jonge ME, Huitema AD, Schellens JH et al. Individualised cancer chemotherapy: strategies and performance of prospective studies on therapeutic drug monitoring with dose adaptation: a review. *Clin Pharmacokinet* 2005; 44: 147-73.
20. European Medicines Agency (EMA). Tarceva: EPAR - Scientific Discussion. Available at: http://www.ema.europa.eu/docs/en_GB/document_library/EPAR_-_Scientific_Discussion/human/000618/WC500033991.pdf. Date accessed July 17, 2012. 2-11-2005.
21. European Medicines Agency (EMA). Glivec: EPAR - Scientific Discussion. Available at: http://www.ema.europa.eu/docs/en_GB/document_library/EPAR_-_Scientific_Discussion/human/000406/WC500022203.pdf. Date accessed July 17, 2012. 28-10-2005.
22. Lankheet NA, Hillebrand MJ, Rosing H et al. Method development and validation for the quantification of dasatinib, erlotinib, gefitinib, imatinib, lapatinib, nilotinib, sorafenib and sunitinib in human plasma by liquid chromatography coupled with tandem mass spectrometry. *Biomed Chromatogr* 2012.
23. Wang Y, Chia YL, Nedelman J et al. A therapeutic drug monitoring algorithm for refining the imatinib trough level obtained at different sampling times. *Ther Drug Monit* 2009; 31: 579-84.
24. Guilhot F, Hughes TP, Cortes J et al. Plasma exposure of imatinib and its correlation with clinical response in the Tyrosine Kinase Inhibitor Optimization and Selectivity Trial. *Haematologica* 2012; 97: 731-8.
25. Hughes AN, O'Brien ME, Petty WJ et al. Overcoming CYP1A1/1A2 mediated induction of metabolism by escalating erlotinib dose in current smokers. *J Clin Oncol* 2009; 27: 1220-6.
26. Duong S, Leung M. Should the concomitant use of erlotinib and acid-reducing agents be avoided? The drug interaction between erlotinib and acid-reducing agents. *J Oncol Pharm Pract* 2011; 17: 448-52.
27. Haouala A, Widmer N, Duchosal MA et al. Drug interactions with the tyrosine kinase inhibitors imatinib, dasatinib, and nilotinib. *Blood* 2011; 117: e75-e87.
28. Pauli-Magnus C, Rekersbrink S, Klotz U et al. Interaction of omeprazole, lansoprazole and pantoprazole with P-glycoprotein. *Naunyn Schmiedeberg's Arch Pharmacol* 2001; 364: 551-7.
29. Breedveld P, Pluim D, Cipriani G et al. The effect of Bcrp1 (Abcg2) on the in vivo pharmacokinetics and brain penetration of imatinib mesylate (Gleevec): implications for the use of breast cancer resistance protein and P-glycoprotein inhibitors to enable the brain penetration of imatinib in patients. *Cancer Res* 2005; 65: 2577-82.
30. Beal SL, Sheiner L. NONMEM Users guides. 1989. Ellicott City, Maryland, USA, Icon Development Solutions.
31. Kawaguchi T, Hamada A, Hirayama C et al. Relationship between an effective dose of imatinib, body surface area, and trough drug levels in patients with chronic myeloid leukemia. *Int J Hematol* 2009; 89: 642-8.
32. Sohn SK, Oh SJ, Kim BS et al. Trough plasma imatinib levels are correlated with optimal cytogenetic responses at 6 months after treatment with standard dose of imatinib in newly diagnosed chronic myeloid leukemia. *Leuk Lymphoma* 2011; 52: 1024-9.
33. George S, Blay JY, Casali PG et al. Clinical evaluation of continuous daily dosing of sunitinib malate in patients with advanced gastrointestinal stromal tumour after imatinib failure. *Eur J Cancer* 2009; 45: 1959-68.
34. Eechoute K, Fransson MN, Reyners AK et al. A long-term prospective population pharmacokinetic study on imatinib plasma concentrations in GIST patients. *Clin Cancer Res* 2012.

R1
R2
R3
R4
R5
R6
R7
R8
R9
R10
R11
R12
R13
R14
R15
R16
R17
R18
R19
R20
R21
R22
R23
R24
R25
R26
R27
R28
R29
R30
R31
R32
R33
R34
R35
R36
R37
R38
R39

R1
R2
R3
R4
R5
R6
R7
R8
R9
R10
R11
R12
R13
R14
R15
R16
R17
R18
R19
R20
R21
R22
R23
R24
R25
R26
R27
R28
R29
R30
R31
R32
R33
R34
R35
R36
R37
R38
R39

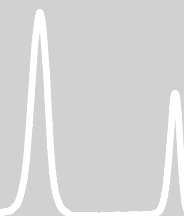
35. Pursche S, Schleyer E, von BM et al. Influence of enzyme-inducing antiepileptic drugs on trough level of imatinib in glioblastoma patients. *Curr Clin Pharmacol* 2008; 3: 198-203.
36. Di Gion P, Kanefendt F, Lindauer A et al. Clinical pharmacokinetics of tyrosine kinase inhibitors: focus on pyrimidines, pyridines and pyrroles. *Clin Pharmacokinet* 2011; 50: 551-603.
37. Hu S, Chen Z, Franke R et al. Interaction of the multikinase inhibitors sorafenib and sunitinib with solute carriers and ATP-binding cassette transporters. *Clin Cancer Res* 2009; 15: 6062-9.
38. Tang SC, Lagas JS, Lankheet NA et al. Brain accumulation of sunitinib is restricted by P-glycoprotein (ABCB1) and breast cancer resistance protein (ABCG2) and can be enhanced by oral elacridar and sunitinib coadministration. *Int J Cancer* 2012; 130: 223-33.
39. Thomas F, Rochaix P, White-Koning M et al. Population pharmacokinetics of erlotinib and its pharmacokinetic/pharmacodynamic relationships in head and neck squamous cell carcinoma. *Eur J Cancer* 2009; 45: 2316-23.

Chapter 2.2

Pharmacokinetically-guided sunitinib dosing: A feasibility study in patients with advanced solid tumors

Nienke A.G. Lankheet
Jacqueline S.L. Kloth
Christa G.M. Gadellaa-van Hooijdonk
Geert A. Cirkel
Ron. H.J. Mathijssen
Martijn P.J.K. Lolkema
Jan H.M. Schellens
Emile E. Voest
Maja J.A. de Jonge
John B.A.G. Haanen
Stefan Sleijfer
Jos H. Beijnen
Alwin D.R. Huitema
Neeltje Steeghs

Manuscript in preparation



R1
R2
R3
R4
R5
R6
R7
R8
R9
R10
R11
R12
R13
R14
R15
R16
R17
R18
R19
R20
R21
R22
R23
R24
R25
R26
R27
R28
R29
R30
R31
R32
R33
R34
R35
R36
R37
R38
R39

Abstract

Background: Due to large inter-individual variations in the plasma exposure of sunitinib, target total trough levels (TTL) are frequently not reached with the current dosing schedule. Therefore, a pharmacokinetic (PK) study was performed to determine the safety and feasibility of PK-guided sunitinib dosing.

Methods: Patients were treated continuously with sunitinib 37.5 mg once daily. At day 15 and 29 of treatment, plasma trough levels of sunitinib and N-desethyl sunitinib were measured. If the TTL was <50 ng/mL and the patient did not show any grade ≥ 3 toxicity, the daily sunitinib dose was increased by 12.5 mg. If the patient suffered from grade ≥ 3 toxicity, the sunitinib dose was lowered by 12.5 mg. After 8 weeks a final TTL evaluation was performed.

Results: Twenty-nine out of 43 patients were evaluable for PK assessments. With a median TTL of 49.5 ng/mL, target TTLs were not reached in 15 patients (52%) at the starting dose of 37.5 mg per day. Of these patients, 5 patients (17%) reached target TTL after dose escalations without additional toxicity. Eight patients (27%) reached target TTL at the starting dose with acceptable toxicities. Grade ≥ 3 were experienced in seven patients (24%) at the starting dose and in nine patients (31%) after PK guided dose escalation.

Conclusion: In a third of the patients that did not reach target TTL at standard dose, the sunitinib dose could be increased without additional toxicities. This could be the basis for future studies and the implementation of a PK-guided dosing strategy in clinical practice.

Introduction

Sunitinib (Sutent®) has proven efficacy as single agent in several solid tumor types and is approved for use in advanced renal cell cancer (RCC), imatinib-resistant or -intolerant gastrointestinal stromal tumors (GISTs) and pancreatic neuroendocrine tumors (pNET) [1-3]. Recent findings demonstrated a positive dose-efficacy relationship for sunitinib treatment [4]. As deduced from pharmacokinetic/pharmacodynamic preclinical data, target total plasma concentrations of sunitinib plus active metabolite (N-desethyl sunitinib) are in the range of 50 to 100 ng/mL [5-9]. In line with these preclinical data, total trough levels (TTLs) below 50 ng/mL have been associated with decreased therapeutic efficacy in patients compared to patients with TTL above this level [7]. It is therefore hypothesized that for optimal sunitinib therapy a TTL above 50 ng/mL should be reached in each individual patient. However, sunitinib exposure shows considerable variation due to patient non-compliance (for example due to drug-related toxicity), drug interactions with co-medication, variability in oral drug availability and many other factors [10]. Despite this considerable inter-patient variability in systemic exposure, sunitinib is currently prescribed at a fixed dose. Given the low therapeutic index, the large inter-individual variability in systemic exposure, and the positive exposure-efficacy relationship, there is a strong rationale for pharmacokinetically (PK) guided dosing also known as therapeutic drug monitoring (TDM) of sunitinib. [4,7,11]. Such an approach could contribute to a tailor made sunitinib treatment with improved therapeutic efficacy and decreased risk for toxicity.

Thus far, no prospective clinical trials investigating the safety and efficacy of PK guided dosing for sunitinib therapy have been performed. Hence, the ultimate proof that reaching target trough concentrations increases treatment efficacy remains to be awaited. As a first step towards individualized PK based dosing, we investigated the safety and feasibility of PK-guided sunitinib dosing in a pilot study by measuring sunitinib trough levels. Establishing a feasible and safe PK-guided dosing strategy could provide a rationale for a large prospective clinical trial.

Materials and Methods

Patient population

This multicenter prospective pilot trial (NCT01286896) was initiated in 2011 and was performed in three medical centers in The Netherlands. Eligible patients were patients with histologically or cytologically confirmed advanced tumors for which sunitinib was considered standard therapy or patients with advanced or metastatic tumors for whom no standard therapy was available.

Other inclusion criteria included age \geq 18 years; an Eastern Cooperative Oncology Group (ECOG) performance status \leq 1; measurable or evaluable disease according to Response Evaluation Criteria Solid Tumors (RECIST) 1.1 criteria; estimated life expectancy $>$ 12 weeks; adequate hematologic, hepatic and renal function; no cardiac instability within the previous six months. Additionally,

R1
R2
R3
R4
R5
R6
R7
R8
R9
R10
R11
R12
R13
R14
R15
R16
R17
R18
R19
R20
R21
R22
R23
R24
R25
R26
R27
R28
R29
R30
R31
R32
R33
R34
R35
R36
R37
R38
R39

R1 patients should be able and willing to undergo blood sampling; and patients should be able to
R2 swallow oral medication.

R3 The protocol was approved by local independent ethics committees, and the study was
R4 conducted in accordance with the Declaration of Helsinki. All patients received information
R5 regarding the purpose and conduct of this study and provided written informed consent.
R6

R7 ***Study design***

R8 Eligible patients started treatment at a dose level of 37.5 mg sunitinib once daily continuously.
R9 At day 15 of sunitinib treatment, TTLs of sunitinib plus N-desethyl sunitinib were measured. If the
R10 TTL was <50 ng/mL and the patient did not experience any grade ≥ 3 toxicity (CTCAE 4.02), the
R11 daily sunitinib dose was increased by 12.5 mg at day 22. At day 29, seven days after the first dose
R12 adjustment, the second TTL was measured. If indicated, a second dose adjustment based on TTL
R13 and/or toxicity was performed at day 36, as described before. After 8 weeks a final TTL evaluation
R14 was performed. No further dose increments were allowed.

R15 If the patient suffered from grade ≥ 3 toxicity or intolerable grade 2 toxicity despite supportive
R16 care at any moment during the study, the sunitinib treatment was interrupted until adequate
R17 recovery (CTC grade <2) was achieved. Subsequently, sunitinib treatment was resumed at the next
R18 lowest dose level. Sunitinib dose levels allowed within this study were 12.5, 25, 37.5, 50 and 62.5
R19 mg QD. Patients experiencing grade >2 toxicity with sunitinib 12.5 mg once daily, discontinued the
R20 treatment and went off study. No dose escalations were allowed after a previous dose reduction
R21 for toxicity. Treatment was continued until progressive disease, until patient refusal or until adverse
R22 events which required discontinuation of therapy were observed.
R23

R24 ***Pharmacokinetic analyses***

R25 Samples for pharmacokinetics (PK) were collected at day 15 \pm 1 day, day 29 \pm 1 day and after 8
R26 weeks (day 57 \pm 1 day) of sunitinib treatment. EDTA blood samples were collected and, thereafter,
R27 directly sent to the laboratory by ordinary mail at ambient temperature. After receipt of the
R28 samples, within 36 h after blood collection, plasma was harvested and stored at -20°C until analysis.
R29 Trough levels of sunitinib and N-desethyl sunitinib in plasma were measured by LC-MS/MS as
R30 described before (see Chapter 1.2). TTLs were determined by calculating the sum of sunitinib and
R31 N-desethyl sunitinib plasma levels and were reported to the treating physician within one week
R32 after blood collection. Patients were evaluable for pharmacokinetic analyses if they had undergone
R33 all three PK blood samplings.
R34

R35 ***Safety assessments***

R36 Adverse events (AE), serious adverse events (SAE) and their relationship with study medication
R37 were assessed throughout the study. The incidence and severity of AEs were evaluated and graded
R38 using the National Cancer Institute Common Toxicity Criteria for Adverse Events version 4.02
R39

(CTCAE 4.02). Patients who received at least one dose of the study treatment were included in the safety evaluation.

Statistical analysis

The number of patients recruited was based on the number estimated to be required to evaluate at least 8 patients for toxicity after PK guided dose escalation. It was expected that 45% of patients would experience clinically relevant toxicity at the starting dose of 37.5 mg once daily [12-16]. In addition, it was expected that about 50% of the patients without toxicity (55%) would have TTL \geq 50 ng/mL [13,14]. In both occasions, patients were not eligible for dose escalation. Thus, to be able to evaluate at least 8 patients after dose escalation, it was necessary to include about four times as many patients (at least 30 patients).

Descriptive statistics were used to summarize the patient characteristics, toxicity data, response data and sunitinib TTLs.

Results

Patient population

From April 2011 until June 2012, 43 patients with a variety of advanced solid tumors were enrolled (18 patients at the Netherlands Cancer Institute - Antoni van Leeuwenhoek Hospital Amsterdam, 15 patients at the University Medical Center Utrecht and 10 patients at the Erasmus Medical Center Rotterdam). Forty-two patients received at least one dose of sunitinib and were evaluable for toxicity assessments. Twenty-nine patients were evaluable for pharmacokinetic assessments (see Figure 1 for CONSORT diagram). At the time of the database lock (August 2012), four patients (9.5%) were still on sunitinib therapy. Demographical and clinical characteristics for all patients are provided in Table 1.

R1
R2
R3
R4
R5
R6
R7
R8
R9
R10
R11
R12
R13
R14
R15
R16
R17
R18
R19
R20
R21
R22
R23
R24
R25
R26
R27
R28
R29
R30
R31
R32
R33
R34
R35
R36
R37
R38
R39

R1
R2
R3
R4
R5
R6
R7
R8
R9
R10
R11
R12
R13
R14
R15
R16
R17
R18
R19
R20
R21
R22
R23
R24
R25
R26
R27
R28
R29
R30
R31
R32
R33
R34
R35
R36
R37
R38
R39

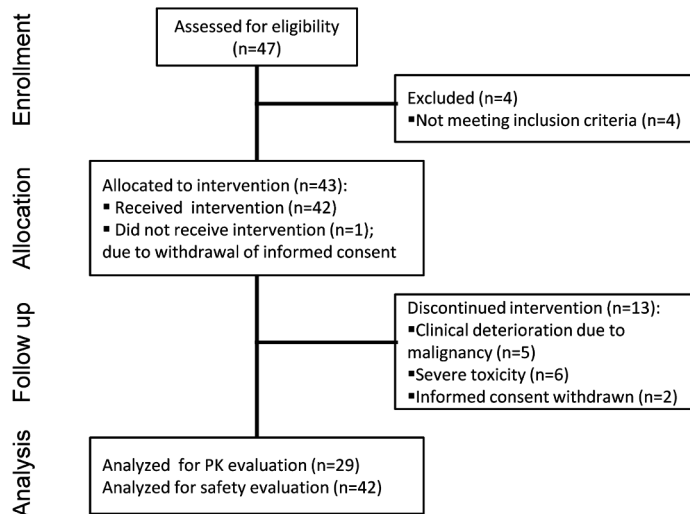


Figure 1. Patient flow diagram

Target trough levels

After 14 days of sunitinib treatment, the median TTL was 49.5 ng/mL [IQR 41.8 – 64.0] (see Table 2). Considerable inter-patient variability of TTLs was observed at the starting dose with a coefficient of variation (CV%) of 32.1%. Moreover, 15 out of 29 patients (52%) did not reach the target TTL of 50 ng/mL at the starting dose of 37.5 mg per day. Therefore, dose escalations to 50 mg per day were indicated in 15 patients. However, in one patient it was not possible to increase the sunitinib dose due to haematological toxicity. At the second PK evaluation (day 29), the median TTL was increased to 57.6 ng/mL [IQR 48.3 – 61.9] with an inter-patient variability of 35.2%. Moreover, 19 out of 29 patients (66%) reached the target TTL. Of the 10 patients below the target level, the sunitinib dose was increased to 62.5 mg per day in 3 patients and dose escalations were not possible due to toxicity in 7 patients. At the final PK evaluation (day 57), the median TTL was reduced to 51.8 ng/mL [40.3 – 63.7] with an inter-patient variability of 45.0% and 15 patients (52%) reached the target TTL. In Figure 2, the measured TTLs of individual patients at day 15, day 29 and day 57 are presented.

Table 1. Baseline characteristics of all evaluable patients.

Characteristic	Patients (n=42)
Gender (number (%))	
Male	28 (67)
Female	14 (33)
Age (y) (median (range))	61 (28 – 74)
Bodyweight (kg) (median (range))	77 (44 – 108)
Ethnicity (number (%))	
Caucasian	42 (100)
ECOG Performance status (number (%))	
0	10 (24)
1	32 (76)
Primary tumor (number (%))	
Neuroendocrine carcinoma	8 (19)
Colorectal carcinoma	8 (19)
Renal cell carcinoma	6 (14)
Adenocarcinoma of unknown primary (ACUP)	3 (7)
Uveal melanoma	3 (7)
Miscellaneous*	14 (33)
Clinical stage, pretreatment (number (%))	
Locally advanced	2 (5)
Metastatic	40 (95)
Prior treatment (number (%))	
TKI therapy	5 (36)
Chemotherapy	31 (74)
1 regimen	12 (29)
2 regimens	3 (7)
≥3 regimens	17 (40)
Surgery	28 (67)
Radiotherapy	16 (38)

*Miscellaneous: pancreatic carcinoma (n=2), hepatocellular carcinoma (n=2), oesophageal carcinoma (n=2), prostate carcinoma, cervix carcinoma, head and neck carcinoma, mesothelioma, liposarcoma, ewing sarcoma, myo-epithelioma, osteosarcoma.

R1
R2
R3
R4
R5
R6
R7
R8
R9
R10
R11
R12
R13
R14
R15
R16
R17
R18
R19
R20
R21
R22
R23
R24
R25
R26
R27
R28
R29
R30
R31
R32
R33
R34
R35
R36
R37
R38
R39

R1
R2
R3
R4
R5
R6
R7
R8
R9
R10
R11
R12
R13
R14
R15
R16
R17
R18
R19
R20
R21
R22
R23
R24
R25
R26
R27
R28
R29
R30
R31
R32
R33
R34
R35
R36
R37
R38
R39

Table 2. Therapy outcomes regarding reached total trough level (TTL), dose and target TTL, stratified by patient group.

Outcome	Group 1a TTL<50 TOX- (n=5)	Group 1b TTL<50 TOX+ (n=10)	Group 2a TTL>50 TOX- (n=6)	Group 2b TTL>50 TOX+ (n=8)	Total (n=29)
TTL (ng/mL) (median [IQR])					
day 15	44.0 [41.8 – 48.8]	39.1 [30.1 – 43.0]	65.5 [56.8 – 67.9]	62.2 [56.0 – 64.7]	49.5 [41.8 – 64.0]
day 29	51.8 [45.6 – 61.5]	50.2 [43.3 – 56.3]	61.4 [58.7 – 79.3]	53.1 [40.1 – 65.8]	57.6 [48.3 – 61.9]
day 57	63.9 [56.2 – 78.3]	39.6 [31.1 – 48.2]	61.9 [55.0 – 69.6]	46.4 [37.5 – 53.6]	51.8 [40.3 – 63.7]
Dose (mg) (mean (SD))					
day 29	50.0 (-)	47.5 (7.9)	37.5 (-)	33.3 (6.5)	42.7 (7.8)
day 57	55.0 (6.8)	35.0 (5.3)	37.5 (-)	25.0 (-)	37.9 (9.7)
Pts on target TTL (number (%))					
day 15	0 (0)	0 (38)	8 (100)	6 (100)	14 (48)
day 29	3 (60)	5 (50)	8 (100)	3 (50)	19 (66)
day 57	5 (100)	1 (25)	6 (75)	3 (50)	15 (52)

IQR, interquartile range; SD, standard deviation; TTL, total trough level, TOX, toxicity.

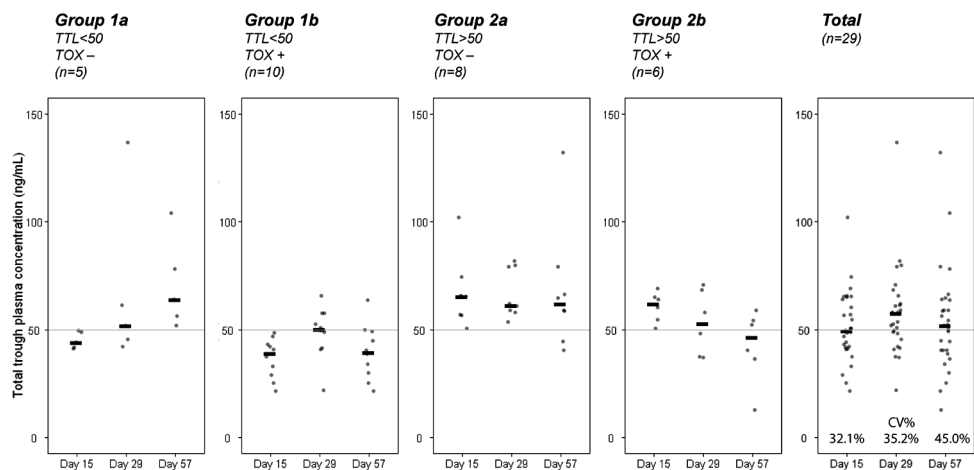


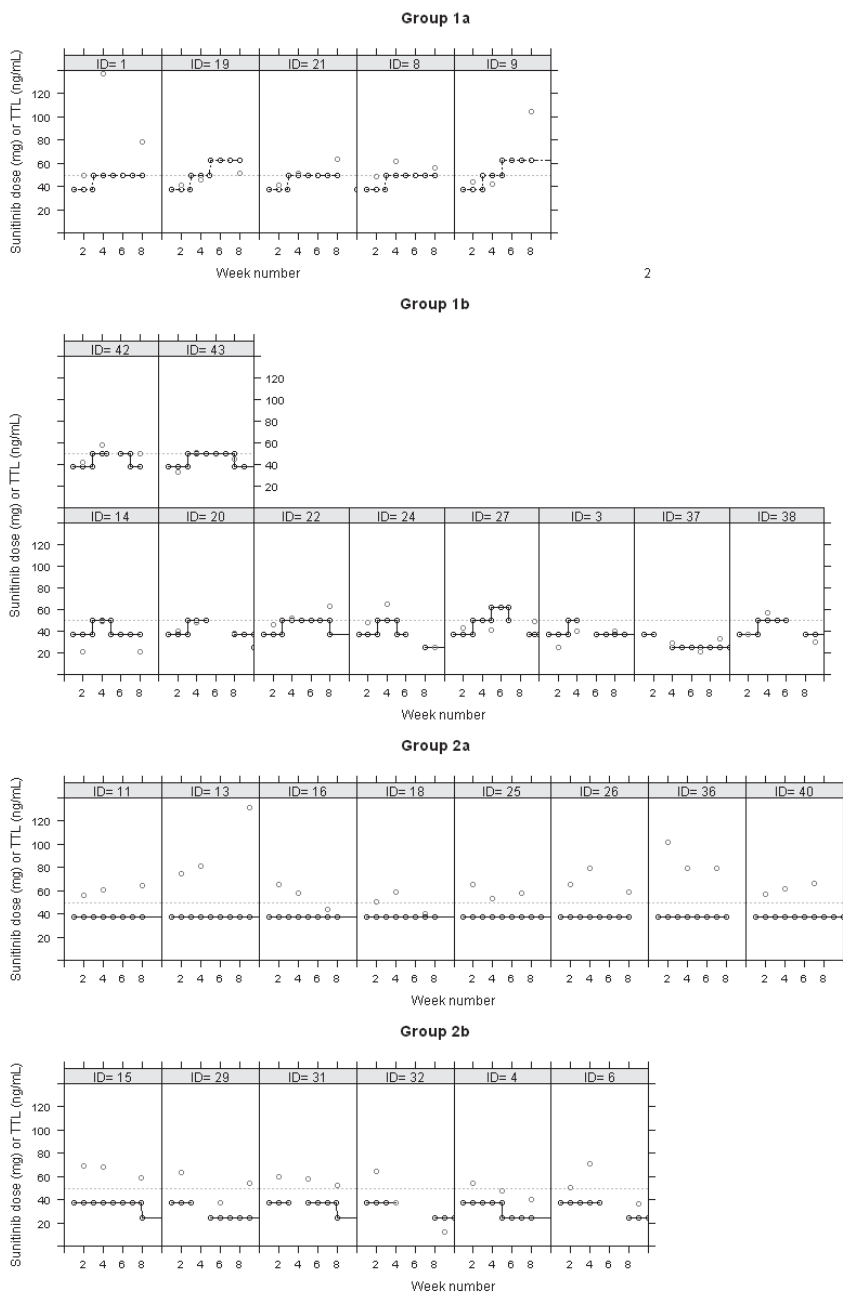
Figure 2. TTLs measured at day 15, day 29 and day 57 of sunitinib treatment of all patients who were evaluable for PK evaluation, stratified by patient group. The black bars represent the median TTL.

PK guided dosing

Based on TTL reached at day 15, two patient groups were distinguished: Group 1 consisted of patients who did not reach target TTL and Group 2 of patients who reached target TTL. Based on toxicity in the first 8 weeks of treatment, these groups could be subdivided further into four patient subgroups with different results of the PK guided dosing strategy. The defined groups were as follows: Group 1a patients with TTL < 50 ng/mL at day 15 and no relevant toxicity (n=5; 17%), Group 1b patients with TTL < 50 ng/mL at day 15 with relevant toxicity (n=10; 34%), Group 2a patients with TTL > 50 ng/mL at day 15 and no relevant toxicity (n=8; 28%), Group 2b patients with TTL > 50 ng/mL at day 15 with relevant toxicity (n=6; 21%). As shown in Table 2, the 5 patients (17%) who did not reach target TTL at day 15 and had PK-guided dose elevations without relevant toxicity, tolerated treatment with 47% higher mean daily dose compared to standard therapy. In Figure 3, an overview of all dose adjustments and TTLs is shown per individual patient within the 8 week study period.

R1
R2
R3
R4
R5
R6
R7
R8
R9
R10
R11
R12
R13
R14
R15
R16
R17
R18
R19
R20
R21
R22
R23
R24
R25
R26
R27
R28
R29
R30
R31
R32
R33
R34
R35
R36
R37
R38
R39

R1
R2
R3
R4
R5
R6
R7
R8
R9
R10
R11
R12
R13
R14
R15
R16
R17
R18
R19
R20
R21
R22
R23
R24
R25
R26
R27
R28
R29
R30
R31
R32
R33
R34
R35
R36
R37
R38
R39



2

Figure 3. Course of sunitinib dose levels and TTLs during the first 8 weeks of treatment of all individual patients who were evaluable for PK evaluation, stratified by patient group. Grey dots represent TTLs. Black dots represent dose levels. The dashed line represents the target TTL. Group 1a: patients with TTL<50 ng/mL at day 15 and without toxicity; Group 1b: patients with TTL<50 ng/mL at day 15 and with toxicity; Group 2a: patients with TTL>50 ng/mL at day 15 and without toxicity; Group 2b: patients with TTL> 50 ng/mL at day 15 and with toxicity.

Treatment toxicity

The most frequently occurring treatment related adverse events are listed in Table 3. Grade ≥ 3 adverse events were observed in 29 patients (69%). The main grade ≥ 3 adverse events attributed to study treatment included hypertension (14%), fatigue (12%), anemia (12%), thrombocytopenia (12%) and hand-foot syndrome (HFS) (10%). Common grade 1 or 2 non-haematologic treatment-related toxicities were fatigue (60%), nausea (50%), dysgeusia (55%), oral mucositis (52%), diarrhea (40%), HFS (33%) and vomiting (29%).

Six patients discontinued sunitinib treatment (at the standard dose of 37.5 mg per day) due to adverse events before the final PK-evaluation at day 57; five of these discontinuations were considered treatment related and included fatal cardiac failure (n=1, grade 5), fatigue, increased blood bilirubin, nausea (all n=1, grade 3) and fatigue (n=1, grade 2). Dose reductions of sunitinib due to treatment related adverse events during the PK evaluation period were performed in sixteen patients (Group 1b + 2b). Moreover, nine of these patients (56%) (Group 1b) who had an initial TTL guided dose increase did not tolerate this higher dose level, as shown in Figure 2. In addition, five patients discontinued sunitinib treatment due to toxicity after the PK evaluation period; two of these discontinuations were considered treatment related and included a combination of anemia and thrombocytopenia (n=2, grade 3).

The main purpose of the study was to assess whether PK-guided dosing could be performed without causing additional toxicities. Therefore, the occurrence of toxicities in the patients who required dose escalations (Group 1) was compared with patients who did not need dose interventions based on PK and remained at the standard dose (Group 2). In all patient groups, the frequency of grade ≤ 2 toxicity was similar. In addition, the frequency of grade ≥ 3 adverse events was comparable between Group 1a and Group 2a and between Group 1b and Group 2b. TTLs above the target level at day 15 of therapy did not correlate to frequency of severe toxicity (grade ≥ 3). Moreover, in Group 1, 10 out of 15 patients (67%) experienced severe toxicities and in Group 2 with TTL > 50 ng/mL, 6 out of 14 patients (43%) experienced severe toxicity.

R1
R2
R3
R4
R5
R6
R7
R8
R9
R10
R11
R12
R13
R14
R15
R16
R17
R18
R19
R20
R21
R22
R23
R24
R25
R26
R27
R28
R29
R30
R31
R32
R33
R34
R35
R36
R37
R38
R39

R1
R2
R3
R4
R5
R6
R7
R8
R9
R10
R11
R12
R13
R14
R15
R16
R17
R18
R19
R20
R21
R22
R23
R24
R25
R26
R27
R28
R29
R30
R31
R32
R33
R34
R35
R36
R37
R38
R39

Table 3. Toxicity data

Adverse event	Grades ≤ 2												Grade ≥ 3												Any grade		
	Discon- tinued (n=13)			Group 1			Group 2			Total (n=42)			Discon- tinued (n=13)			Group 1			Group 2			Total (n=42)			Total (n=42)		
	n	%	n	Group 1a (n=5)		Group 1b (n=10)		Group 2a (n=8)		Group 2b (n=6)		n	%	n	Group 1a (n=5)		Group 1b (n=10)		Group 2a (n=8)		Group 2b (n=6)		n	%	n	%	
				n	%	n	%	n	%	n	%				n	%	n	%	n	%	n	%					
<i>Treatment-related non-heamatological adverse events (occurring in ≥10% of patients)</i>																											
fatigue	7	54	4	80	6	60	5	63	3	50	25	60	2	15	0	0	2	20	0	0	1	17	5	12	30	71	
nausea	6	46	3	60	4	40	4	50	4	67	21	50	2	15	0	0	0	0	1	13	0	0	3	7	24	57	
dysgeusia	6	46	4	80	5	50	4	50	4	67	23	55	0	0	0	0	0	0	0	0	0	0	0	0	23	55	
oral mucositis	3	23	2	40	8	80	5	63	4	67	22	52	0	0	0	0	0	0	0	0	1	17	1	2	23	55	
diarrhea	3	23	3	60	3	30	4	50	4	67	17	40	0	0	1	10	1	10	1	13	0	0	3	7	20	48	
hand-foot syndrome	2	15	3	60	5	50	2	25	2	33	14	33	0	0	0	0	3	30	1	13	0	0	4	10	18	43	
vomiting	4	31	5	100	2	20	1	13	0	0	12	29	0	0	0	0	0	0	1	13	0	0	1	2	13	31	
hypertension	1	8	1	20	0	0	3	38	0	0	5	12	2	15	2	40	0	0	1	13	1	17	6	14	11	26	
anorexia	2	15	0	0	2	20	0	0	2	33	6	14	1	8	0	0	0	0	0	0	0	0	0	1	2	7	17
dry skin	2	15	2	40	2	20	0	0	2	33	8	19	0	0	0	0	0	0	0	0	0	0	0	0	0	8	19
rash	0	0	0	0	3	30	4	50	1	17	8	19	0	0	0	0	0	0	0	0	0	0	0	0	0	8	19
constipation	1	8	1	20	3	30	1	13	0	0	6	14	1	8	0	0	0	0	0	0	0	0	1	2	7	17	
epistaxis	2	15	0	0	2	20	2	25	0	0	6	14	0	0	0	0	0	0	0	0	1	17	1	2	7	17	
dyspnea	2	15	0	0	2	20	1	13	0	0	5	12	1	8	0	0	0	0	0	0	0	0	1	2	6	14	
skin yellow discoloration	2	15	0	0	1	10	2	25	1	17	6	14	0	0	0	0	0	0	0	0	0	0	0	0	0	6	14
dyspepsia	0	0	2	40	1	10	1	13	1	17	5	12	0	0	0	0	0	0	0	0	0	0	0	0	0	5	12
hair depigmentation	0	0	2	40	1	10	2	25	0	0	5	12	0	0	0	0	0	0	0	0	0	0	0	0	0	5	12
oral pain	1	8	0	0	0	0	4	50	0	0	5	12	0	0	0	0	0	0	0	0	0	0	0	0	0	5	12
periorbital edema	2	15	0	0	2	20	0	0	1	17	5	12	0	0	0	0	0	0	0	0	0	0	0	0	0	5	12
periph. neuropathy	1	8	0	0	2	20	1	13	1	17	5	12	0	0	0	0	0	0	0	0	0	0	0	0	0	5	12

Laboratory abnormalities																										
<i>Haematology</i>																										
anemia	1	8	0	0	0	0	0	0	0	1	2	1	8	0	0	1	10	1	13	2	33	5	12	6	14	
white blood cells	0	0	0	0	0	1	13	1	17	2	2	0	0	0	0	1	10	0	0	1	17	2	5	4	10	
neutrophils	0	0	1	20	2	20	0	0	3	50	6	14	1	8	1	20	2	20	0	0	1	17	5	12	11	26
platelets	1	8	1	20	0	0	2	25	0	4	10	0	0	0	0	1	10	0	0	2	33	3	7	7	17	
<i>Clinical Chemistry</i>																										
ALAT	0	0	0	0	1	10	2	25	0	3	7	0	0	1	20	0	0	1	13	0	0	2	5	5	12	
ASAT	0	0	0	0	0	0	1	13	0	1	2	0	0	1	20	1	10	1	13	0	0	3	7	4	10	
creatinine increased	0	0	0	0	0	1	10	1	13	1	17	3	7	1	8	0	0	0	0	0	0	1	2	4	10	
<i>Cardiac events</i>																										
heart failure	0	0	0	0	0	0	0	0	0	0	0	0	1	8	1	20	0	0	0	0	0	2	5	2	5	
acute coronary syndrome	0	0	0	0	0	0	0	0	0	0	0	1	8	0	0	0	0	0	0	0	0	1	2	1	2	
prolonged QT interval	0	0	0	0	0	0	0	0	0	0	0	0	0	0	0	0	0	1	13	0	0	1	2	1	2	
myocardial infarction	0	0	0	0	0	0	0	0	0	0	0	0	0	0	0	0	0	1	13	0	0	1	2	1	2	
Any toxicity	13	100	5	100	10	100	8	100	6	100	100	7	54	3	60	9	90	5	62.5	5.0	83.3	29	69	100	100	

ASAT, aspartate aminotransferase; ALAT, alanine aminotransferase. Group 1a: patients with TTL<50 ng/mL at day 15 and without toxicity; Group 1b: patients with TTL<50 ng/mL at day 15 and with toxicity; Group 2a: patients with TTL>50 ng/mL at day 15 and without toxicity; Group 2b: patients with TTL>50 ng/mL at day 15 and with toxicity.

R1
R2
R3
R4
R5
R6
R7
R8
R9
R10
R11
R12
R13
R14
R15
R16
R17
R18
R19
R20
R21
R22
R23
R24
R25
R26
R27
R28
R29
R30
R31
R32
R33
R34
R35
R36
R37
R38
R39

Discussion

In this pilot study, the safety and feasibility of PK guided sunitinib dosing was investigated. At the standard dose of 37.5 mg, 15 patients (52%) did not reach target TTLs of sunitinib after 14 days of sunitinib treatment. Ultimately, 5 out of 29 patients (17%) had successful dose escalations with a mean dose escalation of 47% leading to TTLs above the target without causing additional toxicities. This implies that PK guided sunitinib dose escalations rather than fixed doses can contribute to optimization of therapy in a considerable part of the patients.

Similar to classical anticancer chemotherapy regimens, it is often reasoned that increasing the dose of an anticancer drug in patients who lack toxicity might increase the likelihood of treatment efficacy [17-20]. Fixed dosing may lead to underdosing due to inadequate drug exposure in some patients. Dosing to toxicity might lead to overdosing and unnecessary side effects since in some patients adequate drug exposure will already be accomplished with a lower dose. This is complex since drug exposure, toxicity and efficacy generally do not show a linear relationship. Therefore, therapeutic drug monitoring for the individualization of dosing of anticancer drugs with an considerable and unpredictable inter-patient variability in pharmacokinetics is gaining popularity. For example, PK-guided dosing has been mentioned for docetaxel leading to a decrease in the inter-patient variability of drug exposure [21]. However, to our knowledge, the current study is the first study in which PK guided dosing is applied to sunitinib treatment.

The sunitinib starting dose of 37.5 mg (continuously once-daily) was based on previously reported studies investigating a continuous dosing strategy for sunitinib [12-14]. Since no safety data were available regarding long term continuously daily dosing of high doses sunitinib, the highest dose level was maximized to 62.5 mg per day [12-14,22].

A limitation of this study is that target TTL have not been established in clinical studies, thus far. The association between sunitinib exposure and efficacy was based on the steady state area under the concentration-time curve (AUC) [4]. Hence, the target plasma levels used in this study were deduced from preclinical studies [5,6,8,9]. Furthermore, our study was performed in a small cohort of patients with a large variety of advanced solid tumors and without a control group. Therefore, it was not possible to investigate the relationship between plasma exposure and treatment efficacy.

In the previously reported studies, mean TTLs were approximately 40-65 ng/mL and inter-patient variability was high with a coefficient of variation (CV) of more than 30% [12-14,22]. Our patient cohort showed comparable results after 14 days of treatment with median TTL of 49.5 ng/mL and an inter-patient variability of 31.2%. When assuming that target TTLs are needed for adequate treatment responses, this meant that more than half of the patients were at subtherapeutic levels (< 50 ng/mL) at the standard dose.

The inter-patient variability in TTL was not reduced using the PK-guided dosing strategy. This can be explained by the fact that 10 of the 15 patients who did not reach TTL at day 15 (Group 1) and 6 of the 14 patients who did reach TTL at day 15 (Group 2) required dose reductions due

to toxicity and could not receive optimal sunitinib doses. Moreover, based on the elimination half life of sunitinib (± 40 h) and N-desethyl sunitinib (± 80 h) [23], it was expected that steady state concentrations would be reached within 14 days of treatment. However, in some patients TTLs still tended to increase after two weeks of sunitinib treatment even when the dose remained equal. A longer period before collection of the first TTL sample was considered, but this would postpone potential beneficial dose increments. In addition, it was observed that TTLs in 2 out of 8 patients decreased to below the target TTL without a dose reduction after 8 weeks of treatment. It is not known whether this is due to unexplained intra-patient variability or whether sunitinib levels tend to decrease after long term treatment as was shown for imatinib [24] and sorafenib [25,26]. Hence, further insights in TTLs and inter-patient pharmacokinetic variability during sunitinib treatment are warranted to allow rational design of future PK-guided dosing studies.

The total occurrence of toxicity grade 3 or higher observed in this study was consistent with previously reported studies on continuous daily dosing regimens of sunitinib [12-14,22]. One patient died on study due to a probably treatment related adverse event (diffuse cardiac ischemia followed by cardiac failure). However, it could not be excluded that this patient was already predisposed to cardiac events and, moreover, the event could not be due to the PK guided dosing strategy since it occurred at the start dose of 37.5 mg per day. Due to the small patient number this study was underpowered to compare the occurrence of toxicities within the different patient subgroups. However, results indicated that the frequency of severe toxicities (grade ≥ 3) was not correlated to TTL at day 15, as this was comparable in the patients with TTL < 50 ng/mL (Group 1) and TTL > 50 ng/mL (Group 2). Of all 16 patients who required dose reductions due to toxicity (Group 1b + 2b), 7 patients suffered from toxicities at the standard dose and would also have experienced these toxicities if they were treated without the PK-guided dosing strategy. In addition, 9 patients experienced severe toxicities after PK guided dose escalation. These toxicities were manageable by dose reductions. Thus, in 9 patients (31%) of the total patient cohort, PK-guided dose escalations were harmful but well manageable. On the other hand, if an effective TTL could not be reached in these patients at a dose level with tolerable toxicity, TTL assessments could substantiate the choice to switch to another more effective therapy. Moreover, in patients of Group 1a (n=5) and Group 2a (n=8), target TTLs were reached without experiencing severe toxicity. Thus, using the PK-guided dosing strategy, additional toxicities could be avoided, since dosing to toxicity was not necessary to reach adequate drug exposure in 45% of patients. Accordingly, the possibility of avoiding unnecessary toxicities and minimizing under-dosing after toxicity induced dose reductions together with the 5 patients (17%) that reached target TTL after dose escalations without additional toxicities, make it worthwhile to implement further research on PK-guided dosing of sunitinib.

In conclusion, 15 patients (52%) did not reach target TTLs at standard sunitinib doses and needed PK guided dose adjustments to increase the probability of a therapeutic effect. Nine patients (31%) experienced clinically relevant adverse events after dose increase, that required

R1
R2
R3
R4
R5
R6
R7
R8
R9
R10
R11
R12
R13
R14
R15
R16
R17
R18
R19
R20
R21
R22
R23
R24
R25
R26
R27
R28
R29
R30
R31
R32
R33
R34
R35
R36
R37
R38
R39

dose reductions. Five patients (17%) reached target TTL after sunitinib dose escalations. Thus, a third of the patients that did not reach target TTL at standard doses, did potentially benefit from the implemented dose escalations without additional toxicities. Further research is required to investigate the safety and therapeutic efficacy of PK guided dosing of sunitinib in order to reach a systemic exposure above the target TTL compared with that from a standard fixed dose.

R1
R2
R3
R4
R5
R6
R7
R8
R9
R10
R11
R12
R13
R14
R15
R16
R17
R18
R19
R20
R21
R22
R23
R24
R25
R26
R27
R28
R29
R30
R31
R32
R33
R34
R35
R36
R37
R38
R39

References

1. Demetri GD, van Oosterom AT, Garrett CR et al. Efficacy and safety of sunitinib in patients with advanced gastrointestinal stromal tumour after failure of imatinib: a randomised controlled trial. *Lancet* 2006; 368: 1329-38.
2. Motzer RJ, Michaelson MD, Redman BG et al. Activity of SU11248, a multitargeted inhibitor of vascular endothelial growth factor receptor and platelet-derived growth factor receptor, in patients with metastatic renal cell carcinoma. *J Clin Oncol* 2006; 24: 16-24.
3. Raymond E, Dahan L, Raoul JL et al. Sunitinib malate for the treatment of pancreatic neuroendocrine tumors. *N Engl J Med* 2011; 364: 501-13.
4. Houk BE, Bello CL, Poland B et al. Relationship between exposure to sunitinib and efficacy and tolerability endpoints in patients with cancer: results of a pharmacokinetic/pharmacodynamic meta-analysis. *Cancer Chemother Pharmacol* 2010; 66: 357-71.
5. Abrams TJ, Murray LJ, Pesenti E et al. Preclinical evaluation of the tyrosine kinase inhibitor SU11248 as a single agent and in combination with "standard of care" therapeutic agents for the treatment of breast cancer. *Mol Cancer Ther* 2003; 2: 1011-21.
6. Abrams TJ, Lee LB, Murray LJ et al. SU11248 inhibits KIT and platelet-derived growth factor receptor beta in preclinical models of human small cell lung cancer. *Mol Cancer Ther* 2003; 2: 471-8.
7. Faivre S, Delbaldo C, Vera K et al. Safety, pharmacokinetic, and antitumor activity of SU11248, a novel oral multitarget tyrosine kinase inhibitor, in patients with cancer. *J Clin Oncol* 2006; 24: 25-35.
8. Mendel DB, Laird AD, Xin X et al. In vivo antitumor activity of SU11248, a novel tyrosine kinase inhibitor targeting vascular endothelial growth factor and platelet-derived growth factor receptors: determination of a pharmacokinetic/pharmacodynamic relationship. *Clin Cancer Res* 2003; 9: 327-37.
9. Murray LJ, Abrams TJ, Long KR et al. SU11248 inhibits tumor growth and CSF-1R-dependent osteolysis in an experimental breast cancer bone metastasis model. *Clin Exp Metastasis* 2003; 20: 757-66.
10. Klumpen HJ, Samer CF, Mathijssen RH et al. Moving towards dose individualization of tyrosine kinase inhibitors. *Cancer Treat Rev* 2011; 37: 251-60.
11. de Jonge ME, Huitema AD, Schellens JH et al. Individualised cancer chemotherapy: strategies and performance of prospective studies on therapeutic drug monitoring with dose adaptation: a review. *Clin Pharmacokinet* 2005; 44: 147-73.
12. Escudier B, Roigas J, Gillessen S et al. Phase II study of sunitinib administered in a continuous once-daily dosing regimen in patients with cytokine-refractory metastatic renal cell carcinoma. *J Clin Oncol* 2009; 27: 4068-75.
13. George S, Blay JY, Casali PG et al. Clinical evaluation of continuous daily dosing of sunitinib malate in patients with advanced gastrointestinal stromal tumour after imatinib failure. *Eur J Cancer* 2009; 45: 1959-68.
14. Novello S, Scagliotti GV, Rosell R et al. Phase II study of continuous daily sunitinib dosing in patients with previously treated advanced non-small cell lung cancer. *Br J Cancer* 2009; 101: 1543-8.
15. van der Veldt AA, Boven E, Helgason HH et al. Predictive factors for severe toxicity of sunitinib in unselected patients with advanced renal cell cancer. *Br J Cancer* 2008; 99: 259-65.
16. van Erp NP, Eechoute K, van der Veldt AA et al. Pharmacogenetic pathway analysis for determination of sunitinib-induced toxicity. *J Clin Oncol* 2009; 27: 4406-12.
17. Gao B, Yeap S, Clements A et al. Evidence for Therapeutic Drug Monitoring of Targeted Anticancer Therapies. *J Clin Oncol* 2012; Published ahead of print.

R1
R2
R3
R4
R5
R6
R7
R8
R9
R10
R11
R12
R13
R14
R15
R16
R17
R18
R19
R20
R21
R22
R23
R24
R25
R26
R27
R28
R29
R30
R31
R32
R33
R34
R35
R36
R37
R38
R39

18. Mita AC, Papadopoulos K, de Jonge MJ et al. Erlotinib 'dosing-to-rash': a phase II inpatient dose escalation and pharmacologic study of erlotinib in previously treated advanced non-small cell lung cancer. *Br J Cancer* 2011; 105: 938-44.
19. Pond GR, Berry WR, Galsky MD et al. Neutropenia as a potential pharmacodynamic marker for docetaxel-based chemotherapy in men with metastatic castration-resistant prostate cancer. *Clin Genitourin Cancer* 2012; 10: 239-45.
20. Rini BI, Grunwald V, Fishman NM et al. Axitinib for first-line metastatic renal cell carcinoma (mRCC): Overall efficacy and pharmacokinetic (PK) analyses from a randomized phase II study (Abstract 4503). *J Clin Oncol* 30[(suppl; abstr 4503)]. 2012.
21. Engels FK, Loos WJ, van der Bol JM et al. Therapeutic drug monitoring for the individualization of docetaxel dosing: a randomized pharmacokinetic study. *Clin Cancer Res* 2011; 17: 353-62.
22. Motzer RJ, Hutson TE, Olsen MR et al. Randomized phase II trial of sunitinib on an intermittent versus continuous dosing schedule as first-line therapy for advanced renal cell carcinoma. *J Clin Oncol* 2012; 30: 1371-7.
23. European Medicines Agency (EMA). Sutent: EPAR - Scientific Discussion. Available at: http://www.ema.europa.eu/docs/en_GB/document_library/EPAR_-_Scientific_Discussion/human/000687/WC500057733.pdf. Date accessed: July 17, 2012. 2007.
24. Eechoute K, Fransson MN, Reyners AK et al. A Long-term Prospective Population Pharmacokinetic Study on Imatinib Plasma Concentrations in GIST Patients. *Clin Cancer Res* 2012; 18: 5780-7.
25. Arrondeau J, Mir O, Boudou-Rouquette P et al. Sorafenib exposure decreases over time in patients with hepatocellular carcinoma. *Invest New Drugs* 2012; 30: 2046-9.
26. Boudou-Rouquette P, Ropert S, Mir O et al. Variability of Sorafenib Toxicity and Exposure over Time: A Pharmacokinetic/Pharmacodynamic Analysis. *Oncologist* 2012; 17: 1204-12.

Chapter 2.3

The effect of seasonal variation and secretion of sunitinib in sweat on the development of hand foot syndrome

Nienke A.G. Lankheet
Alwin D.R. Huitema
Henk Mallo
Sandra Adriaansz
John B.A.G. Haanen
Jan H.M. Schellens
Jos H. Beijnen
Christian U. Blank

Submitted for publication



R1
R2
R3
R4
R5
R6
R7
R8
R9
R10
R11
R12
R13
R14
R15
R16
R17
R18
R19
R20
R21
R22
R23
R24
R25
R26
R27
R28
R29
R30
R31
R32
R33
R34
R35
R36
R37
R38
R39

Abstract

Background. Skin toxicities, such as Hand Foot Syndrome (HFS), are side effects of sunitinib with a considerable impact on quality of life. For conventional anti-neoplastic agents studies have indicated a relationship between hyperhydrosis and development of HFS. Possibly seasonal variation is correlated to occurrence of HFS and, therefore, we proposed to study the prevalence of HFS in different seasons retrospectively. When summertime could be related to increased occurrence of severe HFS, we would hypothesize that aggravation of skin toxicities is caused by the secretion of sunitinib in sweat and, accordingly, we would propose to study the relationship between sunitinib sweat secretion and skin toxicity prospectively.

Patients and methods. A retrospective cohort of nineteen patients treated with sunitinib at the same four seasons was used to determine the prevalence of HFS in summertime compared to wintertime by scoring the skin toxicity. In a prospective study, twenty-five patients treated with sunitinib QD, applied two sweat patches for seven consecutive days; one patch during the last week of the on-treatment phase and one during the last week of the off-treatment phase. Sunitinib and metabolite levels in sweat were quantified by liquid chromatography coupled to tandem mass spectrometry (LC-MS/MS). Skin toxicity was graded using the National Cancer Institute Common Toxicity Criteria version 3.0.

Results. In the retrospective cohort, the patients suffered from more severe HFS during summertime (July to September) compared with the rest of the year. In the prospective study, the cumulative amounts of sunitinib plus N-desethyl sunitinib measured in the patches of the on-treatment phase (median 129.4 ng/patch) were higher than the amounts in the patches of the off-treatment phase (median 39.5 ng/patch ($p < 0.0001$)). A tendency was observed in which increasing amounts of total drug per patch were observed with increasing severity of HFS.

Conclusion. Patients experienced more HFS in summer time compared to other seasons. However, no statistically significant correlation between sunitinib sweat secretion and severity of HFS could be demonstrated within our patient cohort.

Introduction

Sunitinib (Sutent®) is an orally available inhibitor of multiple tyrosine kinases. Sunitinib has proven efficacy as single agent in several solid tumor types and is approved for use in advanced renal cell cancer (RCC), imatinib-resistant or -intolerant gastrointestinal stromal tumors (GIST) and neuroendocrine tumors (NET) [1-3].

Recent findings demonstrated a positive dose-efficacy relationship for sunitinib treatment, indicating that it can be beneficial to dose patients as high as possible [4]. Target plasma concentrations of sunitinib plus active metabolite (N-desethyl sunitinib) are in the range of 50 to 100 ng/mL, as deduced from pharmacokinetic/pharmacodynamic preclinical data [5-9]. However, within this target range some patients already develop severe toxicities [1].

The clinically most relevant side effect of sunitinib aside diarrhea and fatigue is the development of Hand-Foot Syndrome (HFS). HFS (all grades) occurred in 19% of patients in a pooled analysis of published clinical trials of sunitinib of whom 5% experienced severe HFS (grade 3 or 4) [10]. This skin toxicity severely impacts the quality of life of patients treated with sunitinib. Moreover, it can lead to unavoidable dose modifications or dose interruptions, which have a negative impact on treatment efficacy [11,12]

The exact pathogenesis of HFS is unknown, but some hypotheses exist concerning the mechanism by which HFS is caused. To confirm physicians' conjectures that there could be a relationship between occurrence of HFS and seasonal variation, we proposed to study the prevalence of HFS in different seasons retrospectively. When summertime could be related to increased occurrence of severe HFS, we would hypothesize that aggravation of skin toxicities is caused by the secretion of sunitinib in sweat. For conventional anti-neoplastic agents, such as liposomal doxorubicin, previous studies have namely indicated a positive relationship between hyperhidrosis on the palms and plantae and the development of skin toxicity [13]. The primarily affected sites in HFS, the palmoplantar surfaces, have a high density of eccrine glands which continuously excrete sweat [13,14]. Sweat can contain virtually any substance present in blood [15]. This indicates that sweat functions as a carrier of drug to the skin surface. After secretion on the skin surface, sweat containing the drug may penetrate into the stratum corneum and cause toxicity [13]. We have recently shown that sunitinib and its active metabolite N-desethyl sunitinib are secreted in sweat in patients treated with sunitinib [16]. For confirmation of our hypothesis we previously developed and validated a LC-MS/MS method for the quantitative analysis of cumulative sunitinib and N-desethyl sunitinib in human sweat samples according to the FDA guidelines [16].

In this article we present the results of a retrospective study about the occurrence of HFS in different seasons a cohort of patients treated with sunitinib, which formed the basis for a prospective exploratory clinical study about the relationship between sunitinib sweat secretion and skin toxicity in 25 patients on sunitinib therapy.

R1
R2
R3
R4
R5
R6
R7
R8
R9
R10
R11
R12
R13
R14
R15
R16
R17
R18
R19
R20
R21
R22
R23
R24
R25
R26
R27
R28
R29
R30
R31
R32
R33
R34
R35
R36
R37
R38
R39

R1
R2
R3
R4
R5
R6
R7
R8
R9
R10
R11
R12
R13
R14
R15
R16
R17
R18
R19
R20
R21
R22
R23
R24
R25
R26
R27
R28
R29
R30
R31
R32
R33
R34
R35
R36
R37
R38
R39

Patients and Methods

Patient cohorts and study design

Retrospective observations were performed in a cohort of patients, who had been included in an expanded access program of sunitinib. Patients were selected based on sunitinib treatment for advanced renal cell carcinoma in the Netherlands Cancer Institute for at least a full year's period and inclusion in the extended access program between November 2005 and September 2006 [17]. Within this study, patients were treated with sunitinib 50 mg once daily during the on-treatment phase of 4 weeks followed by an off-treatment phase of 2 weeks. For safety assessment, toxicity was graded using the National Cancer Institute Common Toxicity Criteria version 3.0. The prevalence of HFS was scored and thereby HFS was divided in non-clinically relevant HFS (CTC grade 1) and clinically relevant HFS (CTC grade >1). Both, high temperature and high humidity are circumstances that may lead to a higher sweat exposure to the skin [18]. Therefore, the mean ambient temperature and humidity during the months of the study were extracted from the archives of the Royal Dutch Meteorological Institute (KNMI) [19].

For the prospective analysis of sunitinib in sweat eligibility criteria were: age above 18 years, life expectancy of at least 6 weeks, and sunitinib indicated as therapy. Additionally, patients were willing and able to undergo sampling by application of sweat patches and venous sampling for collection of paired plasma samples. The study was approved by the local institutional review board. All patients received information regarding the purpose and conduct of this study and provided written informed consent in accordance with institutional guidelines. Patients were treated with sunitinib once daily. The sunitinib regimen consisted of an on-treatment phase of 4 weeks (days 1-28) followed by an off-treatment phase of 2 weeks (days 29-42). Each patient applied two sweat patches for seven consecutive days; one patch during the last week of the on-treatment phase (days 22-28) and one during the last week of the off-treatment phase (days 36-42) (see Figure 1). From 12 patients paired plasma samples for trough level determination were collected on day 28 and 42 of the treatment cycle. Additionally, one patient had patches applied on both upper arm and palmoplantar surfaces for 30 hours during the on-treatment phase. Patients received standard care related to sunitinib therapy including the standard follow-up examinations. Thus, complete medical history, physical examination, Karnofsky performance status, complete blood count with differential and platelet count, biochemical profile, urinalysis, ECGs were recorded before start of treatment and repeated during every treatment cycle. Toxicity was graded using the National Cancer Institute Common Toxicity Criteria version 3.0 during every treatment phase, similarly to toxicity assessment in the retrospective study. Data on mean ambient temperature during patch application were collected retrospectively by using the monthly overviews in the archive of the Royal Dutch Meteorological Institute (KNMI) [19].



Figure 1. Time scheme of patch application during the 6 weekly cycle (4 weeks treatment followed by 2 weeks of no treatment) of sunitinib therapy. Black bars represent the weeks on which the patches were applied. Arrows represent the time points of plasma sampling.

Sweat and plasma analysis

To collect sweat samples, patients were instructed to apply sweat patches (PharmChek™ Drugs of Abuse patches, PharmChem Inc. (Forth Worth, TX, USA)) onto their upper arm during seven consecutive days. Patches were used in concordance with the manufacturers' application and removal instructions [20]. After removal the patches were stored in accessory plastic bags at -20 °C until analysis. In 12 patients 3.0 mL K-EDTA blood was drawn on the last day of patch application (day 28 and 42 of the treatment cycle) for sunitinib and N-desethyl sunitinib trough level determination. Plasma was collected by centrifugation and stored at -20°C until analysis.

For the determination of both compounds in human sweat a liquid chromatography-tandem mass spectrometry method was developed and validated, with limits of quantification of 1.00-200 ng/patch [16]. The cumulative amount of sunitinib and its metabolite in the patches was used as a measure of skin exposure. Plasma samples were analysed by using a liquid chromatography-tandem mass spectrometry method, with limits of quantification of 2.50-500 ng/mL for both sunitinib and N-desethyl sunitinib (see Chapter 1.2).

Statistical analysis

Descriptive statistics were used to summarize the patient characteristics. To identify outliers within the bio-analytical results The Dixon's Q-test was performed [21]. Non-parametric methods were used to analyse the data. All statistical tests were performed with and without rejecting bio-analytical outliers. For the assessment of the seasonal variation in occurrence of HFS it was not possible to perform a statistical test, since the observations within the two periods of the year were not independent (some patients suffered from HFS in more than one month). For this reason, descriptive statistics were used and data were graphically explored. The Wilcoxon Rank Sum Test was used for comparison of the amounts of drug in sweat in different treatment periods. The Kruskal-Wallis Test was used for the comparison of the amounts of total drug in sweat in three patient groups with increasing severity of HFS (HFS CTC grade 0, HFS CTC grade 1, HFS CTC grade > 1). Spearman's rank correlation coefficient was used as a measure of the association between two variables.

R1
R2
R3
R4
R5
R6
R7
R8
R9
R10
R11
R12
R13
R14
R15
R16
R17
R18
R19
R20
R21
R22
R23
R24
R25
R26
R27
R28
R29
R30
R31
R32
R33
R34
R35
R36
R37
R38
R39

R1
R2
R3
R4
R5
R6
R7
R8
R9
R10
R11
R12
R13
R14
R15
R16
R17
R18
R19
R20
R21
R22
R23
R24
R25
R26
R27
R28
R29
R30
R31
R32
R33
R34
R35
R36
R37
R38
R39

Results

Patients' characteristics

Nineteen patients were enrolled for the retrospective sunitinib cohort of whom 63% suffered from any grade of HFS, as shown in Table 1. Twenty-five patients were enrolled onto the prospective study between September 2009 and January 2012. One patient was excluded from the final analysis, because of protocol deviation concerning the time scheme of patch application. Twenty-four evaluable patients, whose characteristics are detailed in Table 1, underwent at least one complete treatment cycle of six weeks. More than half of the patients suffered from any grade of HFS and half of the patients were male. No considerable differences in patient characteristics were found between patients suffering from any grade of HFS and patients without HFS. However, the mean daily dose of sunitinib was slightly lower in patients suffering from HFS, which was due to previous dose reductions related to toxicity. Namely, seven patients already had a dose adjustment before inclusion in the study and three patients had a dose adjustment during the study. Additionally, a lower Karnofsky Performance Status was found in patients suffering from HFS, which is possibly related to occurrence of this skin toxicity.

Table 1. Patients' characteristics

Study	Characteristic	Number of patients (%) or Mean (SD)*		
Retrospective		Total (n=19)	No HFS (n=7)	HFS CTC > 0 (n=12)
	Gender			
	Male	13 (68.4)	6 (85.7)	7 (58.3)
	Female	6 (31.6)	1 (14.3)	5 (41.7)
	Age (y)*	56.2 (10.5)	53.9 (14.4)	57.6 (7.9)
	Mean daily dose (mg)*	46.7 (5.3)	48.4 (4.3)	45.6 (5.8)
Prospective		Total (n=24)	No HFS (n=11)	HFS CTC > 0 (n=13)
	Gender			
	Male	12 (50.0)	4 (36.4)	8 (61.5)
	Female	12 (50.0)	7 (63.6)	5 (38.5)
	Age (y)*	60.1 (9.5)	61.1 (8.2)	59.2 (10.7)
	Mean daily dose (mg)*	46.1 (11.0)	47.7 (12.3)	44.7 (10.2)
	Length (cm)*	178 (9.9)	177 (11.2)	179 (11.5)
	Weight (kg)*	82.1 (13.6)	81.1 (15.4)	83.0 (12.4)
	MSKCC grade			
	0	8 (33)	4 (36)	4 (31)
	1	7 (29)	4 (36)	3 (23)
	2	4 (17)	1 (9)	3 (23)
	3	4 (17)	1 (9)	3 (23)
	4	1 (4)	1 (9)	0 (0)
	Fuhrmann grade			
NA	5 (21)	3 (27)	2 (15)	
1	2 (8)	2 (18)	0 (0)	
2	5 (21)	2 (18)	3 (23)	
3	11 (46)	4 (36)	7 (54)	
4	1 (4)	0 (0)	1 (8)	
Karnofsky Performance status				
>80	21 (88)	11 (100)	10 (77)	
<80	3 (12)	0 (0)	3 (23)	

CTC, common toxicity criteria; HFS, hand foot syndrome; SD, standard deviation; MSKCC, Memorial Sloan-Kettering Cancer Center criteria.

R1
R2
R3
R4
R5
R6
R7
R8
R9
R10
R11
R12
R13
R14
R15
R16
R17
R18
R19
R20
R21
R22
R23
R24
R25
R26
R27
R28
R29
R30
R31
R32
R33
R34
R35
R36
R37
R38
R39

Seasonal impact on HFS prevalence

Within the retrospective cohort of patients, 12 patients (63.2%) suffered from any grade of HFS of whom 3 patients (15.8%) suffered from non-clinically relevant HFS (CTC grade 1) and 9 patients (47.4%) suffered from clinically relevant HFS (CTC grade > 1) at any time during the one-year observational period. The prevalence of HFS per month is shown in Figure 2. Additionally, the course of mean ambient temperature and humidity per month are shown. We observed that patients suffered from more severe HFS in months with a mean ambient temperature of $\geq 15^\circ\text{C}$ (June to September) compared with the rest of the year. In these four months, 7 patients suffered from clinically relevant HFS (CTC grade > 1) compared with 5 patients in the remaining eight months of the year. Moreover, our observation supported the assumption that the development of HFS during sunitinib treatment is correlated with seasons and temperature and possibly with hyperhydrosis.

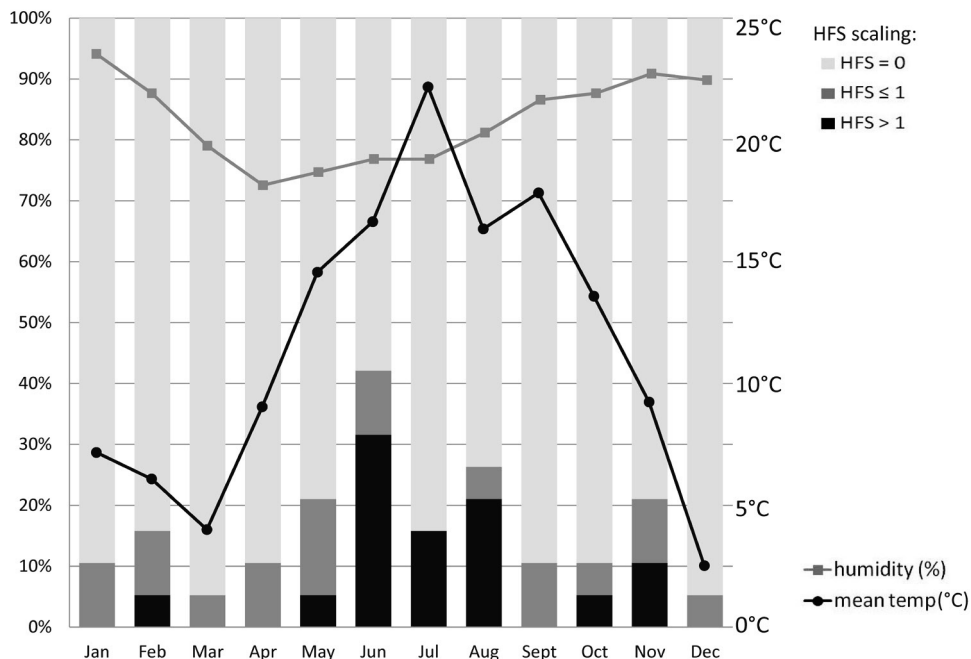


Figure 2. Monthly prevalence (%) of HFS in a cohort of patients treated with sunitinib for at least one year combined with the mean ambient temperature (in $^\circ\text{C}$ at right axis) and mean humidity (% at left axis) at that time. Severity of HFS was stratified in three different groups: HFS absent (CTC grade 0); non-clinically relevant HFS (CTC grade 1); and clinically relevant HFS (CTC grade >1).

Amounts of sunitinib and metabolite in sweat

All patients had worn a sweat patch on their upper arm during the on-treatment phase and off-treatment phase of sunitinib therapy. As expected, the cumulative amounts of sunitinib, N-desethyl sunitinib and the total drug (sunitinib plus N-desethyl sunitinib) measured in the patches of the on-treatment phase were higher than the amounts in the patches of the off-treatment phase (see Figure 3). For the amount of sunitinib and the amount of total drug the differences between the on-treatment and off-treatment phase were significant with median values of 129.4 and 39.5 ng/patch, respectively ($p < 0.0001$). No significant difference between treatment phases was found for the amount of N-desethyl sunitinib per patch ($p = 0.14$). The range of total amount of drug in the patches during the on-treatment and off-treatment phase were 3.51 – 969 ng/patch and 1.84 – 150 ng/patch, respectively. Even in the off-treatment phase (second week after the administration of sunitinib) all cumulative amounts of sunitinib in the sweat patches were far above the lower limit of quantification (LLOQ = 1.0 ng/patch) of the assay. Moreover, in only four patients the cumulative amount of N-desethyl sunitinib in the off-treatment phase was below the LLOQ.

Additionally, one patient applied three patches simultaneously on the upper arm and the palmar and plantar surfaces for 30 hours during the on-treatment phase. The highest amounts of sunitinib and its metabolite were detected on the upper arm. The detected amounts of sunitinib and N-desethyl sunitinib on the plantar and palmar surface, respectively, were approximately 40% and 2% compared to the upper arm, most likely due to problems with attachment of the patches to the skin in these areas.

R1
R2
R3
R4
R5
R6
R7
R8
R9
R10
R11
R12
R13
R14
R15
R16
R17
R18
R19
R20
R21
R22
R23
R24
R25
R26
R27
R28
R29
R30
R31
R32
R33
R34
R35
R36
R37
R38
R39

R1
R2
R3
R4
R5
R6
R7
R8
R9
R10
R11
R12
R13
R14
R15
R16
R17
R18
R19
R20
R21
R22
R23
R24
R25
R26
R27
R28
R29
R30
R31
R32
R33
R34
R35
R36
R37
R38
R39

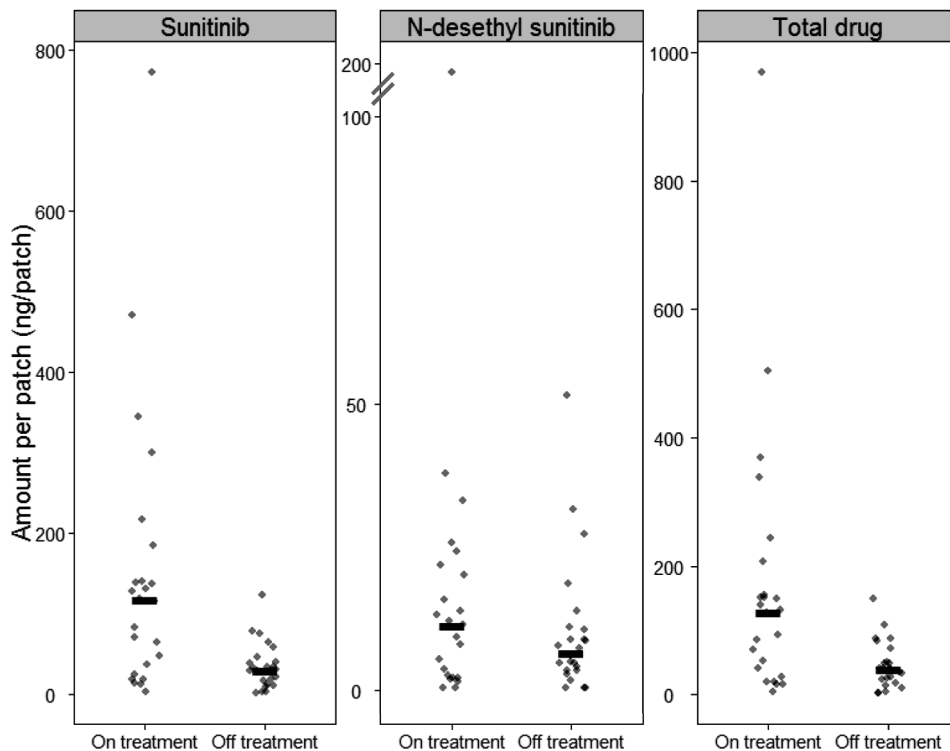


Figure 3. The amount of sunitinib, N-desethyl sunitinib and total drug in the sweat patches; comparing the amounts during the on-treatment phase and the off-treatment phase of sunitinib therapy. Bars represent the median amount per patch.

Relationship between sunitinib skin exposure and skin toxicity

During the on-treatment phase of sunitinib therapy 13 patients suffered from any grade HFS. In Figure 4 the cumulative amount of total drug measured per patch is stratified by CTC grade HFS. Sweat patches of one patient without HFS showed strong colour change of the patches and extremely high amounts of sunitinib and N-desethyl sunitinib were detected in these patches, which were identified as outliers and could be rejected at 99% and 95% confidence level, respectively, based on the Dixon's Q-test [21]. However, since rejection of the outliers did not substantially affect study outcomes and no explanation was found for the high amounts detected, these data were not excluded from the final analysis.

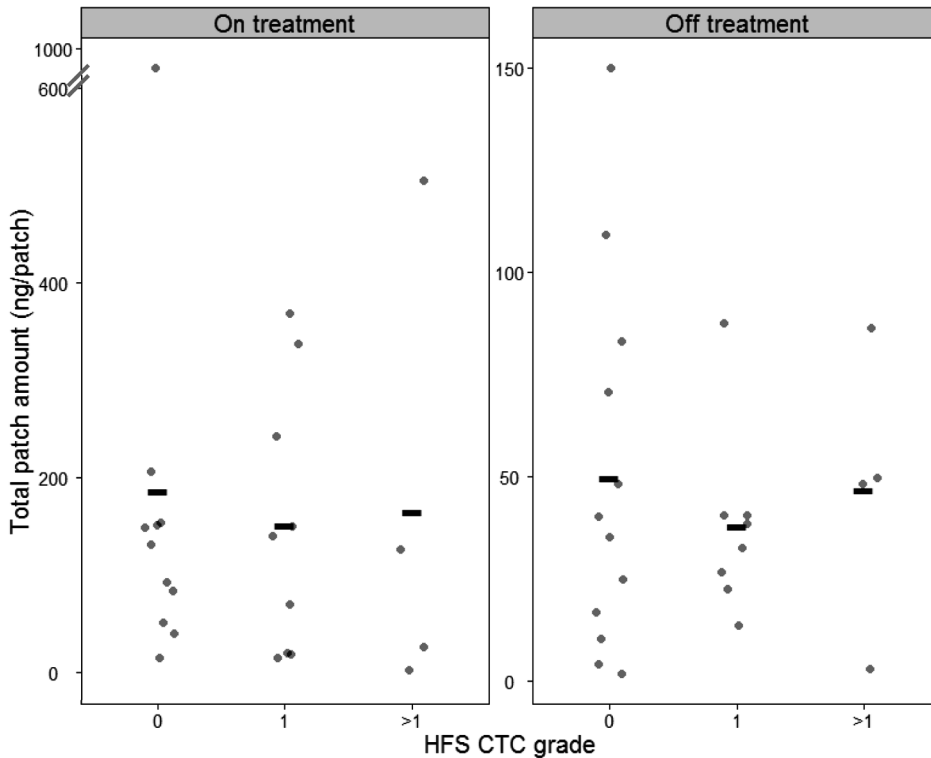


Figure 4. The amount of total drug (sunitinib + N-desethyl sunitinib) during the on-treatment and the off-treatment phase of sunitinib therapy; stratified by HFS CTC grade: HFS absent (CTC grade 0), non-clinically relevant HFS (CTC grade 1), and clinically relevant HFS (CTC grade >1). Bars represent the median amount per patch.

In the on-treatment phase an increase in the total amount of drug per patch was observed when comparing patients without HFS (CTC grade 0 (n=10)) and patients with HFS (CTC grade 1 (n=9)). Only four patients developed HFS CTC grade > 1 within our study and these patients showed a wide variability in total amounts of drug per patch. In the off-treatment phase a tendency was observed in which the highest median amounts of drug per patch were measured in patients with the highest severity of HFS (CTC grade >1 (n=4)). However, due to small patient numbers and large inter-patient variability in amounts of total drug per patch no significant correlation was established between median total amount of drug per patch and severity of HFS in both treatment phases.

R1
R2
R3
R4
R5
R6
R7
R8
R9
R10
R11
R12
R13
R14
R15
R16
R17
R18
R19
R20
R21
R22
R23
R24
R25
R26
R27
R28
R29
R30
R31
R32
R33
R34
R35
R36
R37
R38
R39

Possible determinants of skin exposure

Three determinants expected to be possibly correlated to the total amount of drug secreted in sweat were: administered daily dose of sunitinib, total drug trough levels in plasma, and ambient temperature during sweat patch application. However, in our prospective population none of these determinants showed statistically significant correlation with sunitinib skin exposure (see Table 2).

Table 2. Correlation coefficients of sunitinib skin exposure during on-treatment phase of therapy and three possible determinants.

Skin exposure	Determinants	Correlation coefficient (R)	p-value
Amount of total drug per patch (ng/patch)	Administered daily dose of sunitinib (mg)	0.298	0.157
	Total drug trough plasma levels (ng/mL)	-0.491	0.154
	Mean ambient temperature (°C)	-0.049	0.820

Discussion

In this study we have addressed the question of a possible correlation between seasonal variation and development of HFS. In our retrospective analysis, we could clearly show that patients experienced more severe HFS during summer time compared to other seasons. In the prospective patient cohort, the relationship between the severity of skin toxicities and the sunitinib skin exposure via sweat did not reach statistical significance. However, a tendency towards higher amounts of total drug in sweat of patients with more severe HFS was established. These hypothesis generating results can probably contribute to elucidation of the mechanisms involved in the development of HFS during sunitinib therapy.

To our knowledge, no studies investigating the effects of seasonal variation and sunitinib sweat secretion on the development of HFS have been reported thus far. Our work extends ideas from other studies towards sunitinib induced HFS, since previous studies have indicated a positive relationship between hyperhidrosis on the palms and plantae and the development of skin toxicity for conventional antineoplastic agents, as for example liposomal doxorubicin [13]. Moreover, in case of sunitinib it would be unlikely that HFS was only correlated with systemic exposure to sunitinib (i.e. high sunitinib plasma levels), since previous studies have indicated that occurrence of skin toxicity was not always accompanied by occurrence of other adverse events of sunitinib like thrombocytopenia, liver and kidney function disorders [22,23]. For sorafenib, a multikinase inhibitor like sunitinib, the association between sweat secretion and HFS has been studied by Jain et al. In contrast to our approach, these investigators were not able to detect instant sorafenib concentrations in sweat of two patients included in this study based on assay's sensitivity [24]. On the contrary, we collected cumulative amounts of sweat using sweat patches and measured detectable amounts of sunitinib and its metabolite in all patients' sweat samples collected during

the on-treatment phase. Unfortunately, due to technical reasons it was not possible to detect sunitinib in the regions of skin which are prevalent for the onset of HFS. Nevertheless, the consistent detection of sunitinib on the arm skin allowed us to investigate whether the local toxicity to the skin through sweat secretion could apply to the targeted multikinase inhibitor sunitinib.

In our prospective patient cohort, the proposed relationship between skin toxicity and the sunitinib skin exposure by secretion of sunitinib and metabolite in sweat was explored. For this purpose, the cumulative amount of drug in the patches was used instead of the concentration of drug in sweat as a measure for skin exposure. According to the manufacturers' information, the sweat patches can be used to estimate the cumulative drug exposure over a period up to ten days [20]. This cumulative amount of drug in the patch is a measure of absolute exposure of drugs to the skin during a certain period of time and depends on both the concentration of drugs in sweat and the degree of sweat secretion.

Previous clinical studies clearly showed a relationship between sunitinib plasma exposure and efficacy [4]. This relationship was also observed for the active metabolite of sunitinib, N-desethyl sunitinib, because pharmacological activity of the metabolite is comparable to the parent drug [4]. Therefore, the correlation between HFS and sweat secretion of the total drug (sum of sunitinib and N-desethyl sunitinib) was determined.

The site of patch application could have affected the results of the skin exposure measurements, since palmoplantar surfaces exhibit different types of eccrine glands compared to the upper arm. However, given the manufacturers' recommendations for patch application (i.e. application at lower back or upper arm for validated use) [20] and patients' high discomfort of patches applied on palmoplantar surfaces, patch application on the upper arm was seen as most feasible option for measuring sunitinib skin exposure in this study. Moreover, all patients applied the sweat patches on their upper arms to ensure that results of patients enrolled for this study were comparable and, therefore, the patch application site would not be expected to be a source of bias.

Levels of sunitinib and its metabolite were quantifiable in sweat patches during the on- and off-treatment phase. The sustained secretion of metabolite in the off-treatment phase can be explained by the long elimination half life, namely 80-110 h for N-desethyl sunitinib compared to 40-60 h for sunitinib [25]. In contrast, in the paired plasma samples collected during the off-treatment phase no sunitinib and metabolite could be detected for most patients. This lack of correlation between plasma and sweat samples was expected, since the cumulative amount of sunitinib in the patch is a result of drug concentrations in sweat and the rate of sweat secretion during seven consecutive days, while paired plasma samples solely reflect drug plasma concentrations at time point of blood collection.

In the retrospective study, it was observed that patients suffered from more severe HFS during summertime compared with wintertime. Since the increased ambient temperature during summer time seemed to be related to the prevalence of HFS, ambient temperature was also expected to be a determinant in the sunitinib sweat secretion. Namely, secretion of sweat is expected to

R1
R2
R3
R4
R5
R6
R7
R8
R9
R10
R11
R12
R13
R14
R15
R16
R17
R18
R19
R20
R21
R22
R23
R24
R25
R26
R27
R28
R29
R30
R31
R32
R33
R34
R35
R36
R37
R38
R39

R1
R2
R3
R4
R5
R6
R7
R8
R9
R10
R11
R12
R13
R14
R15
R16
R17
R18
R19
R20
R21
R22
R23
R24
R25
R26
R27
R28
R29
R30
R31
R32
R33
R34
R35
R36
R37
R38
R39

be correlated to ambient temperatures [15,18]. However, in the prospective study no correlation was found between mean ambient temperature during the period of patch application and the amount of sunitinib secreted in sweat or development of HFS. This lack of correlation between may be caused by the low number of patients with skin toxicity or more pronounced supportive care by the clinicians. Namely, the prospective cohort patients were treated two years later and thus the experience about managing HFS has increased. In line with this, within the retrospective study cohort 47% of patients suffered from severe HFS, in contrast to 17% of patients in the prospective study. Additionally, the mean ambient temperature alone is probably not an adequate representation of all circumstances that provoke sweat secretion during summertime.

No significant correlation could be established between the total amount of drug per patch and severity of HFS in both treatment phases. In addition, no clear correlation between administered dose and sunitinib skin exposure could be established. This is remarkable, since dose reduction has shown to be effective in reducing skin toxicity in individual patients [7]. However, large inter-patient variability in skin exposure was observed in our study. Similarly, plasma exposure to sunitinib shows large variability [7]. The absence of a correlation between skin exposure and administered dose is, therefore, possibly due to large inter-patient variability in skin exposure.

Despite the limitation of small patient numbers, our study revealed that the occurrence of severe HFS was increased during summertime and that there is a tendency towards increasing sunitinib secretion in sweat of patients with more severe HFS. Since HFS is often a cause of undesirable dose reductions, treatment delays or treatment discontinuation, it would be worthwhile to study skin exposure of sunitinib more extensively in a larger cohort of patients. As has previously been suggested for doxorubicin, skin exposure due to sweat secretion could namely be limited by the same preventive measures (e.g. iontophoresis or topically applied aluminum chloride) as proposed for hyperhidrosis [13]. Moreover, preventive measures for hyperhidrosis could be considered to reduce this side effect.

Conclusion

To our knowledge, this is the first exploratory study in which the correlation between seasonal variation, secretion of sunitinib in sweat of patients and the development of skin toxicities was assessed. Patients experienced more HFS in summer time compared to other seasons. Besides, a tendency was seen towards higher amounts of total drug in sweat of patients with more severe HFS. Therefore, further exploration of determinants of sunitinib sweat secretion and seasonal variation in relation to development of skin toxicities in a larger cohort of patients is justified.

References

1. Demetri GD, van Oosterom AT, Garrett CR et al. Efficacy and safety of sunitinib in patients with advanced gastrointestinal stromal tumour after failure of imatinib: a randomised controlled trial. *Lancet* 2006; 368: 1329-38.
2. Motzer RJ, Michaelson MD, Redman BG et al. Activity of SU11248, a multitargeted inhibitor of vascular endothelial growth factor receptor and platelet-derived growth factor receptor, in patients with metastatic renal cell carcinoma. *J Clin Oncol* 2006; 24: 16-24.
3. Raymond E, Dahan L, Raoul JL et al. Sunitinib malate for the treatment of pancreatic neuroendocrine tumors. *N Engl J Med* 2011; 364: 501-13.
4. Houk BE, Bello CL, Poland B et al. Relationship between exposure to sunitinib and efficacy and tolerability endpoints in patients with cancer: results of a pharmacokinetic/pharmacodynamic meta-analysis. *Cancer Chemother Pharmacol* 2010; 66: 357-71.
5. Abrams TJ, Murray LJ, Pesenti E et al. Preclinical evaluation of the tyrosine kinase inhibitor SU11248 as a single agent and in combination with "standard of care" therapeutic agents for the treatment of breast cancer. *Mol Cancer Ther* 2003; 2: 1011-21.
6. Abrams TJ, Lee LB, Murray LJ et al. SU11248 inhibits KIT and platelet-derived growth factor receptor beta in preclinical models of human small cell lung cancer. *Mol Cancer Ther* 2003; 2: 471-8.
7. Faivre S, Delbaldo C, Vera K et al. Safety, pharmacokinetic, and antitumor activity of SU11248, a novel oral multitarget tyrosine kinase inhibitor, in patients with cancer. *J Clin Oncol* 2006; 24: 25-35.
8. Mendel DB, Laird AD, Xin X et al. In vivo antitumor activity of SU11248, a novel tyrosine kinase inhibitor targeting vascular endothelial growth factor and platelet-derived growth factor receptors: determination of a pharmacokinetic/pharmacodynamic relationship. *Clin Cancer Res* 2003; 9: 327-37.
9. Murray LJ, Abrams TJ, Long KR et al. SU11248 inhibits tumor growth and CSF-1R-dependent osteolysis in an experimental breast cancer bone metastasis model. *Clin Exp Metastasis* 2003; 20: 757-66.
10. Rosenbaum SE, Wu S, Newman MA et al. Dermatological reactions to the multitargeted tyrosine kinase inhibitor sunitinib. *Support Care Cancer* 2008; 16: 557-66.
11. Lacouture ME, Wu S, Robert C et al. Evolving strategies for the management of hand-foot skin reaction associated with the multitargeted kinase inhibitors sorafenib and sunitinib. *The Oncologist* 2008; 13: 1001-11.
12. Lacouture ME, Reilly LM, Gerami P et al. Hand foot skin reaction in cancer patients treated with the multikinase inhibitors sorafenib and sunitinib. *Ann Oncol* 2008; 19: 1955-61.
13. Jacobi U, Waibler E, Schulze P et al. Release of doxorubicin in sweat: first step to induce the palmar-plantar erythrodysesthesia syndrome? *Ann Oncol* 2005; 16: 1210-1.
14. Lipworth AD, Robert C, Zhu AX. Hand-foot syndrome (hand-foot skin reaction, palmar-plantar erythrodysesthesia): focus on sorafenib and sunitinib. *Oncology* 2009; 77: 257-71.
15. Rivier L. Techniques for analytical testing of unconventional samples. *Bailliere's Clinical Endocrinology and Metabolism*, 2000 edition. 2010;147-65.
16. Lankheet NAG, Blank CU, Mallo H et al. Determination of sunitinib and its active metabolite N-desethylsunitinib in sweat of a patient. *J Anal Toxicol* 2011; 35: 558-65.
17. Gore ME, Szczylik C, Porta C et al. Safety and efficacy of sunitinib for metastatic renal-cell carcinoma: an expanded-access trial. *Lancet Oncol* 2009; 10: 757-63.
18. Staiger H, Laschewski G, Gratz A. The perceived temperature - a versatile index for the assessment of the human thermal environment. Part A: scientific basics. *Int J Biometeorol* 2012; 56: 165-76.

R1
R2
R3
R4
R5
R6
R7
R8
R9
R10
R11
R12
R13
R14
R15
R16
R17
R18
R19
R20
R21
R22
R23
R24
R25
R26
R27
R28
R29
R30
R31
R32
R33
R34
R35
R36
R37
R38
R39

R1
R2
R3
R4
R5
R6
R7
R8
R9
R10
R11
R12
R13
R14
R15
R16
R17
R18
R19
R20
R21
R22
R23
R24
R25
R26
R27
R28
R29
R30
R31
R32
R33
R34
R35
R36
R37
R38
R39

19. KNMI. Royal Dutch Meteorological Institute (KNMI): Monthly Climatology overviews (ambient temperature, humidity). Available at: http://www.knmi.nl/klimatologie/maand_en_seizoensoverzichten/. Date accessed: July 17, 2012 . 2012.
20. Hartley M, Crook D. PharmChek Drugs of Abuse Sweat Patch (Training manual). Available at: http://www.pharmchem.com/pharmchem/files/download_files/Patch_Training_Manual_Rev_Feb_2012_Final.pdf Date accessed: July 17, 2012. 2012. Product Information.
21. Rorabacher DB. Statistical treatment for rejection of deviant values: critical values of Dixon's "Q" parameter and related subrange ratios at the 95% confidence level. *Anal.Chem.* 63[2], 139-146. 1991.
22. Bex A, van der Veldt AA, Blank C et al. Neoadjuvant sunitinib for surgically complex advanced renal cell cancer of doubtful resectability: initial experience with downsizing to reconsider cytoreductive surgery. *World J Urol* 2009; 27: 533-9.
23. van der Veldt AA, Boven E, Helgason HH et al. Predictive factors for severe toxicity of sunitinib in unselected patients with advanced renal cell cancer. *Br J Cancer* 2008; 99: 259-65.
24. Jain L, Gardner ER, Figg WD et al. Lack of association between excretion of sorafenib in sweat and hand-foot skin reaction. *Pharmacotherapy* 2010; 30: 52-6.
25. European Medicines Agency (EMA). Sutent: EPAR - Scientific Discussion. Available at: http://www.ema.europa.eu/docs/en_GB/document_library/EPAR_-_Scientific_Discussion/human/000687/WC500057733.pdf Date accessed: July 17, 2012. 2007.

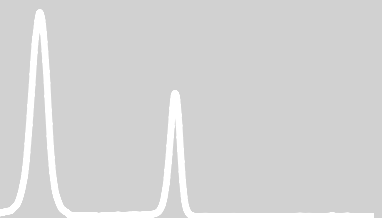
Chapter 2.4

Correlation between plasma erlotinib concentrations and treatment outcome during alternating erlotinib-chemotherapy dosing schedules and erlotinib monotherapy in non-small cell lung cancer

Subanalysis of the NVALT10 study

Nienke A.G. Lankheet
Joachim G. Aerts
Henk E. Codrington
Andrew D. Vincent
Jos H. Beijnen
Jan. H. M. Schellens
Alwin D.R. Huitema
Jacques A. Burgers

*On behalf of the NVALT10 study group
Submitted for publication*



R1
R2
R3
R4
R5
R6
R7
R8
R9
R10
R11
R12
R13
R14
R15
R16
R17
R18
R19
R20
R21
R22
R23
R24
R25
R26
R27
R28
R29
R30
R31
R32
R33
R34
R35
R36
R37
R38
R39

Abstract

Introduction. A phase II study comparing alternating dosing schedules of erlotinib and pemetrexed or docetaxel, with erlotinib monotherapy in non-small cell lung cancer (NSCLC) was performed. Antagonistic, pharmacodynamic drug-drug interactions between chemotherapeutic agents and erlotinib have been reported, for which a erlotinib free interval before chemotherapy was implemented in this study. The potential negative impact of therapeutic erlotinib concentrations on the day of administration of chemotherapeutic agents is currently unknown. Therefore, a pharmacokinetic substudy was performed within this phase II study to investigate (1) whether nadir erlotinib plasma concentrations after an erlotinib wash-out period of five days were low enough to avoid antagonistic interactions during combination therapy and (2) whether trough erlotinib plasma concentrations were high enough to reach therapeutic effects during monotherapy.

Methods. Patients with advanced NSCLC, after failure of first line platinum base therapy, were randomized between erlotinib monotherapy or an alternating treatment schedule of chemotherapy and erlotinib. In the monotherapy arm patients received 150 mg erlotinib continuously. In the combination arm, on day 1 of a 21-day cycle patients received pemetrexed or docetaxel. On day 2 through day 16 patients were treated with erlotinib 150 mg/day once daily. On the first day of the second cycle (day 22 of treatment) a plasma sample was drawn for pharmacokinetic analyses before administration of chemotherapy. HPLC-MS/MS analysis was used to determine erlotinib and O-desmethyl erlotinib concentrations in plasma. Additionally, safety was assessed every 3 weeks using CTC-AE criteria and clinical response was assessed every 6 weeks using RECIST-criteria.

Results. Of the 231 patients included in 66 patients adequate blood samples were obtained. In four out of 34 patients treated with alternating combination therapy, erlotinib plasma concentrations were above the IC_{50} (183 ng/mL) after an erlotinib free period of five days, namely 187, 232, 238 and 394 ng/mL. This was not related to a lower probability of treatment responses. In 32 patients treated with erlotinib monotherapy, median total plasma concentrations were 1538, 1853 and 1530 ng/mL for patients with PD (n=20), SD (n=10) and PR (n=2), respectively. Better clinical response and severe toxicity (CTC grade>3) were not significantly associated with higher erlotinib plasma concentrations.

Conclusions. In 12% of patients the five day wash-out period was insufficient. However, high erlotinib concentrations before chemotherapy administration were not associated with decreased treatment responses. Erlotinib trough concentrations during monotherapy were not associated with better treatment response and with increasing occurrence of severe toxicity.

Introduction

Erlotinib is an epidermal growth factor receptor (EGFR) tyrosine kinase inhibitor. Erlotinib is approved for first-line treatment of non-small cell lung cancer (NSCLC) with mutated EGFR, second-line treatment of NSCLC irrespective of the mutation status, and first-line treatment of advanced pancreatic adenocarcinoma.

Erlotinib plasma exposure can be influenced by many factors, such as patient nonadherence, variability in oral drug availability, and pharmacokinetic drug-drug interactions leading to high inter-patient variability in plasma concentrations [1]. It has been established in vitro that tyrosine kinase inhibition by erlotinib is concentration dependent. Moreover, in clinical studies trough plasma concentrations of erlotinib and its metabolite (O-desmethyl erlotinib) have been correlated with treatment outcome [2-4]. At the recommended daily dose of erlotinib (150 mg/day) typical plasma trough concentrations of 1200 (\pm SD 620) ng/mL have been observed [2]. Based on animal pharmacodynamic studies, it has been established that minimal trough plasma concentrations of approximately 500 ng/mL are required to provide an adequate level of tyrosine kinase inhibition [2]. So far, no clear cut-off values for efficacy and toxicity have been established in humans [1,2]. Therefore, further pharmacokinetic investigations are needed to allow individual treatment optimization.

Additionally, pharmacodynamic drug-drug interactions between chemotherapeutics and erlotinib can negatively influence treatment outcome [5]. Erlotinib induces G1-phase cell cycle arrest, which may interfere with cell cycle-dependent toxicity of chemotherapeutic agents, like pemetrexed (active during synthesis (S) phase of cell cycle) and docetaxel (active during mitosis (M) phase of cell cycle) [5,6]. For this reason, alternating dosing schedules with a wash-out period for erlotinib have been introduced for combination therapy regimens [5,7]. Using this strategy, a randomized phase II study to compare efficacy and safety of chemotherapy – erlotinib combination therapy with single agent erlotinib therapy in NSCLC was initiated. Results of this study have already been published separately [8]. The minimal effective therapeutic level of erlotinib for wild-type EGFR, as deduced from half maximal inhibitory concentration (IC_{50}) after adjusting for plasma protein binding, is approximately 183 ng/mL [9,10]. Theoretically, the erlotinib concentration at the moment of administration of chemotherapeutic agents has to be below 183 ng/mL to prevent any pharmacodynamic antagonism. The optimal alternating treatment schedule of erlotinib with chemotherapeutic agents remains to be confirmed. Moreover, the clinical consequences of high erlotinib plasma levels on the day of administration of chemotherapeutics is currently unknown. Therefore, a translational substudy was performed within the phase II study. The objectives of this translational substudy were to investigate (1) whether nadir erlotinib plasma concentrations after an erlotinib wash-out period of five days were low enough to avoid antagonistic interactions during combination therapy with docetaxel or pemetrexed and (2) whether trough erlotinib plasma concentrations were high enough to provide therapeutic effects during monotherapy. Therefore, we proposed to correlate erlotinib plasma concentrations to treatment outcome.

R1
R2
R3
R4
R5
R6
R7
R8
R9
R10
R11
R12
R13
R14
R15
R16
R17
R18
R19
R20
R21
R22
R23
R24
R25
R26
R27
R28
R29
R30
R31
R32
R33
R34
R35
R36
R37
R38
R39

R1
R2
R3
R4
R5
R6
R7
R8
R9
R10
R11
R12
R13
R14
R15
R16
R17
R18
R19
R20
R21
R22
R23
R24
R25
R26
R27
R28
R29
R30
R31
R32
R33
R34
R35
R36
R37
R38
R39

Materials and Methods

Patient population

The randomized multicenter phase II trial (NCT00835471) was initiated in 2009. Eligible patients had histologically or cytologically confirmed NSCLC, locally advanced and metastatic disease (stage IIIb and IV), and evidence of disease progression after one or two cytotoxic treatment regimens. Other inclusion criteria included age ≥ 18 years; an Eastern Cooperative Oncology Group (ECOG) performance status ≤ 2 ; measurable or evaluable disease according to Response Evaluation Criteria Solid Tumors (RECIST) criteria; estimated life expectancy > 12 weeks; and adequate hematologic, hepatic and renal function.

Main exclusion criteria included previous treatment with an EGFR tyrosine kinase inhibitor; inability to interrupt acetyl salicylic acid or other non-steroidal anti-inflammatory agents for a 5-day period; patients unsuitable for adequate follow-up.

In ten selected centers, this translational substudy was conducted. For a patient to be evaluable in the present translational substudy, one plasma erlotinib concentration should be available during the first four cycles of therapy.


The protocol was approved by local independent ethics committees, and the study was conducted in accordance with the Declaration of Helsinki. All patients received information regarding the purpose and conduct of this study and provided written informed consent.

Study design

Patients were randomized to receive erlotinib monotherapy, or a combination of erlotinib and chemotherapy (see Figure 1). In the monotherapy schedule, patients were continuously treated with erlotinib at a dose of 150 mg/day until disease progression. In the combination therapy schedule, patients were treated with an alternating regimen of erlotinib and chemotherapy. On day one of the schedule (q21 days) patients received pemetrexed (500 mg/m²) or docetaxel (75 mg/m²), depending on tumor type (non-squamous or squamous carcinoma, respectively). On days 2 through 16 patients were treated with erlotinib 150 mg/day once daily. Chemotherapy was given for a maximum of four cycles. Thereafter, continuously daily dosing of erlotinib was continued until disease progression. The primary objective of the randomized study was to compare progression free survival and overall survival of patients in both treatment groups. The primary objective of the translational substudy was to assess the correlation between pharmacokinetics and treatment responses and safety. Plasma samples were drawn for pharmacokinetic analyses during treatment of patients on monotherapy and during erlotinib-free interval of patients on combination therapy.

Pharmacokinetic analyses

For patients on erlotinib monotherapy the plasma sample for PK analysis was drawn at day 22 or otherwise at least 7 days after start of erlotinib therapy. From patients on the alternating combination schedule the plasma sample for PK analysis was drawn on day 22 (or alternatively at start of cyclus 3 or 4) or during another day of the erlotinib free interval. The EDTA blood samples were centrifuged within 12 hours after blood draw and subsequently, EDTA plasma was stored at -20°C until analysis.



Monotherapy	Day 1 -21		Day 22-...
Erlotinib	X		X
Chemotherapy			

Combination therapy	Day 1	Day 2-16	Day 17-21	Day 22-...
Erlotinib		X		
Chemotherapy	X			X

Figure 1. Study design with randomization of patients to monotherapy or combination therapy schedule. Black arrow represents time point of blood collection.

Concentrations of erlotinib and its primary metabolite, O-desmethyl erlotinib (isomers OSI-420 plus OSI-413), in human EDTA plasma were determined using high-performance liquid chromatography and detection with tandem mass spectrometry (HPLC-MS/MS). This method was validated over a range from 5.0 to 2,500 ng/mL for both compounds and showed adequate accuracy and precision, as described before [11]. The lower limit of detection (LLOD) of the assay was established at 2.0 ng/mL for both compounds with a signal to noise ratio of 3. All measured concentrations above 2.0 ng/mL were included in the data analysis and, consequently, all concentrations below 2.0 ng/mL were defined as <LLOD. The investigators performing the pharmacokinetic analyses were blinded to patient characteristics and clinical outcomes.

For patients on alternating combination therapy, the PK parameters assessed in this study were the nadir erlotinib and O-desmethyl erlotinib concentrations at moment of chemotherapy administration (day 22). For some patients a sample was collected within the erlotinib-free interval but not directly before chemotherapy. The nadir plasma concentrations for these patients were estimated using the interval between blood sampling and chemotherapy administration and the mean elimination half life of the drug. Mean elimination half life used in the calculation was 36 hours for erlotinib and O-desmethyl erlotinib [12] according to the method previously described by Wang et al [13]. The formula used for this purpose, was:

R1
R2

$$1) \text{ Conc}_{\text{nadir}} = \text{Conc}_{\text{measured}} \cdot 0.5^{\left(\frac{\text{interval}}{t_{1/2}}\right)}$$

- R3
R4
R5
R6
R7
R8
- $\text{Conc}_{\text{nadir}}$ = estimated nadir plasma concentration in ng/mL.
 - $\text{Conc}_{\text{measured}}$ = measured drug plasma concentration in ng/mL
 - Interval = interval between between blood sampling and chemotherapy administration in hours
 - $t_{1/2}$ = mean terminal half life of the drug in hours

R9

Safety and efficacy assessments

R10
R11
R12
R13

Tumor response was determined every second treatment cycle during study treatment by computed tomography (CT) until disease progression and every 3 months thereafter. Tumor response was assessed according to RECIST. For a patient to be evaluable for efficacy assessments, tumor response had to be assessed 6 weeks after the start of treatment (2 cycles).

R14
R15
R16
R17
R18

Adverse events were assessed at three-weekly intervals and were graded using the National Cancer Institute Common Toxicity Criteria for Adverse Events (version 3.0). All patients treated with erlotinib monotherapy of whom an erlotinib plasma concentration was available, were considered evaluable for toxicity assessments.

R19

Additional data collection

R20
R21
R22
R23

Case report forms were reviewed to collect data on patient and medication related factors that could have contributed to variations in erlotinib plasma concentrations. Data were collected on age, gender, bodyweight, tumor type, performance status, cigarette smoking habits and concomitant medication.

R24
R25
R26
R27
R28
R29
R30
R31

Concomitant medication could influence erlotinib plasma levels by pharmacokinetic interactions. Proton pump inhibitors and histamine-2-receptor antagonists are known to decrease erlotinib plasma levels by decreasing the gastro-intestinal absorption of erlotinib through increasing the gastric pH [14]. Additionally, ciprofloxacin can increase the erlotinib plasma levels substantially by inhibition of cytochrome P450 enzyme (CYP) 1A2 and 3A4 [15]. Smoking of cigarettes leads to induction of CYP1A2 and thereby substantially decrease erlotinib concentrations in plasma [16]. For this reason, data on concomitant use of proton pump inhibitors, histamine-2-receptor antagonists, ciprofloxacin and smoking status were collected.

R32
R33
R34
R35
R36
R37
R38
R39

KRAS and EGFR-mutations have been related to treatment outcome in erlotinib therapy. Namely, KRAS mutations decrease the sensitivity of tumor cells for erlotinib, whereas various EGFR-mutations increase the sensitivity of cells for erlotinib [9,17,18]. Additionally, patients with NSCLC and EGFR mutations have a better prognosis than patients with wild-type EGFR, regardless of treatment received [19]. However, patients were not selected based on mutational status before enrolment into the phase II study. Therefore, data on mutational status of KRAS and EGFR were collected retrospectively whenever available.

Statistics

Descriptive statistics were used to summarize the patient characteristics and erlotinib and O-desmethyl erlotinib plasma concentrations. Correlations of plasma concentrations with response and safety were graphically explored and tested with non-parametric statistic tests when graphics indicated relevant differences between groups. The Jonckheere-Terpstra Trend Test was used for the comparison of erlotinib trough plasma concentrations in three patient groups with different early clinical responses (PD, progressive disease; SD, stable disease; PR, partial response). The Wilcoxon Rank Sum Test was used for comparison of erlotinib plasma concentrations in patients with or without clinically relevant toxicities.

Results

Patient characteristics

In total, 231 patients were included in the phase II study. From 73 patients plasma concentrations were available and thereof 66 patients were evaluable for response, as shown in Figure 2. Characteristics of the evaluable patients of this translational substudy are detailed in Table 1. Patients were equally distributed to the two treatment schedules with 32 patients (48.5%) treated with erlotinib monotherapy and 34 patients (51.5%) treated with combination therapy. The percentages of males in the monotherapy and combination therapy schedule were 62.5% and 64.7%, respectively. Moreover, the patient characteristics in this substudy were not relevantly different compared to the whole study population (data not shown).

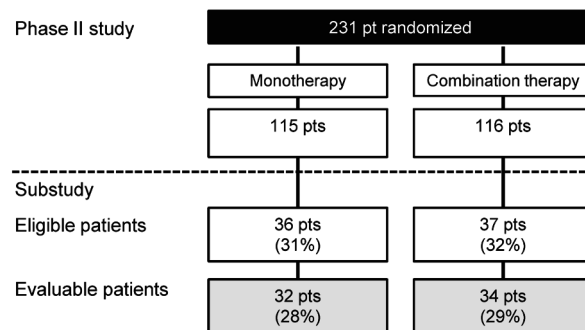


Figure 2. Overview of included patients in Phase II study and translational substudy.

The mean daily erlotinib dose of patients in the monotherapy and combination therapy schedule were 147 mg and 149 mg per day, respectively. In the alternating combination schedule 10 patients (29.4%) were treated with docetaxel and 24 patients (70.6%) were treated with pemetrexed. Concomitant medication, e.g. proton pump inhibitors, histamine-2-receptor antagonists and ciprofloxacin, was more frequently used in patients treated with combination therapy.

Table 1. Patients' characteristics

Characteristic	Number of patients (%) or Mean (SD) *		
	Total (n=66)	Erlotinib monotherapy (n=32)	Combination therapy (n=34)
Gender			
Male	42 (63.6)	20 (62.5)	22 (64.7)
Female	24 (36.4)	12 (37.5)	12 (35.3)
Age (y)*	62.5 (9.1)	61.4 (7.6)	63.6 (10.3)
Bodyweight (kg)*	78.4 (14.7)	83.0 (16.8)	74.3 (11.2)
Tumor histology			
Not specified	8 (12.1)	5 (15.6)	3 (8.8)
Adenocarcinoma	26 (39.4)	11 (34.4)	15 (44.1)
Squamous carcinoma	20 (30.3)	11 (34.4)	9 (26.5)
Large cell carcinoma	12 (18.2)	5 (15.6)	7 (20.6)
WHO Performance status			
0	31 (47.0)	15 (46.9)	16 (47.0)
1	34 (51.5)	17 (53.1)	17 (50.0)
2	1 (1.5)	0 (0.0)	1 (3.0)
Smoking status			
Never smoker	4 (6.1)	0 (0.0)	4 (11.8)
Former smoker	33 (50.0)	16 (50.0)	17 (50.0)
Current smoker	22 (33.3)	13 (40.6)	9 (26.5)
Unknown	7 (10.6)	3 (9.4)	4 (11.8)
KRAS mutation status			
Negative	17 (25.8)	8 (25.0)	9 (26.5)
Positive	3 (4.5)	2 (6.3)	1 (2.9)
Unknown	46 (69.7)	22 (68.7)	24 (70.6)
EGFR mutation status			
Negative	17 (25.8)	8 (25.0)	9 (26.5)
Positive	2 (3.0)	2 (6.3)	0 (0.0)
Unknown	47 (71.2)	22 (68.7)	25 (73.5)
Mean daily erlotinib dose (mg)*	148 (13.7)	147 (17.7)	149 (8.6)
Chemotherapy			
Docetaxel	10 (29.4)	-	10 (29.4)
Pemetrexed	24 (70.6)	-	24 (70.6)
Co-medication			
PPIs	13 (19.7)	4 (12.5)	9 (26.3)
Ciprofloxacin	1 (1.5)	0 (0.0)	1 (2.9)

EGFR, epidermal growth factor receptor; KRAS, K-ras gene; SD, standard deviation; WHO, world health organization.

Plasma concentrations of erlotinib and O-desmethyl erlotinib

Plasma concentrations of the evaluable patients are summarized in Table 2. In general, the inter-patient variability of erlotinib and O-desmethyl erlotinib plasma concentrations was high (63.3% and 133.2%, respectively).

Table 2. Erlotinib and O-desmethyl erlotinib concentrations in patients treated with erlotinib monotherapy or a combination therapy of erlotinib and chemotherapy sequentially.

Characteristic	Number of patients (%) or Median (IQR)			
	Erlotinib monotherapy (n=32)		Combination therapy (n=34)	
	Erlotinib	O-desmethyl erlotinib	Erlotinib	O-desmethyl erlotinib
Median trough level at day 22 of therapy* (ng/mL [IQ R])	1575 [815 – 1934]	233 [161 – 306]	74.1 [7.34 - 148]	15.3 [8.52 – 21.7]
(number of pt (%))	30 (92.7)	30 (92.7)	16 (47.1)	12 (35.3)
Number of pt below LLOD (2 ng/mL) (number (%))	2 (6.3)	2 (6.3)	18 (52.9)	22 (64.7)
Number of pt ≥ therapeutic target level (500 ng/mL) (number (%))	28 (87.5)	NA	1 (2.9)	NA
Number of pt > IC ₅₀ (183 ng/mL) (number (%))	29 (90.6)	NA	5 (14.7)	NA

* median trough level of all patients with concentration > LLOD (= 2.0 ng/mL).

IC₅₀, concentration at which 50% of cells is inhibited; IQ R, inter quartile range; LLOD, lower limit of quantification; pt, patients; NA, not available.

From eight patients treated with the alternating schedule (23.5%), erlotinib concentrations were not available on the day of the subsequent chemotherapy administration, but rather during the preceding erlotinib free interval (median time before administration of chemotherapy 48h [IQR: 24-72h]). Nadir concentrations for these patients were estimated using Formula 1. Median nadir concentrations on the day of chemotherapy administration of patients on alternating schedule were 4.46 and <LLOD (2.0 ng/mL) for erlotinib and O-desmethyl erlotinib, respectively. For one patient the concentration at day 22 was at a therapeutic level (2195 ng/mL), since no erlotinib free period was used, as deduced from medical records. This patient was, therefore, excluded from further analyses. In addition, four patients (11.8%) had erlotinib concentrations above the IC₅₀ (183 ng/mL) after a five day erlotinib-free period, namely 187, 232, 238 and 394 ng/mL (see Figure 3). Erlotinib and O-desmethyl concentrations below the LLOD (2.0 ng/mL) were observed in 18 and 22 patients, respectively.

Median steady state trough concentrations of patients on continuous erlotinib monotherapy were 1528 ng/mL [interquartile range (IQR) 783 – 1890] and 228 ng/mL [IQR 82.0 – 284] for erlotinib and O-desmethyl erlotinib, respectively. Four patients (12.5%) had erlotinib concentrations below the pre-defined therapeutic target level (500 ng/mL). Additionally, thereof 2 patients even experienced erlotinib and O-desmethyl erlotinib trough levels below the lower limit of detection (LLOD = 2.0 ng/mL).

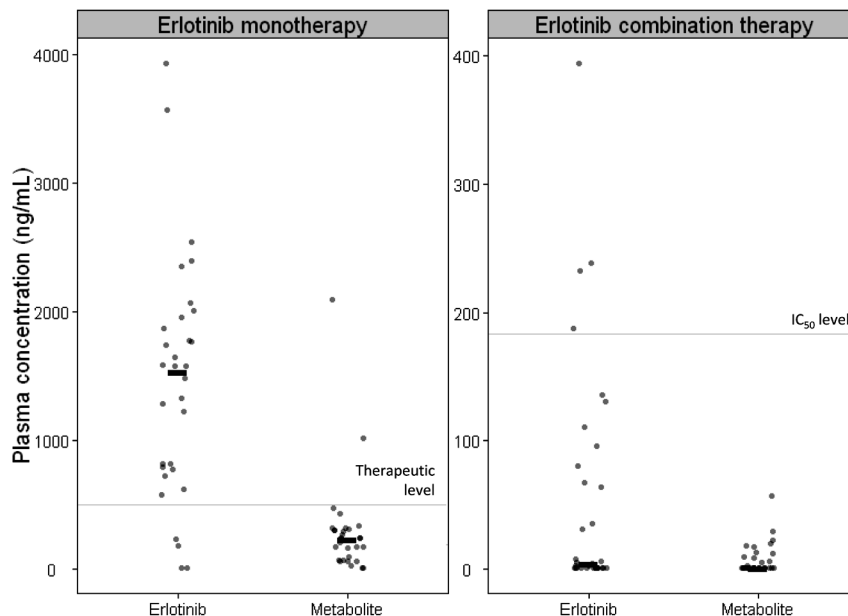


Figure 3. Erlotinib and O-desmethyl erlotinib plasma concentrations during erlotinib monotherapy and at the day of chemotherapy administration during erlotinib plus chemotherapy combination therapy. Black bars represent median concentrations.

Correlation between erlotinib plasma concentrations and response

The correlation between total plasma concentrations of erlotinib plus O-desmethyl erlotinib and best overall response were assessed for patients in both treatment groups.

For patients treated with the alternating combination therapy, no relationship between plasma levels and response was observed (see Figure 4). The median total plasma concentrations at moment of chemotherapy administration were <LLOD (2.0 ng/mL) [IQR: < LLOD – 11.7], 4.58 ng/mL [<LLOD – 105] and 8.89 ng/mL [5.16 – 133] in patients with progressive disease (n=8), stable disease (n=16) and partial response (n=9), respectively. A statistically significant relationship was found relating higher total nadir plasma concentrations with better response (p=0.04). Moreover, of the four patients with nadir erlotinib plasma concentrations above the IC₅₀ (183 ng/mL), none showed progressive disease as early clinical response, two patients showed stable disease and two patients showed a partial response.

For the patients treated with erlotinib monotherapy, median plasma concentrations observed in patients with progressive disease (n=20), stable disease (n=10) and partial response (n=2) were 1538 ng/mL [IQR 814 – 2214], 1853 ng/mL [928 – 2181], 1350 ng/mL [1126 – 1574]), respectively, as shown in Figure 3. Since only two patients reached partial response within this treatment cohort and inter-patient variability was high, no statistically significant relationship was found towards increasing total plasma concentrations with better response (p=0.97).

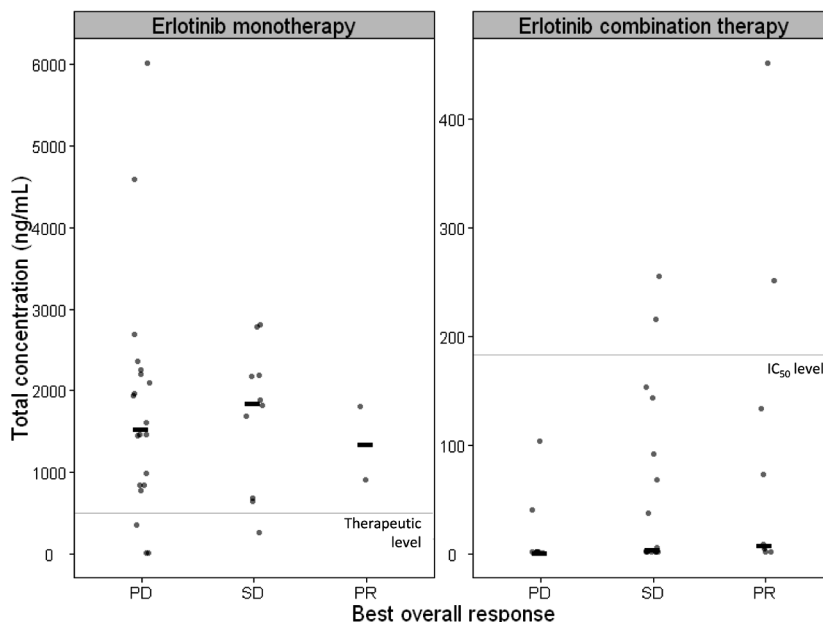


Figure 4. Total plasma concentrations (erlotinib plus O-desmethyl erlotinib) during erlotinib monotherapy and at the day of chemotherapy administration during alternating combination therapy stratified by best overall response classifications (PD, progressive disease; SD, stable disease; PR, partial response). Black bars represent median concentrations.

Correlation between erlotinib plasma concentrations and toxicity

Erlotinib and O-desmethyl erlotinib concentrations during erlotinib therapy were available of patients treated in the monotherapy arm. Therefore, all patients on erlotinib monotherapy for whom plasma concentrations were available, were evaluable for toxicity assessment. In total, 35 patients were included in the toxicity assessment. All non-hematological adverse events, which occurred within the first four cycles of treatment, were included in the analysis. Subsequently, patients were categorized by severity of adverse events, namely patients with non-hematological toxicity CTC grade <3 (n=26) or CTC grade ≥3 (n=9). As shown in Figure 5, higher total plasma concentrations were not correlated to increased severity of adverse events in our population (p=0.36).

Factors influencing erlotinib concentrations

Only a small number of patients used concomitant medication during erlotinib monotherapy. Therefore, no correlation between use of proton pump inhibitors or histamine-2 receptor antagonists and erlotinib trough plasma concentrations during erlotinib therapy could be established within our study. Of the current smokers (n=13), ten patients did reach therapeutic erlotinib concentrations. Two current smokers experienced erlotinib plasma concentrations <LLOD

R1
R2
R3
R4
R5
R6
R7
R8
R9
R10
R11
R12
R13
R14
R15
R16
R17
R18
R19
R20
R21
R22
R23
R24
R25
R26
R27
R28
R29
R30
R31
R32
R33
R34
R35
R36
R37
R38
R39

(2 ng/mL) and, therefore, it is more likely that other factors such as nonadherence contributed to these extremely low plasma concentrations rather than pharmacokinetic variability. Thus, it was not possible to relate low erlotinib concentrations directly to concurrently administered drugs or cigarette smoking.

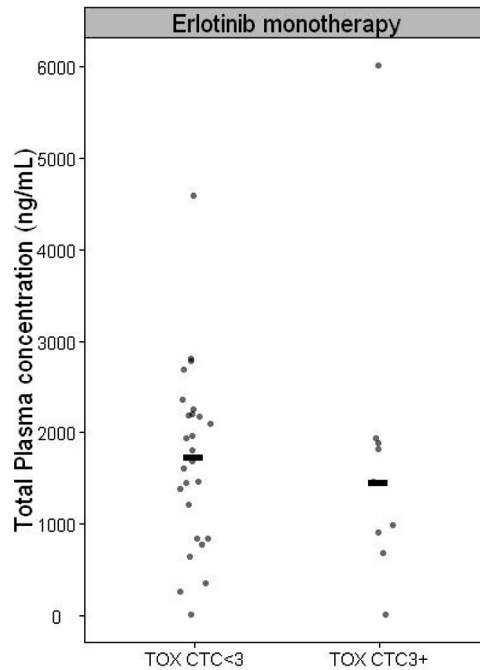


Figure 5. Total plasma concentrations (erlotinib plus O-desmethyl erlotinib) of patients with non-hematological toxicities CTC grade <3 (n=26) and CTC grade \geq 3 (n=9) during erlotinib monotherapy. Black bars represent median concentrations.

Discussion

This translational study was conducted to investigate whether nadir erlotinib plasma concentrations after an erlotinib wash-out period of five days were low enough to avoid antagonistic interactions during combination therapy. In four patients treated with alternating combination therapy, erlotinib plasma concentrations were above the IC_{50} for wildtype-EGFR inhibition (183 ng/mL) after an erlotinib free period of five days. However, these relatively high erlotinib concentrations were not associated with decreased treatment efficacy. Possibly, an erlotinib wash-out period shorter than 5 days would also be adequate to avoid an antagonistic interaction. This implies that further exploration of the mechanism behind the pharmacodynamic interaction and its clinical consequences are required. Additionally, it was investigated whether trough erlotinib plasma concentrations were high enough to reach therapeutic effects during monotherapy.

Erlotinib trough concentrations during monotherapy were not significantly associated with better treatment response and with increasing occurrence of severe toxicity. However, data imply that the exposure-response correlation may be stronger than the exposure-safety correlation in erlotinib therapy.

Various studies combining EGFR targeted therapy concurrently with chemotherapy were unable to show survival benefit of combination therapy compared with chemotherapy alone [20-23]. These negative results may have been due to either using a population not enriched for EGFR-mutations or an antagonistic interaction between the EGFR targeted therapy and the chemotherapeutic agents [24]. Moreover, preclinical data suggests that concomitant use of EGFR targeted therapy and chemotherapy may result in a negative cell cycle-specific pharmacodynamic drug-drug interaction [5,25]. For this reason, studies investigating alternating dosing schedules have been initiated [10,26-28]. In three previously reported phase I/II clinical studies (total: n = 12) erlotinib and O-desmethyl erlotinib concentrations were determined on day 22 of the treatment cycle, after a wash-out period of five days [10,26,27]. Within these studies, erlotinib on days 2 through 16 was combined with docetaxel or pemetrexed on the first day of a 21 day treatment cycle. In one out of twelve patients the plasma samples showed erlotinib levels far above the IC_{50} , namely 372 ng/mL. Therefore, we collected pharmacokinetic data of a larger cohort of patients (n=34) treated with alternating erlotinib plus chemotherapy to confirm whether pharmacodynamic separation was achieved using a five day wash-out period for erlotinib. To our knowledge, this is the first study in which correlation between nadir erlotinib plasma concentrations and treatment response was assessed in an alternating treatment schedule.

Four patients (11.8%) treated with alternating erlotinib showed erlotinib concentrations above the IC_{50} after a five day erlotinib free interval. The erlotinib free interval incorporated in the alternating schedule included four times the mean elimination half life of erlotinib (36 hours). Consequently, only approximately 6% of the maximum plasma concentration (C_{max}) was expected to be remaining after the wash-out period. Accordingly, only patients with extremely high maximum plasma concentrations ($C_{max} > 3000$ ng/mL) are expected to have nadir erlotinib concentrations > 183 ng/mL. Hence, it is remarkable that almost 12% of the patients in our study showed nadir erlotinib concentrations > 183 ng/mL. No pharmacokinetic interactions between erlotinib and pemetrexed or docetaxel have been described or are to be expected and low metabolic clearance of erlotinib in those patients could, therefore, not be contributed to concomitant medication [29,30]. This may indicate that an erlotinib wash-out period of five days does not ensure that nadir concentrations < 183 ng/mL are reached in all patients.

In the combination therapy arm, a significant relationship was observed between increased median nadir erlotinib concentrations and better response during alternating therapy. Moreover, the highest nadir erlotinib concentrations (>183 ng/mL) during combination therapy were found in patients with stable disease or partial response and not in patients with progressive disease. Additionally, the patient whom did not use an erlotinib free period before chemotherapy

R1
R2
R3
R4
R5
R6
R7
R8
R9
R10
R11
R12
R13
R14
R15
R16
R17
R18
R19
R20
R21
R22
R23
R24
R25
R26
R27
R28
R29
R30
R31
R32
R33
R34
R35
R36
R37
R38
R39

R1
R2
R3
R4
R5
R6
R7
R8
R9
R10
R11
R12
R13
R14
R15
R16
R17
R18
R19
R20
R21
R22
R23
R24
R25
R26
R27
R28
R29
R30
R31
R32
R33
R34
R35
R36
R37
R38
R39

administration showed stable disease as early clinical response. This is remarkable, since it was expected that nadir plasma concentrations at the moment of chemotherapy administration would be inversely related to early clinical response [7]. Possibly, the erlotinib plasma concentration at which the interaction takes place is much higher than the IC_{50} of 183 ng/mL. Moreover, it might be that erlotinib concentrations at the tumor site were much lower than in plasma and did not exceed the IC_{50} at moment of chemotherapy administration. Alternatively, response may have been primarily due to the erlotinib and less due to the chemotherapy. Then patients with the highest erlotinib concentrations and/or sensitizing EGFR mutations are expected to have a better clinical response [18]. However, no EGFR mutations were observed in the five patients with high erlotinib concentrations during combination therapy (EGFR-mutation negative (n=2), EGFR-mutation unknown (n=3)).

In contrast with the negative results of concurrently administered combination therapies with EGFR tyrosine kinase inhibitors (e.g. erlotinib) and chemotherapy, concurrent use of cetuximab (EGFR targeted antibody) and chemotherapy showed a more favorable response than chemotherapy alone in clinical studies [31-34]. Moreover, combination therapy of cetuximab and chemotherapy (oxaliplatin, irinotecan and fluorouracil) has been approved for use in metastasized colorectal cancer with wild-type KRAS and EGFR over-expression and locally advanced or metastasized squamous cell carcinoma of head and neck [31,33,34]. Given the similar mechanism of action of cetuximab and erlotinib (G1 phase cell cycle arrest via inhibition of downstream EGFR signaling) and the cell cycle-dependent pharmacological activity of the chemotherapeutic agents, a cell cycle-specific antagonism might also be expected with these drug combinations [35]. However, no interference of cetuximab and chemotherapy was observed [31-34]. This is in line with our results, since we did not observe negative interactions of erlotinib plasma concentrations exceeding the IC_{50} level for EGFR inhibition in combination with chemotherapy. Therefore, more pharmacokinetic/pharmacodynamic studies on EGFR-targeted therapies in combination with chemotherapy are needed to assess whether pharmacodynamic separation is required to increase treatment efficacy.

Twenty-eight patients (87.5%) reached therapeutic erlotinib concentrations during erlotinib monotherapy. The extremely low plasma concentrations of the remainder of patients may indicate nonadherence rather than pharmacokinetic variability or pharmacokinetic drug-drug interactions. As expected, a tendency towards higher erlotinib trough concentrations with better response was observed in patients treated with erlotinib monotherapy. Soulieres *et al.* reported a significant relationship between overall survival and trough concentrations in 89 patients [3]. Possibly, the statistical power of our study was too limited to identify a significant association with only 2 patients with a partial response. In addition, in our study no association between erlotinib trough levels and occurrence of severe non-hematological toxicities was observed. This result is comparable to previously reported studies in which severity of rash and diarrhea did not correlate with erlotinib exposure (area under the curve (AUC)) and large overlap was observed for AUCs of

patients with and without toxicities [4,36]. This implies that dose-adjustments based on toxicities may lead to subtherapeutic erlotinib exposure. Therefore, further prospective clinical studies are needed to assess whether erlotinib trough levels are prognostic for clinical response in erlotinib therapy and, subsequently, to define a therapeutic target level.

Conclusion

In 12% of patients erlotinib concentrations after a five day erlotinib-free interval exceeded the IC_{50} of erlotinib (183 ng/mL). However, these relatively high erlotinib concentrations before chemotherapy administration were not associated with decreased treatment responses. Thus, more studies on alternating erlotinib and chemotherapy therapies are warranted to establish the optimal dosing schedule and to assess whether pharmacodynamic separation is required for adequate clinical responses.

Erlotinib trough concentrations during monotherapy were not significantly associated with better treatment response or with increased severe toxicity. Therefore, prospective clinical studies should be initiated to assess whether erlotinib trough levels are prognostic for clinical response in erlotinib therapy.

R1
R2
R3
R4
R5
R6
R7
R8
R9
R10
R11
R12
R13
R14
R15
R16
R17
R18
R19
R20
R21
R22
R23
R24
R25
R26
R27
R28
R29
R30
R31
R32
R33
R34
R35
R36
R37
R38
R39

R1
R2
R3
R4
R5
R6
R7
R8
R9
R10
R11
R12
R13
R14
R15
R16
R17
R18
R19
R20
R21
R22
R23
R24
R25
R26
R27
R28
R29
R30
R31
R32
R33
R34
R35
R36
R37
R38
R39

References

1. Thomas F, Rochaix P, White-Koning M et al. Population pharmacokinetics of erlotinib and its pharmacokinetic/pharmacodynamic relationships in head and neck squamous cell carcinoma. *Eur J Cancer* 2009; 45: 2316-23.
2. Hidalgo M, Siu LL, Nemunaitis J et al. Phase I and pharmacologic study of OSI-774, an epidermal growth factor receptor tyrosine kinase inhibitor, in patients with advanced solid malignancies. *J Clin Oncol* 2001; 19: 3267-79.
3. Soulieres D, Senzer NN, Vokes EE et al. Multicenter phase II study of erlotinib, an oral epidermal growth factor receptor tyrosine kinase inhibitor, in patients with recurrent or metastatic squamous cell cancer of the head and neck. *J Clin Oncol* 2004; 22: 77-85.
4. Lu JF, Eppler SM, Wolf J et al. Clinical pharmacokinetics of erlotinib in patients with solid tumors and exposure-safety relationship in patients with non-small cell lung cancer. *Clin Pharmacol Ther* 2006; 80: 136-45.
5. Li T, Ling YH, Goldman ID et al. Schedule-dependent cytotoxic synergism of pemetrexed and erlotinib in human non-small cell lung cancer cells. *Clin Cancer Res* 2007; 13: 3413-22.
6. Mahaffey CM, Davies AM, Lara PN, Jr. et al. Schedule-dependent apoptosis in K-ras mutant non-small-cell lung cancer cell lines treated with docetaxel and erlotinib: rationale for pharmacodynamic separation. *Clin Lung Cancer* 2007; 8: 548-53.
7. Davies AM, Ho C, Lara PN, Jr. et al. Pharmacodynamic separation of epidermal growth factor receptor tyrosine kinase inhibitors and chemotherapy in non-small-cell lung cancer. *Clin Lung Cancer* 2006; 7: 385-8.
8. Aerts JG, Codrington H, Burgers JA et al. A randomized phase II study comparing erlotinib (E) versus E alternating with chemotherapy in relapsed non-small cell lung cancer (NSCLC) patients. The NVALT10 study. (Abstract LBA29). *Ann Oncol* 2012; 23: IXe21.
9. Carey KD, Garton AJ, Romero MS et al. Kinetic analysis of epidermal growth factor receptor somatic mutant proteins shows increased sensitivity to the epidermal growth factor receptor tyrosine kinase inhibitor, erlotinib. *Cancer Res* 2006; 66: 8163-71.
10. Sangha R, Davies AM, Lara PN, Jr. et al. Intercalated Erlotinib-Docetaxel Dosing Schedules Designed to Achieve Pharmacodynamic Separation: Results of a Phase I/II Trial. *J Thorac Oncol* 2011; 6: 2112-9.
11. Lankheet NAG, Schaake EE, Rosing H et al. Quantitative determination of erlotinib and O-desmethyl erlotinib in human EDTA plasma and lung tumor tissue. *Bioanalysis* 4[21]. 2012.
12. European Medicines Agency (EMA). Tarceva: EPAR - Scientific Discussion. Available at: http://www.ema.europa.eu/docs/en_GB/document_library/EPAR_-_Scientific_Discussion/human/000618/WC500033991.pdf. Date accessed July 17, 2012. 2-11-2005.
13. Wang Y, Chia YL, Nedelman J et al. A therapeutic drug monitoring algorithm for refining the imatinib trough level obtained at different sampling times. *Ther Drug Monit* 2009; 31: 579-84.
14. Duong S, Leung M. Should the concomitant use of erlotinib and acid-reducing agents be avoided? The drug interaction between erlotinib and acid-reducing agents. *J Oncol Pharm Pract* 2011; 17: 448-52.
15. Scheffler M, Di GP, Doroshyenko O et al. Clinical pharmacokinetics of tyrosine kinase inhibitors: focus on 4-anilinoquinazolines. *Clin Pharmacokinet* 2011; 50: 371-403.
16. Hughes AN, O'Brien ME, Petty WJ et al. Overcoming CYP1A1/1A2 mediated induction of metabolism by escalating erlotinib dose in current smokers. *J Clin Oncol* 2009; 27: 1220-6.
17. Metro G, Chiari R, Duranti S et al. Impact of specific mutant KRAS on clinical outcome of EGFR-TKI-treated advanced non-small cell lung cancer patients with an EGFR wild type genotype. *Lung Cancer* 2012; 87: 81-6.

18. Tokumo M, Toyooka S, Kiura K et al. The relationship between epidermal growth factor receptor mutations and clinicopathologic features in non-small cell lung cancers. *Clin Cancer Res* 2005; 11: 1167-73.
19. Eberhard DA, Johnson BE, Amler LC et al. Mutations in the epidermal growth factor receptor and in KRAS are predictive and prognostic indicators in patients with non-small-cell lung cancer treated with chemotherapy alone and in combination with erlotinib. *J Clin Oncol* 2005; 23: 5900-9.
20. Gatzemeier U, Pluzanska A, Szczesna A et al. Phase III study of erlotinib in combination with cisplatin and gemcitabine in advanced non-small-cell lung cancer: the Tarceva Lung Cancer Investigation Trial. *J Clin Oncol* 2007; 25: 1545-52.
21. Giaccone G, Herbst RS, Manegold C et al. Gefitinib in combination with gemcitabine and cisplatin in advanced non-small-cell lung cancer: a phase III trial--INTACT 1. *J Clin Oncol* 2004; 22: 777-84.
22. Herbst RS, Giaccone G, Schiller JH et al. Gefitinib in combination with paclitaxel and carboplatin in advanced non-small-cell lung cancer: a phase III trial--INTACT 2. *J Clin Oncol* 2004; 22: 785-94.
23. Herbst RS, Prager D, Hermann R et al. TRIBUTE: a phase III trial of erlotinib hydrochloride (OSI-774) combined with carboplatin and paclitaxel chemotherapy in advanced non-small-cell lung cancer. *J Clin Oncol* 2005; 23: 5892-9.
24. Gandara DR, Gumerlock PH. Epidermal growth factor receptor tyrosine kinase inhibitors plus chemotherapy: case closed or is the jury still out? *J Clin Oncol* 2005; 23: 5856-8.
25. Cheng H, An SJ, Zhang XC et al. In vitro sequence-dependent synergism between paclitaxel and gefitinib in human lung cancer cell lines. *Cancer Chemother Pharmacol* 2011; 67: 637-46.
26. Davies AM, Hesketh PJ, Beckett LA et al. Pharmacodynamic separation of erlotinib and docetaxel (DOC) in advanced non-small cell lung cancer (NSCLC): overcoming hypothesized antagonism. *J.Clin.Oncol.* 25[18S]. 2007.
27. Davies AM, Ho C, Beckett L et al. Alternating erlotinib in combination with pemetrexed: phase I schedules designed to achieve pharmacodynamic separation. *J Thorac Oncol* 2009; 4: 862-8.
28. Mok TS, Wu YL, Yu CJ et al. Randomized, placebo-controlled, phase II study of sequential erlotinib and chemotherapy as first-line treatment for advanced non-small-cell lung cancer. *J Clin Oncol* 2009; 27: 5080-7.
29. Kraut EH, Rhoades C, Zhang Y et al. Phase I and pharmacokinetic study of erlotinib (OSI-774) in combination with docetaxel in squamous cell carcinoma of the head and neck (SSCHN). *Cancer Chemother Pharmacol* 2011; 67: 579-86.
30. Ranson M, Reck M, Anthony A et al. Erlotinib in combination with pemetrexed for patients with advanced non-small-cell lung cancer (NSCLC): a phase I dose-finding study. *Ann Oncol* 2010; 21: 2233-9.
31. Bokemeyer C, Cutsem EV, Rougier P et al. Addition of cetuximab to chemotherapy as first-line treatment for KRAS wild-type metastatic colorectal cancer: pooled analysis of the CRYSTAL and OPUS randomised clinical trials. *Eur J Cancer* 2012; 48: 1466-75.
32. Herbst RS, Kelly K, Chansky K et al. Phase II selection design trial of concurrent chemotherapy and cetuximab versus chemotherapy followed by cetuximab in advanced-stage non-small-cell lung cancer: Southwest Oncology Group study S0342. *J Clin Oncol* 2010; 28: 4747-54.
33. Vermorken JB, Mesia R, Rivera F et al. Platinum-based chemotherapy plus cetuximab in head and neck cancer. *N Engl J Med* 2008; 359: 1116-27.
34. Van Cutsem E, Kohne CH, Lang I et al. Cetuximab plus irinotecan, fluorouracil, and leucovorin as first-line treatment for metastatic colorectal cancer: updated analysis of overall survival according to tumor KRAS and BRAF mutation status. *J Clin Oncol* 2011; 29: 2011-9.
35. Gandara DR, Davies AM, Gautschi O et al. Epidermal growth factor receptor inhibitors plus chemotherapy in non-small-cell lung cancer: biologic rationale for combination strategies. *Clin Lung Cancer* 2007; 8 Suppl 2: S61-S67.

R1
R2
R3
R4
R5
R6
R7
R8
R9
R10
R11
R12
R13
R14
R15
R16
R17
R18
R19
R20
R21
R22
R23
R24
R25
R26
R27
R28
R29
R30
R31
R32
R33
R34
R35
R36
R37
R38
R39

R1
R2
R3
R4
R5
R6
R7
R8
R9
R10
R11
R12
R13
R14
R15
R16
R17
R18
R19
R20
R21
R22
R23
R24
R25
R26
R27
R28
R29
R30
R31
R32
R33
R34
R35
R36
R37
R38
R39

36. Mita AC, Papadopoulos K, de Jonge MJ et al. Erlotinib 'dosing-to-rash': a phase II inpatient dose escalation and pharmacologic study of erlotinib in previously treated advanced non-small cell lung cancer. *Br J Cancer* 2011; 105: 938-44.

Chapter 2.5

Intratumoral and serum concentrations of erlotinib in non-small cell lung cancer patients treated with neo-adjuvant erlotinib therapy

*Nienke A.G. Lankheet

*Eva E. Schaake

Renée van Pel

Jacques A. Burgers

Jos H. Beijnen

Alwin D.R. Huitema

Houke Klomp

*both authors contributed equally to the manuscript

Submitted for publication



R1
R2
R3
R4
R5
R6
R7
R8
R9
R10
R11
R12
R13
R14
R15
R16
R17
R18
R19
R20
R21
R22
R23
R24
R25
R26
R27
R28
R29
R30
R31
R32
R33
R34
R35
R36
R37
R38
R39

Abstract

Introduction. Tumors might not benefit optimal from systemic therapy as minimal effective therapeutic levels are not reached within the tumor. However, since erlotinib has been studied mainly in the adjuvant or palliative setting, little is known about erlotinib tumor penetration. Therefore, the purpose of this exploratory study was to investigate lung tumor tissue concentrations after neoadjuvant erlotinib therapy for non-small cell lung cancer (NSCLC).

Methods. Patients were treated with preoperative erlotinib (150 mg QD for 3 weeks) up to 48 hours prior to surgery. Plasma samples were collected during treatment. Surgical resection involved radical resection of the lung tumor and tumor biopsies were frozen directly after surgery. Erlotinib and O-desmethyl erlotinib concentrations in lung tumor tissue and plasma were determined using high performance liquid chromatography coupled to tandem mass spectrometry (HPLC-MS/MS).

Results. Thirteen evaluable patients were included. The mean plasma and lung tumor tissue erlotinib levels were 1222 ng/mL (standard deviation (SD) 678) and 149 ng/g (SD 153), respectively. In two individual patients, erlotinib and O-desmethyl erlotinib concentrations in lung tumor tissue were detectable up to 13 days and 7 days after erlotinib intake, respectively. Mean erlotinib tissue concentrations extrapolated to a time point directly after intake of erlotinib were approximated at >200 ng/g tissue.

Conclusion. No strong accumulation of erlotinib in lung tumor tissue was observed. Nevertheless, extrapolated intratumoral concentrations during erlotinib therapy were above the IC_{50} of wild-type EGFR of 183 ng/mL.

Introduction

The epidermal growth factor receptor tyrosine kinase inhibitor (EGFR-TKI) erlotinib is a targeted agent which has been approved for second-line treatment of patients with non-small cell lung cancer (NSCLC) regardless of the EGFR genotype and in first-line treatment of patients with activating mutations in EGFR [1]. It has been established that the magnitude of the pharmacological effect of erlotinib (EGFR tyrosine kinase inhibition) in vitro is concentration dependent [2]. Moreover, in clinical studies trough plasma concentrations of erlotinib and its metabolite (O-desmethyl erlotinib) have been correlated with treatment outcome [3]. The minimal effective therapeutic level of erlotinib for wild-type EGFR, as deduced from half maximal inhibitory concentration (IC_{50}) in vitro after correction for plasma protein binding, is 183 ng/mL [2,4].

Penetration of drugs into tumor tissue may be affected by different factors including tumor vascularisation, plasma protein binding, drug efflux pumps in tumor cells and intratumoral drug metabolism [5-9]. Tumors might not benefit optimal from systemic therapy as minimal effective therapeutic levels are not reached within the tumor [2]. However, since erlotinib has been studied mainly in the adjuvant or palliative setting, little is known about tumor penetration in NSCLC [10-12]. Due to tumor location and risk of complications it is difficult to obtain sufficient tumor samples of NSCLC patients. However, the introduction of neo-adjuvant treatments with targeted agents enables to get insights into tissue penetration of erlotinib, as the remainder of the tumor is available for analysis after neo-adjuvant therapy combined with a radical resection. Therefore, an explorative and observational substudy was performed within a multicenter phase II study of neo-adjuvant erlotinib monotherapy in early stage NSCLC patients [13]. The purpose of this study was to investigate erlotinib plasma and lung tumor tissue concentrations after neo-adjuvant erlotinib therapy.

Patients and Methods

The explorative study was part of a larger multicentre phase II trial performed in the Netherlands [13]. The study protocol was approved by the institutional review board and was conducted in accordance with guidelines established by the World Medical Association Declaration of Helsinki.

Eligibility

Patients with newly diagnosed resectable NSCLC, over 18 years of age could enter the study. Patients had to have an Eastern Cooperative Oncology Group (ECOG) performance status of 0 or 1, and were neither pregnant nor breastfeeding. The diagnosis had to be histologically proven or highly probable (> 95%) based on medical history, chest X-ray, spiral CT-scan, bronchoscopy and [18F]-FDG-Positron Emission Tomography (PET scan). Exclusion criteria were continuation of smoking, prior malignancy treated with HER1/EGFR inhibitors, ophthalmologic abnormalities

R1
R2
R3
R4
R5
R6
R7
R8
R9
R10
R11
R12
R13
R14
R15
R16
R17
R18
R19
R20
R21
R22
R23
R24
R25
R26
R27
R28
R29
R30
R31
R32
R33
R34
R35
R36
R37
R38
R39

R1 (especially those causing dry eyes) or the unwillingness or inability to wear glasses instead of
R2 contact lenses during treatment.

R3 For a patient to be evaluable in the present explorative study, a tissue sample collected after
R4 erlotinib therapy and data on the duration of the interval between last intake of erlotinib and
R5 surgery should be available.

R6 *Treatment schedule*

R7 Preoperative treatment consisted of 150 mg erlotinib once daily for a period of at least 3 weeks.
R8 Surgical resection involved a radical resection of the tumor, preferably by lobectomy, and regional
R9 lymph nodes (at least three hilar and three mediastinal lymph node stations). Erlotinib was taken
R10 up to 48 hours prior to surgery to prevent bleeding complications at resection. The treatment
R11 duration of three weeks was chosen to fit within the 'preoperative window'; not extending the time
R12 to surgery and using the workup time to study the effect of erlotinib in early stage NSCLC.

R13 *Pharmacokinetics of tumor tissue and plasma*

R14 Plasma samples were collected in the afternoon between day 14 and 21 of the erlotinib treatment.
R15 Patients were instructed to take erlotinib at dinnertime, therefore, time between intake and blood
R16 collection was between 18 and 24 hours. All plasma samples were snap frozen and stored at -80 °C
R17 until analysis. The resection specimens were snap frozen at -80 °C directly after surgery until
R18 further processing. A 50 to 150 mg specimen from each resected tumor was weighted accurately.
R19 Subsequently, an accurate volume of 500 to 1500 µL of drug-free human plasma was added to
R20 obtain samples containing 100 mg of lung tumor tissue per 1.0 mL of plasma. Lung tumor tissue
R21 homogenate was prepared by using a rotor/stator-type mechanical homogenizer for minimal
R22 three minutes per sample. Tissue homogenate samples were stored at nominally -20 °C until use.
R23 Bio-analytical quantification of erlotinib and its metabolite, O-desmethyl erlotinib, in plasma and
R24 lung tumor tissue homogenates was performed by using high-performance liquid chromatography
R25 and detection with tandem mass spectrometry (HPLC-MS/MS) as described before [14]. The lower
R26 limit of detection (LLOD) of the assay for both compounds was established at 2.0 ng/mL and 20
R27 ng/g in plasma and tumor tissue samples, respectively.

R28 *Statistical analyses*

R29 Descriptive statistics were used to summarize the patient characteristics and erlotinib and
R30 O-desmethyl erlotinib plasma and tissue concentrations.

Results

Patients' characteristics

Between December 2006 and November 2010 tumor tissue and plasma samples were collected from 14 NSCLC patients receiving preoperative erlotinib. One patient was not evaluable, since no data on period of erlotinib treatment was available. Clinical and histological data for all evaluable patients are listed in Table 1.

Table 1. Patient characteristics

Characteristic	Number of patients (%) or Mean (SD)*	
	Total (n=13)	
Gender		
	Male	5 (38.5)
	Female	8 (61.5)
Age (y)*		63 (8.0)
Tumor histology		
	Adenocarcinoma	10 (76.9)
	Squamous cell carcinoma	1 (7.7)
	Large cell carcinoma	2 (15.4)
Smoking status		
	Never smoker	3 (23.1)
	Former smoker	7 (53.8)
	Current smoker	3 (23.1)
KRAS mutation status		
	Negative	11 (84.6)
	Positive	2 (15.4)
EGFR mutation status		
	Negative	10 (76.9)
	Positive	3 (23.1)
Mean erlotinib treatment duration (days)*		21 (3.6)
Mean period between erlotinib treatment and surgery (days)*		7 (4.9)

Plasma and tumor tissue concentrations

An overview of measured erlotinib and N-desmethyl erlotinib concentrations in plasma and lung tumor tissue samples of all patients is presented in Table 2. Mean plasma trough erlotinib and O-desmethyl erlotinib levels were 1222 ng/mL (SD 678) and 179 ng/mL (SD 140), respectively. Mean lung tumor tissue levels of erlotinib were 149 ng/g (SD 153). The mean number of days between last erlotinib administration and surgery was 7 days with a wide range from 1 to 19 days. In one patient erlotinib tissue concentrations were quantifiable up to at least 13 days after intake of erlotinib. In two patients erlotinib tissue concentrations (collected 7 and 19 days after intake of erlotinib) were below the lower limit of detection (20 ng/g). O-desmethyl erlotinib concentrations were quantifiable in three patients up to 7 days after intake of erlotinib with mean lung tumor tissue concentrations of 79.2 ng/g (SD 78.0).

Table 2. Erlotinib and O-desmethyl erlotinib concentrations in plasma and lung tumor tissue

Patient	Plasma concentration (ng/mL)		Tumor tissue concentration (ng/g)		Time Period between last erlotinib intake and surgery (days)
	Erlotinib	O-desmethyl erlotinib	Erlotinib	O-desmethyl erlotinib	
1	1407	161	105	<LLD	6
2	NA	NA	441	57.7	3
3	701	85.7	<LLD	<LLD	7
4	993	83.0	450	187	1
5	2521	520	52.0	<LLD	3
6	1189	162	77.6	<LLD	4
7	633	52.6	33.2	<LLD	10
8	862	126	48.3	<LLD	3
9	782	76.0	197	46.9	7
10	NA	NA	<LLD	<LLD	19
11	2440	348	84.8	<LLD	4
12	596	212	110	<LLD	13
13	1321	141	39.3	<LLD	7
Mean	1222	179	149	79.2	7
SD	678	140	153	78.0	4.9

LLD, lower limit of detection; NA, not available; SD, standard deviation.

Figure 1 shows the erlotinib and O-desmethyl erlotinib lung tumor tissue concentrations versus the interval between erlotinib administration and tumor tissue collection during surgery. Using extrapolation, lung tumor tissue concentrations during erlotinib therapy (time after erlotinib intake = 0 days) were approximated at 200 ng/g tissue, which is above the IC50 level of wild-type EGFR inhibition by erlotinib (183 ng/mL).

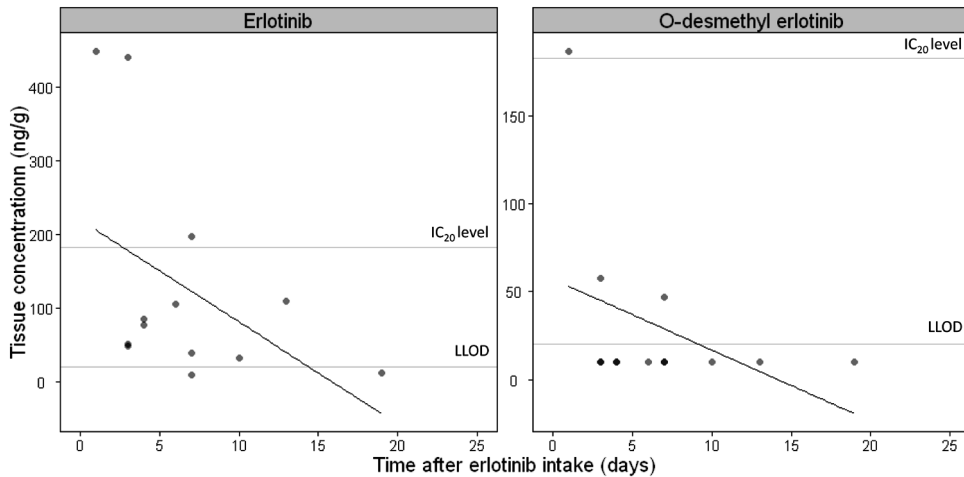


Figure 1. Tumor tissue concentrations of erlotinib and O-desmethyl erlotinib of patients (n=13) plotted against the interval between erlotinib administration and tumor tissue collection during surgery. The horizontal grey lines represent the lower limit of detection (20 ng/g) and the minimal effective therapeutic concentration (IC_{50} level:183 ng/mL). The black line represents the linear regression line with correlation coefficients (R) of -0.481 ($p=0.096$) and -0.451 ($p=0.122$) for erlotinib and O-desmethyl erlotinib, respectively.

Discussion

This exploratory study was conducted to investigate erlotinib concentrations in lung tumor tissue after neo-adjuvant erlotinib therapy. Only limited data of erlotinib and O-desmethyl erlotinib concentrations in lung tumor tissue were available thus far. A large drawback of assessment of intratumoral drug concentrations is the availability of only one tissue sample per patient per time point [15,16]. Therefore, it is not possible to investigate changes in tumor levels over time. In previously reported studies of erlotinib and gefitinib, lung tumor tissue was obtained during tyrosine kinase inhibitor (TKI) treatment [10-12]. In our observational study, however, treatment with erlotinib was interrupted at least 48 hours before surgery to decrease risk of surgical bleeding complications. Therefore, we could measure erlotinib and O-desmethyl erlotinib concentrations in lung tumor tissue samples that were collected at different time points up to 19 days after administration of erlotinib.

Available data concerning TKI levels in lung tumor tissue, including the data of the present study, showed wide variability. Variability in tumor tissue concentrations could be due to a wide variability in TKI plasma levels. The observed plasma concentrations and corresponding inter-patient variability within our study were comparable to previously reported trough plasma concentrations by Hidalgo et al. (1200 ng/mL (\pm SD 620)) [3]. Moreover, no correlation between trough plasma levels and tumor tissue concentrations could be established, taking into account the time point of tissue collection. Therefore, observed variability could probably be contributed

R1
R2
R3
R4
R5
R6
R7
R8
R9
R10
R11
R12
R13
R14
R15
R16
R17
R18
R19
R20
R21
R22
R23
R24
R25
R26
R27
R28
R29
R30
R31
R32
R33
R34
R35
R36
R37
R38
R39

R1 to large heterogeneity of tumor tissue samples. Tumors exist of different types of cells and, thereof,
R2 vital tissue is supposed to have a better blood supply than non-vital tissue (fibrotic and necrotic
R3 tissue). It is unclear what the effect on erlotinib concentration is when the resection sample
R4 remains with erlotinib non-sensitive cells after neo-adjuvant therapy. Within one tumor, therefore,
R5 areas with different concentrations of drugs might exist [9]. When only a small part of the tumor is
R6 used for drug concentration measurement, the processed part of the tumor could strongly affect
R7 the measured concentrations. Additionally, contamination of tissue samples with blood clots can
R8 affect measured intratumoral TKI levels as was experienced in the study of Lassman et al [15]. In our
R9 study no blood clots were observed in tumor samples, however, tumor heterogeneity of samples
R10 could not be ruled out as this is inherent to tumor tissue analysis [17].

R11 A part of the lung tumor tissue samples showed undetectable amounts of erlotinib (15.4%)
R12 and O-desmethyl erlotinib (76.9%). However, the lower limit of detection of our assay for erlotinib
R13 and O-desemethyl erlotinib in tissue samples (20 ng/g) was far below the minimal effective
R14 therapeutic level of erlotinib for wild-type EGFR (183 ng/mL) [2,4]. Therefore, exact quantification
R15 of concentrations below 20 ng/g was not supposed to be clinically relevant.

R16 The means of detectable lung tumor tissue concentrations were 179 ng/g (SD 140) and 79.2
R17 ng/g (SD 78.0) for erlotinib and O-desmethyl erlotinib, respectively. In two individual patients,
R18 erlotinib and O-desmethyl erlotinib concentrations in lung tumor tissue were detectable up to
R19 13 days and 7 days, respectively. Due to the observational setting, tissue collection occurred at
R20 various time points. Therefore, direct comparison of erlotinib and O-desmethyl erlotinib tissue
R21 concentrations between patients within our study and with previously reported data was not
R22 possible. For this reason, lung tumor tissue concentrations were extrapolated to a time point
R23 directly after intake of erlotinib and estimated at >200 ng/g tissue. This estimated concentration
R24 was lower than the concentrations measured in a previous study including 3 patients with NSCLC
R25 and 1 patient with laryngeal cancer treated with erlotinib (150 mg QD for 9 days). In these tumors,
R26 resected within 90 minutes after erlotinib intake, mean erlotinib and O-desmethyl erlotinib tumor
R27 concentrations were 1185 ng/g (range 94.0 - 3028) and 160 ng/g (range 125 - 184), respectively
R28 [12,18]. The discrepancy between the observed intratumoral concentrations in both studies could
R29 probably be explained by the small patient number and high inter-patient variability.

R30 In our study no indication for accumulation of erlotinib in lung tumor tissue was observed,
R31 which was consistent with reported data (tissue to plasma ratio's (n=4) of 0.05 - 1.61 and 0.88 -
R32 1.30 for erlotinib and O-desmethyl erlotinib, respectively) [12,18]. In contrast, for gefitinib, another
R33 EGFR-TKI, lung tumor concentrations during gefitinib therapy in 23 patients with NSCLC were
R34 40-fold elevated compared to plasma concentrations which suggested that gefitinib strongly
R35 accumulated in lung tumor tissue [10]. Since physicochemical properties of gefitinib and erlotinib
R36 are similar, this difference remains unexplained. Possibly, this could be due to interaction with drug
R37 efflux pumps P-glycoprotein (P-gp) or Breast Cancer Resistance Protein (BCRP) in tumor cells for
R38 which erlotinib is a substrate [6,19,20] or due to metabolism of erlotinib by CYP1A1/1A2 within lung
R39

tumor tissue [7,21]. Nevertheless, the mean erlotinib lung tumor tissue concentration extrapolated to a time point directly after intake of erlotinib was >200 ng/g tissue, which exceeds the IC50 level of wild-type EGFR inhibition by erlotinib (183 ng/mL). This indicates that even without tissue accumulation, therapeutic levels of erlotinib are reached within lung tumors.

Conclusion

Erlotinib and O-desmethyl erlotinib concentrations in lung tumor tissue were detectable up to 13 days and 7 days after drug intake, respectively. The extrapolated tumor tissue concentration of approximately 200 ng/g were much lower than the mean plasma concentrations of 1222 ng/mL, thus, no strong accumulation of erlotinib in tumor tissue was observed. Nevertheless, extrapolation of tumor tissue concentrations assumed that intratumoral erlotinib concentrations during erlotinib therapy were above the minimal effective therapeutic concentration of 183 ng/mL.

R1
R2
R3
R4
R5
R6
R7
R8
R9
R10
R11
R12
R13
R14
R15
R16
R17
R18
R19
R20
R21
R22
R23
R24
R25
R26
R27
R28
R29
R30
R31
R32
R33
R34
R35
R36
R37
R38
R39

R1
R2
R3
R4
R5
R6
R7
R8
R9
R10
R11
R12
R13
R14
R15
R16
R17
R18
R19
R20
R21
R22
R23
R24
R25
R26
R27
R28
R29
R30
R31
R32
R33
R34
R35
R36
R37
R38
R39

References

1. Thomas F, Rochaix P, White-Koning M et al. Population pharmacokinetics of erlotinib and its pharmacokinetic/pharmacodynamic relationships in head and neck squamous cell carcinoma. *Eur J Cancer* 2009; 45: 2316-23.
2. Carey KD, Garton AJ, Romero MS et al. Kinetic analysis of epidermal growth factor receptor somatic mutant proteins shows increased sensitivity to the epidermal growth factor receptor tyrosine kinase inhibitor, erlotinib. *Cancer Res* 2006; 66: 8163-71.
3. Hidalgo M, Siu LL, Nemunaitis J et al. Phase I and pharmacologic study of OSI-774, an epidermal growth factor receptor tyrosine kinase inhibitor, in patients with advanced solid malignancies. *J Clin Oncol* 2001; 19: 3267-79.
4. Sangha R, Davies AM, Lara PN, Jr. et al. Intercalated Erlotinib-Docetaxel Dosing Schedules Designed to Achieve Pharmacodynamic Separation: Results of a Phase I/II Trial. *J Thorac Oncol* 2011; 6: 2112-9.
5. Bergan T, Engeset A, Olszewski W. Does serum protein binding inhibit tissue penetration of antibiotics? *Rev Infect Dis* 1987; 9: 713-8.
6. de Vries NA, Buckle T, Zhao J et al. Restricted brain penetration of the tyrosine kinase inhibitor erlotinib due to the drug transporters P-gp and BCRP. *Invest New Drugs* 2012; 30: 443-9.
7. Gharavi N, El-Kadi AO. Expression of cytochrome P450 in lung tumor. *Curr Drug Metab* 2004; 5: 203-10.
8. Gottesman MM. Mechanisms of cancer drug resistance. *Annu Rev Med* 2002; 53: 615-27.
9. Graves EE, Maity A, Le QT. The tumor microenvironment in non-small-cell lung cancer. *Semin Radiat Oncol* 2010; 20: 156-63.
10. Haura EB, Sommers E, Song L et al. A pilot study of preoperative gefitinib for early-stage lung cancer to assess intratumor drug concentration and pathways mediating primary resistance. *J Thorac Oncol* 2010; 5: 1806-14.
11. McKillop D, Partridge EA, Kemp JV et al. Tumor penetration of gefitinib (Iressa), an epidermal growth factor receptor tyrosine kinase inhibitor. *Mol Cancer Ther* 2005; 4: 641-9.
12. Petty WJ, Dragnev KH, Memoli VA et al. Epidermal growth factor receptor tyrosine kinase inhibition represses cyclin D1 in aerodigestive tract cancers. *Clin Cancer Res* 2004; 10: 7547-54.
13. Schaake EE, Kappers I, Codrington HE et al. Tumor Response and Toxicity of Neoadjuvant Erlotinib in Patients With Early-Stage Non-Small-Cell Lung Cancer. *J Clin Oncol* 2012; Epub July 2012.
14. Lankheet NAG, Schaake EE, Rosing H et al. Quantitative determination of erlotinib and O-desmethyl erlotinib in human EDTA plasma and lung tumor tissue. *Bioanalysis* 4[21]. 2012.
15. Lassman AB, Rossi MR, Raizer JJ et al. Molecular study of malignant gliomas treated with epidermal growth factor receptor inhibitors: tissue analysis from North American Brain Tumor Consortium Trials 01-03 and 00-01. *Clin Cancer Res* 2005; 11: 7841-50.
16. Reck M, Hermes A, Tan EH et al. Tissue sampling in lung cancer: a review in light of the MERIT experience. *Lung Cancer* 2011; 74: 1-6.
17. Pitz MW, Desai A, Grossman SA et al. Tissue concentration of systemically administered antineoplastic agents in human brain tumors. *J Neurooncol* 2011; 104: 629-38.
18. European Medicines Agency (EMA). Tarceva: EPAR - Scientific Discussion. Available at: http://www.ema.europa.eu/docs/en_GB/document_library/EPAR_-_Scientific_Discussion/human/000618/WC500033991.pdf. Date accessed July 17, 2012. 2005.

19. Marchetti S, de Vries NA, Buckle T et al. Effect of the ATP-binding cassette drug transporters ABCB1, ABCG2, and ABCC2 on erlotinib hydrochloride (Tarceva) disposition in in vitro and in vivo pharmacokinetic studies employing Bcrp1^{-/-}/Mdr1a/1b^{-/-} (triple-knockout) and wild-type mice. *Mol Cancer Ther* 2008; 7: 2280-7.
20. Wang XK, Fu LW. Interaction of tyrosine kinase inhibitors with the MDR- related ABC transporter proteins. *Curr Drug Metab* 2010; 11: 618-28.
21. Hughes AN, O'Brien ME, Petty WJ et al. Overcoming CYP1A1/1A2 mediated induction of metabolism by escalating erlotinib dose in current smokers. *J Clin Oncol* 2009; 27: 1220-6.

R1
R2
R3
R4
R5
R6
R7
R8
R9
R10
R11
R12
R13
R14
R15
R16
R17
R18
R19
R20
R21
R22
R23
R24
R25
R26
R27
R28
R29
R30
R31
R32
R33
R34
R35
R36
R37
R38
R39



Conclusions and perspectives



R1
R2
R3
R4
R5
R6
R7
R8
R9
R10
R11
R12
R13
R14
R15
R16
R17
R18
R19
R20
R21
R22
R23
R24
R25
R26
R27
R28
R29
R30
R31
R32
R33
R34
R35
R36
R37
R38
R39

Conclusion and perspectives

The aim of the studies described in this thesis was to develop bio-analytical assays to quantify tyrosine kinase inhibitors (TKIs) in different biological matrices, and to apply these assays to clinical studies for optimal use of these promising new agents. In this chapter these aims are evaluated and the results are discussed. In addition, the results of the presented studies are put in a broader perspective and some approaches for future research are proposed.

Bio-analytical aspects

Availability of adequate compound specific bio-analytical methods is pivotal in determination of drug exposure in cancer patients. High-performance liquid chromatography coupled to tandem mass-spectrometry (HPLC-MS/MS) is the gold standard analytical method for pharmacokinetic (PK) analysis in clinical trials and therapeutic drug monitoring (TDM).

To support large (pre)clinical studies it is useful to develop very sensitive bio-analytical assays that are optimized to quantify a single TKI (with its active metabolite). However, to support routine pharmacokinetically guided dosing in individual patients, it is useful to have a method available in which small batches of samples with various TKIs can be quantified in a single analytical run. The applicability of the method for simultaneous quantification of eight TKIs in plasma for routine TDM purposes has been demonstrated. The used chromatographic system was suitable for quantification of analytes with a wide range in polarity and may, therefore, also allow inclusion of newly developed TKIs. Moreover, for the assay of sunitinib in plasma a shorter analytical run with a strongly reduced set of calibration standards (three concentration levels) and validation samples (one concentration level) has proven to be interchangeable with the conventional extended analytical run composition. Thus, for cases of TDM that require a fast turnaround time, it has been established that the time-saving analytical run composition can give adequate results of this assay within a much shorter time frame.

Compared to venous blood collection to obtain plasma samples, a more patient-friendly technique to collect patient samples for TDM is dried blood spot (DBS) sampling by means of a simple finger prick. This technique has several advantages over the classic way of performing TDM, allowing self-sampling in non-hospital based settings and less complicated logistics and sample storage. Therefore, we have developed a method for the quantitative analysis of sunitinib and N-desethyl sunitinib in DBS using pretreated DBS paper cards to prevent conversion of sunitinib in its metabolite during drying of the blood spot. However, the quality of patient DBS samples was highly variable due to spot inhomogeneity and the influence of volume of blood spotted on the paper card. Therefore, no correlation between sunitinib and N-desethyl sunitinib trough concentrations in paired patient plasma and DBS samples was observed. Hence, we concluded that patient self-sampling by means of a finger prick using these pretreated DBS paper cards is not feasible for accurate trough level determinations of sunitinib and N-desethyl sunitinib. However,

R1
R2
R3
R4
R5
R6
R7
R8
R9
R10
R11
R12
R13
R14
R15
R16
R17
R18
R19
R20
R21
R22
R23
R24
R25
R26
R27
R28
R29
R30
R31
R32
R33
R34
R35
R36
R37
R38
R39

R1 since DBS sampling remains an attractive, patient-friendly alternative for venous sampling for TDM
R2 purposes, further investigations are recommended to enable clinical use of DBS sampling of these
R3 compounds.

R4 Systemic exposure to TKIs can be investigated using plasma samples. However, assessment
R5 of the local exposure to TKIs is important to gain knowledge about drug uptake at the site of
R6 action or adverse reaction. We demonstrated clinical applicability of a method for quantification
R7 of sunitinib and its active metabolite in sweat in order to assess local skin exposure of sunitinib
R8 and its active metabolite. In addition, a method measuring tissue erlotinib concentrations in lung
R9 tumor resections of patients treated with neo-adjuvant erlotinib has been developed and applied.
R10 Complementary to analysis of TKI plasma concentrations, in the near future, tissue concentration
R11 analysis may be increasingly used to determine the distribution of targeted anticancer drugs into
R12 their target tissues. However, inconsistency between extraction recovery of the drug in calibration
R13 samples and patient samples remains one of the major challenges of tissue and sweat patch
R14 analysis.

R15 ***Pharmacological aspects***

R16 For several TKIs, relationships between plasma concentrations and treatment efficacy or toxicity
R17 have been described. Pharmacokinetic variability (both inter-patient and intra-patient) may,
R18 therefore, have important clinical consequences. Hence, better understanding of factors that
R19 contribute to variability in drug exposure, as for instance drug interactions with co-medication,
R20 patient non-compliance (for example due to drug-related toxicity), and variability in oral drug
R21 availability or metabolic clearance, could support optimization of TKI therapy.

R22 ***Drug-drug interactions***

R23 TKIs are extensively metabolized by cytochrome P450 (CYP) enzymes and, therefore, a risk
R24 of considerable variation in drug exposure when administered concomitantly with strong
R25 inducers or inhibitors of CYP enzymes exists. In our observational study, it was clearly shown that
R26 concomitantly administered CYP3A4 enzyme inducers, such as phenytoin and carbamazepine,
R27 decreased imatinib trough concentrations. In one patient, even a doubling of the daily imatinib
R28 dose was not sufficient to overcome the effect of CYP3A4 induction by carbamazepine. Moreover,
R29 the CYP1A enzyme inducing effect of cigarette smoking was correlated to a substantial decrease
R30 of erlotinib concentrations. Concomitant use of proton pump inhibitors, which increase gastric pH,
R31 led to decreased oral bioavailability of erlotinib. Since multiple factors affect the plasma exposure
R32 of TKIs and the magnitude of effect of drug-drug interactions on TKI plasma exposure is not easily
R33 predictable, monitoring of TKI plasma levels could give an indication of systemic exposure.

R34 Besides pharmacokinetic drug-drug interactions, also pharmacodynamic drug-drug
R35 interactions have been mentioned regarding TKIs. Erlotinib can negatively influence treatment
R36 outcome in a combination schedule with chemotherapeutics as erlotinib induces G1-phase
R37
R38
R39

cell cycle arrest, which may interfere with cell cycle-dependent toxicity of chemotherapeutic agents. For this reason, intermittent dosing schedules with a wash-out period for erlotinib have been introduced for combination therapy regimens. However, in contrast to expectations, erlotinib concentrations above the IC50 for wildtype-EGFR inhibition at the day of chemotherapy administration were not associated with decreased treatment efficacy. This implies that further exploration of the mechanism behind the pharmacodynamic interaction in relation to erlotinib plasma or tissue exposure is required to establish the clinical consequences of this drug-drug interaction.

Toxicities

Despite the fact that TKIs are targeted against tumor cells, toxicity of healthy cells during TKI treatment has shown to be inevitable. Moreover, severe toxicities may lead to unavoidable dose modifications or dose interruptions of TKIs, which have a negative impact on treatment efficacy. Thus far, no clear cut-off plasma levels for toxicity have been established for TKIs in humans. Therefore, further exploration of toxicity in relation to systemic and local TKI exposure is warranted. In our observational study, no difference was observed between mean trough TKI plasma concentrations of patients with or without toxicities. In addition, no association between erlotinib trough concentrations and occurrence of severe non-hematological toxicities was observed in the phase II study. Hence, toxicities also occurred at subtherapeutic concentrations. This implies that dose-adjustments based on toxicities may lead to subtherapeutic TKI exposure. Therefore, further prospective clinical studies are needed to assess whether TKI trough plasma concentrations are prognostic for clinical response in TKI therapy and, subsequently, to define a therapeutic window of for TKI concentrations in plasma.

The clinically most relevant side effect of sunitinib aside diarrhea and fatigue is Hand-Foot Syndrome (HFS). It would be unlikely that HFS was only correlated with systemic exposure to sunitinib, since previous studies have indicated that occurrence of skin toxicity was not always accompanied by occurrence of other adverse events of sunitinib. In a retrospective patient cohort, patients experienced more severe HFS in summer time compared to other seasons. Prospectively, a tendency was seen towards higher levels of total drug in sweat of patients with more severe HFS. Therefore, further exploration of determinants of sunitinib sweat secretion and seasonal variation in relation to development of skin toxicities in a larger cohort of patients is justified. If the hypothesis that aggravation of skin toxicities is caused by the secretion of sunitinib in sweat can be substantiated, skin toxicity due to sweat secretion could possibly be limited by preventive measures for hyperhidrosis in future.

R1
R2
R3
R4
R5
R6
R7
R8
R9
R10
R11
R12
R13
R14
R15
R16
R17
R18
R19
R20
R21
R22
R23
R24
R25
R26
R27
R28
R29
R30
R31
R32
R33
R34
R35
R36
R37
R38
R39

R1
R2
R3
R4
R5
R6
R7
R8
R9
R10
R11
R12
R13
R14
R15
R16
R17
R18
R19
R20
R21
R22
R23
R24
R25
R26
R27
R28
R29
R30
R31
R32
R33
R34
R35
R36
R37
R38
R39

Therapeutic drug monitoring

Dosing to toxicity is an approach for treatment individualization that has dominated cancer treatment for decades as it was reasoned that increasing the dose of an anticancer drug in patients who lack toxicity might increase the likelihood of treatment efficacy. However, since the toxicity of some newly developed targeted agents is minimal, dosing to toxicity would not be necessary to achieve adequate drug exposure in all patients. Therefore, TDM is gaining popularity for the individualization of dosing of anticancer drugs with a considerable and unpredictable inter-patient variability in pharmacokinetics. In addition, the oral administration of newly developed targeted agents also entails the possibility of considerable variation in drug exposure due to patient non-compliance (for example due to drug-related toxicity), drug interactions with co-medication and variability in oral drug availability. Large inter-individual variability in systemic exposure in combination with the positive exposure-efficacy relationship and low therapeutic index, form a rationale for individualized dosing of TKIs.

In our unselected outpatient population, wide inter-patient variability of TKI trough plasma concentrations was observed and, moreover, almost half of the trough plasma concentrations in this population appeared to be subtherapeutic with a risk of treatment failure or development of drug resistance. It was not possible to predict which patients were at risk of subtherapeutic plasma concentrations based on patient- or medication related factors. This indicated that therapeutic drug monitoring (TDM) is paramount and should be fully implemented in routine cancer care to identify patients that are in need of individual adjusted dosages.

As a proof of concept for TDM of one of the TKIs, sunitinib, a pharmacokinetic pilot study was performed to investigate the safety and feasibility of the pharmacokinetically guided dosing strategy. At the standard dose of 37.5 mg, more than half of the patients did not reach target total trough concentrations of sunitinib after 14 days of treatment and, therefore, needed pharmacokinetically guided dose adjustments to increase the probability of a therapeutic effect. Of these patients, 60% experienced clinically relevant adverse events after dose increase, which were, however, manageable by subsequent dose reductions. Ultimately, a third of the patients that did not reach target total sunitinib trough levels at standard doses, did potentially benefit from the implemented dose escalations without causing additional toxicities. In these patients, the mean dose was increased by 47%. This implies that pharmacokinetically guided sunitinib dose escalations rather than fixed doses would contribute to optimization of therapy in a considerable part of the patients.

TKI tissue concentrations may be even more informative than trough plasma concentrations. However, tissue sampling is highly invasive compared to blood sampling and, therefore, it would be worthwhile to investigate which factors affect the blood and tissue distribution of TKIs and to determine whether monitoring of plasma concentrations adequately reflects TKI concentrations reached within tumor tissue.

Future perspectives

The ultimate proof that reaching adequate drug exposure increases treatment efficacy of TKIs remains to be awaited. Moreover, much effort will be needed to define target trough plasma concentrations that are associated with therapeutic efficacy for each drug in different tumor types. To acquire distinct clinical evidence for the benefit of individualized TDM compared with that from a standard fixed dose of TKIs, prospective randomized clinical trials should be performed. Moreover, to allow a rational design of TDM studies, it is paramount to gain further insights in inter- and intra-patient variability in pharmacokinetics in order to select accurate and specific time points for PK sampling of each TKI. For newly developed TKIs, clinical trials with overall survival as study end point can be initiated. However, for TKIs currently used in clinical practice, there may be resistance to initiate new large prospective trials. In these cases, routinely performed determinations of TKI trough plasma concentrations could increase insights in factors that affect variability in drug exposure. In addition, retrospective analyses of these data could contribute to the determination of target plasma concentrations and, moreover, a subsequent clinical trial with progression free survival, metabolic responses (by positron emission tomography (PET)) or reaching target plasma concentrations (as described in Chapter 2.2) as surrogate end point could give an indication of the benefits of TDM.

In some cases, TKI therapy fails due to induction of therapy resistance leading to reduced or transient responses. Dose escalations may help when the effect of a TKI is reduced. Moreover, combining different TKIs or addition of a TKI to conventional chemotherapies may possibly lead to a better and faster therapy response in order to prevent development of resistance. This hypothesis is based on the assumption that more complete responses prevent cells to escape from therapy, analogous to the development of resistance in case of incomplete response to antimicrobial agents. To make individual dosing of TKIs within combination regimens possible in future, firstly therapeutic plasma concentrations should be defined in monotherapy regimens and, secondly, pharmacokinetic studies should be initiated to determine the optimal dose and schedule of combination therapies and the effect of drug-drug interactions on TKI plasma concentrations.

In conclusion, bio-analytical methods to quantify TKIs in plasma, sweat and tissue were successfully developed and validated. Moreover, the application of these bio-analytical methods to clinical studies provided profound insights in the pharmacokinetics of TKIs. The insights and hypotheses generated in this thesis could be used as starting point for further research on the pharmacological aspects of TKIs and to further optimize TKI treatment.

R1
R2
R3
R4
R5
R6
R7
R8
R9
R10
R11
R12
R13
R14
R15
R16
R17
R18
R19
R20
R21
R22
R23
R24
R25
R26
R27
R28
R29
R30
R31
R32
R33
R34
R35
R36
R37
R38
R39





Summary

Nederlandse samenvatting

Dankwoord

Curriculum Vitae

List of publications





Summary

Cancer is the second leading cause of death worldwide, after cardiovascular diseases. Tyrosine kinase inhibitors (TKIs) are recently developed targeted anticancer agents that target molecular abnormalities which are unique to cancer cells and, hence, provide an anticancer therapy that is potentially less toxic to healthy cells. To date, eleven TKIs (eg. erlotinib, sunitinib and imatinib) have been approved for use in several types of cancer. However, considerable inter-individual variability in safety and efficacy has been observed for all TKIs. Therefore, there is an urgent need to gain insight into factors that are involved in this large interindividual variability for optimal use of these important novel drugs. One of the most important determinants for safety and efficacy of TKIs may be systemic drug exposure (pharmacokinetics). A better understanding of efficacy and toxicity in relation to plasma exposure might contribute to optimization and individualization of TKI therapy. To be able to study the pharmacokinetics of TKIs, quantitative analysis of TKIs and their metabolites in plasma and other biological matrices is pivotal.

In this thesis the development of bio-analytical assays to quantify TKIs in different biological matrices using high performance liquid chromatography coupled to mass spectrometry (HPLC-MS/MS) is described. In addition, these assays were applied to clinical studies to further increase the knowledge of clinical pharmacology of TKIs.

Bioanalysis of Tyrosine Kinase Inhibitors

The development of six bio-analytical methods to quantify the exposure of TKIs and their active metabolites in different biological matrices is described in **Chapter 1**. The development and validation of a fast and accurate method for simultaneous determination of the TKIs dasatinib, erlotinib, gefitinib, imatinib, lapatinib, nilotinib, sorafenib and sunitinib in human plasma using HPLC-MS/MS to support pharmacokinetic (PK)-guided dosing in individual patients is described in **Chapter 1.1**. This method was validated over clinically relevant concentration ranges for all analytes. Moreover, this method was successfully applied for routine therapeutic drug monitoring (TDM) in patients treated with these TKIs.

In **Chapter 1.2** a sensitive and specific method for determination of sunitinib and its active metabolite (N-desethyl sunitinib) is described. To accelerate the turnaround time of this assay for TDM purposes, the results of 25 analytical runs with full calibration and quality control sample set (8 calibrators and 3 levels of quality control samples) were compared with the results of analyses with a strongly reduced set (3 calibrators and 1 quality control sample). The method with the rapid turnaround time gave adequate results with a non-clinically relevant mean absolute difference of only -0.66 ng/mL compared to the conventional extended analytical run. Thus, both methods were found to be interchangeable for TDM purposes.

Dried blood spot (DBS) sampling for TDM enables sample collection by means of a simple fingerprick instead of plasma collection using venapuncture. In **Chapter 1.3** the development

R1
R2
R3
R4
R5
R6
R7
R8
R9
R10
R11
R12
R13
R14
R15
R16
R17
R18
R19
R20
R21
R22
R23
R24
R25
R26
R27
R28
R29
R30
R31
R32
R33
R34
R35
R36
R37
R38
R39

R1
R2
R3
R4
R5
R6
R7
R8
R9
R10
R11
R12
R13
R14
R15
R16
R17
R18
R19
R20
R21
R22
R23
R24
R25
R26
R27
R28
R29
R30
R31
R32
R33
R34
R35
R36
R37
R38
R39

of a method for determination of sunitinib and its active metabolite (N-desethyl sunitinib) in DBS is described. Since conversion of sunitinib to its N-desethyl metabolite occurred on conventional pure cellulose based DBS paper cards, these cards could only be used to quantify the sum of sunitinib and N-desethyl concentrations. On DMPK-B paper cards, impregnated with thiocyanate salts to denature catabolic enzymes, the conversion of sunitinib was blocked and, therefore, these paper cards could be used to quantify sunitinib and N-desethyl sunitinib separately. However, DBS specific method validation parameters, e.g. spotted blood volume, haematocrit level and spot homogeneity were found to strongly influence the accuracy and precision of the assay using DBS on DMPK-B cards. Additionally, when comparing sunitinib and N-desethyl sunitinib concentrations in paired plasma and DBS patient samples using DMPK-B paper cards, the two methods did not show adequate correlation making these cards unsuitable for use in clinical practice. Therefore, further research is warranted for the development of a clinically applicable DBS method for sunitinib and N-desethyl sunitinib.

To study the pathogenesis of skin toxicities in patients treated with sunitinib, the development of a method to quantify sunitinib and its metabolite in sweat is outlined in **Chapter 1.4**. Sweat samples of a patient treated with sunitinib were collected using sweat patches to determine cumulative amounts of sunitinib and metabolite. In a proof of principle experiment ranges of 76-119 and 7.9-10.5 ng/patch for cumulative secretion of sunitinib and metabolite, respectively, were found in patient samples which was within the validated ranges of the assay. Using this method, these analytes were quantified in human sweat for the first time.

In **Chapter 1.5**, the development of a sensitive and accurate method for determination of erlotinib and O-desmethyl erlotinib (OSI-420) in human plasma and lung tumor tissue is described in order to increase knowledge of lung tumor tissue and plasma levels. During method development it was a challenge to overcome mutual suppression of erlotinib and stable isotopically labelled erlotinib responses due to competition in the electrospray ionisation (ESI) process of the mass spectrometer. The internal standard concentration which showed the smallest fluctuation in response over the entire calibration range was eventually used in the validation experiments. Since tumor tissue is scarce, calibration curves in plasma were used to quantify analytes in lung tumor tissue homogenate. This method has been successfully validated and applied to determine plasma and lung tumor tissue concentrations of erlotinib and O-desmethyl erlotinib in patients with non-small cell lung cancer.

The final chapter of this section (**Chapter 1.6**) describes the development of a sensitive and accurate method for the determination of vatalanib in human EDTA plasma using HPLC-MS/MS. The method was easy to perform and has been used to determine plasma vatalanib concentrations in patients with advanced solid tumors, enrolled in a Phase I pharmacokinetic trial with the drug.

Clinical Pharmacology of Tyrosine Kinase Inhibitors

Clinical studies to further explore the efficacy and toxicity in relation to systemic and local exposure of TKIs are discussed in **Chapter 2**. An observational study in an unselected cohort of patients using TKIs for cancer treatment was performed to evaluate plasma concentrations of TKIs imatinib, erlotinib and sunitinib in routine clinical practice and to find possible factors related to subtherapeutic plasma concentrations, as outlined in **Chapter 2.1**. Almost half of the plasma concentrations in the outpatient population appeared to be subtherapeutic with a risk of treatment failure or development of drug resistance. It was not possible to predict which patients were at risk of subtherapeutic plasma concentrations based on patient- or medication related factors. Thus, TDM could play a crucial role in routine cancer care to identify patients that are in need of individual adjusted dosages.

Before large prospective clinical trials can be initiated to determine the efficacy of TDM in TKI treatment, safety and feasibility of the PK guided dosing strategy should be investigated in a pilot study. Therefore, the primary objective of the pharmacokinetic study in described in **Chapter 2.2** was to assess the safety and feasibility of PK-guided sunitinib treatment. In this study, patients were treated continuously with sunitinib 37.5 mg once daily. At day 15 and 29 of treatment, plasma trough levels of sunitinib and N-desethyl sunitinib were measured. If the total trough level (TTL) was < 50 ng/mL and the patient did not show any grade ≥ 3 toxicity, the daily sunitinib dose was increased by 12.5 mg. If the patient suffered from grade ≥ 3 toxicity, the sunitinib dose was lowered by 12.5 mg. With a median TTL of 49.5 ng/mL, target TTLs were not reached in 15 patients (52%) at the starting dose of 37.5 mg per day. In a third of the patients (17%) that did not reach target TTL at standard dose, the sunitinib dose could be increased without additional toxicity. Nine patients (31%) experienced grade ≥ 3 toxicity after PK guided dose escalation. These toxicities were manageable by dose reductions. Hence, the results justify further research to investigate the safety and therapeutic efficacy of PK guided sunitinib dosing.

Skin toxicities, such as Hand Foot Syndrome (HFS), are side effects of sunitinib with a considerable impact on quality of life. In **Chapter 2.3**, the relation between HFS and seasonal variation is investigated by determining the effect of seasonal variation and secretion of sunitinib in sweat on the development of HFS. In a retrospective cohort, patients suffered from more severe HFS during summertime (July to September) compared with the rest of the year. In a prospective study, a tendency was observed in which increasing amounts of total drug per patch were observed with increasing severity of HFS. However, no statistically significant correlation between sunitinib sweat secretion and severity of HFS could be demonstrated within our small cohort of 25 patients. Therefore, further exploration of determinants of sunitinib sweat secretion and seasonal variation in relation to development of skin toxicities in a larger cohort of patients is warranted.

In **Chapter 2.4**, a pharmacokinetic study is described of 66 patients participating in a phase II study comparing alternating dosing schedules of erlotinib and pemetrexed or docetaxel, with erlotinib monotherapy in non-small cell lung cancer (NSCLC). It was investigated (1) whether nadir

R1
R2
R3
R4
R5
R6
R7
R8
R9
R10
R11
R12
R13
R14
R15
R16
R17
R18
R19
R20
R21
R22
R23
R24
R25
R26
R27
R28
R29
R30
R31
R32
R33
R34
R35
R36
R37
R38
R39

R1
R2
R3
R4
R5
R6
R7
R8
R9
R10
R11
R12
R13
R14
R15
R16
R17
R18
R19
R20
R21
R22
R23
R24
R25
R26
R27
R28
R29
R30
R31
R32
R33
R34
R35
R36
R37
R38
R39

erlotinib plasma concentrations after an erlotinib wash-out period of five days were low enough to avoid antagonistic interactions in combination with chemotherapeutics and (2) whether trough erlotinib plasma concentrations were high enough to reach therapeutic effects during monotherapy. In 12% of patients erlotinib concentrations after the erlotinib-free interval exceeded the half minimal inhibitory concentration of erlotinib (183 ng/mL). In contrast to expectations, these relatively high erlotinib concentrations before chemotherapy administration were not associated with decreased treatment responses. Thus, more studies on alternating erlotinib and chemotherapy therapies are warranted to establish the optimal dosing schedule and to assess whether pharmacodynamic separation is required for adequate clinical responses. In addition, erlotinib trough concentrations during monotherapy were not significantly associated with better treatment response or with increased severe toxicity.

Since erlotinib has been studied mainly in the adjuvant or palliative setting, little is known about erlotinib tumor penetration. **Chapter 2.5** describes an exploratory study investigating lung tumor tissue concentrations after neo-adjuvant erlotinib therapy for NSCLC. Plasma samples were collected during erlotinib therapy and lung tumor tissue was collected during surgical resection of the tumor at least 48 hours after stop of erlotinib therapy. Mean erlotinib tissue concentrations extrapolated to a time point directly after intake of erlotinib were estimated at >200 ng/g tissue and plasma concentrations were around 1222 ng/mL. Therefore, no strong accumulation of erlotinib in lung tumor tissue was observed. Nevertheless, extrapolated intratumoral concentrations during erlotinib therapy were above the IC_{50} of wild-type EGFR of 183 ng/mL. This indicates that even without tissue accumulation, therapeutic levels of erlotinib are reached within lung tumors.

In conclusion, bio-analytical methods to quantify TKIs in plasma, sweat and tissue were successfully developed, validated and applied to clinical studies. However, regarding the patient-friendly method using dried blood spots to quantify sunitinib and N-desethyl sunitinib levels further research is warranted, since this method is not applicable in clinical practice yet. Monitoring the exposure of TKIs in individual patients in various circumstances as for instance in daily practice, in case of specific toxicities, in case of drug-drug interactions and during PK guided dosing regimens provided insights in the clinical pharmacology of TKIs. Pharmacokinetically adjusted dosing might probably contribute to individualization and optimization of TKI therapy by increasing treatment efficacy and limiting treatment related toxicities. However, more research should be performed to determine the relationships between exposure and efficacy/toxicity of TKIs and to define TKI target trough plasma concentrations.

Samenvatting

Kanker is wereldwijd de op één na meest voorkomende doodsoorzaak, na hart- en vaat ziekten. Tyrosinekinaseremmers (TKI's) zijn recentelijk ontwikkelde doelgerichte antikankergeneesmiddelen. TKI's hebben unieke afwijkingen in kankercellen als doelwit. Daarom vormen deze middelen een effectieve behandeling die weinig schadelijk is voor gezonde cellen. Tot nu toe zijn elf TKI's (bijv. erlotinib, sunitinib, imatinib) beschikbaar voor toepassing bij verschillende soorten kanker. Echter, voor alle TKI's worden grote verschillen tussen patiënten waargenomen in de veiligheid en werkzaamheid. Voor optimaal gebruik van deze belangrijke nieuwe middelen is er daarom dringend behoefte aan verbeterd inzicht in de oorzaken van deze grote verschillen tussen patiënten. Eén van de meest belangrijke oorzaken voor het verschil in veiligheid en werkzaamheid is waarschijnlijk de blootstelling van het lichaam aan de geneesmiddelen. Deze blootstelling, oftewel de concentratie van het geneesmiddel in het lichaam (bijv. in bloedplasma), wordt ook wel farmacokinetiek genoemd. Een beter inzicht in de blootstelling in relatie tot werkzaamheid en bijwerkingen van TKI's kan mogelijk bijdragen aan het optimaliseren en individualiseren van TKI therapie. Om de farmacokinetiek van TKI's te kunnen bestuderen, is bepaling van concentraties van TKI's en hun metabolieten (afbraakproducten) in plasma en andere lichaamsvloeistoffen en/of -weefsels essentieel.

In dit proefschrift wordt de ontwikkeling van bioanalytische methoden voor het meten van concentraties van TKI's in verschillende lichaamsvloeistoffen en -weefsel behandeld. Voor deze methoden wordt gebruik gemaakt van vloeistof chromatografie (scheiding van mengsels van verschillende stoffen) gevolgd door massa spectrometrie (gevoelige en specifieke detectie van afzonderlijke stoffen) ook wel afgekort tot HPLC-MS/MS. Daarnaast worden deze methoden toegepast in klinische onderzoeken om de kennis van de klinische farmacologie van TKI's te vergroten. Klinische farmacologie is het vakgebied dat gaat over de effecten van het geneesmiddel op het lichaam (bijv. werkzaamheid en bijwerkingen) en de effecten van het lichaam op het geneesmiddel (bijv. opname vanuit de darmen en afbraak in de lever).

Bioanalyse van tyrosine kinase remmers

De ontwikkeling van zes bioanalytische methoden voor het meten van concentraties van TKI's en hun metabolieten in het lichaam is beschreven in **Hoofdstuk 1**. De ontwikkeling en validatie van een snelle en accurate methode voor gelijktijdige bepaling van de TKI's dasatinib, erlotinib, gefitinib, imatinib, lapatinib, nilotinib, sorafenib en sunitinib in bloedplasma wordt behandeld in **Hoofdstuk 1.1**. Deze methode is ontwikkeld over een klinisch relevante concentratiereeks voor alle acht TKI's. Bovendien is deze methode succesvol toegepast voor routinematig monitoren van TKI plasmaconcentraties met eventuele dosis aanpassingen (ook wel therapeutische drug monitoring (TDM) genoemd) bij patiënten behandeld met deze TKI's.

R1
R2
R3
R4
R5
R6
R7
R8
R9
R10
R11
R12
R13
R14
R15
R16
R17
R18
R19
R20
R21
R22
R23
R24
R25
R26
R27
R28
R29
R30
R31
R32
R33
R34
R35
R36
R37
R38
R39

R1
R2
R3
R4
R5
R6
R7
R8
R9
R10
R11
R12
R13
R14
R15
R16
R17
R18
R19
R20
R21
R22
R23
R24
R25
R26
R27
R28
R29
R30
R31
R32
R33
R34
R35
R36
R37
R38
R39

In **Hoofdstuk 1.2** wordt een gevoelige en specifieke methode voor het meten van sunitinib en zijn werkzame metabooliet (N-desethyl sunitinib) in bloedplasma beschreven. Om de tijd die nodig is voor het uitvoeren van de methode voor TDM te verkorten, werd gekeken of de methode versneld kon worden. Hiervoor werden de resultaten van 25 metingen met de gebruikelijke ijklijn en controlemonsters (8 ijkpunten en controle monsters op 3 verschillende concentraties) vergeleken met de resultaten van de metingen met een sterk ingeperkte set monsters (3 ijkpunten en 1 controle monster). De methode met de kortere meettijd gaf goede resultaten met een niet-klinisch relevant gemiddeld verschil van -0.66 ng/ml vergeleken met de methode met de langere meettijd. Daarom kunnen de beide methodes gebruikt worden voor het uitvoeren van TDM.

Het gebruik van droge bloed spots op papier (DBS) voor TDM maakt het mogelijk om bloed af te nemen met een simpele vingerprik in plaats van uit een bloedvat in de arm. In **Hoofdstuk 1.3** wordt de ontwikkeling van een methode voor het meten van de concentratie van sunitinib en zijn metabooliet (N-desethyl sunitinib) in DBS beschreven. Echter, sunitinib wordt omgezet in zijn metabooliet in DBS op gewoon (cellulose) papier. Daarom kon alleen de som van deze twee stoffen juist worden bepaald. Op een nieuwere soort DBS papier (DMPK-B papier) worden de enzymen die sunitinib omzetten geremd. Hiermee kon op dit DMPK-B papier de hoeveelheid sunitinib en metabooliet wel afzonderlijk bepaald worden. Echter, het bleek moeilijk om de concentraties in de DBS te meten met voldoende juistheid en precisie. De gemeten geneesmiddelconcentraties in de DBS worden namelijk sterk beïnvloed door de hoeveelheid bloed die is opgebracht (bloed volume), de hematocrietwaarde van de patiënt en de mate waarin het bloed verdeeld is (spot homogeniteit). Bovendien, bleek bij het vergelijken van DBS op DMPK-B papier en plasmamonsters die tegelijkertijd bij patiënten waren afgenomen dat er geen samenhang was in de daarin gemeten sunitinib concentraties. Daarom is het DMPK-B papier ongeschikt om te gebruiken voor het meten van sunitinib concentraties in bloed van patiënten. Er is dus nog verder onderzoek nodig voor het ontwikkelen van een DBS methode voor sunitinib en zijn metabooliet die bruikbaar is in de praktijk.

Om het ontstaan van bijwerkingen van de huid door sunitinib te bestuderen, is een methode ontwikkeld om sunitinib en zijn metabooliet in zweet te meten (zie **Hoofdstuk 1.4**). Zweetmonsters van een patiënt die werd behandeld met sunitinib, werden verzameld met behulp van zweetpleisters. In de pleisters, die een week waren gedragen op de bovenarm, werd de opgehoopte hoeveelheid sunitinib en metabooliet gemeten. Hiermee werd aangetoond dat sunitinib en zijn metabooliet konden worden gemeten in zweet in concentraties van 76-119 ng/pleister voor sunitinib en 7.9 – 10.5 ng/pleister voor de metabooliet. Deze concentraties lagen binnen het concentratie bereik van de analysemethode. Met behulp van deze nieuwe methode werden deze stoffen voor het eerst in zweet gemeten.

In **Hoofdstuk 1.5** is de ontwikkeling beschreven van een gevoelige methode voor het meten van erlotinib en zijn metabooliet (O-desmethyl erlotinib) in bloedplasma en in longtumorweefsel. Met deze methode kan de kennis van plasma-, en weefselconcentraties van dit geneesmiddel worden vergroot. Omdat longtumorweefsel lastig verkrijgbaar is, werden ijklijnen in plasma

gebruikt om de geneesmiddelconcentraties in longtumorweefsel te bepalen. Deze methode is succesvol getest en toegepast om plasma- en longtumorweefsel concentraties van erlotinib en O-desmethyl erlotinib te meten in patiënten met niet-kleincellige longkanker.

Het laatste hoofdstuk van dit deel (**Hoofdstuk 1.6**) beschrijft de ontwikkeling van een gevoelige methode voor het meten van vatalanib concentraties in menselijk bloedplasma met behulp van HPLC-MS/MS. Deze methode is gebruikt om plasmaconcentraties van vatalanib te meten in patiënten met solide tumoren die deelnamen aan een fase I farmacokinetische studie met dit geneesmiddel.

Klinische Farmacologie van tyrosine kinase remmers

Klinische onderzoeken om de werkzaamheid en bijwerkingen van TKI's en het verband met de blootstelling aan TKI's verder uit te zoeken, zijn beschreven in **Hoofdstuk 2**. Een observatieonderzoek werd uitgevoerd in een niet-geselecteerde groep van patiënten die TKI's gebruiken voor de behandeling van kanker. Hierin werden de plasmaconcentraties van TKI's imatinib, erlotinib en sunitinib in de dagelijkse praktijk bestudeerd. Daarnaast werd in **Hoofdstuk 2.1** ook gekeken welke factoren (bijv. gewicht, leeftijd, geslacht of combinatie met andere geneesmiddelen) mogelijk betrokken waren bij het ontstaan van te lage (niet-werkzame) TKI plasmaconcentraties. Bijna de helft van de patiënten had te lage TKI plasmaconcentraties waardoor zij het risico lopen op het falen van de behandeling of resistentie tegen de behandeling. Het was niet mogelijk om op basis van de onderzochte factoren te voorspellen welke patiënten het grootste risico hadden op te lage plasma concentraties. Daarom zou het regelmatig meten van TKI plasmaconcentraties (TDM) een belangrijke rol kunnen spelen in de behandeling met TKI's. TDM zou namelijk kunnen helpen om te bepalen welke patiënten een individuele, aangepaste dosering van de TKI nodig hebben.

Voordat grote klinische onderzoeken kunnen worden gestart naar de toegevoegde waarde van TDM in behandeling met TKI's, moeten eerst de veiligheid en haalbaarheid van het doseren op basis van plasmaconcentraties worden onderzocht in een kleine groep patiënten. Daarom was het doel van de farmacokinetische studie in **Hoofdstuk 2.2** om de veiligheid en haalbaarheid van TDM in de behandeling met sunitinib vast te stellen. In deze studie werden patiënten behandeld met een dosering van eenmaal daags 37.5 mg sunitinib. Op dag 15 en 29 van de behandeling werden plasmaconcentraties van sunitinib en zijn metaboliet gemeten. Als de totale dalconcentratie kleiner was dan 50 ng/mL en de patiënt geen last had van ernstige (graad \geq 3) bijwerkingen, dan werd de dosering verhoogd met 12.5 mg. Als de patiënt last had van ernstige (graad \geq 3) bijwerkingen, dan werd de sunitinib dosis verlaagd met 12.5 mg. Met gemiddelde dalconcentratie van 49.5 ng/mL werd bij 15 van de 29 patiënten (52%) de gewenste dalconcentratie (50 ng/mL) niet bereikt op de standaard dosering van 37.5 mg per dag. Bij een derde van de patiënten (17%) die de gewenste plasmaconcentratie niet behaalden op de standaard sunitinib dosering, kon de dosering worden verhoogd zonder extra bijwerkingen. Negen patiënten (31%) hadden ernstige (graad \geq 3) bijwerkingen na de dosisverhoging. Deze bijwerkingen waren behandelbaar door de

R1
R2
R3
R4
R5
R6
R7
R8
R9
R10
R11
R12
R13
R14
R15
R16
R17
R18
R19
R20
R21
R22
R23
R24
R25
R26
R27
R28
R29
R30
R31
R32
R33
R34
R35
R36
R37
R38
R39

R1 dosis weer te verlagen. De resultaten van dit onderzoek rechtvaardigen verder onderzoek naar de
R2 veiligheid en werkzaamheid van TDM in de behandeling met sunitinib.

R3 Bijwerkingen van de huid, zoals Hand Voet Syndroom (HFS: pijnlijke zwelling, blaren, kloven
R4 op handpalmen en voetzolen), zijn bijwerkingen van sunitinib met een aanzienlijke invloed op
R5 de kwaliteit van leven. In **Hoofdstuk 2.3** wordt de relatie tussen HFS en de verandering van
R6 seizoenen onderzocht. Hierbij werden de effecten van de verandering van de seizoenen en van
R7 de uitscheiding van sunitinib in zweet op het ontstaan van HFS bepaald. Uit gegevens die zijn
R8 verzameld uit eerdere observaties bleek dat patiënten meer last hadden van ernstig HFS tijdens
R9 de zomertijd (juli tot september) vergeleken met de rest van het jaar. Vervolgens werd een nieuwe
R10 studie opgestart. Hierin werd een trend gezien waarbij verhoogde hoeveelheden sunitinib in
R11 de zweetpleister werden gemeten bij patiënten met ernstigere klachten van HFS. Echter, er kon
R12 geen statistisch significant verband tussen sunitinib uitscheiding in zweet en de ernst van HFS
R13 worden aangetoond in de kleine patiëntengroep van 25 patiënten. Daarom is verder onderzoek
R14 naar uitscheiding van sunitinib in zweet en de verandering van de seizoenen in relatie tot de
R15 ontwikkeling van HFS vereist in een grotere groep patiënten.

R16 In **Hoofdstuk 2.4** is een farmacokinetische studie beschreven van 66 patiënten die deelnamen
R17 aan een groot fase II onderzoek. In het fase II onderzoek werden een behandeling met een
R18 combinatie van afwisselend erlotinib en chemotherapie (pemetrexed of docetaxel) vergeleken
R19 met een behandeling met alleen erlotinib in patiënten met niet-kleincellige longkanker. In de
R20 farmacokinetische substudie werd onderzocht:

- R21 - (1) of de erlotinib dal plasmaconcentraties na een erlotinib-vrije periode van 5 dagen laag
R22 genoeg waren om een negatieve geneesmiddeleninteractie in combinatie met chemotherapie
R23 te voorkomen;
- R24 - (2) of de erlotinib plasmaconcentraties tijdens de behandeling met alleen erlotinib hoog genoeg
R25 waren om werkzaam te zijn.

R26 In 12% van de patiënten waren de erlotinib concentraties na de erlotinib-vrije periode hoger
R27 dan de concentratie die nodig is voor de helft van het maximale effect van erlotinib (183 ng/mL).
R28 Tegen de verwachting in, waren deze relatief hoge erlotinib concentraties tijdens de toediening
R29 van de chemotherapie niet gerelateerd aan verminderde werkzaamheid van de behandeling. Er
R30 zijn dus meer onderzoeken nodig om het optimale doseringsschema van erlotinib in combinatie
R31 met chemotherapie vast te stellen. Bovendien moet verder worden onderzocht of gescheiden
R32 toediening van erlotinib en chemotherapie echt nodig is voor een goede werkzaamheid van
R33 de behandeling. Daarnaast waren de erlotinib plasmaconcentraties tijdens de behandeling met
R34 alleen erlotinib niet significant gerelateerd aan betere werkzaamheid of ernstigere bijwerkingen.

R35 Omdat erlotinib voornamelijk is onderzocht als adjuvante behandeling (na een operatieve
R36 verwijdering van de tumor) of palliatieve (symptoom verlichtende) behandeling is er weinig bekend
R37 over de mate waarin erlotinib doordringt in de tumor. **Hoofdstuk 2.5** beschrijft een verkennend
R38 onderzoek waarin longtumor weefselconcentraties werden gemeten na een neo-adjuvante
R39

behandeling (voorafgaand aan een operatieve verwijdering van de tumor) met erlotinib voor niet-kleincellige longkanker. Plasmamonsters werden verzameld gedurende de erlotinib behandeling. Longtumorweefsel werd verkregen tijdens de operatieve verwijdering van de longtumor minstens 48 uur na stop van de erlotinib behandeling. De gemiddelde erlotinib weefselconcentraties werden omgerekend naar een tijdstip direct na inname van erlotinib en werden geschat op >200 ng erlotinib per gram weefsel. De erlotinib plasmaconcentraties waren ongeveer 1222 ng/mL. Er werd dus geen sterke ophoping van erlotinib in longtumorweefsel waargenomen. De geschatte erlotinib concentraties in de tumor tijdens de behandeling met erlotinib waren hoger dan de concentratie die nodig is voor de helft van het maximale remmende effect van erlotinib (183 ng/mL). Dit geeft de indicatie dat werkzame erlotinib concentraties worden bereikt in longtumoren, zelfs zonder sterke ophoping van erlotinib in weefsel.

Concluderend kan worden gesteld dat bioanalytische methoden om TKI concentraties te meten in plasma, zweet en weefsel succesvol zijn ontwikkeld, getest en toegepast in klinische onderzoeken. Echter, voor de patiëntvriendelijke methode die gebruik maakt van droge bloed spots om sunitinib en zijn metaboliet te meten is nog niet bruikbaar in de praktijk. Daarom is hiernaar nog meer onderzoek nodig. Het meten van de blootstelling aan TKI's in individuele patiënten in verschillende omstandigheden (bijv. in de dagelijkse praktijk, in het geval van specifieke bijwerkingen, in het geval van geneesmiddeleninteracties en tijdens behandelingen met doseringen gebaseerd op TKI plasmaconcentraties) hebben het inzicht in de klinische farmacologie van TKI's vergroot. Doseren op basis van TKI plasmaconcentraties kan waarschijnlijk bijdragen aan het individualiseren en optimaliseren van TKI behandelingen door het verbeteren van de werkzaamheid en het beperken van bijwerkingen. Er moet echter nog meer onderzoek worden uitgevoerd om de relatie tussen blootstelling en werkzaamheid/veiligheid van TKI's vast te stellen en om voor elke TKI te bepalen wat de optimale plasmaconcentraties zijn.

R1
R2
R3
R4
R5
R6
R7
R8
R9
R10
R11
R12
R13
R14
R15
R16
R17
R18
R19
R20
R21
R22
R23
R24
R25
R26
R27
R28
R29
R30
R31
R32
R33
R34
R35
R36
R37
R38
R39



Dankwoord

Vier jaar lang leek dit moment heel ver weg, maar ik ben nu toch echt toegekomen aan het schrijven van het laatste en misschien wel meest gelezen hoofdstuk van mijn proefschrift. Vanaf september 2008 tot nu zijn er velen die er aan hebben bijgedragen dat ik mijn promotieonderzoek en dit proefschrift heb kunnen voltooien. Deze personen hebben ervoor gezorgd dat mijn promotietraject een onvergetelijke en zeer leerzame periode is geworden. Ik wil iedereen die mij op enige wijze heeft ondersteund hiervoor hartelijk bedanken. Een aantal mensen daarvan wil ik in het bijzonder bedanken.

Allereerst wil ik de patiënten bedanken voor hun vrijwillige bijdrage aan de klinische studies die zijn beschreven in dit proefschrift.

Mijn promotoren, Jos Beijnen en Jan Schellens, ik wil jullie bedanken dat ik de afgelopen jaren met veel plezier heb mogen werken binnen de inspirerende werkomgeving die jullie hebben gecreëerd binnen de onderzoeksgroep in het Slotervaartziekenhuis en Antoni van Leeuwenhoekziekenhuis. Beste Jos, iets meer dan vier jaar geleden kwam ik als stagiaire terecht in de apotheek van het Slotervaartziekenhuis. Het werd me meteen al duidelijk dat dit niet zomaar een ziekenhuisapothek was. Ik ben dan ook heel blij dat je mij de kans hebt gegeven om binnen deze apotheek het 'NIB'-project op te starten. Ik waardeer het heel erg dat ik alle vrijheid en vertrouwen heb gekregen om me bezig te houden met de verschillende projecten die vanuit de kliniek op mijn pad kwamen. Beste Jan, jou wil ik bedanken voor de snelle en kritische commentaren op mijn manuscripten. Daarnaast heb je, ondanks je zeer drukke baan, tijdens grote visites en andere besprekingen altijd de tijd genomen om je taak als opleider zeer serieus te nemen. Dit waardeer ik heel erg.

Beste Alwin, mede dankzij jou, en niet te vergeten de recruitment-activiteiten van je vrouw Jenny, ben ik als stagiaire en vervolgens als onderzoeker in het Slotervaartziekenhuis beland. Ik vraag me vaak af waar ik terecht zou zijn gekomen als ik niet bij Jenny in de openbare apotheek stage zou hebben gelopen. Maar nog vaker bedenk ik me dat ik echt heel blij ben dat het zo gelopen is. Alwin, als co-promotor stond jouw deur altijd open voor overleg. Zelfs vanaf een camping in Zuid-Frankrijk of een congres, informeerde je hoe het ervoor stond met de laatste loodjes en was je bereikbaar voor commentaar. Dat geeft aan hoe betrokken je bent bij al je onderzoekers en dat waardeer ik enorm. Jij was ook degene die altijd feilloos de lijn van mijn manuscripten en experimenten wist vast te houden. Het was heel verhelderend hoe jij in onze overleggen complexe situaties altijd weer wist te reduceren tot een overzichtelijk en oplosbaar probleem. Daarnaast heeft jouw aanstekelijke enthousiasme ervoor gezorgd dat vele obstakels werden omgezet in uitdagingen. Bedankt voor de fijne samenwerking.

Voor het ontwikkelen van de bioanalytische assays en het meten van alle patiëntenmonsters, heb ik heel veel tijd doorgebracht op het lab van de apotheek. Pas nu ik de laatste maanden voornamelijk aan het schrijven ben geweest, merk ik hoeveel ik de gezelligheid op het lab mis.

R1 Hilde, ik vind het bewonderenswaardig dat jij, ondanks dat er vele eigenwijze onderzoekers op
R2 het lab rondlopen, alles toch in goede (GLP-) banen weet te leiden. Daarnaast maakte jij altijd tijd
R3 om mee te denken over de meest uiteenlopende analyseproblemen. Ik heb dan ook veel geleerd
R4 van jouw analytische aanpak van HPLC-MS/MS-problemen. Bij het verlaten van jouw kamer had
R5 ik meestal weer een heel concreet plan met uit te voeren experimenten. Bovendien was jij ook
R6 degene die mijn analysemanuscripten zeer grondig heeft bekeken. Bedankt voor de prettige
R7 samenwerking. Abadi en Luc, bedankt dat jullie mij de eerste weken met heel veel geduld de
R8 wondere wereld van de bioanalyse hebben laten zien en ervoor hebben gezorgd dat ik daarna
R9 snel zelfstandig op het lab aan de slag kon. Bovendien kon ik altijd bij jullie en bij Bas, Matthijs en
R10 Michel terecht voor een brainstormsessie over een analyseprobleem of wanneer de MS weer eens
R11 niet deed wat hij moest doen. Bedankt voor al jullie geduld en hulp. Ik hoop dat ik jullie na al die
R12 jaren heb kunnen overtuigen dat het echt niet alleen aan mij lag dat de Quantum Ultra's weer
R13 eens kuren hadden, want uiteindelijk zijn er toch vijf assays ontwikkeld op deze apparaten! Niels, ik
R14 weet zeker dat de NIB-assay bij jou in zeer goede handen is. Nu jij het stokje van ondergetekende
R15 'NIBjes-koningin' hebt overgenomen, wil ik jou bij deze tot 'NIBjes-koning' benoemen. Heel veel
R16 succes met het uitvoeren van deze bepalingen. Joke, Lianda en Ciska bedankt voor al jullie
R17 gezelligheid op het lab. Alle gesprekken over koetjes en kalfjes hebben er voor gezorgd dat zelfs
R18 het bijvullen van pipetpuntjes nog gezellig werd. Roel, bedankt voor je hulp bij HR-, ICT-, GLP-, QA-,
R19 enzenz-gerelateerde vragen. Jouw humor en vermogen om mensen te stangen, maakten dat je
R20 bij jou altijd op je hoede moest zijn, maar zorgden ook voor heel wat vermakelijke conversaties.
R21 Denise, toen we samen het keuzevak Natural Product Research volgden had ik nooit kunnen
R22 bedenken dat wij ooit collega's zouden worden in een ziekenhuisapotheek. Bas, Dieuwke, Kees
R23 en Jan, jullie zorgden ervoor dat ik werd ingelicht als er weer een 'groen monster' voor mij was
R24 gearriveerd. Ook hebben jullie, op de dagen dat ik afwezig was, de opslag van de binnengekomen
R25 patiëntenmonsters overgenomen, waarvoor dank. Het was fijn om te weten dat ik dit met een
R26 gerust hart aan jullie over kon laten.

R27 Voor het opzetten en uitvoeren van klinische studies heb ik nauw samengewerkt met een
R28 aantal oncologen van het Antoni van Leeuwenhoekziekenhuis.

R29 Christian, jouw tomeloze enthousiasme en 'Deutsche Grundligkeit' hebben ervoor gezorgd
R30 dat we een innovatieve studie hebben kunnen doen naar de uitscheiding van sunitinib in zweet.
R31 Jouw mailtjes, waar het enthousiasme van afspatte ('das wird ja super cool!'), motiveerden enorm
R32 bij het opzetten van de zweet-assay en het uitvoeren van het onderzoek. Bedankt voor de fijne
R33 samenwerking.

R34 Sjaak, dankzij jou heb ik twee mooie projecten kunnen uitvoeren met erlotinib, waarvoor
R35 dank. Jij hebt me geïntroduceerd bij de NVALT-10 werkgroep en ervoor gezorgd dat we hier een
R36 mooie substudie konden uitvoeren. Daarnaast heb je me ook laten kennismaken met Eva, zodat
R37 we samen nog meer interessante data uit de neo-adjuvante erlotinib studie konden halen. Eva,
R38 ik vond het leuk dat jij als arts-onderzoeker veel interesse toonde in de bioanalyse en zelfs graag
R39

een keertje mee wilde kijken op het lab. Dankzij jou hadden we genoeg tumorweefsel om de assay te valideren en een mooi manuscript te kunnen schrijven. Veel succes met de rest van je manuscripten en het afronden van je proefschrift.

Neeltje, samen met jou heb ik mijn eerste interventiestudie kunnen uitvoeren. De TDM-studie sloot precies aan bij mijn promotieonderwerp en ik ben dan ook heel blij dat ik deze studie met jou heb mogen opzetten en uitvoeren. We hebben samen moeten ontdekken wat de exacte procedures voor klinische multicenter studies binnen het NKI waren. Daar heb ik veel van geleerd. Hopelijk kunnen je vervolgstudies nu zonder kinderziektes in het eCRF van start gaan. Jouw enthousiasme heeft ervoor gezorgd dat de studie een zeer snelle inclusie had, zodat ik deze nog kon opnemen in mijn proefschrift. Ook was het jou idee om een abstract voor de ASCO in te dienen. Het was een leuke en leerzame ervaring om een poster te mogen presenteren op zo'n groot congres. Heel erg bedankt voor de samenwerking en veel succes met je andere studies.

Daarnaast wil ik alle andere medisch oncologen en verpleegkundig specialisten van het NKI en het Slotervaartziekenhuis bedanken voor hun interesse in mijn onderzoek. Velen van jullie hebben direct of indirect bijgedragen aan de klinische studies. Bovendien hebben velen van jullie spiegelbepalingen van tyrosine kinase remmers bij mij aangevraagd waardoor ik mijn bepaling ook direct kon inzetten voor individuele patiëntenzorg. Dit was heel leerzaam. Henk en Sandra, bedankt voor het includeren van patiënten en het verzamelen van de sweatpatches. Emmy, jij hebt ervoor gezorgd dat de M10PKS studie in het NKI op rolletjes liep, waarvoor veel dank. Yvonne, bedankt dat jij als monitor van de M10PKS studie veel nuttige input hebt gegeven bij het implementeren van de studie en bovendien heel hard hebt gewerkt om alle data op tijd te monitoren.

Het samenwerkingsverband van het Center for Personalized Cancer Treatment (CPCT) heeft gezorgd voor een snelle inclusie en dataverwerking van de M10PKS studie. Iedereen van het CPCT wil ik daarvoor hartelijk danken. Jacqueline, Christa en Geert, bedankt voor de samenwerking en veel succes met het afronden van jullie proefschriften. Martijn Lolkema, Ron Mathijssen, Emile Voest en Stefan Sleijfer, ik wil jullie bedanken voor de snelle en nuttige commentaren op het manuscript.

Joachim Aerts, Henk Codrington, Harry Groen, Anne-Marie Dingemans, Egbert Smit en de rest van de NVALT-10 werkgroep van de Nederlandse Vereniging van Artsen voor Longziekten en Tuberculose (NVALT), ik wil jullie bedanken dat jullie de mogelijkheid hebben geboden om een farmacokinetische studie als amendement op de NVALT-10 studie uit te voeren. Otilia Dalesio and Andrew Vincent, you did a great job by matching my sample-database with the NVALT10-database and I want to thank you for making me aware of the suitability of the 'Jonckheere-Terpstra test'.

Tijdens het laatste jaar van mijn promotietraject heb ik twee enthousiaste farmaciestudenten mogen begeleiden. Sander en Lotte, ik vond het heel leuk om met jullie te mogen samenwerken. Het was erg leerzaam voor mij om jullie in te werken en te begeleiden. Bovendien heeft het ook mooie data voor dit proefschrift opgeleverd. Bedankt daarvoor. Sander, als sinterklaas wist je voor grote oproer in de keet te zorgen en dit jaar hebben we je dan ook erg gemist rond 5 december. Veel succes met de laatste loodjes van je studie. Lotte, hopelijk bevalt het je goed in Maastricht. Succes met je opleiding; binnenkort komen we elkaar daarbij vast wel eens tegen.

R1
R2
R3
R4
R5
R6
R7
R8
R9
R10
R11
R12
R13
R14
R15
R16
R17
R18
R19
R20
R21
R22
R23
R24
R25
R26
R27
R28
R29
R30
R31
R32
R33
R34
R35
R36
R37
R38
R39

R1
R2
R3
R4
R5
R6
R7
R8
R9
R10
R11
R12
R13
R14
R15
R16
R17
R18
R19
R20
R21
R22
R23
R24
R25
R26
R27
R28
R29
R30
R31
R32
R33
R34
R35
R36
R37
R38
R39

Vier jaar lang is 'de keet' mijn uitvalsbasis geweest. Hier heb ik al die tijd met heel veel plezier gewerkt. Het was fijn te weten dat je er als onderzoeker niet alleen voor stond en er altijd wel een mede-onderzoeker aanwezig was om goede resultaten of tegenslagen mee te delen. Ook de Is-het-al-vrijdag?-borrels en de zeer succesvolle taartenbakcompetitie zal ik niet snel vergeten. In mijn Slotervaart-tijd heb ik vele onderzoekers zien gaan en komen. Ron, Stijn, David, Ly, Mariska, Joost, Johannes, Carola, Claudia, Elke, Annemieke, Marie-Christine en Corine, tijdens mijn stage zaten jullie al in de keet en jullie enthousiasme heeft mij dan ook het laatste zetje gegeven om als onderzoeker aan de slag te gaan. Bas, als echte MS-expert stond jij altijd klaar met handige tips wanneer het niet helemaal wilde lukken met de API's of QU's. Dat heeft me goed op weg geholpen, veel dank daarvoor. Het werd trouwens wel heel rustig op het lab en in de keet toen jij vertrokken was... Rob, het was leuk om te zien dat jij na je vertrek naar Amersfoort ook helemaal into de NIBjes was. Jij hebt me scherp gehouden door te opperen dat je ook met een alles-in-één NIB-assay aan de slag wilde gaan. Daarnaast heeft jou enthousiasme twee mooie case reports opgeleverd waaraan ik met mijn assay een bijdrage heb mogen leveren. Coen, jou ben ik veel dank verschuldigd omdat je altijd klaar stond als R- en NONMEM-helpdesk en je me de benodigde skills hebt geleerd om mooie figuren te maken. Zonder jouw uitzonderlijke kennis van R en ggplot was dat zeker niet gelukt. Rik, mijn reismaatje in Chicago, bedankt voor de gezelligheid tijdens het congres, bij de match van de Whitesox met de heerlijke Chicagostyle hotdogs en in het vliegtuig met de welverdiende fles Cava. Iris en Susanne, het was heel leuk om met twee mede-volleyballers en spelletjesfanaten in de keet te zitten. Wanneer plannen we ons volgende potje Regenwormen? Robert en Anne-Charlotte, het was heel fijn dat jullie er achtereenvolgens voor zorgden dat er elke dag een warm welkom was bij het binnentreden van de keet. Nynke en Cynthia, veel succes met het opstarten van jullie DBS-assays; hopelijk kunnen jullie de valkuilen die ik daarbij tegenkwam een beetje omzeilen. Anita, week in, week uit, in zon en in regen hebben wij baantjes getrokken (en onze ogen goed de kost gegeven) in het Mirandabad. Zonder jou als zwemmaatje had ik het vast niet volgehouden om totaal verkleumd en met blauwe lippen toch nog de geplande baantjes uit te zwemmen. Jelte, jij bent de echte doorzetter van de keet; jij hebt lang moeten zaaien om nu artikelen te kunnen oogsten. Je kunt er trots op zijn dat 'jouw' product nu in een klinische studie kan worden toegepast. Emilia, het zal ook vast niet lang meer duren voordat 'jouw' tablet de kliniek in kan. Nalini, jouw vrolijke lach en je grote interesse in de projecten van alle onderzoekers maakten je een heel fijne collega. Jeroen, het was altijd gezellig om met jou naar het station te fietsen; wel jammer dat jij vaak de trein wel haalde en ik de deur weer voor mijn neus zag dichtgaan... Huixin, I hope you will have a great time in The Netherlands; good luck with your PhD-project. Thomas, dat jij al jaren Dr. Dorlo wordt genoemd is niet voor niets; iedereen kon al voorzien dat er een mooie carrière in de wetenschap op jou lag te wachten. Hopelijk kan jij in de toekomst kwakzalverij uitbannen en de toegankelijkheid van geneesmiddelen in derdewereldlanden verbeteren. Tine, als dierenarts tussen alle apothekers en als enige Belg in onze keet wist jij te zorgen voor een welkome afwisseling in de gespreksonderwerpen tijdens koffiepauzes en borrels. Geert, Ruud, Aarti, Bojana

en Susanne, ik vond het leuk om in mijn reservetijd nog even jullie kamergenoot in het AVL te mogen zijn. Hebben jullie inmiddels al uitgevonden wat het mysterieuze geluid is? Jolanda, ik vind het een hele eer dat ik jouw paranimf mocht zijn; nu weet ik al iets beter wat me te wachten staat op d-day. Ik weet zeker dat ik de ontelbare gezellige, gezamenlijke trein- en fietstochtjes ga missen. De spelletjesavonden moeten we natuurlijk gewoon blijven volhouden; dan hoef ik ook niet bang te zijn dat ik iets mis van wat zich in de keet afspeelt. En ik wil natuurlijk ook zien of je promotiecadeau een mooi plaatsje heeft gekregen in je (nieuwe) huis.

Nu ontbreken in dit verhaal nog de twee collega's waarmee ik de meeste tijd samen heb doorgebracht. Ellen en Wiete, als kamergenoten in de Vrouwenvleugel hebben we de afgelopen jaren lief en leed gedeeld. Daarom ben ik heel blij dat jullie mij ook op de laatste dag van mijn promotietraject willen bijstaan. Het heeft veel voor mij betekend dat ik al die tijd precies wist wat ik aan jullie had. Dankzij jullie heb ik mijn boksbal niet veel hoeven gebruiken. Alles hebben we samen kunnen bespreken: analyseproblemen, promotieperikelen, privé zaken, maar ook veel minder serieuze gespreksonderwerpen. Onze vieruurtjes zal ik zeker erg gaan missen. Elke dag was het vaste prik dat er om vier uur weer 3x 'the usual' werd besteld om vervolgens even gezellig bij te kletsen en daarna nog even een 'blokje te knallen'. Wat zullen ze bij de kiosk veel chocolademuffins overhouden als wij weg zijn... Ik weet zeker dat de afgelopen vier jaar zonder jullie echt niet zo soepel en snel voorbij zouden zijn gevlogen. We zijn alle drie vlak na elkaar begonnen en dat ik nu als eerste van de Vrouwenvleugel ga promoveren, betekent dat jullie snel zullen volgen. Heel veel succes met jullie laatste loodjes! Het gaat helemaal goed komen!

Gelukkig waren er buiten het ziekenhuis ook veel familieleden, vrienden, huisgenoten en teamgenoten met wie ik leuke activiteiten kon ondernemen om het werk even helemaal te vergeten. Promoveren is geen standaardbaan en het zal voor jullie vast niet gemakkelijk zijn geweest om een voorstelling te maken van de onderzoekswereld. Ik hoop dat mijn Nederlandse samenvatting kan helpen om een beetje een beeld te krijgen van wat ik de afgelopen jaren heb gedaan.

Heleen, al 28 jaar kennen we elkaar en in die jaren zijn we elkaar nooit uit het oog verloren. We hebben zoveel samen meegemaakt dat het altijd als vanouds is als we elkaar weer eens zien. Dat we allebei voor studie en werk in Amsterdam terecht kwamen, heeft ervoor gezorgd dat we heel regelmatig gezellige eet-dates konden plannen. En nu we allebei tegelijk begonnen zijn aan onze opleiding, hebben we vast weer veel ervaringen om met elkaar te delen. Marlies, op de allereerste dag van de studie farmacie (meer dan 10 jaar geleden alweer!!) heb ik jouw leren kennen en de hele rest van de studie hebben we samen doorlopen. Alle leuke uitjes (musicals, uitwaaien aan het strand, winkelen, koninginnennacht vieren, kanoën, een weekje Mallorca enz.) hebben ervoor gezorgd dat ik me weer kon opladen voor een werkweek. Ik hoop dat we dit nog heel lang kunnen doorzetten! Willeke en Willemijn, ook jullie hebben altijd veel interesse getoond voor mijn onderzoek. Wanneer plannen we weer een high tea om gezellig bij te kletsen? Loes en Nihan, met jullie heb ik vele jaren doorgebracht in villa Bdd. Bedankt voor de fijne tijd samen!

R1
R2
R3
R4
R5
R6
R7
R8
R9
R10
R11
R12
R13
R14
R15
R16
R17
R18
R19
R20
R21
R22
R23
R24
R25
R26
R27
R28
R29
R30
R31
R32
R33
R34
R35
R36
R37
R38
R39

Loes, we hebben zoveel gemeen: dezelfde roots, hetzelfde vakgebied, dezelfde stageplekken, dezelfde sportvereniging en ook nog hetzelfde huis... Dat gaf genoeg gespreksstof voor de gezellige bijna dagelijkse deuropeningsgesprekken, die ik heel erg ga missen als we beiden villa Bdd gaan verlaten. Trouwens, al die heerlijke brownies en stroopwafels van jou kwamen altijd precies op het moment dat ik het heel erg nodig had! Bedankt voor al je steun; ik ben heel erg blij met jou als huisgenootje!

Volleyballen was dé manier om hoofd even helemaal leeg te maken en volleybal had ik ook echt nodig om energie op te doen om er de volgende werkdag weer vol enthousiasme tegenaan te kunnen. Teamgenootjes en trainer, afgelopen jaar hebben jullie veel begrip getoond voor het feit dat ik heel druk was met werk en dus soms moest afhaken bij trainingen, veel dank daarvoor. Laura, ik wil je bedanken dat jij als oud-teamgenootje wilde helpen om mijn ontwerp voor de omslag van mijn proefschrift helemaal technisch uit te werken. Hij is echt precies geworden zoals ik wilde!

Bert en Tom, 'kleine' broertjes, nu jullie dit boekje in jullie handen hebben, weten jullie waar ik me al die tijd zo druk voor heb gemaakt. Het afgelopen jaar hebben we elkaar veel te weinig gezien en nu ik in het oosten van het land ga werken, gaan we daar zeker verandering in brengen. In alle telefoongesprekken hebben jullie veel interesse getoond in mijn onderzoek en werd het duidelijk dat jullie je zelfs een beetje zorgen maakten over hoe druk ik het had. Dat heb ik erg gewaardeerd, maar ik zou zeggen: 'Dat werkende leven staat jullie binnenkort ook te wachten, dus geniet nu nog maar even van het studentenleven!'

Papa en mama, de laatste alinea van dit dankwoord is voor jullie. Jullie zijn de belangrijkste mensen in mijn leven. De brede interesse die jullie mij van jongs af aan hebben meegegeven, heeft zeker een bijdrage geleverd in de afronding van mijn studie en dit promotieonderzoek. Jullie hebben altijd veel interesse getoond in mijn onderzoek en erg jullie best gedaan om te begrijpen wat ik allemaal deed. Bedankt voor jullie liefde en onvoorwaardelijke steun bij alles wat ik heb gedaan en bij alle keuzes die ik heb gemaakt.

Nienke
Utrecht 2013

Curriculum Vitae



Nienke Lankheet werd geboren op 27 april 1984 te Haaksbergen. In 2002 behaalde zij haar VWO-diploma aan Scholengemeenschap Het Assink te Haaksbergen. Aansluitend werd begonnen aan de studie Farmacie aan de Universiteit Utrecht. In augustus 2005 behaalde zij bachelordiploma. Ter afsluiting van de masteropleiding, werd een wetenschappelijke stage verricht op de afdeling 'Biomedical Research' van Numico Research B.V. te Wageningen. Hier heeft zij gewerkt aan een in vitro onderzoek naar het moduleren van immuunresponsen tegen respiratoir syncytiaal virus (RSV) met behulp van oligosacchariden. In augustus 2008 werd het masterdiploma Farmacie (met profilering 'Meervoudige ziektebeelden') behaald. Direct na haar studie, in september 2008, begon zij in de Apotheek van het Slotervaartziekenhuis en het Nederlands Kanker Instituut te Amsterdam aan het promotieonderzoek dat is beschreven in dit proefschrift. Het onderzoek werd uitgevoerd onder begeleiding van Prof.dr. J.H. Beijnen en Prof.dr. J.H.M. Schellens, en co-promotor Dr. A.D.R. Huitema. Naast het promotieonderzoek werd tevens de opleiding tot klinisch farmacoloog gevolgd. Sinds januari 2013 is zij werkzaam als ziekenhuisapotheker in opleiding in het UMC St. Radboud te Nijmegen en het TweeSteden ziekenhuis te Tilburg.

Nienke Lankheet was born on April 27th 1984 in Haaksbergen, The Netherlands. In 2002 she finished secondary school at 'Scholengemeenschap Het Assink' in Haaksbergen. Thereafter, she started studying Pharmaceutical Sciences at Utrecht University. In August 2005 she received her Bachelor's degree. During the Master's programme a scientific internship was performed at de Department of Biomedical Research of Numico Research B.V. in Wageningen, The Netherlands. Here she worked at a research project to investigate the modulation of immune responses to respiratory syncytial virus (RSV) by oligosaccharides in vitro. In August 2008 she obtained the Master's degree in Pharmacy (with specialization 'Pharmaceutical care'). Immediately after graduation, in September 2008, she started with the PhD project described in this thesis at the Department of Pharmacy & Pharmacology of Slotervaart Hospital and The Netherlands Cancer Institute in Amsterdam, The Netherlands. This research project was supervised by Prof.dr. J.H. Beijnen, Prof.dr. J.H.M. Schellens and joint-supervisor Dr. A.D.R. Huitema. Simultaneously with the PhD project she started a traineeship in Clinical Pharmacology. Since January 2013 she started working as a trainee Hospital Pharmacist at the University Medical Center St. Radboud in Nijmegen and the TweeSteden Hospital in Tilburg, The Netherlands.

R1
R2
R3
R4
R5
R6
R7
R8
R9
R10
R11
R12
R13
R14
R15
R16
R17
R18
R19
R20
R21
R22
R23
R24
R25
R26
R27
R28
R29
R30
R31
R32
R33
R34
R35
R36
R37
R38
R39



List of publications

Lankheet NA, Steeghs N, Rosing H, Schellens JH, Beijnen JH, Huitema ADR. Quantification of sunitinib and N-desethyl sunitinib in human EDTA plasma by liquid chromatography coupled with electrospray ionization tandem mass spectrometry: validation and application in routine therapeutic drug monitoring. *Therapeutic Drug Monitoring*, in press.

Lankheet N, Schaake E, Rosing H, Burgers J, Schellens J, Beijnen J, Huitema A. Quantitative determination of erlotinib and O-desmethyl erlotinib in human EDTA plasma and lung tumor tissue. *Bioanalysis*. 2012 Nov;4(21):2563-77.

Lankheet NA, Hillebrand MJ, Rosing H, Schellens JH, Beijnen JH, Huitema AD. Method development and validation for the quantification of dasatinib, erlotinib, gefitinib, imatinib, lapatinib, nilotinib, sorafenib and sunitinib in human plasma by liquid chromatography coupled with tandem mass spectrometry. *Biomed Chromatogr*. 2012 Sep 17. [Epub ahead of print]

Kroiss M, Quinkler M, Johanssen S, van Erp NP, **Lankheet N**, Pöllinger A, Laubner K, Strasburger CJ, Hahner S, Müller HH, Allolio B, Fassnacht M. Sunitinib in Refractory Adrenocortical Carcinoma: A Phase II, Single-Arm, Open-Label Trial. *J Clin Endocrinol Metab*. Epub 2012 Jul 26.

Tang SC, **Lankheet NA**, Poller B, Wagenaar E, Beijnen JH, Schinkel AH. P-glycoprotein (ABCB1) and breast cancer resistance protein (ABCG2) restrict brain accumulation of the active sunitinib metabolite N-desethyl sunitinib. *J Pharmacol Exp Ther*. 2012 Apr;341(1):164-73. Epub 2012 Jan 11.

Ter Heine R, van den Bosch RT, Schaefer-Prokop CM, **Lankheet NA**, Beijnen JH, Staaks GH, van der Westerlaken MM, Malingré MM, van den Brand JJ. Fatal interstitial lung disease associated with high erlotinib and metabolite levels. A case report and a review of the literature. *Lung Cancer*. 2012 Mar;75(3):391-7. Epub 2011 Nov 17.

Lankheet NA, Blank CU, Mallo H, Adriaansz S, Rosing H, Schellens JH, Huitema AD, Beijnen JH. Determination of sunitinib and its active metabolite N-desethylsunitinib in sweat of a patient. *J Anal Toxicol*. 2011 Oct;35(8):558-65.

Tang SC, Lagas JS, **Lankheet NA**, Poller B, Hillebrand MJ, Rosing H, Beijnen JH, Schinkel AH. Brain accumulation of sunitinib is restricted by P-glycoprotein (ABCB1) and breast cancer resistance protein (ABCG2) and can be enhanced by oral elacridar and sunitinib coadministration. *Int J Cancer*. 2012 Jan 1;130(1):223-33. doi: 10.1002/ijc.26000. Epub 2011 Apr 7.

R1
R2
R3
R4
R5
R6
R7
R8
R9
R10
R11
R12
R13
R14
R15
R16
R17
R18
R19
R20
R21
R22
R23
R24
R25
R26
R27
R28
R29
R30
R31
R32
R33
R34
R35
R36
R37
R38
R39

R1
R2
R3
R4
R5
R6
R7
R8
R9
R10
R11
R12
R13
R14
R15
R16
R17
R18
R19
R20
R21
R22
R23
R24
R25
R26
R27
R28
R29
R30
R31
R32
R33
R34
R35
R36
R37
R38
R39

Lankheet NA, Padberg RD, de Kluiver EM, Wilhelm AJ, van Woensel JB, Beijnen JH, Huitema AD. Relatively mild symptoms after an olanzapine intoxication in a 2-year-old girl with excessively high serum levels. *J Child Adolesc Psychopharmacol*. 2011 Feb;21(1):93-5. Epub 2011 Feb 2.

Ter Heine R, Fanggiday JC, **Lankheet NA**, Beijnen JH, Van Der Westerlaken MM, Staaks GH, Malingré MM. Erlotinib and pantoprazole: a relevant interaction or not? *Br J Clin Pharmacol*. 2010 Dec;70(6):908-11.

De Boer MP, van der Veldt AA, **Lankheet NA**, Wijnstok NJ, van den Eertwegh AJ, Boven E, Serné EH. Sunitinib-induced reduction in skin microvascular density is a reversible phenomenon. *Ann Oncol*. 2010 Sep;21(9):1923-4. Epub 2010 Jul 5.

Langenberg MH, Witteveen PO, **Lankheet NA**, Roodhart JM, Rosing H, van den Heuvel IJ, Beijnen JH, Voest EE. Phase 1 study of combination treatment with PTK 787/ZK 222584 and cetuximab for patients with advanced solid tumors: safety, pharmacokinetics, pharmacodynamics analysis. *Neoplasia*. 2010 Feb;12(2):206-13.

Lankheet AG, Hillebrand MJ, Langenberg MH, Rosing H, Huitema AD, Voest EE, Schellens JH, Beijnen JH. A validated assay for the quantitative analysis of vatalanib in human EDTA plasma by liquid chromatography coupled with electrospray ionization tandem mass spectrometry. *J Chromatogr B Analyt Technol Biomed Life Sci*. 2009 Nov 1;877(29):3625-30. Epub 2009 Sep 6.

Lankheet AG, Hillebrand MJX, Beijnen JH. Hoe natuurlijk is een '100% natuurlijke' erectiepijl? *PW Wetenschappelijk Platform* 2009;3(9): 164-5.

Lankheet AG, Beijnen JH, Schellens JHM, Huitema ADR. Resistentie tegen tyrosinekinaseremmers. *PW Wetenschappelijk Platform* 2009;3(7/8):122-12.

Abstracts

Lankheet NA, Kloth JS, Gadellaa-van Hooijdonk CG, Cirkel GA, Mathijssen RH, Lolkema MP, Schellens JH, Voest EE, Sleijfer S, Beijnen JH, Huitema ADR, Steeghs N. Individual PK-guided sunitinib dosing: A feasibility study in patients with advanced solid tumors. *J Clin Oncol*. 2012; 30 (suppl; abstr 2596). Poster presentatie tijdens ASCO Annual Meeting 2012, Chicago, Illinois.

Lankheet NA, Mallo H, Haanen JB, Huitema ADR, Schellens JHM, Beijnen JH, Blank CU. Quantification of sunitinib in sweat secretion. *J Clin Oncol*. 2010; 28 (suppl; abstr e15094).